

# Consolidation of Stressed and Lifting Decorative Coatings on Wood

---

The effect of consolidant choice on the structural integrity  
of multilayered East Asian lacquer coatings with  
gesso-type foundation layers

Inauguraldissertation  
zur Erlangung des Grades eines Doctor rerum naturalium  
im Fachgebiet  
Kunsttechnologie, Konservierung und Restaurierung von Kunst- und Kulturgut  
an der  
Hochschule für Bildende Künste Dresden

vorgelegt von

Nanke C. Schellmann

Tag der öffentlichen Verteidigung: 03. März 2012

Die Forschungsarbeiten für diese Dissertation wurden in den Labors und Werkstätten des Imperial College London, Mechanical Engineering Department, und dem Victoria and Albert Museum, London, durchgeführt.

Betreuer: Prof. Dr. Christoph Herm  
Hochschule für Bildende Künste Dresden

Gutachter: Prof. Dr. Christoph Herm  
Hochschule für Bildende Künste Dresden  
Dr. Ambrose C. Taylor  
Imperial College London, UK

Tag der Einreichung der Dissertation bei der HfBK Dresden:  
02. September 2011

Tag der öffentlichen Verteidigung:  
05. März 2012

Druckjahr 2012

# Consolidation of Stressed and Lifting Decorative Coatings on Wood

---

The effect of consolidant choice on the structural integrity  
of multilayered East Asian lacquer coatings with  
gesso-type foundation layers

Inaugural Dissertation  
for obtaining the Degree of Doctor rerum naturalium  
in the field of Art Technology,  
Conservation and Restoration of Artefacts and Cultural Heritage Assets,  
of the  
Academy of Fine Arts Dresden

submitted by

Nanke C. Schellmann

Date of public defence at the Academy of Fine Arts Dresden:

03 March 2012



Text and tables: © Nanke C. Schellmann

Images: © Nanke C. Schellmann, except as stated otherwise in the List of Figures

Image of shrine: © Victoria and Albert Museum London, UK

All Rights Reserved. No part of the work, published in either book or electronic form, may be reproduced or transmitted in any form or by any means, electronic or mechanical, including photocopy, recording or any other information storage and retrieval system without prior permission from the author and/or the Victoria and Albert Museum London.

For information please contact: [nschellmann@gmx-topmail.de](mailto:nschellmann@gmx-topmail.de)



# Zusammenfassung

Die Bestimmung von Effizienz und Verhalten polymerer Festigungsmittel für spröde, mehrschichtige dekorative Fassungen ist eine große Herausforderung für Restauratoren. Diese Arbeit beschäftigt sich daher mit einem neuen methodischen Ansatz zur Untersuchung des mechanischen Festigungseffekts von Konsolidierungsmitteln, die in die Fassungsstruktur eingezogen sind. Exemplarisch wurde diese Arbeit an ostasiatischen Lackfassungen durchgeführt, die als typisches Beispiel für durch spröde Brüchigkeit, Delamination und Abblätterungserscheinungen gekennzeichnete, mehrschichtige dekorative Fassungen gelten.

Eine an ausgewählten Beispielen durchgeführte Untersuchung zu der Frage, welche Schichten in derartigen Lackfassungen die geringste Widerstandsfähigkeit besitzen und was der Hauptgrund für ihr mechanisches Versagen ist, ergab, dass proteingebundene (kreidegrundähnliche) Grundierungen am anfälligsten für Brüche und Delamination sind. Mechanische Festigkeitstest wurden mit einem Ansatz aus der werkstoffkundlichen Bruchmechanik unter Verwendung der Doppelbalkenprobe (double-cantilever beam, DCB-Test) durchgeführt. Der Materialwert Bruchenergie ( $G_{Ic}$ ) wurde gemessen und das Bruchverhalten der spröden proteingebundenen Grundierung charakterisiert. Die DCB-Proben wurden unter kontrollierten Bedingungen gebrochen, danach mit verschiedenen polymeren Konsolidierungsmitteln gefestigt und schließlich erneut gebrochen, um Messdaten für einen direkten Vergleich zu erhalten. Getestet wurden Rinderhautleim, kaltflüssiger Fischleim, Störleim, Stärkekleister/Störleim, Lascaux Medium für Konsolidierung, Paraloid B 72 und B 48 N, Mowiol 3-83, Mowilith 50, Mowilith DMC2 und ostasiatische Lackmischungen (Roh-Urushi und Mugi-Urushi). Bei erstmaligem Bruch der Grundierung wurden unabhängig von der Schichtstärke Werte von  $47 (\pm 22) \text{ J/m}^2$  gemessen. Die Ergebnisse für die gefestigten Proben variierten stark. Die mit Paraloid und kaltflüssigem Fischleim gefestigten Proben zeigten die größte Reduzierung der gemittelten  $G_{Ic}$  (reduziert bis um -98 %), Lascaux Medium für Konsolidierung und Mowilith DMC2 die größten Steigerungen (bis auf + 180 %).

Vor dem zweiten Bruchtest der gefestigten DCB-Proben wurden Querschlitze angefertigt, um das Eindringverhalten und Verfüllungsvermögen der Konsolidierungsmittel zu untersuchen. Die Ergebnisse dieser Untersuchung korrespondierten gut mit den zuvor gemessenen Bruchenergien. Zusätzlich wurden die verschiedenen Festigungsmittel noch auf kleine Testbrettchen aufgetragen, auf denen zuvor delaminierende Lackschichten künstlich nachgebildet worden waren. Diese Tests lieferten ergänzende, empirische Informationen zu den Verhaltens-

und Handhabungseigenschaften der Festigungsmittel.

Diese Arbeit zeigt deutlich, dass die verwendete Untersuchungsmethode messbare Unterschiede in der Bruchenergie und dem Eindringverhalten der Konsolidierungsmittel feststellen kann sowie detaillierte Informationen über die Lage der Bruchebenen liefert. Zusammengefasst ergeben diese Daten ein verbessertes Verständnis des Festigungsvermögens verschiedener Konsolidierungsmittel.



# Abstract

Determining the efficiency and performance of polymer formulations used as consolidants for fragile, multilayered decorative coatings is a great challenge for conservators. To tackle this problem, this thesis presents a new methodical approach to detail the mechanical strengthening effect that consolidants have on coatings once they are applied to and allowed to penetrate through their structure. Research was undertaken using East Asian lacquer coatings as a typical example of a multilayered coating that shows brittle fracture, delamination and flaking.

A survey was conducted to identify the least stable layers in these coatings and the causes responsible for their failure. Protein-bound (gesso-type) foundation layers were found to be the most prone to develop failure and delamination. Mechanical strength tests were performed with a fracture mechanics approach using the standardised double cantilever beam (DCB) method. The fracture energy ( $G_{Ic}$ ), a material property, was measured and the fracture behaviour of the brittle, protein-bound foundation layers were characterised. DCB specimens were fractured, then consolidated with various polymer formulations and re-fractured to provide data for direct comparison. The tested consolidants included hide glue, cold-liquid fish glue, isinglass, starch/isinglass, Lascaux Medium for Consolidation, Paraloid B 72 and B 48 N, Mowiol 3-83, Mowilith 50, Mowilith DMC2 and East Asian lacquer-based formulations (raw urushi, mugi-urushi). For undamaged foundation layers,  $G_{Ic}$  values of  $47 (\pm 22) J/m^2$  were measured, independent of the layer thickness. The results for the consolidated specimens varied widely. Specimens consolidated with Paraloid and fish glue showed the greatest decreases in mean  $G_{Ic}$  (down to -98 %) and Lascaux Medium for Consolidation and Mowilith DMC2 gave the greatest increases (up to +180 %).

Cross-sections were prepared from the DCB specimens before second-phase fracture to determine penetration behaviour and void-filling ability of the consolidants. These data reflected the results of the measured fracture energies. In addition, the consolidants were applied to small test boards, which had been artificially aged beforehand to replicate lifting lacquer coatings. This provided complementary empirical information on the performance and handling properties of the consolidants.

The results clearly show that the methods can determine measurable differences in the fracture energy and the penetration behaviour of the consolidants. Detailed information on the location of crack path propagation can also be determined. Together, these data provide a much improved understanding of the strengthening capability of different consolidants.



*To my family.*



# Acknowledgements

I am indebted to my Doktorvater Professor Dr. Christoph Herm, HOCHSCHULE FÜR BILDENDE KÜNSTE DRESDEN, Shayne Rivers, VICTORIA AND ALBERT MUSEUM, FURNITURE CONSERVATION and THE MAZARIN CHEST PROJECT, and to Dr. Ambrose C. Taylor, IMPERIAL COLLEGE LONDON, for encouraging and supporting so strongly the idea of this collaborative PhD project. Without the continued guidance and expertise of my academic supervisors, their extensive support for all aspects of my work at the three institutions and the most generous access to facilities, this work would not have been possible.

My sincerest thanks also go to Arlen Heginbotham, THE J. PAUL GETTY MUSEUM, and Michael Schilling, THE GETTY CONSERVATION INSTITUTE, for their invaluable assistance and the PyGC/MS analysis of the lacquer samples; Dr. Heinrich Piening, RESTAURIERUNGSZENTRUM BAYERISCHE VERWALTUNG DER STAATL. SCHLÖSSER, GÄRTEN UND SEEN, MÜNCHEN, and Yannick Chastang for helping out with inspiring suggestions, materials and equipment; Dr. Ralph Kay, and Dr. Adrian Hayes, for the kind provision of stains; and to Günther Heckmann for assisting me in getting my research started.

For financial support, which enabled research and training in Japan, discussions and exchange with fellow international professionals, I am very grateful to THE DAIWA ANGLO-JAPANESE FOUNDATION, THE GREAT BRITAIN SASAKAWA FOUNDATION, ICCROM, the BROMMELLE MEMORIAL FUND and COST ACTION IE0601 WOODCULTHER.

The colleagues I would like to acknowledge are too numerous for all to be listed here – if I have missed your name please be assured that my gratitude is no less. At the V&A, I am especially thankful to Dr. Nigel Bamforth, Dr. Rupert Faulkner, Boris Pretzel and Yoshihiko Yamashita. At IMPERIAL COLLEGE, MECHANICAL ENGINEERING DEPARTMENT, my sincerest thanks go to Hugh MacGillivray, Dr. Ruth Brooker and Dr. Eric Hagan for their technical assistance in the laboratories. I am also particularly grateful to Dr. Kunal Masania, Hari Arora, Dr. Paul Hooper, Dr. Yatish Patel, Tim Hault and Dr. Idris Mohammed, not only for all the discussions and their support in engineering matters, but also for proof-reading my work, and for including me as “one of the boys”.

Special thanks are further due to Carola Schüller, Dr. Carolyn McSharry, Dr. Cristina Gentilini, Johanna Lang and Dr. Lisa Wagner for continuously sharing their thoughts on conservation matters and chemistry; and to a friend of yore, for the long conversations we have had that increased my understanding of the subtleties of the English language, which helped me write this thesis.

Last, but not least, my deepest gratitude goes to my family. Without their unlimited support, encouragement and their belief in me, my work and my endurance, I would not have got this far.



# Contents

List of Figures	5
List of Tables	11
Nomenclature	13
1. Introduction	17
1.1. Problem of consolidation . . . . .	18
1.2. Aims and objectives . . . . .	19
1.3. Thesis outline . . . . .	20
2. The Multilayered Structure of East Asian Lacquer Coatings	23
2.1. Introduction . . . . .	23
2.2. Lacquer – the characteristic constituent . . . . .	24
2.3. Complexity of layer structures . . . . .	24
2.4. The problem of stresses . . . . .	25
2.5. Wood substrates in composite structures . . . . .	25
2.6. The quality of lacquer coating structures . . . . .	26
2.6.1. Mechanical strength of lacquer composites . . . . .	26
2.6.2. Effect of surrogate binders . . . . .	27
2.6.3. Types of lacquer ware . . . . .	27
2.7. Effect of moisture on multilayered coatings . . . . .	28
2.8. Implications . . . . .	30
3. Review of Damage to East Asian Lacquer Objects	31
3.1. Introduction . . . . .	31
3.2. Object choice . . . . .	31
3.3. Analysis of coating structures and components – Materials and methods . . . . .	36
3.3.1. Optical microscopy and staining . . . . .	36
3.3.2. FTIR and PyGC/MS analysis . . . . .	42
3.4. Analysis results and discussion . . . . .	47
3.4.1. Results of coating layer analysis . . . . .	47
3.4.2. Comparison of identification techniques . . . . .	51
3.4.3. Discussion of the causes of binding media failure – Influence of exposure to water and high humidity levels . . . . .	68

## Contents

3.4.4. Remarks on the durability of coatings with high lacquer content . . . . .	71
3.5. Conclusions . . . . .	75
4. Consolidation of East Asian Lacquer Objects . . . . .	77
4.1. Introduction . . . . .	77
4.2. Literature review . . . . .	78
4.2.1. Approaches to the consolidation of delaminating lacquer coatings . . . . .	78
4.2.2. Natural polymers . . . . .	81
4.2.3. Synthetic polymers . . . . .	84
4.2.4. Major challenges encountered during consolidation . . . . .	86
4.3. Criteria for consolidant selection . . . . .	88
4.3.1. Requirements for consolidants . . . . .	88
4.3.2. Factors influencing consolidant properties and performance . . . . .	90
4.4. Consolidant choice for lifting lacquer coatings . . . . .	98
4.4.1. Class I, Protein-based consolidants . . . . .	99
4.4.2. Class +, Polysaccharides (starch) . . . . .	100
4.4.3. Class II, <i>Urushi</i> lacquer . . . . .	100
4.4.4. Class III, Acrylics . . . . .	101
4.4.5. Class IV, Poly(vinyl alcohols) . . . . .	102
4.4.6. Class V, Poly(vinyl acetates) . . . . .	103
4.4.7. Summary of polymers selected for testing . . . . .	104
4.5. Chapter summary . . . . .	104
5. Testing of Material Strength and Fracture Behaviour . . . . .	109
5.1. Introduction . . . . .	109
5.2. Material properties definitions . . . . .	110
5.3. Previous research . . . . .	111
5.3.1. Properties of East Asian Lacquer films and coatings . . . . .	112
5.3.2. Properties of filled polymers and complex systems . . . . .	112
5.3.3. Methods for determining the mechanical behaviour of adhesives or consolidants . . . . .	113
5.4. Fracture mechanics approach – Choice of test method . . . . .	115
5.4.1. Testing of fracture energy under mode I – Double cantilever beam testing . . . . .	117
5.4.2. Determination of flexural modulus . . . . .	123
5.5. Choice of materials for test specimens . . . . .	124
6. Experimental: Fracture Behaviour – Materials and Methods . . . . .	127
6.1. Preparation of test specimens . . . . .	127
6.1.1. Double Cantilever Beam (DCB) specimens for initial testing . . . . .	127
6.1.2. Consolidation of fractured DCB specimens . . . . .	134
6.1.3. Specimens for tensile and compression testing . . . . .	138



6.1.4.	Replication of lifting lacquer for empirical consolidation testing . . . . .	139
6.2.	Mechanical properties testing . . . . .	143
6.2.1.	Mode I fracture tests . . . . .	143
6.2.2.	Flexural modulus of the wood substrate . . . . .	147
6.2.3.	Tensile modulus of foundation . . . . .	147
6.2.4.	Yield stress of foundation . . . . .	149
6.3.	Determination of consolidant distribution . . . . .	149
6.3.1.	Cross-section sampling . . . . .	149
6.3.2.	Staining of consolidants . . . . .	150
6.3.3.	Optical microscopy . . . . .	151
7.	Experimental: Fracture Behaviour – Results and Discussion	153
7.1.	Introduction . . . . .	153
7.2.	Initial DCB fracture tests . . . . .	153
7.2.1.	Fractography . . . . .	153
7.2.2.	Fracture energy $G_{Ic}$ . . . . .	162
7.2.3.	Dependence of $G_{Ic}$ on layer thickness . . . . .	167
7.2.4.	Flexural modulus . . . . .	171
7.3.	Second-phase DCB fracture tests (consolidated specimens) . . . . .	173
7.3.1.	Validity of measured data . . . . .	173
7.3.2.	Fracture results for specimen sets . . . . .	175
7.3.3.	Summary of DCB fracture tests . . . . .	199
7.4.	Examination of DCB cross-sections . . . . .	207
7.4.1.	Bondline thickness and penetration behaviour . . . . .	207
7.4.2.	Notes on the efficiency of the stains used . . . . .	221
7.5.	Empirical evaluation of consolidants . . . . .	222
7.5.1.	Wetting and handling properties deduced from DCB specimens . . . . .	222
7.5.2.	Consolidation of lifting lacquer specimens . . . . .	224
7.6.	Discussion of experimental results and conclusions . . . . .	230
7.6.1.	State of bondline and accuracy of joint fit . . . . .	231
7.6.2.	Implications of Penetration Depth . . . . .	232
7.6.3.	Level of strengthening and significance of $G_{Ic}$ . . . . .	233
7.6.4.	Suitability of consolidants for protein-based foundations in lacquer coatings . . . . .	235
7.6.5.	Remarks on the DCB test method . . . . .	238
7.7.	Chapter summary . . . . .	240
8.	Conclusions	243
8.1.	Failure causes in export-type lacquer coatings . . . . .	243
8.2.	Fracture behaviour of foundation layers . . . . .	244
8.2.1.	Initial fracture behaviour . . . . .	244
8.2.2.	Fracture behaviour after consolidation . . . . .	244

*Contents*

8.2.3. Advantages of test methodology . . . . .	246
8.3. Future Work . . . . .	246
References	249
A. Staining Assays	277
B. Wood Specifications	279
C. List of Materials and Suppliers	281
D. Survey of Damage to East Asian Lacquer Objects	285
D.1. Introduction . . . . .	285
D.2. Table of surveyed objects . . . . .	288
D.3. Survey Results . . . . .	290
E. List of Publications	379

# List of Figures

1.1. Detail of a Japanese shrine panel (W.1-1913) showing losses in the lacquer coating. (Photograph by N. Schellmann, courtesy of the V&A). . . . .	17
3.1. Examples of extensive coating damage on East Asian lacquer objects. (Photographs by N. Schellmann, (a)-(e) courtesy of the V&A).	32
3.2. Cross-sections of lacquer coatings under blue light, showing fluorescence of the lacquer. . . . .	38
3.3. Round box (V&A W.332-1921): cross-section of coating in VIS and in blue light, and stained with AB2 solution. . . . .	40
3.4. Export lacquer reference sample: cross-section of the coating structure in VIS light, stained with AB2 and Nile Blue sulphate solution.	40
3.5. Cabinet stand (V&A 303-1876): cross-section of coating in VIS and in blue light, and stained with Lugol's solution . . . . .	42
3.6. Palanquin (V&A 48-1874): cross-section of coating in VIS and in blue light; unstained and stained with Nile Blue sulphate and Sudan Black B. . . . .	43
3.7. Anacard marker compounds identified by TMAH-PyGC/MS for a reddish foundation sample of the palanquin (Schilling 2010a). . .	57
3.8. Fatty acid profile measured by TMAH-PyGC/MS for the reddish foundation of the palanquin (V&A 48-1874) (Schilling 2010a). . .	59
3.9. Cross-section of priming layer of cabinet stand (V&A 303-1876) after staining with Lugol's solution in blue light. . . . .	60
3.10. Coromandel cabinet (priv. collection): cross-section of coating structure under blue light. . . . .	62
3.11. FTIR spectra of a sample taken from the round box (V&A W.332-1921) and its best matching two reference components (Herm 2009a, p.34). . . . .	65
3.12. Four-fold screen (V&A W.25-1939): cross-section of entire coating structure under blue light. . . . .	67
3.13. Details of Cabinet stand (V&A No. 303-1876) displaying blistering, lifting and flaking lacquer on the top panel and on one of the legs. (Photographs by N. Schellmann, courtesy of the V&A). . . .	69
3.14. Details of the lifting coating on the corner cabinet (493-1872). (Photographs by N. Schellmann, courtesy of the V&A.) . . . . .	70
3.15. Round box (W.332-1921), full view. (Photographs by N. Schellmann, courtesy of the V&A.) . . . . .	71

List of Figures

3.16. Cabinet with fans (W.19-1969) showing cupping and lifting lacquer coating between ivory inlay. (Photograph by N. Schellmann, courtesy of the V&A.) . . . . .	72
3.17. Outside of drop-front of early 15th century Chinese cabinet (F.E.7-1973), showing extensive cracking of the lacquer coating. (Photograph by N. Schellmann, courtesy of the V&A). . . . .	73
3.18. Detail of the Chinese cabinet (F.E.7-1973) drop front inside. (Photograph by N. Schellmann, courtesy of the V&A.) . . . . .	74
3.19. FTIR spectra of a sample from the fifteenth century Chinese lacquer cabinet (F.E.7-1973) and its best matching three reference components (Herm 2009a, p. 28). . . . .	76
5.1. Stress/strain behaviour of materials. . . . .	111
5.2. Modes of loading of a test specimen. . . . .	115
5.3. DCB specimen with end blocks adapted from Standard BS 7991 (2001). . . . .	118
5.4. Schematic load-displacement curve (figure taken from BS 7991:2001, p.14). . . . .	119
5.5. Determination of the crack length correction factor $\Delta$ for the corrected beam theory (CBT) method (figure taken from BS 7991:2001, p.15). . . . .	122
5.6. Slope $n$ determined for the Experimental Compliance Method (ECM) for the DCB specimen (after BS 7991:2001). . . . .	123
5.7. Three-point bending test. . . . .	123
6.1. Cutting of laminae from pine wood log at a $3^\circ$ angle to the wood grain and pairing of lamina boards. . . . .	128
6.2. Method of brush application of <i>urushi</i> lacquer to ensure even spreading. . . . .	131
6.3. Desorption curves for two DCB specimens during equilibration. . . . .	132
6.4. DCB specimen (pine wood/foundation) with attached aluminium end blocks. . . . .	133
6.5. Foundation compression specimens. . . . .	139
6.6. Replication of lifting export lacquer coatings . . . . .	140
6.7. Instron 5584 universal testing machine setup for DCB testing under controlled environmental conditions. . . . .	144
6.8. Principle of DCB testing. . . . .	144
6.9. Stress/strain curve for a foundation tensile test specimen showing the Young's modulus, $E$ , and the tensile strength. . . . .	148
6.10. Stress/strain curve for a cylindrical foundation specimen tested in compression. . . . .	149
7.1. Typical fracture surfaces of DCB specimens type A after initial testing. . . . .	154

7.2. Typical fracture surfaces of DCB specimens type B after initial testing. . . . .	155
7.3. Frequency of occurrence of the proportion of interfacial failure in the tested DCB specimens. . . . .	156
7.4. Type A DCB specimen: detail of fracture surface of foundation layer showing failure on varying levels. . . . .	157
7.5. Type B DCB specimen: detail of fracture surface of foundation layer. Failure predominantly occurred near the lacquer interface. . . . .	158
7.6. Detail of typical DCB specimen fracture surface (type A) resembling the naturally-induced damage on the export-type East Asian lacquer coating. . . . .	158
7.7. Examples of natural coating failure observed on export-type East Asian lacquer objects: corner cabinet (V&A, 493-1872), and cabinet on stand (V&A, 303-1876). (Photographs by N. Schellmann, courtesy of the V&A.) . . . . .	159
7.8. Details of foundation fracture surfaces showing small air bubbles and pin hole-shaped discontinuities. . . . .	160
7.9. SEM image of a DCB type B fracture surface showing irregular-shaped voids and air-bubbles in the foundation. . . . .	161
7.10. SEM image of DCB type B foundation fracture surface at x1000 magnification. . . . .	162
7.11. Typical curves for load versus displacement, and crack length vs. displacement for different failure types in mode I fracture testing. . . . .	163
7.12. Load, $P$ , and crack length, $a$ , as a function of displacement, $\delta$ , for a DCB (type A) test. . . . .	164
7.13. Resistance curves for a DCB specimen during initial testing in mode I, established by the methods of SBT, CBT, and ECM. . . . .	165
7.14. Examples of two type A DCB specimens showing stable and unstable failure during initial testing. . . . .	168
7.15. Distribution of mean $G_{Ic}$ (CBT) values for tested type A DCB specimens in relation to the mean thickness of the foundation layer. . . . .	169
7.16. Plastic zone ahead of crack tip (after Kinloch 1987, p.280). . . . .	170
7.17. Flexural modulus back-calculated using simple beam theory (SBT) plotted against crack length. . . . .	172
7.18. Comparison of the flexural moduli measured by three-point bending test, and from DCB test results back-calculated with corrected beam theory (CBT). . . . .	173
7.19. Load versus displacement curve for a type A DCB specimen showing relatively unstable crack propagation. . . . .	175
7.20. Fracture surfaces of DCB specimen consolidated with 10% isinglass solution. . . . .	176
7.21. Example of typical fracture surface of DCB specimen type A consolidated with cold-liquid fish glue stained with Fast Green. . . . .	178

List of Figures

7.22. Load as a function of displacement for a typical DCB specimen consolidated with cold-liquid fish glue. . . . .	178
7.23. Fracture surfaces of type B DCB specimen consolidated with 10 % bovine hide glue solution stained with Fast Green. . . . .	179
7.24. Type B DCB specimen consolidated with starch/isinglass showing typical fracture surfaces showing SCF and new AF. . . . .	181
7.25. Fracture surface of a DCB specimen treated with <i>mugi-urushi</i> . . .	183
7.26. Fracture surfaces of type A DCB specimen consolidated with <i>ki-urushi</i> . . . . .	184
7.27. R-curves for DCB specimen before and after consolidation with <i>ki-urushi</i> . . . . .	185
7.28. Typical fracture surfaces of a DCB specimen consolidated with Paraloid B 72 (25 %) in acetone stained with Solvent Blue G stain. . . . .	186
7.29. DCB fracture surface showing irregular distribution of Paraloid B 72 stained with Solvent Blue G in the foundation layer. . . . .	188
7.30. Fracture surfaces of DCB specimen consolidated with Paraloid B 48 N in toluene/xylene. . . . .	189
7.31. Details of the fracture surfaces of DCB specimens consolidated with Paraloid resin solutions stained with Solvent Blue G. . . . .	189
7.32. Typical load-displacement curve for a DCB specimen consolidated with Paraloid B 72 in acetone. . . . .	190
7.33. Typical fracture surface of a type B DCB specimen consolidated with Lascaux Medium for Consolidation. . . . .	191
7.34. Details of the fracture surfaces shown in Figure 7.33. . . . .	191
7.35. Load and crack length as a function of displacement, and $G_{Ic}$ as a function of crack length for the specimen consolidated with Lascaux Medium for Consolidation. . . . .	193
7.36. Fracture surfaces of DCB specimens consolidated with Mowiol 3-83 (unstained). . . . .	194
7.37. R-curves for specimens consolidated with Mowiol 3-83, measured during second-phase testing. . . . .	195
7.38. Fracture surface of DCB specimen consolidated with Mowilith 50 in toluene, stained with Lugol's solution. . . . .	196
7.39. Detail of fracture surface of DCB specimen consolidated with Mowilith 50 in toluene after staining with Lugol's solution. . . . .	196
7.40. Fracture surfaces of specimen consolidated with Mowilith DMC2 dispersion, stained with Lugol's solution. . . . .	197
7.41. Details of fracture surfaces of DCB specimen consolidated with Mowilith DMC2, stained with Lugol's solution. . . . .	198
7.42. Detail of DCB specimen consolidated with Mowilith DMC2 during testing, showing bridging of the consolidant. . . . .	198
7.43. Mean fracture energy, $\bar{G}_{Ic}$ , values for each DCB specimen set of type A before and after consolidation. . . . .	200

7.44. Mean fracture energy, $\overline{G}_{Ic}$ , values for each DCB specimen set of type B before and after consolidation. . . . .	201
7.45. Effect of consolidation expressed as mean relative changes in fracture energy, $\overline{\Delta G}_{Ic}$ , measured for types A and B samples during second-phase DCB testing. . . . .	202
7.46. Comparison of the percentage of failure in new areas of the DCB specimens determined after second-phase fracture. . . . .	203
7.47. Examples of DCB cross-section micrographs (type A and B) with unstained foundation layers. . . . .	207
7.48. Cross-sections of DCB specimens consolidated with protein-based polymer formulations, stained with Fast Green. . . . .	209
7.49. Cross-sections of type B DCB specimens consolidated with starch/isinglass. . . . .	211
7.50. Cross-sections of type A DCB specimens consolidated with traditional formulations based on East Asian lacquer. . . . .	213
7.51. Cross-sections of specimens consolidated with acrylate-based consolidant solutions. . . . .	215
7.52. Cross-sections of type A DCB specimens consolidated with the acrylate-based dispersion Lascaux Medium for Consolidation. . . . .	216
7.53. Type B DCB cross-section of specimen consolidated with the poly(vinyl alcohol) Mowiol 3-83. . . . .	217
7.54. Type A DCB cross-sections of specimens consolidated with the poly(vinyl acetate) solution Mowilith 50. . . . .	218
7.55. Cross-sections of type A specimens consolidated with the poly(vinyl acetate) dispersion Mowilith DMC2. . . . .	219
7.56. Lifting lacquer test boards after consolidation showing uneven appearance of the lacquer surface. (Board size 35 x 60 mm) . . . . .	225
7.57. Lifting lacquer specimen consolidated with Lee Valley fish glue. . . . .	226
7.58. Side view of lifting lacquer specimen shown in Fig. 7.57a before consolidation. . . . .	227
7.59. Lifting lacquer specimen consolidated with Paraloid B 72 in acetone (stained with Solvent Blue G). . . . .	229
7.60. Adapted DCB method using a simple bench vice. . . . .	240





# List of Tables

3.1.	Lacquer objects from the V&A collection and a private owner displaying extensive coating damage. (Image of shrine taken by the V&A Photographic Studio, © Victoria and Albert Museum, London. All other photographs taken by N. Schellmann, courtesy of the V&A. Image of Coromandel cabinet courtesy of the private owner).	34
3.3.	Choice of identification methods for different binding media types.	41
3.4.	Characteristic FTIR absorption band frequencies for compounds of lacquer coatings.	44
3.5.	Marker compounds used for interpretation of the PyGC/MS chromatograms (Schilling 2010a).	46
3.6.	Coating layer structures of the lacquer objects analysed.	48
3.7.	Results of the material and binding media analysis.	49
3.8.	Summary of binding media analysis for selected coating layers from the surveyed lacquer objects.	53
4.1.	Surface free energy (surface tension), $\gamma_m$ , and viscosities, $\eta$ , of some solvents commonly used for consolidants, measured at 20 °C.	92
4.2.	Polymers selected for consolidation testing.	106
6.1.	Selection of consolidant formulations.	135
6.2.	Possible failure patterns on DCB specimens based on the definitions given by the British Standard BS EN ISO 10365 (1995)	146
7.1.	Frequency of occurrence of the degree of interfacial failure in the tested DCB specimens.	155
7.2.	Mean fracture energy initiation values, $G_{Ic\,init}$ , for the non-linear (NL), visual (VIS), and the 5% or maximum load (5%/MAX) criteria according to BS 7991 (2001), and the flexural modulus, $E_f$ , of DCB specimens.	166
7.3.	Average foundation layer thicknesses, $h_o$ , of export-type lacquer objects and DCB specimens.	169
7.4.	Mechanical properties of hide glue/tonoko foundation.	171
7.5.	Mean fracture energy, $\overline{G}_{Ic}$ , and mean relative changes in fracture energy, $\overline{\Delta G}_{Ic}$ for specimens consolidated with isinglass.	177
7.6.	Summary of fracture testing results for all DCB specimens (type A and B).	206

*List of Tables*

7.7. Summary of the penetration and fracture behaviour of the consolidants. . . . .	220
7.8. Summary of the consolidant performance for protein-bound foundations of East Asian lacquer coatings. . . . .	235

# Nomenclature

## Latin alphabet

$A$	Surface area; cross-sectional area
$A$	Starter foil length
$A_o$	Initial cross-sectional surface area of tensile specimen
$a$	Crack length (measured from load line to tip of mode I crack)
$a_o$	Starter foil length from load line
$a_p$	Initial crack length (precrack)
$a_s$	Starter foil total length
$B$	Joint width
$C$	Compliance, $C = \delta/P$
$C_o$	Initial compliance
$C_n$	Carbon chain of molecule, with $n$ denoting the number of C-atoms
$d_p$	Diameter of plastic zone
$d_{bl}$	Bondline thickness (of consolidant/adhesive)
$d_{pf}$	Penetration depth of consolidant in foundation
$d_{pw}$	Penetration depth of consolidant in wood substrate
$E$	Young's modulus (modulus of elasticity, stiffness)
$E_f$	Young's modulus, back-calculated from CBT
$E_s$	Young's modulus (flexural), independently measured
$F$	Correction factor for large displacement and end-block tilting
$F_n$	Foundation layer, with $n$ denoting the position number of the layer, counted from substrate (used in Appendix D)
$G$	Fracture energy/energy release rate
$G_{Ic}$	Fracture energy in mode I
$H$	Thickness of end block of DCB specimen
$h$	Thickness of wood substrate beam of DCB specimen
$h_o$	Foundation layer thickness
$h_a$	Adhesive layer thickness
$K_{Ic}$	Critical stress intensity factor
$L$	Support span length (3-point bend test)
$L_o$	Initial length of tensile specimen
$L_n$	Lacquer layer, with $n$ denoting the position number of the layer, counted from substrate (used in Appendix D)
$l$	Total DCB specimen length

## Nomenclature

$l_1$	Distance from the loading pin centre to the mid-plane of the DCB substrate arm to which the end block is attached
$l_2$	Distance from the loading pin centre to the edge of the end block of DCB specimen
$M_w$	Molecular weight
$N$	Correction factor for end-block stiffening
$n$	Sample size (statistical)
$n$	Slope of the graph plotting the logarithm of the normalised compliance, $\log(C/N)$ , versus the logarithm of the crack length, $\log a$ (in Chapter 5.4.2)
$P$	Load
$P_f$	Load at point of failure
$P_{max}$	Load at point of maximum load on load-displacement curve
$P_{5\%}$	Load at intersection point of 5% offset line with load-displacement curve
$r_p$	Radius of plastic zone
$s$	Standard deviation
$T$	Temperature
$T_g$	Glass transition temperature
$x_i$	Population (statistical)
$\bar{x}$	Arithmetic mean

## Units and prefixes

G	Giga
g	Gram
J	Joule
k	Kilo
M	Mega
M	Molarity (of a solution, used in Chapters 3.3.1 and Appendix A)
m	Metre
mm	Millimetre
N	Newton
N	Normality (of a solution, used in Chapters 3.3.1 and Appendix A)
Pa	Pascal
s	Second

## Greek alphabet

$\gamma_m$	Surface free energy
$\delta$	Load-point displacement
$\Delta$	Crack length correction factor in mode 1 (used in Chapter 5)

$\Delta$	Difference/change (when used in front of another variable)
$\overline{\Delta}$	Mean relative change (when used together with $G_{Ic}$ )
$\varepsilon$	Strain
$\eta$	Viscosity
$\mu$	Micro
$\mu_m$	Material constant for pressure dependency
$\nu$	Poisson's ratio
$\sigma$	Axial stress
$\sigma_f$	Stress at failure
$\sigma_{max}$	Ultimate tensile strength/stress
$\sigma_y$	Yield stress (onset of plastic deformation)
$\sigma_{yc}$	Yield stress in compression
$\sigma_{yt}$	Yield stress in tension

### Acronyms and Abbreviations

AB2	Amido Black staining solution (Martin 1977)
ASTM	American Society for Testing and Materials
AF	Adhesive (interfacial) failure
BS	British Standard
CBT	Corrected beam theory
CF	Cohesive failure
C.I.	Colour Index number
CoV	Coefficient of variation
c.	Century
c.	Circa
cf.	Confer/compare with
DAME	Dicarboxylic fatty acid methyl esters
DCB	Double cantilever beam
ECM	Experimental compliance method
EMA/MA	Ethyl methacrylate/methyl acrylate
e.g.	For example
FAME	Fatty acid methyl esters
FTIR	Fourier-transform infrared spectroscopy
i.e.	That is
LEFM	Linear elastic fracture mechanics
MAX	Maximum load on the load-displacement curve
MfC	Medium for Consolidation (Lascaux)
NL	Nonlinear criterion
PVAc	Poly(vinyl acetate)
PVAI	Poly(vinyl alcohol)
PyGC/MS	Pyrolysis-gas chromatography/mass spectrometry
R-curve	Resistance curve
RH	Relative humidity

## *Nomenclature*

SBT	Simple beam theory
SCF	Special cohesive failure (on varying levels of the layer)
SEM	Scanning electron microscope
TMAH	Tetramethyl ammonium hydroxide
UV	Ultra violet radiation
V&A	Victoria and Albert Museum
VIS	Visible light (used in Chapter 3)
VIS	Visible criterion for crack initiation (used in Chapters 5-7)

## *Subscripts*

<i>I</i>	Mode I
<i>init</i>	Initiation values
<i>prop</i>	Propagation values

# 1. Introduction

Decorative coatings on wooden substrates are found on a great variety of cultural heritage objects throughout the world, ranging from furniture and sculptures to panel paintings and architectural elements. Characteristically, many of these coatings are composed of multiple layers which often consist of different materials that have greatly varying properties. Upon ageing and exposure to unsuitable environmental conditions, these coatings can degrade and lose their physical integrity. Over time, this can lead to increasing damage and may eventually render the objects entirely unsuitable for their intended use. Ageing processes and subsequent failure of such structures are typically of a complex nature, but are often manifested in the development of delamination and lifting of coating layers. A prime example of objects that experience this kind of coating failure is East Asian lacquer ware (Fig. 1.1).



Figure 1.1.: Detail of a Japanese shrine panel (W.1-1913) showing losses in the lacquer coating caused by delamination and lifting of its multilayered coating structure. (Photograph by N. Schellmann, courtesy of the V&A).

To preserve these coatings and objects for future generations, efficient stabilisation of their fragile elements is required. This, however, is a challenging task. In the conservation of cultural heritage objects, high demands are made on the stabilising agent (consolidant) used to achieve effective stabilisation (i.e. consolidation) of decorative coatings. Ideally, a suitable stabilisation treatment should

## 1. Introduction

not only appropriately strengthen the object, but also slow down significantly its further course of deterioration. Moreover, no additional degradation should be induced in the future by either the treatment or the material added. In compliance with the relevant professional standards and guidelines (E.C.C.O. 2001; ICOM 2006, p. 6), the choice of consolidant should be governed by various factors: its chemical and physical compatibility with the object, its long-term physico-chemical stability and favourable ageing properties, and last but not least its handling (i.e. application) properties. Hence, conservators are required to predict the performance of stabilising agents to make informed decisions on which agent is most suitable for the purpose. In turn, this necessitates a thorough understanding not only of the properties of both the consolidant and the fragile material in isolation, but also of the stabilised (composite) material. Unfortunately, however, information on these characteristics is often scarce and limited to certain properties only.

### 1.1. Problem of consolidation

Artists' materials, particularly when aged, are rarely thoroughly characterised in their chemical and mechanical state. Hence, it is difficult to know the baseline properties of the fragile material to start with. In addition, the properties of the consolidants may also vary widely, as conservators can choose from a wide variety of available stabilising agents (most commonly polymers), whose character and performance is dependent on many parameters that can be manipulated. These include not only the choice of the stabilising compound or polymer, but also comprise the selection of solvents or diluents, the concentration of the desired consolidant formulation and the application method.

Over the previous decades, much research has been undertaken to characterise the properties of polymers used in conservation, particularly when applied as coatings or as adhesives (e.g. research by Feller 1957, 1958, 1984; Thomson (1963); Feller and Curran 1970, 1975; de la Rie 1988a,b; de la Rie et al. 2002; Down and co-workers 1980, 1984, 1996). Many of these studies were conducted with a focus on the conservation of paintings, and thus often concentrated on investigating the chemical stability and ageing behaviour of the consolidant and the strength properties of the bulk polymer. However, investigations on the strengthening ability of various polymers applied to and partly dispersed into fragile coating structures, such as that undertaken by Simon (2001), have rarely been the focus of comprehensive research. Hence, only limited information is available on the mechanical performance of polymer formulations applied to multilayered coatings on wooden substrates. A further step in this field of research is therefore required.

Knowing the mechanical strength properties of a bulk polymer is not necessarily sufficient to judge the levels of strength improvements achieved by a certain agent in situ on the object. Furthermore, questions remain about how far these consolidants infiltrate the fragile material, and whether they induce uniform property



changes in these structures. Whether or not a sufficient quantity of polymer remains located on the surface to re-adhere the lifting layers, also has to be questioned. All things considered, a thorough methodology which objectively characterises and quantifies the physical and mechanical performance of consolidants is lacking. Such a methodology is, however, necessary to help establish potential differences in their behaviour. Unsurprisingly, conservators often still find it difficult to carefully balance the measures required to stabilise a fragile coating, let alone choose the ‘most suitable’ consolidant for a practical application. The need to further improve the understanding of the interaction between these materials has been widely recognised in the field of conservation (e.g. Olstad and Kucerova 2009).

## 1.2. Aims and objectives

The primary aim of this research is to advance the understanding of the behaviour of polymer formulations that are used to stabilise failing layers in multilayered decorative coating structures. Using the example of East Asian lacquer ware, a methodical approach is presented that is intended to help conservators gain detailed and practically relevant information on the strengthening effect of consolidants. As the approach assumes that failure loci within the coating structure are so far unspecified, the methodology starts by investigating systematically the causes and effects of the failure on the coating structure. Once the least stable layers are identified, this work considers how the fracture behaviour of the failing layer can best be characterised.

Previously, most investigations in this field concentrated on employing more conventional methods for determining mechanical properties, such as tensile, compressive and shear tests (e.g. Schniewind and Kronkright 1984; Schniewind 1998; Down 1984; Weinbeck 2007). Although these give information on some mechanical properties, they are not necessarily ideal methods for characterising materials for conservation purposes. The strength values obtained from conventional tests dependent on the specimen geometry and the exact testing conditions. Furthermore, these tests often neither satisfactorily model the failure observed in real-life objects nor the stresses that cause it. This explains why a new approach, which can provide data on mechanical properties that are more directly applicable and useful for practical conservation purposes, is desirable.

For the purpose of investigating the fracture properties of materials, a standardised test method, known as the double cantilever beam (DCB) method, is borrowed from the field of fracture mechanics. This method is newly adapted to enable the characterisation of the fracture properties of decorative coating structures both before and after consolidation. In the field of conservation research, fracture properties have not been considered in such detail before. Only very recently, some researchers have started to employ fracture mechanics methods using

## 1. Introduction

disk-shaped specimens for investigating adhesives used for the consolidation or bonding of fractured marble (Jorjani et al. 2009; Tan et al. 2011). The current research adopts the DCB method as a more suitable means of investigating the fracture properties of multilayered coating structures applied to wood. The fracture mechanics approach has the great advantage of providing valuable information on how and when structures realistically fail during service in a real-life environment. Furthermore, the fracture behaviour can be described with material properties that are independent of the testing conditions. This makes the data gathered particularly useful as they can be compared universally between different studies. This new approach will help conservators improve their understanding of the overall performance of consolidants, and is therefore a promising tool for providing further criteria upon which the selection of a suitable consolidant can be based.

### 1.3. Thesis outline

This thesis is divided into seven chapters which present the methodology employed to systematically investigate the performance of consolidants that are used for stabilising delaminating and lifting coatings. The problem, aims and objectives of this research are given in this first chapter. The second chapter introduces East Asian lacquer ware as an example of decorative coatings with highly complex, multilayered structures, of which some types typically show severe delamination, lifting and flaking of coating layers with age.

As differences in coating quality and constituents are generally held responsible for the varying levels of damage that occur to these coatings, Chapter 3 examines in more detail the causes of this deterioration. To find out which types of lacquer coatings are most prone to developing extensive delamination failure and flaking, the results of a survey are presented, which was undertaken on a group of East Asian lacquer objects that showed this type of severe damage. The results of various microscopic, spectroscopic and staining techniques undertaken for investigating the coatings of these objects are discussed in detail. The exact failure loci within the multilayered coatings are identified, and the constituent compounds of the materials involved in their failure mechanisms are determined. This gives a clearer understanding of the areas of lowest toughness in the coating structures and identifies specific layer compositions that appear to be predominantly involved in the development of delamination and flaking damage.

Chapter 4 reviews the methods and materials previously used for the consolidation of damaged lacquer coatings. It highlights the problems and challenges encountered when trying to select a suitable consolidant for these structures. Furthermore, the criteria for consolidant selection are reviewed, providing an overview of the factors that influence the performance of consolidants used on porous substrates, such as the protein-bound foundation layers of lacquer coatings. Based on this review, a wide range of consolidants that may be used on

protein-bound lacquer coatings are selected to investigate their mechanical behaviour once applied to test specimens. These tests are presented in the following experimental part of this work.

Chapter 5 develops the reasoning for introducing a new approach for testing the mechanical properties of materials in the context of conservation. Previous methods and their limitations are reviewed, suggesting that an alternative method borrowed from the field of fracture mechanics might be a particularly promising alternative for gaining useful information on the mechanical properties of a consolidant. The double cantilever beam (DCB) test method is introduced as a means to establish the energy required to propagate a crack through both undamaged and consolidated test specimens.

Chapter 6 provides the technical details of the chosen test methodology and describes the preparation of the test specimens required for the individual tests. The specimens comprise those for DCB testing, which contain simplified coating layer structures, and additional tensile and compression test specimens of protein-based foundation material in bulk. These three test methods are used to establish the mechanical properties of the initial fragile material. Furthermore, details are provided about the initial fracture and subsequent consolidation of the DCB specimens with a variety of polymer-based consolidants. The staining methods for the consolidants are also described, as well as the manufacture of additional test specimens for cross-section analysis. Finally, lacquer test boards are manufactured and the delamination and lifting of their lacquer coatings is replicated. These boards are used for the empirical evaluation of the consolidants, which are tested under normal drying conditions and after cycling in a fluctuating environment.

The results of these tests are presented and discussed in Chapter 7.8a. This identifies the similarities and differences in the mechanical and physical performance of the consolidated test specimens, i.e. their fracture properties and the penetration ability of the various consolidants tested. Additionally, these results are compared with those of the empirical consolidation tests undertaken on the replicated lifting lacquer sample boards, the latter of which also highlight the scope and problems encountered with such tests on specimens that were manufactured to show delaminating coatings. The chapter closes with a discussion and evaluation of the consolidants' performance as stabilising agents for the protein-bound foundation layers of lacquer coatings. Furthermore, the wide applicability of the presented test methodology is demonstrated by proposing a simplified DCB test setup, that can be adopted for use even in modestly equipped conservation workshops.

Finally, the main conclusions of this research are summarised in Chapter 8. These give an overview of the performance of the tested consolidants and the scope of the test methodology employed. Recommendations regarding possibilities for future work in this field are presented to encourage further research on suitable materials and methods for consolidating cultural heritage objects that suffer from delaminating and lifting decorative coatings.



## 2. The Multilayered Structure of East Asian Lacquer Coatings

### 2.1. Introduction

A prime example of multilayered coatings on wooden substrates are those on East Asian lacquer ware. Many museums and collections in the Western world that house such lacquer objects are troubled with a small but significant number that have suffered severe damage to their lacquer coatings over the course of time. These coatings dramatically show cracks which cover large areas of the surface, delamination and cupping or tenting of layers. In the worst cases, considerable losses caused by complete adhesive or cohesive failure of the layered coating structures can be observed. In order to prevent any further loss of the decorative and protective coating layers and to successfully preserve these objects, the delaminating and flaking coatings require effective consolidation.

As is the case with panel paintings or many other multilayered decorative coatings on artefacts, the composite structure of East Asian lacquer coatings is usually specific to every individual object. This applies to the exact composition, layer thickness and state of deterioration. Owing to inherent variations of the natural materials used and the non-standardised production of the coatings, it is expected that such coatings may fail in a varied manner. The range of different consolidation methods used in the past and present reflects the diversity of problems encountered during consolidation and the necessity to understand the performance of different consolidation media when applied to complex composite structures.

This chapter introduces the component materials and multilayered structure of typical East Asian lacquer coatings. In order to provide a basic understanding of the general problems encountered with such coatings, the main aspects of stress development and their causes within the decorative coating are explained. Also, the major qualitative differences in specific lacquer coatings are presented to provide a suitable basis for the investigations conducted and reported in the subsequent chapters of this work.

## 2.2. Lacquer – the characteristic constituent

The characteristic and usually major constituent of East Asian lacquer coatings are the saps of certain lacquer trees native to the region. The saps polymerise through an enzyme-catalysed reaction in the presence of oxygen and high relative humidity, forming a tough, cross-linked polymer film. A wide range of lacquer types are used for the decoration of artefacts, each type varying slightly in its chemical constituents depending on the country of origin. The native lacquer originating from Japan, Korea and China derives from the tree *Toxicodendron vernicifluum* (Stokes) F.A. Barkley (previously known as *Rhus vernicifera* D.C. or *Rhus verniciflua* Stokes) of the family *Anacardiaceae* (Garner 1963; Kumanotani 1995; Langhals et al. 2005). It is generally known as *urushi* in Japanese and as *qi* in Chinese. Lacquers from other tree species and thus with different chemical composition exist in countries such as Vietnam and Myanmar (e.g. discussed in detail by Mills and White 1999, p. 118; Golloch and Sein 2004; Lu et al. 2006; Qin et al. 1996; Honda et al. 2008; Niimura 2009). Although countries like Japan have been growing and tapping their own lacquer trees for centuries, lacquer from different species has also sometimes been imported and added to their native *urushi* (Honda et al. 2010; Heginbotham and Schilling 2011). Hence, this makes it hard to know the exact composition of any lacquer coating applied on an object without using chemical analysis.

As for most of the present work the exact chemical nature of the lacquer is of no particular relevance to the subject of study, no distinctions is made between the various lacquer types. They are collectively referred to as ‘East Asian lacquer’ or simply ‘lacquer’ throughout this thesis. However, in the experimental chapters of this thesis the term *urushi* is used, where it specifically denotes the sap of the tree *Toxicodendron vernicifluum*. This sap contains the phenolic lipid urushiol, a 3-substituted catechol derivative with chains of 15 carbon atoms and up to three double bonds (Kumanotani 1976; Kamiya and Miyakoshi 2000). In Section 3.4.1 this compound is referred to when identified by chemical analysis, whilst in Chapters 6 and 7 *urushi* denotes fresh, liquid lacquer purchased in Japan as “Chinese raw *urushi*”.

## 2.3. Complexity of layer structures

Generally, East Asian lacquer coatings are complex multilayered structures. They are built up with one or more foundation layers applied to a substrate – most commonly wood – which consist of mineral filler particles bound by lacquer or some other polymeric matrix (binder). In high quality lacquer coatings the ratio of lacquer binder to filler particles usually increases with increasing number of layers. Sometimes, these foundations contain organic fibres, or incorporate sheets of textile or paper. The foundation layers are followed by a varying number of lacquer top coats that finally produce the highly polished surface typical of East

Asian lacquer ware (for example Quin 1882/1995; Stephan 1927, pp. 30-42; Heckmann and Dei Negri 2002, pp. 78-93; NRICPT 2008, Chapter 2). The complex layer structure is required to achieve perfectly smooth surfaces that can be polished to a mirror-like appearance. It further helps to distribute stresses more evenly between substrate and coating, and also within the coating structure itself. Incorrect choice of materials would result in physical damage to composite materials, leading to failure at the interface between adjacent layers (adhesive failure) or within a layer, i.e. cohesively (e.g. Heckmann and Dei Negri 2002, pp. 82, 176).

## 2.4. The problem of stresses

Stresses occur in all multilayered structures (composite materials) due to the restraint of dimensional changes of individual layers (e.g. Mecklenburg et al. 1998). These are commonly induced during manufacture or service by changing relative humidity (RH) and temperature. Stresses can be evenly distributed within these structures if all individual layers show similar elastic behaviour and adhere strongly to one another. However, in practice this is rarely the case owing to the varied nature and the different mechanical properties of their components. In such cases, stress concentrations occur at or near interfaces and within flaws of individual components. If the stress reaches a critical level, then the material will fail. In composite materials, the interlaminar plane, parallel to the layered structure, is most prone to failure. Therefore, the most common failure mode in composites is delamination – a phenomenon frequently observed by conservators working with decorative coatings on artefacts and other decorative objects.

Exactly when the critical stress level in such structures is reached is largely governed by the toughness of the material (i.e. the amount of energy that a material can absorb before fracturing). This property varies greatly for the individual components of East Asian lacquer coatings and their substrates.

## 2.5. Wood substrates in composite structures

In East Asian lacquer objects, the most common substrate upon which the multilayered coatings are applied is wood. Layered systems including wood are subject to significant stress development during manufacture and service. Not only is wood a hygroscopic material, it is also orthotropic; in that its mechanical properties change with respect to the three mutually perpendicular axes of grain direction. Wood is dimensionally stable when it contains more moisture than necessary to saturate its fibres. However, below the fibre saturation point, wood changes its dimensions with loss or uptake of water. Wood is most responsive when cut in the tangential direction, where it can show changes in dimensions

## 2. *The Multilayered Structure of East Asian Lacquer Coatings*

approximately twice as great as in the radial direction over a broad spectrum of moisture contents, i.e. from fibre saturation point to air-dry condition. In the radial direction, wood commonly shrinks between about 2 % and 4 %, whilst in the longitudinal direction it merely reduces its dimensions by approximately 0.1 % to 0.3 % (Panshin and de Zeeuw 1980, p. 209). Variations in RH between 30 % and 70 % induce the least dimensional changes in wood, however, outside this range, the structural effects are large (Mecklenburg et al. 1998, p. 467). In comparison to coating materials, dimensional changes of wood induced by varying RH can be large and thus cause significant stresses on the coating.

In contrast to wood, the mechanical properties of lacquer films and other polymeric layers are naturally isotropic. In changing RH conditions, any coating materials applied to wood will therefore be exposed to high stresses in the direction across the wood grain, whilst being fully restrained in the longitudinal direction of the wood grain (Mecklenburg 2007). A typical damage pattern showing the effect of across-grain compressive stresses is the cracking of lacquer coatings in the direction parallel to the wood grain, as pointed out by Toishi and Washizuka (1987, pp. 164-65) and Webb (2000, p. 62).

Whether or not East Asian lacquer coating structures can compensate for, or withstand, the stresses induced by the dimensional changes of the wood substrates generally depends on their mechanical characteristics. These mechanical properties are directly related to the composition of the materials involved and the quality of the layer structure.

## 2.6. The quality of lacquer coating structures

### 2.6.1. Mechanical strength of lacquer composites

East Asian lacquer is known for being a strong material. Lacquer films have a glass transition temperature well above room temperature ( $> 80\text{ }^{\circ}\text{C}$ ), they show no abrupt changes in mechanical properties at room temperature and are much less brittle than many synthetic resins (Kuwata et al. 1961; Obataya et al. 2001; Obataya et al. 2002). Lacquer also displays good cohesion and strong adhesion between individual layers (Nishiura 1984). However, cohesion and adhesion of the composite foundation layers in complex lacquer coating structures depend on the amount and nature of the binder enclosing the filler particles and thus may vary considerably.

Foundation layers that incorporate a high volume fraction of lacquer – that is a high binder to pigment ratio – can be considered as reinforced lacquer polymers and their adhesion to the wood substrate and adjacent (non-reinforced) lacquer layers will be strong and durable, reducing the risk of delamination (Nishiura 1984; Webb 2000, p. 60). Foundations with a very low volume fraction of binder will account for layers with comparatively low mechanical strength, even if the



## 2.6. The quality of lacquer coating structures

binder is lacquer. In isolation, such a layer generally does not induce high stresses itself and thus would be less prone to cracking and flaking than a mixture of higher binder to pigment ratio (Nishiura 1984, Michalski 1991a). However, when incorporated into a layer structure, its toughness will be too low to withstand the stresses imposed by the wood and coating, leading to failure. Foundation layers with lower adhesive and cohesive strength properties are also produced when more brittle surrogate binders are used.

### 2.6.2. Effect of surrogate binders

Lacquer has always been very expensive and was therefore often used sparingly in objects of lower quality or replaced entirely by cheaper binders for unseen layers (Nishikawa 1993). This was particularly the case since the seventeenth century, when East Asian lacquer objects became popular in the West and were specifically produced to satisfy the demands of foreign merchants and collectors. In Japanese export ware and Chinese products, common surrogates included animal glue, starch, persimmon juice (a polysaccharide) or pigs' blood and ox gall (Bonanni 1720/2009, p. 23; Kato 2000; Kitamura 2000; Piert-Borgers 2000; Webb 2000, p. 27). Lacquer was also often adulterated with additives, such as oils or even *funori* (an extract from red seaweed) and finely grated sweet potato (Bonanni 1720/2009, pp. 23-26; Stephan 1927; Quin 1882/1995, p. 13; Lu et al. 2006; NRICPT 2008, p. 20). Additives and surrogates in lacquer coatings are known to have significant influence on the coating structure.

Foundations that do not contain a high amount of lacquer, or those introducing less tough binders, such as proteins (e.g. animal glue or pigs' blood) or polysaccharides, will weaken the coating structure. Protein-bound gesso-type foundations are known to be very susceptible to failure as they break after very little deformation (Mecklenburg 2007, p. 19). In comparison, lacquer and wood are much tougher materials, i.e. they can be strained more before failure is induced. Unsurprisingly therefore, Kitamura (2000) describes the "spreading exfoliation" – that is flaking – on objects with simplified foundation layers containing animal glue or persimmon tannin blended with charcoal, calcium carbonate or clay powder, and predicts great problems for their future conservation. Extensive delamination and flaking on Chinese lacquered panels and screens involving protein-bound foundation layers has also been reported by other authors (Breu and Miklin-Kniefacz 1995; Wu and Wu 1995; Miklin-Kniefacz 1999; Breidenstein 2000).

### 2.6.3. Types of lacquer ware

Material choice during manufacture and build-up of the multilayered structure are often strongly influenced by the provenance of the object and its original

## 2. *The Multilayered Structure of East Asian Lacquer Coatings*

designation. For this reason, lacquer objects are commonly divided into two broad categories, which describe their quality:

**High quality domestic ware** Lacquer objects manufactured to the highest standards (particularly in Japan) are characterised by their very complex composite structure, which is thoroughly built up with a relatively high content of East Asian lacquer present in every layer of the coating. Foundation layers would typically be applied in several stages and generally contain a high amount of lacquer binder, which often increases with every subsequent foundation layer applied (e.g. Heckmann and Dei Negri 2002, p. 82). These layers normally also incorporate textile or paper layers that are well adhered with lacquer. These serve as buffering layers to evenly distribute stresses that may occur in the composite structure, thus preventing stress concentration and subsequent damage to the coating (Matsumoto and Kitamura 2008; NRICPT 2008, p. 59). Finally, the upper layers of lacquer coating structures consist of pure East Asian lacquer. It generally applies that the more layers are present, the higher the quality of the final product.

### **Lower quality ('cheap') domestic ware and objects made for export**

A second category of lacquer ware includes those objects manufactured for the domestic market for more 'every-day' use and those specifically made for export to Western countries (often referred to as 'export ware'). Apart from a few examples of early Japanese export ware originating from the first half of the 17th century (such as the Victoria and Albert Museum's Mazarin Chest), which were produced to exceptionally high quality, most other export and cheap domestic ware were generally either mass-produced or made under constraints of limited resources and time. On the whole, they are cheaper in production costs and consequently have a less thoroughly built up layer structure. Also, in the lower foundation layers which are invisible from the coating surface, the rather expensive lacquer is typically replaced with cheaper surrogate binders, such as animal glue, starch or persimmon juice (e.g. Kato 1988; Taguchi et al. 2001; ICCROM/Tobunken 2009; NRICPT 2009, pp. 34, 44, 95).

(For more detailed reading on export lacquer ware, consult for example Impey 1982, 1984, 2000a,b; Hutt 1998, 1999, 2000; Jorg 2000; Impey and Jorg 2005; Hidaka 2009; Rivers et al. 2011)

## 2.7. Effect of moisture on multilayered coatings

As mentioned earlier, varying humidity levels cause wood and any organic coating materials to change dimensions. Most significantly, they do so at different speeds and to different degrees, which increases the stresses within the layers and at their interfaces. Wood and protein binder (such as animal glue), for example,

## 2.7. Effect of moisture on multilayered coatings

take up moisture much faster than lacquer (Miura 2000). Nevertheless, eventually – given sufficient time – lacquer moves approximately the same amount as Japanese cypress wood (*hinoki*) in the radial direction (Bratasz et al. 2008). Lacquer with additives of animal glue, rice- or wheat starch are also extremely sensitive to moisture, much more so than pure lacquer films. These mixtures suffer significant volume increases during water absorption and development of severe shrinkage stresses during desiccation (Thieme 2001). Any textile layers included in the structure will behave differently with the warp and weft and will shrink in high humidity (Berger and Russell 1988; Mecklenburg and Tumosa 1991b), whilst all other organic materials swell under these circumstances. In contrast, composite layers such as protein binder mixed with clay powder generally show comparatively small dimensional response, similar to that of gesso layers of Western paintings (Mecklenburg 2007, pp. 16-19).

Despite being hygroscopic, intact lacquer films effectively act as a barrier for moisture diffusion and sorption in a coating. The rate of water sorption is dependent on the layer thickness of the undamaged lacquer film: the thicker the layer, the slower the process (e.g. Ogawa and Kamei 2000). Lacquer layers therefore significantly slow down moisture uptake and loss in both the foundation layers and wooden substrates during short-term exposure to varying RH. Even extreme changes in RH will not necessarily be detrimental to the structure if they occur for a very short term. Initiation of failure in foundation layers will indeed require rather drastic and/or recurring changes in environmental conditions (for detailed discussions see also Berger and Russell 1986; Berger and Russell 1994; Schaible 1990). Exposure to liquid water is the most extreme case, as water uptake occurs much faster than moisture absorption from the surrounding air.

The effect of water sorption of undamaged, lacquer coatings with lacquer-bound foundation layers on convex wooden substrates has been investigated in detail by Ogawa and Kamei (2000). Using a theoretical model (finite element analysis), they found that during exposure to both 100 % and 0 % RH the tensile-, compressive- and peeling stresses in the coating and at its interface to the substrate were high enough to potentially cause fracture and delamination failure of the coating. However, during practical tests, no failure at all was actually observed in the lacquer coating, suggesting that stress relaxation played a significant role and can be very effective in preventing damage (for a detailed discussion see Ogawa and Kamei 2000).

In already damaged lacquer coatings, however, wood substrates and very hygroscopic foundations containing surrogate binders are affected more quickly by RH changes. Humidity changes are highly likely to induce stresses large enough to cause failure in those layers of the coating that can endure the smallest strain to failure, i.e. the least deformation before breakage.

## 2.8. Implications

Having introduced the basic constituents and layer structures of typical East Asian lacquer coatings, it has become clear that the mechanical behaviour of such multilayered structures is rather complex and difficult to estimate. Therefore, it is now important to identify the common types of failure these coatings experience whilst the coated object is in service, on display and in storage. The following chapter hence investigates in more detail the causes and effects of failing lacquer coatings which are frequently encountered in Western collections. It clarifies whether certain lacquer coating types are typically prone to developing delamination and flaking.

## 3. Review of Damage to East Asian Lacquer Objects

### 3.1. Introduction

It is generally understood that damage to lacquer coatings is caused by unfavourable environmental conditions, such as exposure to ultraviolet radiation (UV) and visible light (VIS), and also frequent or extreme fluctuations of relative humidity (RH) and temperature (see for instance Miura and Ogawa 1999; Miura 2000; Webb 2000, pp. 54-60). This, however, does not explain why some objects are more severely affected than others when exposed to similar environments. Conclusions drawn by Japanese lacquer specialists (Kitamura 1995) and by other reports suggest that quality differences in the lacquer coatings also play a major role in their deterioration behaviour. However, it appears that these findings are mostly based on the examination of individual objects from diverse international collections that have suffered severe deterioration due to rather varied environmental influences and storage conditions (e.g. Chase 1988; Heckmann 1995; Miklin-Kniefacz 1999; Kitamura 2000; Breidenstein 2000). This poses the question as to whether the most severely damaged lacquer objects within a single collection are generally those of lower quality and/or whether specific types of lacquer ware are principally more prone to severe coating damage. A small survey of the collection of Japanese and Chinese lacquer objects at the Victoria and Albert Museum (V&A) was undertaken to identify structural and compositional similarities between the damaged artefacts, which would explain the failure mechanisms involved in the development of lifting and flaking coatings. The aim was to verify current perceptions of failure causes and to assess whether other influences might also play an important role. The following chapter will report the methodology and results of this research.

### 3.2. Object choice

To investigate the causes of severe delamination and flaking, approximately 300 lacquer objects in the V&A stores were viewed with respect to the physical condition of their coatings. Whilst a number of objects showed some coating damage, the objects that displayed the most severe cracking, delamination and flaking

### 3. Review of Damage to East Asian Lacquer Objects



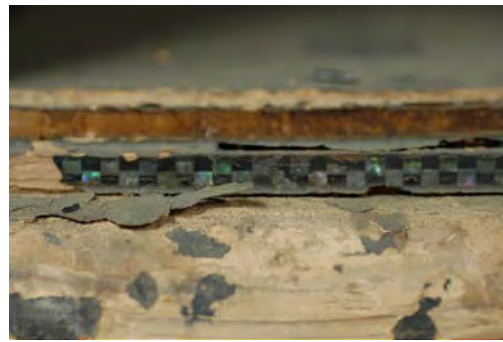
(a) Round box (W.332-1921). Extensive coating losses of the lacquer coating expose the wood substrate. (6.5 x 14.5 cm).



(b) Curved box (Lost.Exp.8). Lifting coating near areas of lost substrate parts, showing some failure in paper layer.



(c) Detail (5 cm length) of palanquin (48-1874). Extensive coating losses due to failure at the wood substrate/textile and textile/foundation layer interfaces.



(d) Corner cabinet (493-1872) detail (c. 7 cm length). Severe lifting and losses of the mother-of-pearl/lacquer layer, exposing the foundation and wood substrate.



(e) Detail (image length 9 cm) of a cabinet stand (303-1876), showing faintly white accretions from water stains on the surface.



(f) Detail of Coromandel cabinet (Private Collection). Losses in the upper coating expose the coarse, fibrous foundation.

Figure 3.1.: Examples of extensive coating damage on East Asian lacquer objects, displaying delaminating, blistering, cupping and tenting lacquer coatings with varying degrees of losses. (Photographs by N. Schellmann, (a)-(e) courtesy of the V&A).

were targeted for further investigation. The progressive failure of these decorative coatings rendered these objects the most in danger of increasing damage, and thus the most in need of conservation to secure their preservation for the future. Examples of this type of damage are shown in Figs. 3.1 a–e. Close examination with the naked eye and a stereo microscope was undertaken to identify objects where the damage had been caused by inherent structural weakness. Objects with the following criteria were excluded:






- pressure marks in the surface of exposed parts (corners, edges, legs, lids etc.) and sharp edges along with small losses in otherwise well adhered lacquer coatings. These gave clear indications of impact induced damage.
- cracked lacquer surfaces showing no delamination or losses due to progressive flaking.
- extensive previous conservation or restoration treatment with no obvious untreated surfaces.

From the V&A collection, nine objects with progressively delaminating and severely flaking coatings apparently caused by inherent structural weaknesses were selected to be studied in more detail (Figs. 3.1 a–e). One privately owned piece of furniture was further included in this group as it showed very similar damage to that of the V&A lacquer objects and was available for analysis (Fig. 3.1f). This object was a lacquer cabinet made from Chinese lacquer panels decorated in the carved lacquer technique known as ‘Coromandel’ ware. The doors of the cabinet were made from former screen panels thought to originate from the 18th century, possibly later. The cabinet itself appeared to be a later assembly with added parts, made for the Western market.

A complete list of the surveyed objects is presented in Table 3.1. Further details, such as object descriptions, appearance of damage and detail images are provided in Appendix D as a comprehensive survey report. Initial assessment of these selected objects based on stylistic features and their place of origin revealed that they bore some similarities: The Japanese objects were either produced for the Western market (frequently referred to as ‘export ware’), or were lower quality products destined for domestic use. They comprised cabinets, boxes, a palanquin and a shrine. Chinese screens were also included in the group of lacquer objects most affected by delamination and flaking. These, too, showed typical features of export-ware in their decoration (e.g. the four-fold screen), or were clearly not manufactured to a particularly high quality. This group of damaged lacquer objects thus confirmed that less prestigious types of lacquer ware deteriorate more dramatically than higher quality objects.






### 3. Review of Damage to East Asian Lacquer Objects

Table 3.1.: Lacquer objects from the V&A collection and a private owner displaying extensive coating damage, which were chosen for further investigation.

OBJECT	V&A No.	ORIGIN	TYPE	DIMENSIONS	IMAGE
Cabinet and stand	303-1876	Japan, late 19 <sup>th</sup> c.	'export ware'	76 x 59 x 38.5 cm  40 x 63.5 x 43.5 cm	
Corner cabinet	493-1872	Japan, late 19 <sup>th</sup> c.	'export ware'	122 x 76 x 33.5 cm	
Cabinet (with fans)	W.19-1969	Japan, 19 <sup>th</sup> c., second half	'export ware'	175 x 145 x 63 cm	
Round box	W.332-1921	Japan, early 18 <sup>th</sup> c.	'cheap' domestic	6.5 x 14.5 (diameter) cm	
Curved box	LOST.EXP.8	Japan, late 19 <sup>th</sup> c.	'cheap' domestic	6.5 x 59.5 x 20 cm	



### 3.2. Object choice

OBJECT	V&A No.	ORIGIN	TYPE	DIMENSIONS	IMAGE
Palanquin	48-1874	Japan, 19 <sup>th</sup> c., second half	'cheap' domestic	125 x 139 x 93 cm	
Shrine	W.1-1913	Japan, late 19 <sup>th</sup> c.	archi- tectural/ 'cheap' domestic	c. 230 x 139 x 107.5 cm	
Five-fold screen	W.9-1943	China, 19 <sup>th</sup> c.	Chinese screen	230 x 62 x 2.7 cm (per each panel)	(detail) 
Four-fold screen	W.25-1939	China, 18th c. (possibly later)	Chinese screen/ 'export ware'	181 x 54 3.7 cm (per each panel)	(detail) 
Coromandel cabinet (made from screen panels)	Private Collection	China, 18 <sup>th</sup> c. (possibly later), adapted	Chinese screen/ 'Coro- mandel lacquer ware'	187.5 x 135.4 x 56.0 cm	

Photograph of Shrine taken by the Photographic Studio of the V&A, reproduced with kind permission, © Victoria and Albert Museum, London. All other images taken by N. Schellmann, courtesy of the V&A. Image of the Coromandel cabinet courtesy of the private owner.

### 3.3. Analysis of coating structures and components – Materials and methods

In order to verify the specific cause for the severe coating failure in the ten objects, their lacquer coatings were optically, chemically and spectroscopically analysed. It was vital to characterise each complex layer structure in its physical form for precisely locating failure zones. Furthermore, determination of material composition provided a possible explanation for the causes of damage. Particular emphasis was placed on the identification of binding media, as low lacquer content and cheaper binders, such as proteins and polysaccharides, were expected to be involved in the failure mechanisms.

#### 3.3.1. Optical microscopy and staining

Samples of the entire coating, ideally including the wood substrate, were chosen from object parts that had not been subjected to previous local consolidation or restoration treatment. Small samples of approximately 1 mm<sup>2</sup> were taken with a scalpel from areas of severe flaking next to losses in the coating. Additional specimens were sampled from flakes that had fallen off the substrate, but which could be traced back to their approximate original position. The multilayered samples were mounted in clear polyester casting resin (Tiranti), and cross section surfaces were polished using dry emery paper (# 360 – # 800) and micro-mesh abrasive cloth (up to # 12 000, Kremer).

Cross sections were analysed with an optical microscope under visible (VIS) and blue light (Figs 3.2a-3.3). Blue light was chosen over ultra violet irradiation due to the availability of appropriate filter cubes and because lacquer has a distinct fluorescence in this wavelength range. VIS analysis was undertaken with an Aristomet microscope in dark field illumination, and analysis with excitation in the blue range was performed in bright field illumination with a Leitz Laborlux 12 ME microscope, fitted with a HBO 50W super pressure mercury light source and an I3 filter cube.

The stratigraphy of the multilayered coating samples was identified and documented photographically as well as in a schematic drawing, summarising its characteristic features gained from several cross section specimens. A full summary of the results is presented in Appendix D for every object included in the survey. Some materials of the individual layers (such as wood, paper, mineral pigment and pure lacquer layers) were ascertained visually, if their characteristics could be unambiguously established due to specific optical characteristics under VIS and blue light. However, most binding media mixed with high amounts of pigment, such as in foundation layers, had to be examined using additional analytical techniques.

## Visual identification of binder types with blue light

Aged bulk lacquer can be detected under irradiation in the blue range due to its distinct caramel-brown to yellow-ochre coloured fluorescence. Personal experience had shown that relatively freshly prepared lacquer samples do not fluoresce, unlike aged samples. The fluorescence appears to increase with increasing ageing and is particularly pronounced in lacquer layers that were exposed to light. These findings were recently confirmed and discussed in detail in a publication by Webb (2011). Examples of typical lacquer fluorescence under blue light are presented in Figure 3.2. The presence of lacquer in these samples was verified by Fourier-transform infrared spectroscopy (FTIR) and pyrolysis-gas chromatography/mass spectrometry (PyGC/MS). Details of these analyses will be reported in Section 3.3.2 of this chapter.

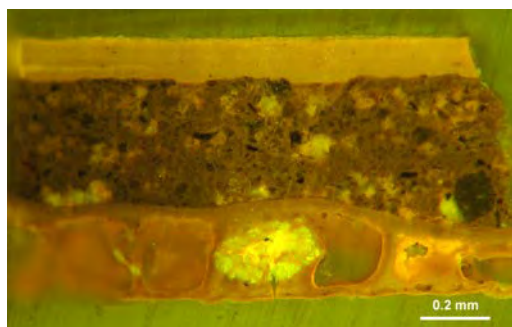
In this study, comparison with reference samples of Japanese and Chinese lacquers of known origin (pure and partly mixed with additives, such as oils and fillers), further suggested that severely photodegraded lacquer and lacquer matrix containing oil show up in distinctly bright yellow fluorescence (see Fig. 3.2b). This appearance contrasts with the caramel-brown to yellow-ochre fluorescence observed in bulk aged lacquer that was more protected from light and did not contain any significant oil additive (Fig. 3.2a, also see other cross-sections in Appendix D for further examples). The identification of lacquer by means of fluorescent microscopy is however limited: if the lacquer is mixed with a high concentration of filler or pigment, it cannot usually be visually identified with sufficient confidence.

## Histochemical staining

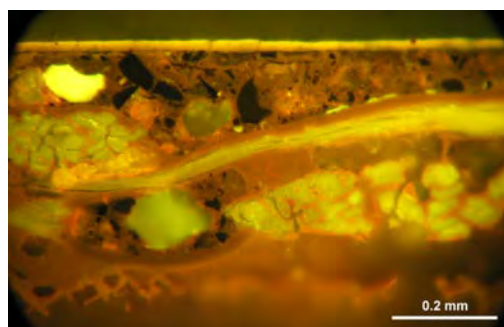
Once fully polymerised, lacquer does not contain functional groups that are characteristic for usual binding media, and hence there are no known stains that have a chemical affinity to this material in solid state. However, other binding media groups and materials which may be present in the layer structure of East Asian lacquer coatings can indeed be identified with staining methods. In conservation, staining of cross-section specimens is a popular identification method for binding media in multilayered composite structures (such as paintings or other decorative coatings on objects). The great advantage of this method is that it also provides information on the spatial distribution of the binder within the sample. Furthermore, staining methods are mostly cheap and relatively easy to conduct even in rather modestly-equipped work environments.

Different types of histochemical staining methods are available, requiring a varying degree of specialist experience and equipment. The simplest method is that of exposing cross section specimens to histological stains. Ostwald (1936), Plesters (1956), Johnson and Packard (1971), Martin (1977) and Schramm and Hering

### 3. Review of Damage to East Asian Lacquer Objects



(a) Chinese cabinet (V&A F.E.7-1973). Caramel-brown to yellow-ochre coloured fluorescence of lacquer. The structure consists of several lacquer top coats, a foundation layer of lacquer mixed with pigment, and a textile layer adhered with lacquer on the wood substrate (latter not shown). (Image length equals 1.49 mm.)



(b) Four-fold screen (V&A W.25-1939). Varying fluorescence of lacquer. Photodegraded (oxidised) or possibly oil-containing top lacquer coating (bright yellow), lacquer-bound foundation with coarse pigment, a textile layer adhered with lacquer (caramel-brown), lacquer priming and the wood substrate. (Image length equals 0.95 mm.)

Figure 3.2.: Cross-sections of lacquer coatings under blue light, showing fluorescence of the layer structures.

(1988) discussed these for use on artist materials. Examination of the staining results can be undertaken with an optical microscope under incident visible light. Staining with fluorochromes is an alternative technique (Wolbers and Landrey 1987; Derrick et al. 1994; Schaefer 1997), but this requires analysis by UV-fluorescence microscopy and the availability of specific filter cubes to enable excitation in the range required for the respective stains. Advantages and disadvantages regarding the staining methods are discussed for example by Matteini and Moles (1990, pp. 52–56) and Nöth (2005, pp. 17-24).

To date, the use of histological stains for the identification of binding media in export-type lacquer has not been investigated systematically. As this method would be very convenient for use on multilayered East Asian lacquer coatings – provided it worked reliably – it was decided to test the scope of this technique in this study. Preliminary tests were conducted with a variety of histological stains, which suggested their general potential to visually mark the respective binder types. Staining is generally performed on embedded samples that are prepared either in thick cross sections or thin (microtomed) sections. Suitability of the respective cross-section type, embedding techniques and preparation methods have been discussed in detail by Tsang and Cunningham (1991), Derrick et al. (1994), Buder and Wülfert (1997) and Khandekar (2003). In this study, thick sections were used for ease of preparation and due to time limitations. The preliminary tests had shown that thick sections were generally suitable for staining and gave sufficiently clear staining results on light coloured sample material.

### 3.3. Analysis of coating structures and components – Materials and methods

**Materials** For identifying proteinaceous media the diazo dye Amido Black 10B (Colour Index C.I. 20470) was used in a formulation and procedure introduced by Martin (1977). Amido Black solution denoted as AB2 by Martin proved to be a superior stain for proteins than other preparations of Amido Black 10B or the alternative protein stain Fast Green (C.I. 42053). It rendered the stained protein binder in reference samples in a darker colour which was more clearly visible under the microscope. This was particularly significant in darker coloured layers (Fig. 3.3c), where positive AB2 staining appeared to be more discernible. Despite personal experience suggesting that Ponceau S (C.I. 27195) generally works very well for identifying proteins, this stain was abandoned during the pre-testing stage. It caused problems on many foundation layers that naturally had a reddish appearance and that only contained a lower concentration of protein. The red dye made it difficult to visually distinguish any subtle, positive staining results from the reddish filler particles. Also, Ponceau S stains calcium carbonate due to acid-base reaction and hence erroneously gives positive staining results for any chalk-containing foundation layers (Herm 2011). Starch content in the cross-sections was identified with iodine potassium-iodide (Lugol’s solution), a stain that very reliably colours starch-based compounds in deep blue (e.g. Chayen and Bitensky 1991, p. 110). Oil-containing matrix was stained with the lipid-soluble dye Sudan Black B (C.I. 26150) following procedures published by Schramm and Hering (1988, pp. 205, 214-215). Sudan Black B stains almost all types of lipid compounds (Chayen and Bitensky 1991, p. 113) and may therefore not only identify drying oils but also other fatty components of the layer. Nile Blue sulphate (C.I. 51180), a compound staining both proteins and oils (Schramm and Hering 1988, p. 218), was added to the test procedure, as it first appeared that Sudan Black B might give ambiguous results in porous layers. In some cases it was suspected that Sudan Black stain may have merely penetrated into the pores of some layers, rather than actually staining lipid media. It was therefore hoped that Nile Blue sulphate would provide additional information on the oil content, and might also give further confirmation on protein content in the cross-section. Control samples had shown that Nile Blue sulphate stained over 10 year-old Japanese hide glue in foundation clearly in a very strong blue colour (Fig. 3.4c).

Table 3.3 summarises the methods for the identification of the individual binders. Staining was undertaken in the following order:

1. staining for proteins with Amido Black 10B,
2. staining for starch with Lugol’s solution,
3. staining for protein and oils with Nile Blue sulphate, and
4. staining for drying oil with Sudan Black B.

Before every subsequent exposure to stain, the cross-sections were very lightly re-polished and pre-soaked in the respective solvent that was used for the staining solution. The only exception was Lugol’s solution which was applied on the sample without pre-soaking. The full details of the staining assay including the solvents used for pre-soaking are given in Appendix A.

### 3. Review of Damage to East Asian Lacquer Objects

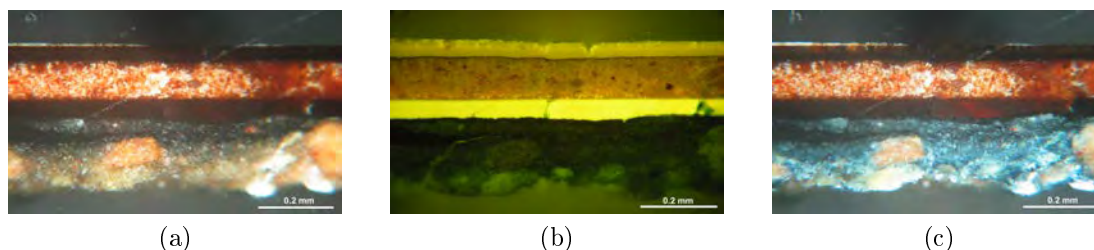


Figure 3.3.: Round box (V&A W.332-1921): cross-section of coating. (a) In VIS showing two lower foundation layers, and an upper foundation layer sandwiched between two lacquer layers; (b) in blue light: the lower lacquer layer fluoresces in a bright yellow colour suggesting some oil additive; the upper lacquer layer is photo-degraded; (c) in VIS: positive staining of protein with AB2 solution in the lower foundation layers. (Image length equals 0.69 mm.)

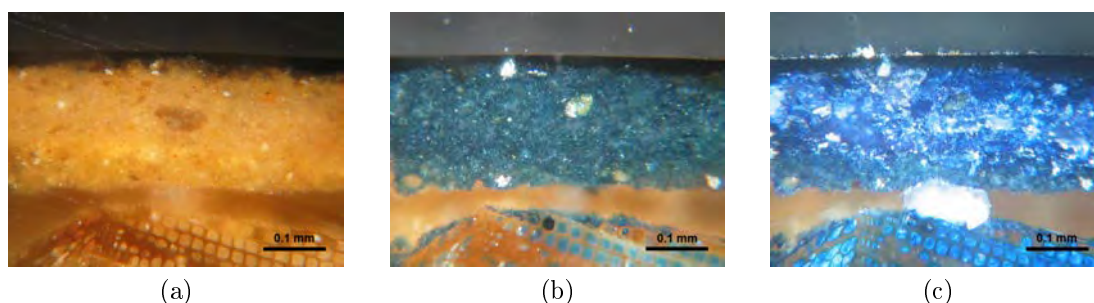


Figure 3.4.: Export lacquer reference sample: cross-section of the coating structure in VIS irradiation. (a) Top lacquer coat with foundation made from hide glue and Japanese clay powder on Japanese cypress wood substrate; (b) as (a) stained with AB2 solution. The hide glue-bound foundation is distinctly stained in blue-black colour; (c) as (a) after staining with Nile Blue sulphate solution. The glue-bound foundation stained in a distinct deep-blue colour. (Image length equals 0.55 mm)

### 3.3. Analysis of coating structures and components – Materials and methods

Table 3.3.: Choice of identification methods for different binding media types.

BINDING MEDIUM		ID METHOD	STAIN/COMMENT	REFERENCE
Protein	bulk and foundation (binder with mineral filler)	Amido Black 10B (AB2) stain	1g Amido Black 10B + 450 ml 1 N acetic acid + 450 ml 0.1 M aqueous sodium acetate solution + 100 ml glycerine	Martin (1977)
	foundation (binder with mineral filler)	NileBlue sulphate stain	50 ml concentrated aqueous solution of Nile Blue + 5 ml sulphuric acid (0.5%) (boiled and filtered)	Schramm and Hering (1988, p.218)
Starch	bulk and foundation (binder with mineral filler)	Iodine potassium-iodide (Lugol's solution)	100 ml distilled water + 2.5 g iodine (I <sub>2</sub> ) + 1.7 g potassium iodide (KI)	Schramm and Hering (1988, p.205); Chayen and Bitensky (1991, p. 110)
Oil	bulk	Sudan Black B stain	Sudan Black B saturated in isopropanol	Schramm and Hering (1988, p.205)
East Asian lacquer	bulk (aged)	blue light irradiation	caramel-brown to yellow-ochre fluorescence	Webb (2011)
	bulk (severely photo-degraded/ highly oxidised or mixed with oil)	blue light irradiation	bright yellow fluorescence	Schellmann (2011), Webb (2011)
All	foundation and bulk	FTIR		Simon et al. (2001), Heginbotham et al. (2008)
		PyGC/MS		Heginbotham et al. (2008), Frade et al. (2009)

### 3. Review of Damage to East Asian Lacquer Objects

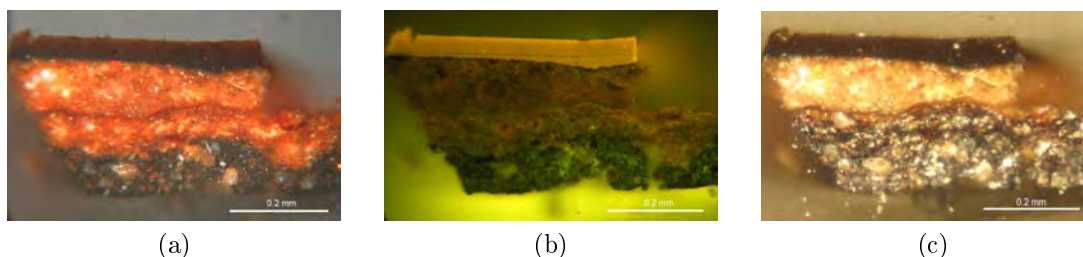


Figure 3.5.: Cabinet stand (V&A 303-1876): cross-section of coating. (a) In VIS showing a coarse dark layer and two fine reddish foundation layers below the top lacquer coating; (b) in blue light: three foundation layers and two lacquer coats are clearly distinguished by their fluorescence; (c) in VIS and stained with Lugol's solution clearly indicating starch content. (Image length equivalent to 0.7 mm).

All the chosen stains appeared to be efficient in marking the respective media (if present) in the comparatively light-coloured foundation layers of the samples. An example for the successful staining of starch in a reddish foundation layer is presented in Figure 3.5. Even though staining is generally not recommended for dark-coloured materials, it was shown that in some layers that appeared very dark under VIS irradiation, positive staining results were nevertheless detectable. If these dark-coloured layers fluoresced under blue light before staining, a positive staining result of black or blue, non-fluorescent stains could be suggested or even determined in some cases by a darkened appearance of these layers under blue light after staining (Fig. 3.6). However, this method was ineffective for previously non-fluorescent layers, and binding media of that kind had to be analysed using other techniques.

As mentioned earlier, staining for oils with SudanBlack B at first seemed to be problematic. The stain appeared to give poor or ambiguous results when used for staining very porous foundation layers, as it seemed to penetrate too far into the layer to be rinsed off sufficiently. One option to avoid this penetration would have been to use thin sections for staining rather than thick cross-sections. However, due to time constraints and other limitations of using thin sections this alternative could not be realised in this study. It was therefore aimed to confirm the staining results with other analytical methods, that are capable of identifying ideally all organic binding media types that may be present in multilayered East Asian lacquer coatings.

#### 3.3.2. FTIR and PyGC/MS analysis

In a number of coating layers the staining methods had given sufficiently clear results for the presence of binding media. Despite this, it was apparent that some layers could not be identified at all or only with insufficient confidence us-



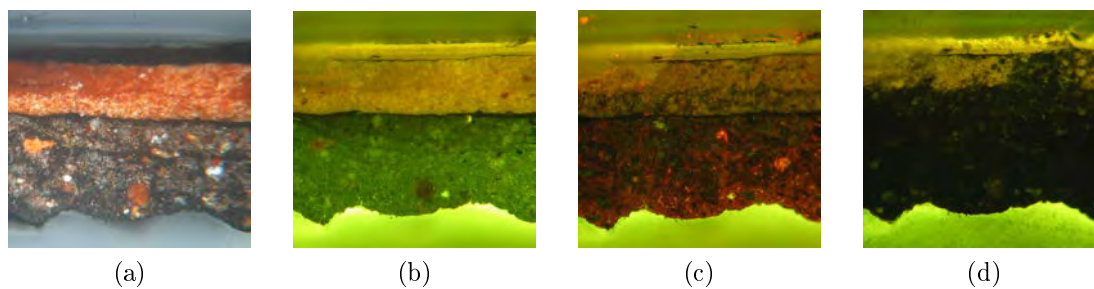


Figure 3.6.: Palanquin (V&A 48-1874): cross-section of coating showing dark grey foundation, thin black-pigmented lacquer layer, reddish foundation in two layers, black layer and three lacquer top coats. (a) VIS, unstained; (b) blue light, unstained, showing dark foundation layer F1/F2 that fluoresces slightly; (c) blue light, stained with Nile Blue sulphate, showing darkened appearance and some red fluorescence of both the dark-grey and lower reddish foundation layers F3; and (d) blue light, stained with Sudan Black B, clearly revealing the black staining of the lower reddish foundation layer F3. (Image length equals 0.7 mm each).

ing staining and fluorescence microscopy. In particular, some doubt remained about the reliability of the staining for oil with Sudan Black. To clarify the accuracy of the staining results and to fill in the missing data, further analytical methods were employed. These were chosen on the basis of their capability of identifying not only organic components of common binding media, but also on their suitability to detect those contained in East Asian lacquer coatings. Only few techniques qualify for this analysis, due to the highly crosslinked nature of the lacquer polymer, which renders lacquer insoluble in most solvents. Therefore, analytical methods that require the test sample to be in a liquid state are unsuitable. Analytical techniques that have been successfully used on lacquer-containing materials include Fourier-transform infrared spectroscopy (e.g. Derrick et al. 1988; Jin et al. 2000; Simon et al. 2001), pyrolysis-gas chromatography/mass spectrometry (e.g. Niimura et al. 1996; Niimura and Miyakoshi 2003, 2006; Lu et al. 2006; Frade et al. 2009; Niimura 2009; Honda et al. 2010; Pitthard et al. 2010) and nuclear magnetic resonance (NMR) spectroscopy (Lambert et al. 1991; Simon et al. 2001). For this study, the first two methods were chosen for further analysing the lacquer samples obtained from the surveyed objects.

## FTIR spectroscopy

Fourier-transform infrared spectroscopy (FTIR) is a relatively common method employed for the identification of organic and inorganic components in artist materials. It has successfully been used to identify organic compounds in paint samples (e.g. Meilunas et al. 1990; Derrick et al. 1999), including aged East Asian

### 3. Review of Damage to East Asian Lacquer Objects

lacquer (e.g. Derrick et al. 1988; Herm 1993; Simon et al. 2001; Ring 2001; Heginbotham et al. 2008). Nevertheless, FTIR is not the most ideal analysis method for identifying all organic compounds contained in lacquer composite samples. It has been pointed out that additives to lacquer are often difficult or impossible to identify with FTIR (Herm 1993; Ring 2001). Despite this limitation, FTIR microspectroscopy was used to confirm some of the results from cross section analysis and chemical staining in this study. The FTIR analysis was undertaken by Herm (2009a) at the laboratories of the Academy of Fine Arts Dresden. With this method it was hoped to identify the presence of lacquer or other binding media in the highly-filled polymer matrix of the foundation layers that could not be determined with the cross-section analysis.

Table 3.4.: Characteristic FTIR absorption band frequencies for compounds of lacquer coatings.

COMPOUND	ABSORPTION BAND WAVE NUMBERS [CM <sup>-1</sup> ]	REFERENCE
Protein	3350 (N-H stretching), 1650 (amide I), 1550 (amide II), 1450 (amide III)	Derrick et al. 1999, p.108
Carbohydrate	3300 (O-H), 1620 (intramolecular bound water/carboxyl group), 1080 (C-O)	Derrick et al. 1999, p.108
Oil	3020 (olefinic C=C-H band), 2926, 2855 (C-H stretching), 1750-1740 (carbonyl band of ester group), 1464, 1379, 725 (aliphatic C-H band), 1240, 1165, 1103 (C-O bands)	Derrick et al. 1999, p.103
<i>Urushi</i> lacquer	3400 (O-H), >3000 (C-H stretches from aromatic and vinyl hydrocarbons), 2926, 2885, 2850 (C-H stretching from alkyl groups), 1715-1695 (strong C=O stretch. This band broadens with increasing ageing and oxidation of the lacquer), 1625 (C=O), 1465-1430, 1407, 1165-1145, 1090-1050, 1033	Kenjo 1978; Derrick et al. 1988; Derrick et al. 1999, p.104 Jin et al. 2000; Simon et al. 2001; Kamiya et al. 2006; Niimura and Miyakoshi 2006

**Method and materials** Small samples were collected from areas of the objects where delamination and flaking of the coating had recently occurred. During sampling, a head-loupe was used for distinguishing between the individual layers. Scrapings were taken with a scalpel from foundation layers which had been determined by microscopic analysis as the failing layers. In the cases where loose flakes had fallen off the object's surface, samples were taken from this source. From the remaining objects, scrapings were sampled directly from damaged coating areas still attached to the object. A few micrograms ( $\mu\text{g}$ ) of each sample were placed

### 3.3. Analysis of coating structures and components – Materials and methods

on a diamond anvil cell (High Pressure Diamond Optics) using a tungsten needle and were analysed in transmission with a Bruker Hyperion 2000 IR microscope connected to a Bruker tensor 27 Fourier-Transform IR spectrometer. Measurement with the attenuated total reflection technique (ATR) was conducted on one cross-section sample embedded in polyester casting resin. These measurements were non-destructive and performed using a Bruker-ATR-objective (25x) and a Germanium-crystal. The measuring areas had a diameter of approximately 0.80 mm (Herm 2009a).

Characteristic transmission bands used for the identification of the compounds area are summarised in Table 3.4.

## Pyrolysis-gas chromatography/mass spectrometry

Pyrolysis-gas chromatography/mass spectrometry (PyGC/MS) appears to be most successful in identifying lacquer in solid state, discriminating even between the different lacquer types from different botanical origins (Niimura et al. 1996; Lu et al. 2006; Frade et al. 2009; Niimura 2009; Honda et al. 2010). Recent research undertaken at the Getty Conservation Institute and The J. Paul Getty Museum has developed an improved methodology for the sampling of lacquer coatings and the analysis of a variety of its organic components by PyGC/MS (Heginbotham et al. 2008; Heginbotham and Schilling 2011). With this methodology, many organic components of East Asian export-type lacquer coatings have since been successfully identified. A collaboration with the Getty Conservation Institute was initiated to enable the analysis of a selected number of coating layers from the surveyed V&A objects by this technique. The analysis was conducted by Schilling (2010a). With this additional analysis, a reliable double-check was possible on whether the previous two identification methods (cross-section microscopy including staining, and FTIR spectroscopy) had given reliable results and could be used with confidence.

**Method and materials** Samples for analysis were sourced from unused sample material previously collected for FTIR and cross-section analysis. The multilayered coating samples were separated layer-by-layer according to a procedure recommended by Heginbotham (2010). This included mounting the sample on a Perspex plate with cyanoacrylate adhesive (Loctite SuperGlue gel) with the top lacquer layer facing down. Then, each individual layer was removed with a steel scalpel under an optical microscope (Nikon SMZ-10A) at 15x magnification. Only the centre part of each layer was collected and placed between two glass-slides (one with depression) or in glass vials. This was to avoid collecting any material contaminated with particles from neighbouring layers. Before the consecutive layer was sampled, all remnants of the previous layer were fully removed with the use of a scalpel and a soft-haired brush.

### 3. Review of Damage to East Asian Lacquer Objects

For pyrolysis, a Frontier Laboratories PY-2020D double-shot pyrolyser system was used, with the pyrolysis interface maintained at 320 °C. The pyrolyser was interfaced to an Agilent Technologies 5975C inert MSD/7890A gas chromatograph/mass spectrometer. For separation, a J&W DB-5MS-UI capillary column was employed (30 m x 0.25 mm x 0.25 µm). By attaching the column to a Frontier Vent-Free adaptor, the effective column length was 40 m. The helium carrier gas was set to 1 ml/minute. The split injector was set to 320 °C with a split ratio of 50:1 and no solvent delay. The GC oven temperature was programmed to 40 °C for 2 minutes, then ramped to 320 °C at 6 °C/minute, followed by a 9 minute isothermal period. The MS transfer line was at 320 °C, the source at 230 °C, and the MS quad at 150 °C. The mass spectrometer was scanned from 10-600 amu at a rate of 2.59 scans per second. The electron multiplier was set to the auto-tune value. Samples were placed into a 50 µl stainless steel Eco-cup fitted with an Eco-stick, and three microlitres of a 25% methanolic solution of tetramethyl ammonium hydroxide (TMAH) were introduced for derivatisation. After three minutes, the cup was placed into the pyrolysis interface where it was purged with helium for three minutes. Samples were pyrolysed using a single-shot method at 550 °C for 6 seconds (Schilling 2010a). The marker compounds used to identify the different materials in the chromatograms are listed in Table 3.5.

Table 3.5.: Marker compounds used for identifying the different materials in the PyGC/MS chromatograms (Schilling 2010a).

MATERIAL	MARKER COMPOUND
Glue	Pyrrole (also methylated derivative) (He et al. 2007)
Blood	Pyrrole, cholesterol (also methylated derivatives)
Carbohydrate	Undetermined pyranose (as methylated derivative)
Drying oil	Azelaic acid (C <sub>9</sub> ), palmitic acid (C <sub>16</sub> ), stearic acid (C <sub>18</sub> ) (as methyl esters)
Lipid	Palmitic acid (C <sub>16</sub> ) and stearic acid (C <sub>18</sub> ), no alezaic acid (as methyl esters)
Persimmon juice	Trimethoxybenzene
Urushi	Dimethoxybenzene nonanoic acid methyl ester, pentadecylcatechol (as dimethoxy derivative), heptyl phenol (Chiavari and Mazzeo 1999; Schilling 2010b)
Thitsi	12-phenyldecyl catechol (as dimethoxybenzene derivative)
Colophony	7-methoxy-tetradecyloabietic acid methyl ester
Cedar oil or pitch	Cedrol, cedrene
Wood oil	Undetermined triterpenes
Gum Benzoin	Cinnamic acid (as methyl ester)
Camphor	Camphor, camphene

(C<sub>n</sub>) gives the number, *n*, of carbon atoms of the respective fatty acids.

## 3.4. Analysis results and discussion

### 3.4.1. Results of coating layer analysis

The materials and binders of the failing lacquer coatings were analysed in as much detail as possible, to characterise more clearly the complex layer structures of each surveyed object in their physical state and material composition. The following section will present the results determined by the survey and the binding media analysis, which help to identify the possible causes for the severe coating damage observed on the selected objects.

#### Macroscopic and microscopic layer structures

Table 3.6 summarises the coating layer structures of the individual objects as analysed using the optical microscope under VIS and blue light irradiation. The fields in the table highlighted in blue italics specify where failure in the coating structure had occurred.

The lower foundation layers were predominantly affected by failure in all coatings, despite the differences in their layer structure. No physical deterioration was apparent in the top coats or the upper fine reddish foundation layers, subject to a further foundation layer being present underneath. The only two exceptions were the corner cabinet and the five-fold screen, which both contained only one type of foundation in their layer structure.

Further analysis of the coating samples revealed that similar constituents could be identified in the failing layers, and particular attention was paid to the identification of the binding media of these layers.

#### Analysis of binding media

Table 3.7 summarises the results of the binding media analysis for all nine lacquer objects. The fields in the table highlighted in blue again identify the layers which had failed. Results were obtained from staining and optical microscopy as well as from FTIR microspectroscopy and PyGC/MS analysis. A detailed report of the analysis results can be found in Appendix D.

#### Top layers and fine upper foundation

Underneath the top East Asian lacquer layers, all objects except the four-fold screen and the Coromandel cabinet doors displayed a reddish foundation layer. In five of these objects, this foundation consisted of finely ground filler particles bound with lacquer, lipids and, in some cases, starch; in two (corner cabinet and

### 3. Review of Damage to East Asian Lacquer Objects

Table 3.6.: Coating layer structures of the lacquer objects that were subjected to analysis.

OBJECT	TOP COATS No.	FINE FOUND. No.	OTHER LAYER MATER.	COARSE FOUND. No.	BUFFERING LAYER MATERIAL	FOUND./ ADHESIVE No.	BUFFERING LAYER MATERIAL	SUBSTRATE MATERIAL
Cabinet stand	2-3	2	-	<i>1</i>	textile or paper	adhesive	-	softwood
Cabinet (on stand)	4	2	-	<i>1</i>	[paper]	-	-	softwood
Corner cabinet	4	<i>2</i>	-	-	[paper (large panels)]	-	-	softwood
Cabinet (with fans)	2	1	-	<i>2</i>	paper	<i>1</i>	<i>textile + adhesive</i>	wood
Round box	1	1	lacquer	<i>2</i>	[paper (base)]	-	-	hardwood
Curved box	2	2	lacquer	-	<i>paper</i>	-	-	softwood
Palanquin	3	2	-	<i>2</i>	textile	<i>adhesive</i>	-	softwood
Shrine	2	2	-	<i>2-3</i>	<i>[paper]</i>	<i>1-2</i>	-	softwood
Four-fold screen (panel f/b)	1	-	-	1	textile	lacquer	-	softwood
Five-fold screen (sides)	1	1	-	<i>1 (or more)</i>	<i>paper</i>	<i>adhesive</i>	-	softwood
Five-fold screen (panels)	3-5	<i>1</i>	-	-	<i>fibres, in binder matrix</i>	-	-	wood
Coromandel cabinet (doors)	1	-	-	<i>1(-3)</i>	plant fibres, in binder matrix	adhesive	-	softwood

'Found.': foundation; 'Mater.': material; 'No.': number of layers; 'f/b': front and back of screen panel, '-' indicates layer not present; '['] denotes presence of layer only in limited areas or on object parts with the location given in round brackets. The fields highlighted in *blue italics* mark the failing layers.

### 3.4. Analysis results and discussion

Table 3.7.: Results of the material and binding media analysis (lacquer- and foundation layers) shown in Table 3.6.

OBJECT	TOP COAT.	BINDER FINE FOUNDATION	BINDER COARSE FOUNDATION	BUFFER LAYER	BINDER / ADHESIVE	BUFF. LAYER
Cabinet stand	lac.	*starch + oil + little lacquer	* <i>starch + oil + lac. (t) + protein (t)</i>	textile / paper	*starch + lipids + camphor	–
Cabinet (on stand)	lac.	starch + lipids + little lacquer	* <i>lipids + protein</i>	[paper]	starch (?)	–
Corner cabinet	lac.	* <i>protein + lipids + lac. + starch (t) + colophony (t)</i>	–	[paper]	<i>[starch or protein] (?)</i>	–
Cabinet (fans)	lac.	lacquer	<i>protein (?) + oil (?)</i>	paper	* <i>oil + carboh. + protein (t) + lacquer (t)</i>	textile + <i>pro-tein (?)</i>
Round box	lac.	lac. + lipids	* <i>lipids + starch + protein</i>	–	* <i>starch + lipids + protein</i>	[paper]
Curved box	lac.	*oil + lac. + starch	–	<i>paper</i>	<i>starch</i>	–
Palanquin	lac.	*oil + starch + lac. + persimmon (t)	* <i>starch + protein + oil + lacquer</i>	textile or paper	<i>starch and/or protein (?)</i>	–
Shrine	lac.	starch + lacquer	<i>protein + lipids</i>	<i>paper + starch</i>	<i>protein + lipids</i>	–
Four-fold screen, f/b	lac.	–	* lipids + lac. + protein (t) + cedar oil(t) + persim. (t)	textile + lacquer	lacquer	–
Four-fold screen, sides	lac.	–	<i>protein + lipids</i>	<i>paper + starch</i>	–	–
Five-fold screen	lac.	* <i>lipids + lacquer + protein + gum benzoin (t)</i>	–	<i>fibres + protein</i>	–	–
Coromandel cabinet (doors)	lac, varn.	–	* <i>lipids + lac. + blood + gum benzoin (t)</i>	<i>fibres + lipids + blood (?)</i>	<i>lipids + blood (?)</i>	–

‘Buff.’ denotes buffer layer; ‘f/b’: front and back of screen panel; ‘lac.’: lacquer; ‘varn.’: natural resin varnish; ‘-’ layer not present; ‘[ ]’ layer present in some areas only; ‘\*’ layer analysed by PyGC/MS, thus giving more detail on the binder composition; ‘(t)’ binder present in traces, as determined by PyGC/MS; ‘?’ binding media not clearly identified due to its low concentration/state of deterioration, or too small sample size. Fields highlighted in *blue italics* indicate the failing layers.

### *3. Review of Damage to East Asian Lacquer Objects*

five-fold screen) the filler was mixed with protein, lipids and little lacquer instead. The four-fold screen had a lacquer-bound foundation consisting of very coarse filler particles on the front and back of its large panels, whilst the panel sides were manufactured from a mixture of finer grey/white translucent pigment (filler), protein and lipids. The layer structure of the Coromandel cabinet doors consisted of one thick dark grey foundation layer which was bound with lipids, lacquer, protein (blood) and some gum benzoin, which appeared to have been built-up by several applications. The Japanese shrine had a fine reddish foundation layer purely bound with starch directly underneath the top lacquer coat. The lower of the two reddish-coloured foundation layers on the cabinet stand also revealed some starch in addition to lacquer. These foundation layers appeared to be stable and had not failed unless they contained protein.

#### **Lower foundation**

The majority of the objects had additional foundation layers directly below the fine reddish layer, typically coarser and darker. Exceptions were the curved box and the panel sides of the four-fold screen, which only contained one finely-pigmented foundation above a paper layer. The corner cabinet also only had the fine reddish foundation applied directly to the wood substrate. The shrine displayed several further fine foundation layers that appeared more like conventional gesso layers prepared from fine white or reddish pigment (filler particles) and protein glue. A single foundation layer only was also applied to the Coromandel cabinet doors. Here, the foundation layer was applied over a buffering layer containing coarse plant fibres (possibly hemp, see de Kesel and Dhont 2002) which were bound or adhered with a similar matrix as that of the foundation layer, containing mainly lipids, blood protein and lacquer.

The other five objects had lower foundation containing densely-packed black, reddish and translucent filler particles of varying size. In some cases this coarse foundation was applied in more than one coat. The binding medium of all these layers contained protein, albeit to varying degrees and with additions of lipids, starch and other organic additives such as persimmon juice (a polysaccharide) or gum benzoin. These protein-containing layers had failed cohesively and/or adhesively on all objects.

#### **Summary**

Analysis on all coatings showed that the protein-containing layers were the most affected by damage, reaffirming the general understanding that such layers are prone to failure. Failure locations as well as weak adhesion between certain materials could be more precisely specified:

In nine out of ten cases foundation layers containing proteins had developed



significant cohesive failure, or had failed adhesively at the interface where they had been applied to starch-containing paper layers (Table 3.7).

Paper layers adhered purely with starch seemed equally problematic and prone to failure. Examples for this were the corner cabinet, the palanquin, the shrine and the curved box, where the paper layer was either lifting from the wood substrate, or was disintegrating.

Foundation containing a large amount of starch and only little lacquer also caused problems. Such layers exhibited adhesive failure from their adjacent wood substrate or textile layer as well as cohesive failure, which promoted delamination (cabinet stand and palanquin). In contrast, a high lacquer concentration within a starch-containing foundation layer provided a comparatively robust layer (reddish foundation of palanquin, curved box, and upper foundation of the cabinet with its matching stand).

More research would be necessary if a critical ratio between the two binder types were to be determined, beyond which the mechanical strength properties of the lacquer/starch paste-bound foundation change significantly.

#### 3.4.2. Comparison of identification techniques

Clearly, it is an ideal situation if sophisticated analytical techniques and equipment are available to identify constituent materials of coatings. However, under most common circumstances one has to make do with less costly and more easily accessible methods instead. It was therefore aimed in this work to investigate whether histological staining methods in combination with visible light and fluorescent microscopy have any scope for use on East Asian lacquer coatings. This line of investigation was particularly interesting as preliminary staining tests had shown some promising results despite the general notion that staining of cross-sections is usually unsuitable for darker-coloured layers (Schramm and Hering 1988, p. 114). Such dark layers are often contained in multilayered East Asian lacquer coatings.

A summary of the analysis results gained from the three analytical methods for a selected number of coating layers are given in Table 3.8. The full list of analysed samples is provided in Appendix D. For the comparison of the analytic methods the identified compounds were partly summarised, so that the effectiveness of the cross-section analysis could be evaluated for the four main binder categories: lacquer, lipid compounds (drying oils and other lipids), carbohydrates (such as starch), and protein (e.g. glue and blood).

Comparison of the results from histological staining and cross-section microscopy using VIS and blue light with those of the FTIR and PyGC/MS analysis showed some very interesting results and trends. As expected, details on a greater number of constituent organic compounds were gained from PyGC/MS analysis. The

### *3. Review of Damage to East Asian Lacquer Objects*

following sections will therefore evaluate the suitability of the cross-section analysis method by firstly comparing its results with those of PyGC/MS. The results obtained from FTIR measurements will be referred to afterwards, as this analytical technique gave less detailed information on the binder types present in the coating samples.

### 3.4. Analysis results and discussion

Table 3.8.: Summary of binding media analysis for selected coating layers from the surveyed lacquer objects, compiled from the analysis reports by Herm (2009a), Schilling (2010a) and Schellmann (Appendix D).

OBJECT	LAYER	DESCRIPTION	METHOD	LAC.	LIPIDS	CARBOH.	PROT.	OTHER
Cabinet (on stand)	F1	Dark grey foundation	PyGC/MS		✓✓✓		✓✓	
			FTIR	i		starch (i)		
			X-section		✓		✓	
	F2	Reddish foundation	FTIR	i				
			X-section	i	✓			
Cabinet stand (legs)	F2	Dark grey foundation	PyGC/MS	t	✓	✓✓✓✓	t	{persim. (t)}
			FTIR			starch (i)		
			X-section		✓	starch ✓		
	F3/F4	Reddish foundation	PyGC/MS	t	oil ✓	✓✓✓✓		{persim. (t)}
			FTIR	✓		starch (i)		
			X-section	i	✓	starch ✓		
Cabinet stand (top)	F1	Black priming	PyGC/MS		✓	✓✓✓		camphor ✓
			FTIR	✓		cellulose ✓		
			X-section	✓		✓		
	F2	Dark grey foundation	PyGC/MS	t	✓	✓✓✓✓		{persim. (t)}
			FTIR			starch (i)		
			X-section		✓	starch ✓		
	F3	Reddish foundation	PyGC/MS	t	✓✓✓	✓✓		{persim. (t)}
			X-section	i	✓	starch ✓		
Corner cabinet	F1	Reddish foundation	PyGC/MS	✓	✓✓	t	✓✓	colophony (t)
			FTIR				✓	
			X-section		✓		✓	
Cabinet with fans	F2	Pale brown foundation	PyGC/MS	t	✓✓✓✓	✓	t	{persim. (t)}
			X-section		✓		i	
Palanquin	F1/F2	Dark grey foundation	PyGC/MS	✓	✓	✓✓✓	✓	
			FTIR				✓	
			X-section		✓	starch (i)	✓	
	F3	Reddish foundation	PyGC/MS	✓	oil ✓✓✓	✓		persim. (t)
			FTIR	✓		starch ✓		
			X-section	i	✓	starch ✓		
	F4	Reddish foundation	FTIR	✓				
			X-section	i	i			

### 3. Review of Damage to East Asian Lacquer Objects

OBJECT	LAYER	DESCRIPTION	METHOD	LAC.	LIPIDS	CARBOH.	PROT.	OTHER	
Round box	F1	Coarse	PyGC/MS		✓	✓✓✓✓	t		
		beige	FTIR	-	-	-	-		
		foundation	X-section		{i}	starch	✓	✓	
	F2	Dark grey	PyGC/MS			✓✓✓✓	✓	✓	
		foundation	FTIR	i				✓	
			X-section			✓	starch (i)	✓	
	L1	Lacquer layer	PyGC/MS	✓		oil✓✓✓			persim. (t), wood oil (t)
			FTIR	i	✓				
			X-section	✓	✓				
F3	Reddish foundation	FTIR	i						
		X-section	i	✓					
Curved box	F2	Reddish	PyGC/MS	✓	oil✓✓✓	✓		{persim. (t)}	
		foundation	FTIR	✓					
			X-section	i	✓				
Five-fold screen	F1	Reddish	PyGC/MS	t	✓✓✓✓		t	cedar oil✓, gum benzoin (t), wax	
		foundation	FTIR				✓		
			X-section	✓	✓		✓		
Four-fold screen	F	Foundation (front panel)	PyGC/MS	✓	oil✓✓✓✓		t	cedar oil (t) {persim. (t)}	
			FTIR	✓					
			X-section	✓	✓		i		
	F	Foundation (side edge)	FTIR		✓		✓		
			X-section		✓		✓		
Coromandel cabinet	F2	Dark grey foundation	PyGC/MS	✓	✓✓✓✓		blood (t)	gum benzoin (t)	
			FTIR				✓		
			X-section		✓		✓		

Abbreviations for the column headers: 'Lac.' is East Asian lacquer; 'Lipids' summarises lipid compounds, such as drying oils (explicitly denoted as 'oil' in the same column) and other fatty lipids; 'Carboh.' are carbohydrates such as starch or cellulose. Persimmon juice (abbreviated 'persim.') is explicitly mentioned in the column named 'Other'; and 'Prot.' denotes glue protein unless stated as blood. '✓' indicates the presence of a binder, with multiple ✓ referring to its increased concentration in the sample as identified by PyGC/MS. 'i' is an indication of binder presence, 't' refers to there being trace amounts of the respective binder. {} marks constituent binder that was not conclusively identified.

## PyGC/MS analysis vs cross-section microscopy

There was a remarkable agreement between the four groups of binding media identified by the PyGC/MS method and that using cross-section microscopy including staining and examination under blue light (cf. Table 3.8). In none of the samples did the cross-section analysis identify binder groups that were not confirmed to be present by PyGC/MS. Eight out of seventeen samples analysed with the two techniques showed total agreement between the binding media types identified (e.g. the layers of the cabinet on stand, the round box, and the four-fold screen). In four further samples, the cross-section method only failed to identify some additional lacquer content, whilst in the remaining four samples bar one, trace amount of protein or some carbohydrate were missed in addition to lacquer. For the last sample, layer F1 of the cabinet stand, the PyGC/MS analysis result differed from that of the cross-section analysis with regards to one binder group. The layer appeared to contain lipids instead of lacquer. The following paragraphs will discuss these analysis results for all four binder types:

**Identification of starch** Exactly why the carbohydrate content was not detected by the staining in two of these samples was unclear. It may have only been present in the sample at very low concentrations and not in the form of rice or wheat starch which was commonly used in foundations of lacquer coatings. Wheat and rice starch are usually added to foundation in the form of very viscous pastes, and thus are not easily finely dispersed in such mixtures. Staining with Lugol's solution was shown to stain these starches well in reference foundation layers. The staining had also been very successful in all other samples in which the PyGC/MS had detected carbohydrates. Other possible additives containing carbohydrates include for example funori, juice of unripe plum, and honey (Quin 1882/1995, pp. 13, 20, 25; Kitagawa 2010; Heginbotham and Schilling 2011). These additives are known to have been used in combination with lacquer, in many cases to achieve certain working properties. As these are mostly fluids of relatively low viscosity, they may render the respective foundation layer with more finely dispersed starch content. In both specimens the PyGC/MS data hinted at the possible presence of persimmon juice, although this result was not conclusive. However, Heginbotham and Schilling (2011) explicitly state that fermented persimmon (be it as juice or aged foundation) has been shown not to contain the marker compounds used for identification of the carbohydrates. It therefore remains unclear which carbohydrate type was present in the sample and, if it were indeed a starch, why exposure of the cross-section to Lugol's solution did not stain it.

**Identification of lacquer** Lacquer additive in foundation was the binder type that was most commonly missed by the cross-section and staining analysis. This is not surprising as this highly cross-linked polymer can only be identified under the optical microscope due to its very typical fluorescence, which is best

### 3. Review of Damage to East Asian Lacquer Objects

visible when present in bulk or at high concentrations. Examples of this fluorescence are shown in Figures 3.2 and 3.9. However, when mixed with considerably high amounts of filler or very dark mineral pigment, this fluorescence may not be discernible. In such cases, confirmation is required through PyGC/MS analysis using TMAH derivatisation. This method clearly identifies characteristic marker compounds that are contained in the lacquers derived from the botanical *Anacardiaceae* family (in the following collectively referred to as ‘anacard marker compounds’).

The top foundation (F3) of the coating of the palanquin is an example of such a highly-filled layer. The corresponding cross-section of the full multilayered coating structure and the staining results were presented earlier in Figure 3.6, where layer F3 is visible underneath the top lacquer coating/thin black layer (cf. also Appendix D, p. 339). Due to the slight caramel/yellow-ochre coloured fluorescence of F3 (Fig. 3.6a), cross-section analysis had tentatively identified the binder of the reddish foundation as lacquer. However, due to the high pigment content, a definite identification of this binder could not be made with confidence. Layer F3 was therefore mechanically isolated from the second half of the coating sample shown in Figure 3.6 and analysed using PyGC/MS (sample X10/003).

Figure 3.7 presents the results for the distribution of the anacard marker compounds identified in the reddish foundation layer F3 of the palanquin (Schilling 2010a). To the very left in each of the three diagrams, the abundance of the anacard markers measured in the foundation sample are given. The other three sets of bar graphs provide the respective abundance of marker compounds identified in reference samples of *ki-urushi*, laccol and ‘thitsi’ lacquer. *Ki-urushi* is the raw urushiol-based lacquer derived from the tree species *Toxicodendron vernicifluum* (Stokes) F.A. Barkley, introduced in Chapter 2.2, which grows in Japan, Korea and China. Its marker compounds are namely dimethoxybenzene-nonanoic acid methyl ester (DMB-nonanoic-AME), pentadecylcatechol (as dimethoxy derivative) and heptyl phenol (Chiavari and Mazzeo 1999; Schilling 2010b; see also Table 3.5). Laccol is the main polymeric constituent of lacquer from *Rhus succedanea*, native to Taiwan and Vietnam (Kumanotani 1976), and ‘thitsi’ denotes lacquer containing the polymer thitsiol (identified by the marker compound 12-phenyldecyl catechol, as dimethoxybenzene derivative; Schilling 2010b), which originates from trees from the *Gluta usitata* species (formerly known as *Melanorrhoea usitata*) native to Thailand and Myanmar (e.g. Jefferson and Wangchareontrakul 1986; Golloch and Sein 2004). Honda et al. (2010) and Heginbotham and Schilling (2011) have recently demonstrated that thitsi lacquer was present as an additive in domestic Japanese and many export-type *urushi* lacquer coatings they had tested, and thus attention was paid to the marker compounds for all possible three lacquer types. The analysis results presented in the graphs clearly show that lacquer was contained in the foundation sample, which could be further identified as *urushi* based on the presence of DMB-nonanoic-AME.

### 3.4. Analysis results and discussion

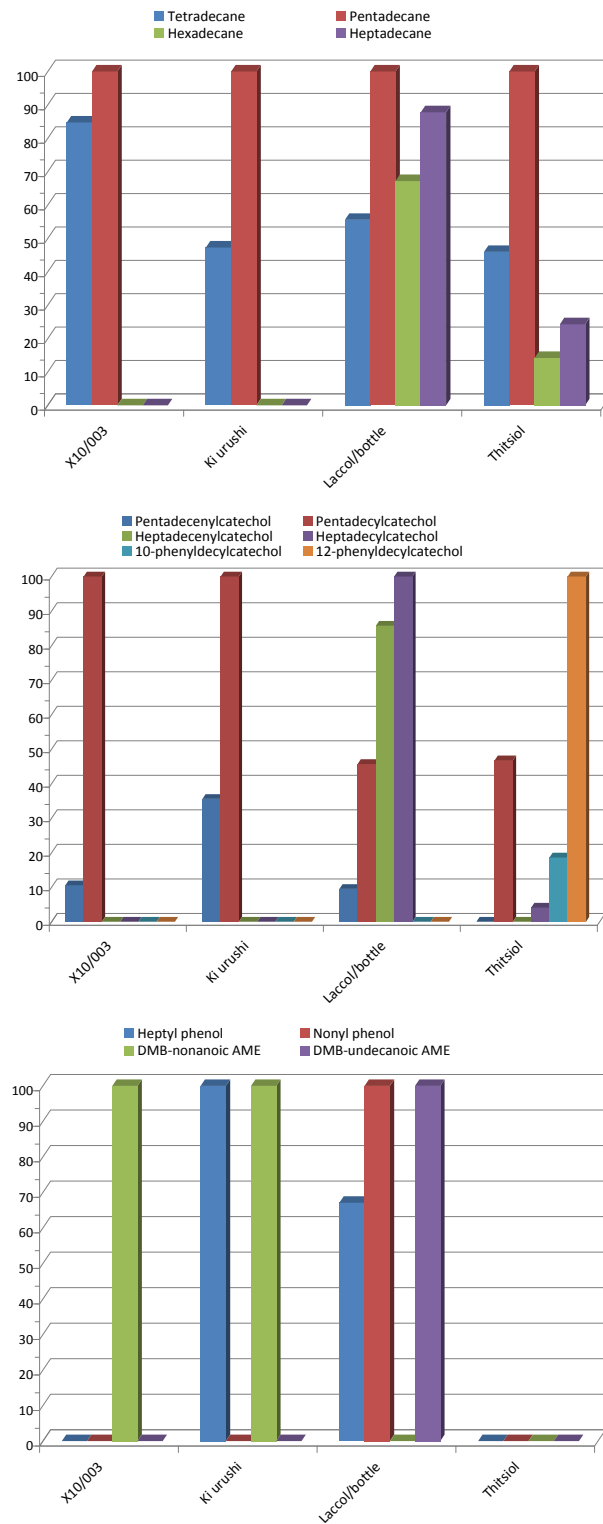


Figure 3.7.: Anacard marker compounds identified by TMAH-PyGC/MS for a sample of the reddish foundation layer (F3) of the palanquin and for three reference samples of East Asian lacquer types (Schilling 2010a).

### 3. Review of Damage to East Asian Lacquer Objects

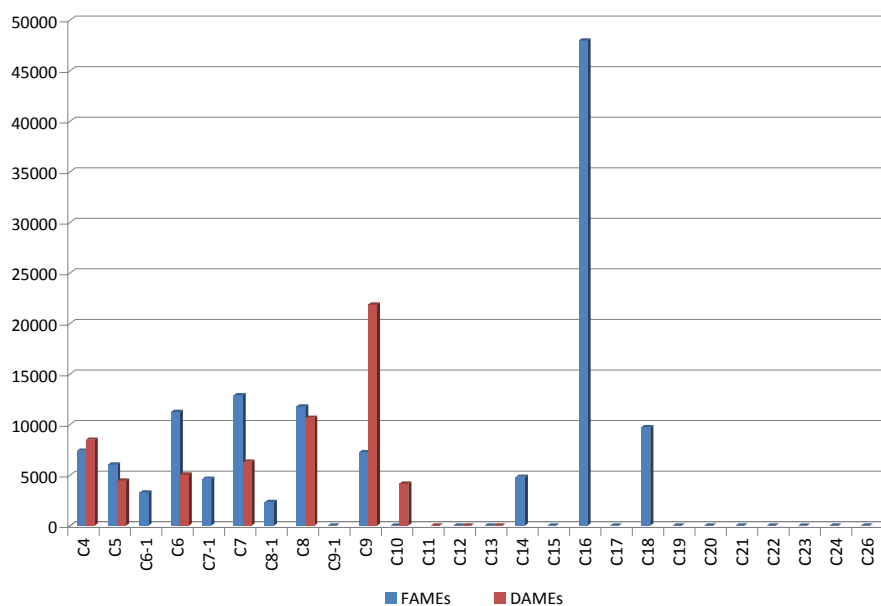
In all the cases where the lacquer had been identified with confidence during cross-section analysis due to its fluorescence, the PyGC/MS analysis confirmed this result (cf. Table 3.8). It can thus be concluded that with a certain degree of experience, lacquer can indeed be reliably identified with fluorescent microscopy techniques. This finding is also supported by research on the fluorescence of East Asian lacquer conducted by Webb (2011).

**Identification of lipids and oil** Clarity on the presence of lipid compounds in the multilayered coating structures was gained by compiling the fatty acids profile from the data measured by PyGC/MS (Schilling 2010a). Referring back to the example of the palanquin's reddish foundation layer F3, the respective fatty acid profile is presented in Figure 3.8. This shows the distribution of fatty acid methyl esters (FAMES) and dicarboxylic fatty acid methyl esters (DAMES) detected in the sample. The saturated fatty acids palmitic and stearic acid (containing sixteen and eighteen carbon atoms,  $C_{16}$  and  $C_{18}$ , respectively) are naturally present in all lipids. It is worth noting that in contrast the phenolic lipids contained in urushiol-based lacquers are characterised by long side chains of mostly fifteen carbon atoms ( $C_{15}$ ) and some side chains of seventeen ( $C_{17}$ ) carbon atoms (Kumanotani 1995, 1998).

FAMES and DAMES were found in all samples tested by PyGC/MS in this work, albeit at varying relative abundance (Schilling 2011). Hence, all tested coating layers were shown to contain lipids of some sort. In the particular example of the palanquin given here, the lipids were more clearly identified as drying oil. Strong evidence for its presence was the relative distribution of dicarboxylic fatty acids, such as azelaic acid ( $C_9$ ), to palmitic and stearic acids. High levels of dicarboxylic fatty acids are a typical feature for aged and oxidised drying oils. Azelaic acid is generally the most abundant one and thus used as a marker compound for their identification (e.g. Mateo-Castro et al. 2001; Schilling 2011).

Altogether five samples were shown to contain drying oil: the reddish foundations of the palanquin (F3), that of the cabinet stand legs (F3/F4), and of the curved box, as well as the foundation of the four-fold screen (F) and the lacquer layer (L1) of the round box (Schilling 2011). The oil content of the lacquer layer had been successfully identified due to its characteristic fluorescence, which was presented in Figure 3.3b. This confirmed that oil content in lacquer changes its fluorescence to a brighter yellow. In contrast, none of the two stains for oil (Sudan Black and Nile Blue sulphate) had induced any colouring of the oil fraction mixed with the lacquer matrix. It thus appears that oil content in a lacquer matrix cannot be stained with either Sudan Black B or Nile Blue sulphate. With respect to the foundation layers, staining of lipid content seemed to be successful, although no distinction could be made between drying oils or other lipid compounds. PyGC/MS confirmed that all samples that had shown positive staining indeed contained lipids. These results also agreed with the positive staining results from the Nile Blue sulphate. It may therefore be concluded that with great





FAMEs = fatty acid methyl esters, DAMEs = dicarboxylic fatty acid methyl esters, C<sub>n</sub> = carbon chain

Figure 3.8.: Fatty acid profile measured by TMAH-PyGC/MS for the reddish foundation F3 of the palanquin (V&A 48-1874) (Schilling 2010a).

likelihood both stains had shown true staining of the lipid compounds. However, it has to be noted that this agreement does not entirely disprove that some of the apparent staining may possibly have derived from stain penetration into the sample pores. As all the foundation layers tested contained lipids, this test series did not provide a control layer for non-lipid-containing porous foundation. The question of stain penetration therefore remains partly unanswered and needs to be investigated further in the future.

As mentioned above, in one sample the PyGC/MS analysis result differed for one binder group from that of the cross-section analysis. The layer appeared to contain lipids instead of lacquer, which had been identified by fluorescent microscopy under blue light according to the characteristic caramel/yellow-ochre colour of the matrix and the absence of staining after exposure to Sudan Black B solution. This discrepancy was explained by the fact that the sample analysed by PyGC/MS was exceptionally small – almost too small to give detectable results –, and was taken from an area with rather inhomogeneous distribution of its constituents (Fig.3.9). Thus, the sample may just not have contained all the components that were actually present in the coating layer.

**Identification of protein** Protein was confirmed by PyGC/MS to be present in ten samples. It was identified in the mass chromatogram by the presence of pyrrole and its methylated derivative which are thought to originate from the pyrolysis of the amino acid derivatives proline and hydroxyproline (He et al.

### 3. Review of Damage to East Asian Lacquer Objects

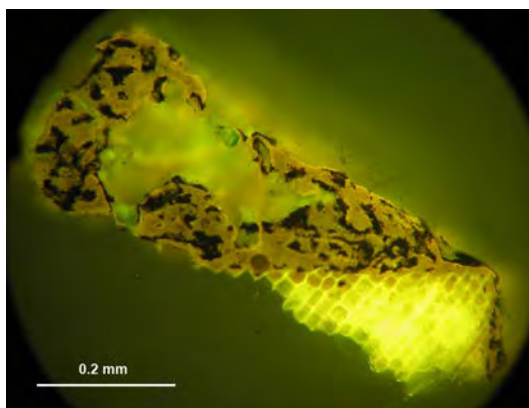


Figure 3.9.: Cabinet stand (V&A 303-1876), top panel: cross-section of priming layer F1 after staining with Lugol's solution in blue light, displaying inhomogeneous dispersion of starch (black) in lacquer matrix.

2007). The exact identification of a specific protein type cannot generally be deduced from these results gained by the TMAH-PyGC/MS method. However, a likely source are thought to be animal glues, which do contain these amino acid derivatives and are commonly used in the manufacture of foundation layers in export-type East Asian coating layers (Heginbotham and Schilling 2011, see also Quin 1882/1995 and de Kesel and Dhont 2002 amongst others). An exception was one sample in which the presence of cholesterol and its methylated derivative were detected. This result was interpreted as an indication of blood, although egg could also have been the source of these marker compounds. Blood was considered the more likely constituent, as historic sources (e.g. Bonanni 1720/2009, p. 23; Wang 1983; Webb 2000, p. 10) mention the use of pig's blood for Chinese lacquer ware. Egg, on the other hand, does not appear to have been used traditionally in the production of lacquer coatings.

Generally, the identification of the protein agreed with all the positive staining results gained from the AB2 solution and subsequent microscopy under visible and blue light. In those cases, where the AB2 stain did not induce sufficient contrast in the colour appearance of a protein-containing layer, staining with Nile Blue sulphate helped to visualise a positive staining result under blue light. An example for this was the dark grey foundation layer of the Coromandel cabinet (which contained the cholesterol). Figure 3.10 presents the cross-section sample in four different stages of staining: before staining (a), the protein content was only visible in very limited areas as whitish fluorescence (marked with red arrows). After staining with AB2 (b), these areas had turned dark, whilst the remaining foundation appeared unchanged. Staining with Nile Blue sulphate (c) indicated some protein and/or lipid content throughout the entire foundation layer, discernible by the reddish-brown fluorescence or darkened appearance of the layer. Eventual staining with Sudan Black (d) finally distinguished the actual lipid content from the protein. The red arrows in (d) mark those areas where oil content coincides

with protein (black appearance). The areas which retained their reddish-brown fluorescence are those containing predominantly protein. It can thus be concluded that the combination of using AB2 stain and NileBlue sulphate was effective in identifying protein content even in dark-coloured foundation layers.

**Summary** In summary these results demonstrated that cross-section analysis was generally capable of identifying all binding media types that were shown to be present in the coating layer at significant concentrations. Not in a single case did the staining and blue light analysis of the cross-sections identify a binder that was not confirmed to be present by PyGC/MS analysis. If binders were missed, it was either because they were only present in trace amounts, or they were lacquer mixed with mineral pigment. Lacquer generally appeared to be identifiable by its characteristic fluorescence with cross-section analysis under blue light, if present in the layer at high concentrations. It was only likely to be missed if contained in dark-coloured foundation layers and when mixed with a high amount of mineral filler particles. Staining for starch with Lugol's solution worked very well, but might be difficult to discern in dark foundation layers. The same applied to the AB2 stain used for proteins. In some cases, microscopic analysis under blue light helped to discern a positive staining result. Furthermore, additional staining with NileBlue sulphate was in several cases able to improve the discernibility of a positive staining result under blue light and helped clarify obscure staining results with AB2. Staining with SudanBlackB appeared to be useful for the identification of oils in darker layers when used in combination with fluorescent microscopy under blue light. In cases of positive staining, a positive staining result could be determined by the darkening of previously fluorescing layers.

### **FTIR analysis vs PyGC/MS and cross-section microscopy**

It has been pointed out previously that the FTIR spectroscopy is not the ideal technique for identifying highly complex mixtures of organic compounds in coating samples, as it lacks sensitivity to low concentrations of such compounds. Unsurprisingly therefore, the number of organic compounds identified by FTIR spectroscopy in this study was much more limited than that by PyGC/MS analysis. In the majority of cases, only one binder type was detected, in 37% a mixture of two binder types. Only in one sample (i.e. the lacquer layer L1 of the round box) did this method identify all the constituent binder groups identified by PyGC/MS, which were lacquer and a large amount of drying oil.

**Agreement of results between methods** Comparison of the cross-section analysis results with those of the FTIR spectroscopy gave a very similar picture (cf. Table 3.8): Nineteen samples were tested by the two methods, and full agreement of their results were achieved in only three samples. These were the priming layer (F1) of the cabinet stand top (containing lacquer and carbohydrate), the

### 3. Review of Damage to East Asian Lacquer Objects

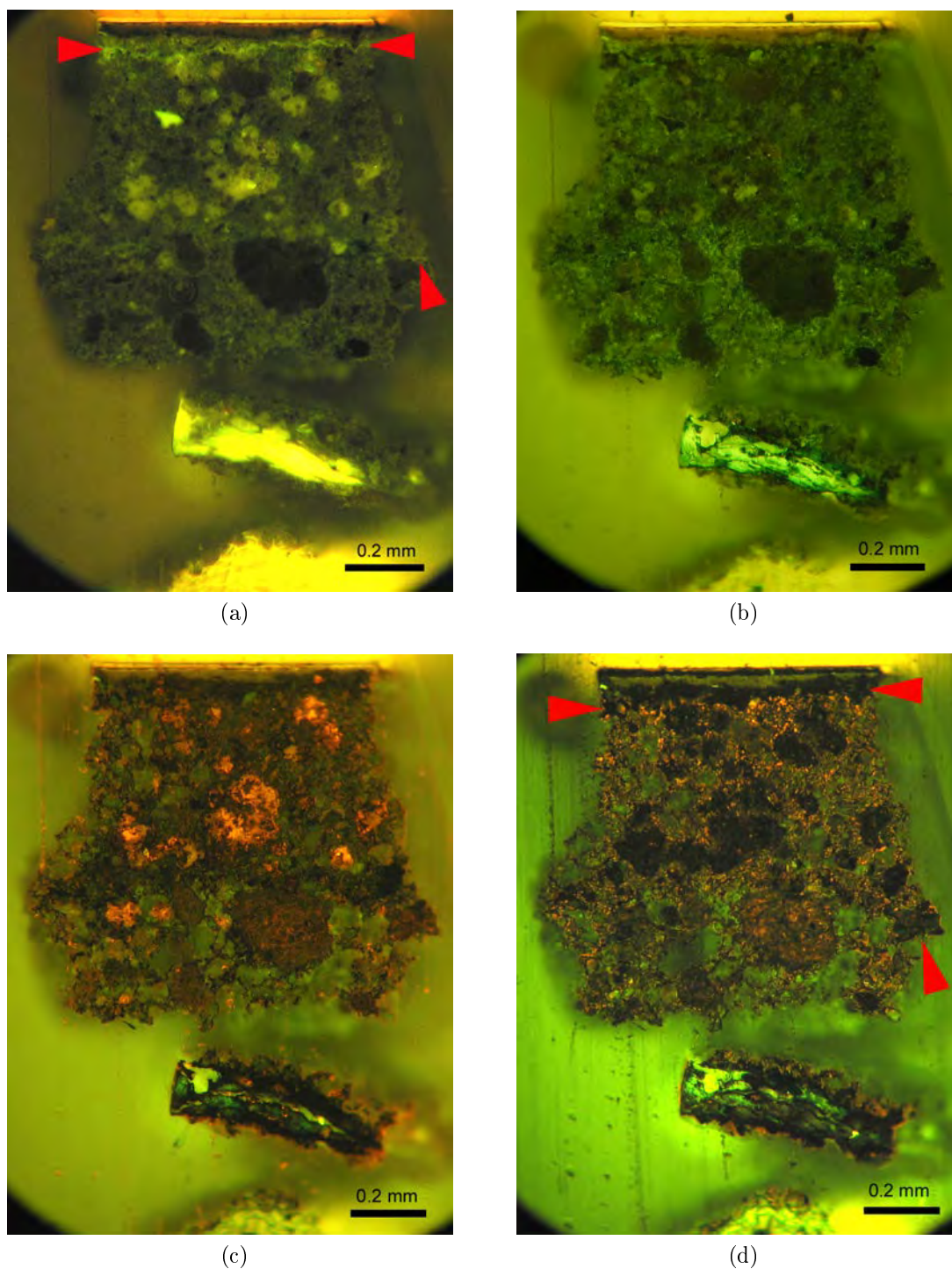


Figure 3.10.: Coromandel cabinet (priv. collection): cross-section of coating structure under blue light. Layer structure from bottom to top: wood, fibrous layer + binder, foundations, lacquer, natural resin varnish. Uneven distribution of binding media in dark grey foundation visible; (a) unstained, (b) stained for protein with AB2, (c) stained for oil and protein with Nile Blue sulphate, and (d) stained for oil with Sudan Black B.

lacquer layer (L1) of the round box (lacquer + oil), and the foundation (F) on the sides of four-fold screen (oil + protein). In two further samples the two techniques agreed on two constituent binder types (starch + lacquer), whilst the FTIR technique missed at least one further type that was identified with cross-section analysis. In the remaining samples agreement was only achieved for one binder group (either protein, starch or lacquer). In summary this meant that in over 80 % of the samples cross-section analysis identified more binder groups than FTIR spectroscopy. In one case, a sample tested by FTIR gave entirely contradictory results to those of the PyGC/MS and cross-section method. The specimen concerned was taken from the cabinet on stand. FTIR analysis identified starch and some indication of lacquer, whilst the other two methods had detected lipids and protein. These discrepancies were mainly ascribed to the sampling technique, which had differed for the three analytical methods. This aspect and details of the respective specimens will be discussed later in this Chapter in the section dedicated to sampling (page 64).

**Limitation of lipid identification** Generally it appeared that protein was relatively reliably identified by FTIR, whilst lacquer and carbohydrates were missed in a few cases. The binder type that appeared to be most problematic to identify with FTIR were the lipids. As was mentioned before, in all the samples in which PyGC/MS detected the marker compounds for lacquer, it also identified the presence of lipids. In contrast, whenever FTIR analysis identified lacquer in a foundation layer (or at least some indication of it), this technique failed to detect the additional lipid content. Only in the case of layer L1 of the round box did it identify oil, together with some indication of lacquer (Fig. 3.11) due to absorbances at 1633 and 1261  $\text{cm}^{-1}$  (Herm 2009a, p. 34). This suggested that in all the other FTIR spectra the lipid content may have been masked by the presence of East Asian lacquer. Mixtures of lacquer and oil are known to be difficult to identify, as these two binder types show rather similar or overlapping absorption bands. These are situated in the proximity of 2930 and 2856  $\text{cm}^{-1}$  (C-H stretching bands), around 1715  $\text{cm}^{-1}$  (carbonyl stretching band, this absorption band of lacquer broadens with increasing oxidation, i.e. ageing), and in the regions around 1443 and 1377 (C-O stretching modes) and near 725  $\text{cm}^{-1}$  (C-H deformation vibrations). These bands can also appear in the spectra of Figure 3.11. In almost all samples in which the FTIR analysis detected lacquer content one of the main absorptions were recorded at the carbonyl (C=O) stretching band around 1710 or 1715  $\text{cm}^{-1}$ . Based on previous investigations this carbonyl band is considered characteristic for polymerised urushiol-based lacquer (Hummel and Scholl 1978, as cited in Simon et al. 2001; Honda et al. 2010). Kamiya et al. (2006) have shown that with increasing oxidation of the urushiol side chains, the C=O stretching vibration near 1715  $\text{cm}^{-1}$  becomes more pronounced. However, absorption in this area can also be induced by the addition of drying oils to lacquer. The characteristic carbonyl ester band of these oils is normally located at approximately 1740  $\text{cm}^{-1}$ . Ring (2001) and Simon et al. (2001) explicitly point out that additives

### 3. Review of Damage to East Asian Lacquer Objects

such as tung oil significantly influence the infrared spectrum of lacquer and reported increased absorption intensity near  $1725\text{ cm}^{-1}$ . Progressive aging of drying oils induces the development of carboxylic acid products, that can also show characteristic absorption near  $1715\text{ cm}^{-1}$  (e.g. Meilunas et al. 1990). It is thus clear that due to these overlaps and shifts, it is very difficult to identify any presence of oils in lacquer mixtures with FTIR. Confirmation for this is provided by Frade et al. (2009), who found that the coatings of two East Asian lacquer shields both showed the typical absorption bands for lacquer, including pronounced carbonyl stretching near  $1715\text{ cm}^{-1}$ . Subsequent analysis by TMAH-PyGC/MS detected the presence of fatty acids in these lacquer samples, which were concluded to have derived from the addition of drying oil.

### Observation on sampling techniques

One of the problems that became obvious during the analysis of the test results was that certain sampling techniques were inadequate for gaining reliable data on the coating constituents. Sampling the entire layer structure of the decorative coating proved a good way to remove material from the object without the risk of contaminating individual layers. From these samples, not only cross-sections could be prepared that gave an undisturbed overview of the stratigraphy and exact locations of the interfaces between the individual layers. Coating specimens including the complete stratigraphy were also extremely useful for providing sample material for PyGC/MS analysis. The method of separating the individual layers by mounting the multilayered sample on a Perspex plate and then separating each layer under the microscope with a scalpel, was very efficient in rendering the collected material relatively uncontaminated. Due to the porosity of the foundation layers, superimposed layers tended to show penetration into the foundation to varying degrees. Differences in layer consistency and appearance could be more easily acknowledged under the microscope and sample material could thus be carefully selected.

In contrast, previous sampling by taking scrapings directly from the object or from loose flakes using a scalpel and a head-loupe, had shown to be problematic. Some samples which were collected in this way had been used for FTIR analysis. They had given ambiguous results compared with those gained from cross-section microscopy and for PyGC/MS analysis. Examples of this were the scrapings of the dark grey foundation F1 of the cabinet stand (leg), or the dark grey foundation F2 of the round box (cf. Table 3.8). Both samples used for FTIR analysis appear not to have been cleanly separated from their adjacent layers, thus giving divergent results from that of the PyGC/MS analysis and the staining and microscopy.

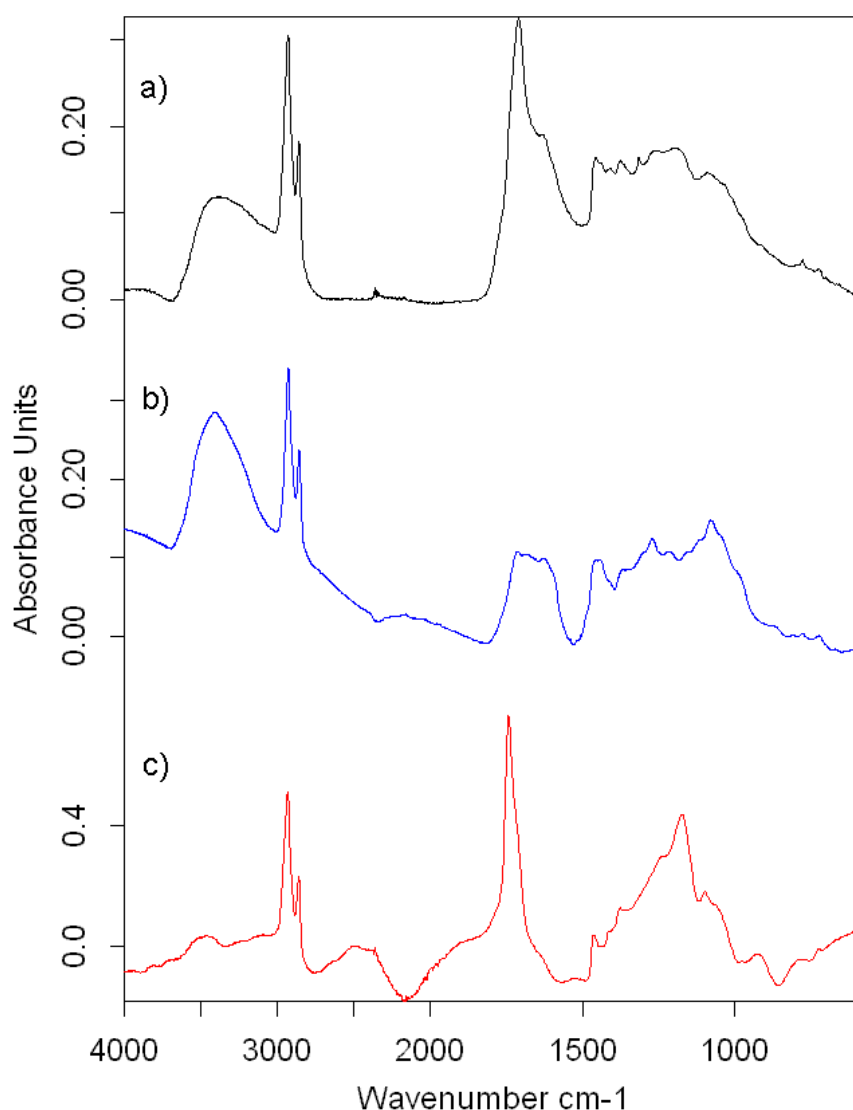


Figure 3.11.: FTIR spectra of a sample taken from the round box (V&A W.332-1921) and its best matching two reference components. Spectra showing from top: (a) Round box, layer L1 (sample X07/028) with characteristic absorbances at 3400, >3000, 2930, 2856, 1710-1715, 1633, 1443, 1377, 1261 and 725  $\text{cm}^{-1}$ ; (b) reference spectrum of Chinese raw lacquer CL1 (Bayerisches Landesamt für Denkmalpflege, Munich 1993); and (c) reference spectrum of Chinese tung oil (Bayerische Schlösserverwaltung, Munich 2007/Piening, Schellmann), dried for 4 months (all spectra taken from Herm 2009a, Figure 30, p.34).

## Advantages of cross-section staining

Fluorescent microscopy in combination with staining of East Asian lacquer coatings has proven to be very useful not only for material identification, but also for determining possible variability in the spatial distribution of specific layer compositions. Without staining, this may not necessarily be visible to the naked eye when relying solely on VIS or blue light microscopy. The staining confirmed that particularly foundation layers of East Asian lacquer coatings can be rather inhomogeneous. This is not surprising: materials for lacquer coating manufacture in East Asian countries, such as Japan or China, are usually mixed with simple wooden spatulas, as opposed to using a muller, which is the traditional way of mixing pigments and binder in the West. If coatings were manufactured quickly – which would be expected for the export-type lacquer ware this study is concerned with – the constituent materials are likely to be less carefully prepared and thus rather inhomogeneous. This has been shown to be true in many of the coatings investigated. Unless this inhomogeneity is recognised in its full extent, any analysis undertaken with techniques that require only tiny samples may provide incomplete results.

Information on the spatial distribution clearly helped to correctly interpret the data measured by FTIR and PyGC/MS analysis. Examples where the staining helped to distinguish between similarly appearing layers were the fine reddish foundations (F3/F4) of the cabinet stand, which contained significantly different amounts of starch (Figure 3.5), as well as the coating structure of the palanquin presented in Figure 3.6. Information gained by staining also explained cases where results differed or some components were missing from the list of identified media. The most striking example for this was the coating structure of the five-fold screen, cross-sections of which are presented in Figure 3.12. It can be clearly seen in the figures before and after staining for protein with AB2 stain that the distribution of the binding media is rather variable: some areas contain a lot of protein (black areas in Figure 3.12b) whilst others contain none or hardly any, but lacquer mixed with oil instead (bright yellowy-caramel fluorescence). This explains why protein was not identified by the FTIR analysis in this particular layer. It was most likely not present in the minute sample that was analysed. Similar observations were also noted for the cabinet on stand (cf. Appendix D) and for the Coromandel cabinet, which both appeared to contain uneven protein distribution. Figure 3.10d had also clearly shown irregular oil content in the dark grey foundation layer. In these samples, too, it was not surprising that the FTIR analysis did not identify unevenly distributed constituents, as they may not have been contained in the fractions of the samples analysed.



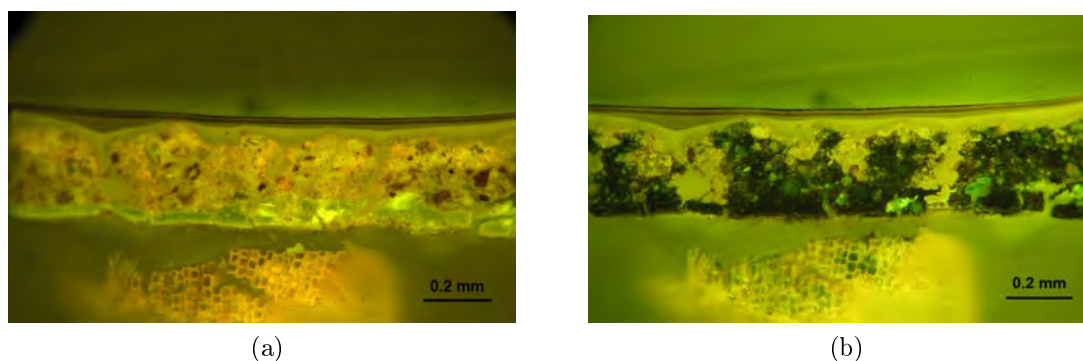


Figure 3.12.: Four-fold screen (V&A W.25-1939): cross-section of entire coating structure under blue light, showing (from bottom to top) wood substrate, paper layer adhered with binder, reddish foundation and five lacquer layers of varying thickness (partly penetrated into foundation layer). (a) before staining, and (b) after staining with AB2 solution, revealing the protein content of the paper and the foundation layer.

## Summary

These results showed that the four binding media groups – lacquer, lipids, starch and protein – were mostly identifiable with cross-section analysis if it was combined with staining and examination under blue light. Correct interpretation of the staining results required significant experience, as first impressions could sometimes be misleading. However, with the use of reference samples, identification of positive staining results were demonstrated to be possible and considerably reliable. Even on dark-coloured layers positive staining results could be discerned, as long as they showed some fluorescence before staining with the non-fluorescent stains. East Asian lacquer layers could be identified in many cases due to its characteristic fluorescence under blue light, provided that it was present in bulk or contained in a foundation layer at relatively high concentrations. Bright yellow to yellowy-caramel coloured fluorescence appeared to be a strong indication for the presence of oil additives in a lacquer layer. Lacquer mixed with a high concentration of dark mineral filler or pigment generally prevented a successful detection by microscopic methods. Last but not least, staining generally proved to be a very useful method to reveal uneven binder concentrations within individual layers. This clearly helped to develop an improved understanding of the layer structure and to clarify any results gained by spectroscopic methods.

### 3.4.3. Discussion of the causes of binding media failure – Influence of exposure to water and high humidity levels

Even though it is often difficult to find out what exactly has caused objects to deteriorate in a specific way over the course of time, some observations may help to explain certain failure mechanisms.

It was noted that several of the objects included in the survey had shown signs of direct exposure to water. This led to the assumption that all objects had been exposed to high levels of humidity or fluctuating environmental conditions, which to some degree was involved in the deterioration of their coatings. This behaviour would be consistent with the theory on RH induced stresses and failure of coatings due to the presence of strongly hygroscopic materials and surrogate binders, introduced in Chapter 2.

To verify the involvement of RH induced stresses, and to identify some of the failure mechanisms involved in the deterioration of the lacquer coating structures, the following section will present a few exemplary case studies from the survey. Even though the failure causes will be discussed in three categories, it has to be noted that they cannot definitely be separated from each other. A certain overlap is to be expected, as all failure causes will be related to changes in RH. Indeed, many of the lacquer objects surveyed most likely deteriorated due to a very complex combination of several individual failure mechanisms. These were either induced or increased by RH changes, however it would go beyond the scope of this work to clearly identify all individual mechanisms involved.

#### Case studies from the survey

**Objects exposed to water/excessively humid conditions** Examples for the consequences of extreme humidification are the cabinet with its matching stand and the corner cabinet. They had clearly been stained by water that had at some point dripped onto parts of their surfaces, leaving behind visible splashes with faintly white accretions. Out of all the surveyed objects, these two pieces exhibited the most severe delamination, tenting, cupping and flaking in all areas close to the water marks (Figs. 3.1e, 3.13 and 3.14a). On the side panels of the corner cabinet, the entire coating layer structure including the paper layer was lifting over a large area, suggesting that the starch binder that had originally attached the paper to the wood substrate had failed completely. The blisters and the tenting of the coating on the horizontal boards of the cabinet indicated blind cleavage and delamination of the multilayered structure caused by plastic (permanent) deformation of the wood substrate. This has occurred due to shrinkage of the wood panel in consequence of the water exposure. In many other areas, particularly near the base and along the lower edges, the lacquer had curled away (Fig. 3.14b). This type of curling is linked with shrinkage or peeling



Figure 3.13.: Cabinet stand (V&A No. 303-1876) displaying blistering, lifting and flaking lacquer on the restrained top panel (a), and on the top edge of the proper right back leg (b), as a consequence of severe water damage. (Photographs by N. Schellmann, courtesy of the V&A).

stresses and plastic deformation of the top lacquer layers during desiccation, which are greater for lacquer than those of the less dimensionally responsive protein-bound, gesso-type foundation layer. The curling is a consequence of exposure to high humidity and subsequent drying: Humidity can induce highly filled and restrained foundation layer/s (i.e. foundation that is fast adhered to its adjacent layers or substrate and therefore not free to move) to crack and lose mechanical strength due to relatively greater swelling of the neighbouring materials. Upon drying, on the other hand, the shrinking stresses of the wood substrate and the lacquer will exert compression stresses on the (still adhered) foundation, which can then cause it to cleave, buckle and finally lift. (For further discussion on this behaviour see Mecklenburg 2007 and Mecklenburg et al. 1998).

**Objects exposed to excessively dry or varying RH conditions** Despite showing no visible signs of direct contact with water, the other surveyed objects also appeared to have suffered from changes in moisture content. An example is the round box (W.332-1921), which predominantly displayed coating failure in the lowest foundation layer near the interface of the wood. Cleavage between the top lacquer-containing layers and the underlying protein-bound foundation had also developed in some areas (see cross-section in Fig. 3.3). Examination of the exposed hardwood substrate showed that the latter had been turned from a wood block with the tangential grain direction running across the lid and the base.

### 3. Review of Damage to East Asian Lacquer Objects

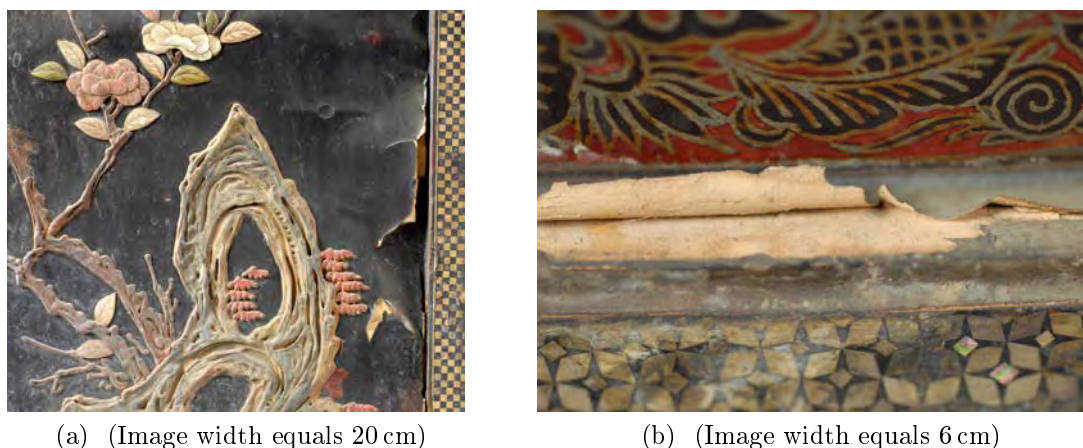


Figure 3.14.: Details of corner cabinet (493-1872). (a) Detail of side panel. The whitish accretions on the lacquer surface and lifting coating layer are caused by exposure to water. (b) Lower proper left hand door, detail of recess. The lacquer is lifting and curling, exposing the protein-bound foundation layer. (Photographs by N.Schellmann, courtesy of the V&A).

Significant shrinkage of the wood in the tangential and radial grain direction had caused the lacquer coating to blister prior to flaking in the respective areas on the side of the box and on the bottom side of its base (Figs 3.15a and 3.15b). It is possible that this substrate shrinkage occurred slowly over time after manufacture due to insufficient initial drying of the wood before the coating was applied. Toishi and Washizuka (1987, p. 164) point out that many uncoated wood substrates are acclimatised to around 80 %RH to accommodate lacquer polymerisation during manufacture. Weintraub et al. (1979) further elaborate that gradual equilibration of exported lacquer ware to generally lower RH conditions in Western countries often causes permanent shrinkage of wooden substrates. This may have been the case in this instance. The protein-bound and thus water-containing foundation layer may also have contributed to initial swelling of the outer wood cells during manufacture. After coating application, transverse wood shrinkage by around 4% compared with the diameter of the box (14.5 cm) in the longitudinal grain direction appears to have exceeded the compressibility of the stiff and brittle protein-bound foundation layer, causing the coating to cleave near the wood interface and to buckle and blister. Alternatively (or additionally), it is also likely that cyclic exposure to varying RH or an excessively dry environment during storage after very humid conditions may have caused the damage. In this case, the coating structure may have fractured in the least dimensionally responsive and least tough protein-bound layer during a humid cycle, stopping it from being restrained in some areas. Upon drying or return to the mid-RH region, the wood will have shrunk more than the unrestrained lacquer coating, thus causing the detached layers to buckle and blister.



(a) Lid showing blistering and flaking of lacquer coating in the area covering end-grain of the turned wood substrate.



(b) Underside of base, showing a large collapsed blister in the lacquer coating parallel to the grain direction of the wood substrate.

Figure 3.15.: Round box (W.332-1921). (Photographs by N. Schellmann, courtesy of the V&A).

**Object with hygroscopic inlays/discontinuities** The cabinet with fans showed the most damage in areas surrounding the ivory inlays, suggesting that significant dimensional responses of the ivory and its adjacent materials relating to humidity changes had occurred (Fig.3.16). Ivory is a very hygroscopic and anisotropic material which can change dimensions by up to 4.2% in the radial direction (Lafontaine and Wood 1982), similar to wood (see also Section 2.5). It may thus be assumed that these ivory inlays act not only as a restraint for the adjacent lacquer coating, but also as effective discontinuities. The observed open joints between the ivory and the lacquer surface, which have developed with time, allow ambient humidity changes to affect the hygroscopic lower layers of the coating and the wood substrate locally at an increased rate compared with the rest of the cabinet. Again, as described earlier, wood shrinkage upon drying along with plastic deformation of the top lacquer layers that most likely occurred due to compressive stresses during a wet cycle, are considered responsible for the permanent distortion and cupping of the coating between the pieces of ivory inlay.

#### 3.4.4. Remarks on the durability of coatings with high lacquer content

Based on the survey of V&A objects, pure lacquer layers and foundation with high lacquer content generally appear to be very durable and the least prone to failure in export-type lacquer ware, even when exposed to unfavourable environmental conditions. This again confirms the general understanding of the comparatively

3. Review of Damage to East Asian Lacquer Objects



Figure 3.16.: Cabinet with fans (W.19-1969) showing cupping and lifting lacquer coating between ivory inlay. (Photograph by N.Schellmann, courtesy of the V&A).



Figure 3.17.: Early 15th century Chinese cabinet (F.E.7-1973). Outside of drop-front showing extensive cracking of the lacquer coating, but no significant coating losses or flaking. (Photograph by N. Schellmann, courtesy of the V&A).

high mechanical strength of lacquer.

An impressive example for the reported durability of lacquer-primed wood and lacquer-containing foundation layers is a Chinese cabinet (V&A F.E.7-1973) from the early fifteenth century that had been included in this survey for comparison. Despite having developed very pronounced mechanical damage in the thick lacquer coating, which consisted of a lacquer-adhered textile layer, lacquer-bound foundation and a thick, partly pigmented top lacquer layer (Fig. 3.2a), the object showed strikingly few losses to its coating (Figs. 3.17 and 3.18).

On the outside of this cabinet, extensive cracks through the entire thickness of the coating and slight cupping had developed in a pattern very similar to that reported to be typical for canvas paintings on wooden stretchers (Keck 1969). This has been shown to be a consequence of the combined effects of both exposure to dropping temperatures and increasingly dry conditions (Mecklenburg and Tumosa 1991a). The extreme cupping of the cracked coating on the inside of the cabinet drop front suggested exposure to very high humidity that was retained over a significant time, while the cabinet desiccated at a faster rate on the outside than on the inside. The wooden panel and frame construction of the drop front restricts the movement of the panel, and therefore changes in RH manifest themselves in stresses which are likely to be responsible for the considerable cracking of the substrate and the coating upon desiccation.

### 3. Review of Damage to East Asian Lacquer Objects



Figure 3.18.: Detail of the Chinese cabinet (F.E.7-1973) drop front inside. Extensive cracking and cupping of the lacquer coating has developed due to shrinkage of the restrained wood substrate. (Photograph by N. Schellmann, courtesy of the V&A).

FTIR analysis of a lacquer sample from this cabinet may also provide a further hint towards deterioration due to high humidity (Herm 2009a). Figure 3.19 a shows the sample spectrum containing characteristic bands at approximately 1713, 1456-1436 and 1079  $\text{cm}^{-1}$  along with absorbances close to 3405, 2930 and 2857  $\text{cm}^{-1}$ , which are an indication of Chinese *qi* (raw) lacquer, shown in Fig.3.19b. The strong bands at approximately 1623 and 1131  $\text{cm}^{-1}$  together with absorbances near 3554, 3490, 3400 and 3245  $\text{cm}^{-1}$  are attributable to gypsum, whilst the small absorption bands at approximately 1316 and 780 suggest the presence of calcium oxalate (Figs.3.19 c-d). The suggested presence of the oxalate in the lacquer coating may be explained by exposure to high humidity levels, which favours mould growth. Oxalic acid and consequently calcium oxalate is a common biodegradation product of carbohydrates generated by mould fungi. However, as no further analysis for the presence of mould was undertaken, the exact source of this compound has yet to be determined, as it may possibly also have other natural origins.

The fact that the severe cracking and cupping did not lead to greater coating losses can be attributed to the very high lacquer concentration present in every layer of the coating. Intense caramel-brown fluorescence throughout the entire thickness of the coating structure, determined in cross-sectional microscopy under blue light irradiation, and FTIR analysis indicated that the foundation layers were bound with a high volume fraction of East Asian lacquer. This thoroughly coated the filler particles and the fibres of the incorporated textile layer, thus providing great cohesion and adhesion between the individual layers and to the



wood substrate (Fig. 3.2a).

A second example of the durability of foundations with a high proportion of lacquer binder was also apparent on the four-fold screen, where the decorated panels, containing lacquer-bound foundations and a lacquer priming of the wood (Fig. 3.2b), did not show significant losses despite some cracking. In contrast, the panel sides were progressively failing in their protein-bound foundation layer.

These results suggest that a high lacquer content throughout the entire thickness of the coating may not necessarily inhibit cracking perpendicular to the layered structure, but is effective in preventing or reducing delamination and flaking. This confirms the general understanding that priming of the wood substrate with lacquer before application of composite foundation, or high lacquer content within the foundation, seems to significantly improve adhesion between the substrate and the coating.

## 3.5. Conclusions

Comparison of the results gained from microscopic cross-sectional analysis and those of the FTIR and PyGC/MS techniques confirmed that the staining method coupled with fluorescent microscopy was a useful and reliable method to analyse the binding media in multilayered lacquer coatings. The binder groups identified for the individual coating layers of the surveyed objects gave further indication of the different failure types that may occur in East Asian lacquer structures. It helped to explain the possible causes of the deterioration mechanisms involved in the development of severe and progressive flaking. As expected, changes in humidity appear to be the major factor inducing the delamination of the export lacquer coatings. Delamination occurs predominantly at or near the interface of lower foundation layers that are bound with a low lacquer concentration or cheaper surrogates. Cohesion and some adhesion failure of foundations that contain protein or starch was found to be the most common cause for flaking of East Asian export lacquer coatings. Layers with high lacquer concentration were confirmed to show good cohesion and adhesion to their adjacent foundations, paper and textile layers and lacquer films.

### 3. Review of Damage to East Asian Lacquer Objects

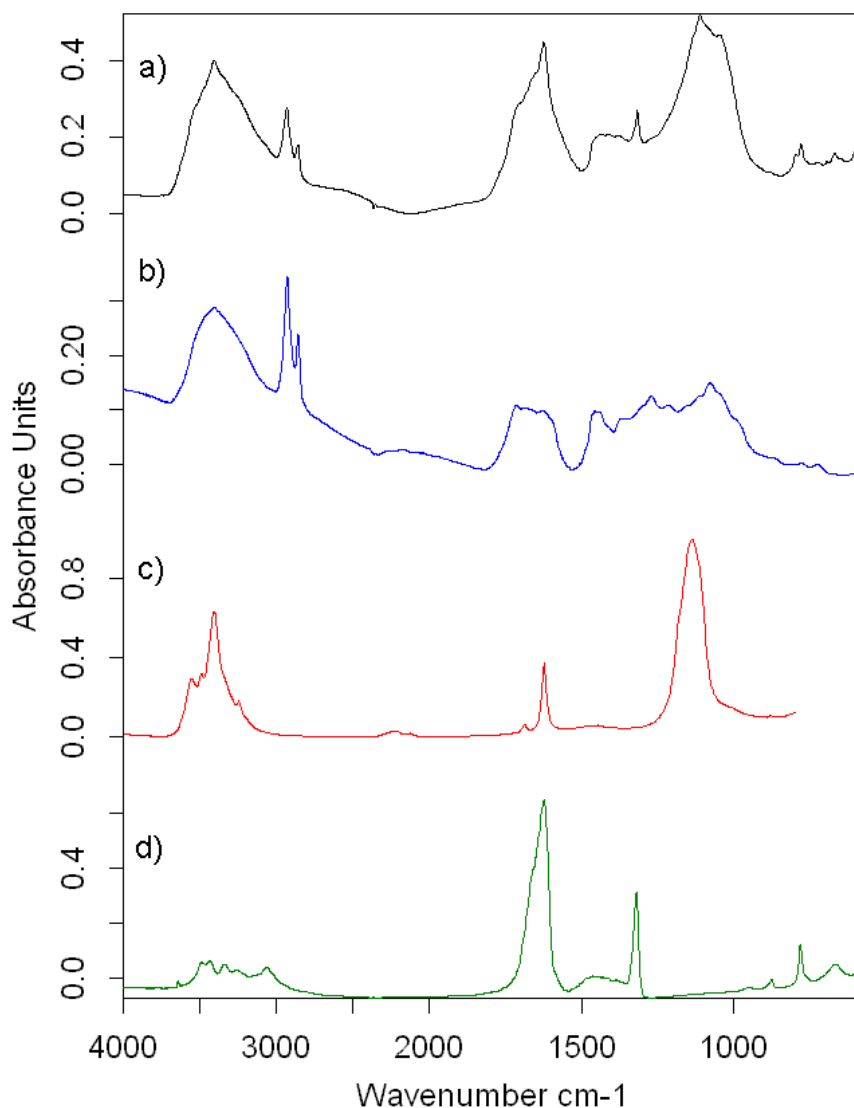


Figure 3.19.: FTIR spectra of a sample taken from the fifteenth century Chinese lacquer cabinet (F.E.7-1973) and its best matching three reference components. Spectra showing from top: (a) Chinese cabinet (F.E.7-1973) foundation, brown particles; (b) reference spectrum of Chinese raw CL1 (Bayerisches Landesamt für Denkmalpflege, Munich 1993) with characteristic absorbances at 3405, 2930, 2857, 1713, 1456-1436 and 1079 cm<sup>-1</sup>; (c) reference spectrum of gypsum from chalk from Bologna (bands at 1623, 1131, 3554, 3490, 3400 and 3245 cm<sup>-1</sup>); and (d) reference spectrum of calcium oxalate dihydrate, precipitated from aqueous solution/dispersion of Ca(OH)<sub>2</sub> and oxalic acid, with absorbances at 1316 and 780 cm<sup>-1</sup> (Herm 2009a, p. 28).

## 4. Consolidation of East Asian Lacquer Objects

### 4.1. Introduction

The lacquer objects analysed in the previous chapter were shown to be prime examples of cultural heritage objects with multilayered decorative coatings that are at severe risk of increasing coating losses during storage and display. Progressive delamination and flaking are continuously induced by even small changes in environmental conditions, and handling becomes impossible without risking further coating damage and losses. In many of these cases, protein-containing foundation layers were identified as a main cause for the development of this type of failure.

The consolidation of such progressively flaking lacquer coatings is a complex problem. Lifting flakes or areas of the coating need to be re-adhered in their original position, which requires an agent or medium that acts as an effective adhesive at the interface of the fracture surfaces. In addition, the fragile layer containing the fracture path has to be strengthened with a consolidant that penetrates well into its structure, preventing it from disintegrating further. These two actions are entirely different from each other and may not necessarily be achieved in one single step. Multi-step approaches are thus often considered inevitable for achieving successful stabilisation of a delaminating multilayered coating.

In conservation, stabilisation of such fragile structures is most commonly achieved with agents based on various natural or synthetic polymers. Choice and mixture of the polymer, solvent and solution concentration are selected depending on the specific purpose they are to fulfill. These parameters determine whether the medium serves as an adhesive or a consolidant, or both. That is, consolidants only differ from adhesives in that they usually are of lower viscosity and capable of penetrating deeply into porous materials, thus ideally providing increased cohesion within the substrate.

Considering these aspects, it is not surprising that a great variety of polymer formulations have been used for the consolidation of East Asian lacquer coatings. Some of these treatments may be more effective than others. In order to assess the existing experiences with consolidants in this field, the following chapter will review the materials and techniques commonly employed for the consolidation of flaking lacquer coatings involving ground layers. Particular emphasis will be placed on East Asian export-type lacquer ware. Based on this overview, the most

important parameters that determine the behaviour of the consolidants will be explored. The degree to which conservators may have control over them will further be highlighted. The final section of this chapter will discuss the choice of consolidants that will be used in the experimental part of this study.

## 4.2. Literature review

### 4.2.1. Approaches to the consolidation of delaminating lacquer coatings

As explained in the previous chapters, export-type lacquer ware forms a specific group in the category of East Asian lacquer objects. It usually contains only small amounts of lacquer, which is mostly prevalent in the uppermost layers of the decorative coating. The foundation layers are however made from clay powder mixed with cheaper binders. These include animal glue, blood and oil, and/or carbohydrates, such as starch or persimmon juice. As generally these types of coatings have always been considered inferior to those containing lacquer-bound foundations they have been rather neglected by Japanese scholars in the past. Hence, very little information on their conservation has been published by Japanese sources (Taguchi et al. 2001). A further complication derives from the fact that constituents of lacquer coatings are rarely clearly identified in the published reports that describe consolidation treatments. Therefore, in many cases it is difficult to clearly grasp the exact nature of the failing coating layers from the limited descriptions provided.

In contrast, Western collections had, and still have, a great need for stabilising numerous export-type lacquer artefacts that have suffered damage over the many years of storage and display. Several published reports are available that describe and discuss in great detail comparative empirical studies on the performance of different consolidants for lifting lacquer coatings. These often clearly identify materials and layer structures. Most of these studies have concentrated on objects of Chinese origin that contained protein-bound foundations (Miklin-Kniefacz 1995, 1999, Breidenstein 2000, Hagedorn 2002; Breidenstein 2000; Hagedorn 2002). These sources are a good starting point for reviewing the materials used in the consolidation of lifting and flaking lacquer coatings.

In addition, sources concerned with similar composite materials, such as traditional panel paintings and gilt wood, are also included in this review, as they resemble typical export-type lacquer structures from a mechanical point of view: they, too, are multilayered composite structures applied to wood substrates, that incorporate brittle gesso-type layers which are finished with a relatively tough top layer, such as oil paint.

## East Asian consolidation methods

In East Asian countries including Japan, lacquer ware is conserved and restored using preferably those materials and techniques that are the most similar to the ones originally employed to manufacture the object (Kitamura 1988; Yamashita 2009a,c). Aesthetic properties of the conservation materials play a very important role. The general aim is not to disturb the aesthetic balance within an object by adding artificial materials or those that were untypical at the object's time of manufacture. Primarily, this follows the aim to "preserve the historic and artistic value of urushi artefacts for future generations and to respect their intrinsic materiality" (Rivers and Yamashita 2006). Even though wider approaches have been followed in recent years that include both traditional and more modern methods and techniques (Rivers 2005; Suzuki 2005), only little information has been published by East Asian sources that report the consolidation with other than traditional materials. Yamashita (2009a) and Kitamura (2009) both suggested that a significant rationale for choosing traditional materials in Japan may be the simple fact that most lacquer conservators are artists. They have not usually been trained to work with many other modern materials and techniques, and hence tend to consistently revert to using traditional methods. Also, the view is widely accepted that traditional materials newly added to lacquer coatings degrade at a similar rate as those of the original material, unlike synthetic adhesives and consolidants (Murose 2001; Kitamura 2009).

**Lacquer-based consolidants, starch and funori** For the consolidation of most types of lacquer ware, adhesives based on lacquer are the most commonly used in Japan and East Asia. Consolidant formulations may consist of pure lacquer, sometimes diluted in hydrocarbon solvents to improve penetration ability. Also, more complex mixtures of lacquer with wheat starch paste (*shofu nori*), rice paste or Japanese hide glue (*nikawa*) are frequently used (NRICPT 2005; Yamashita 2009a). Funori, a polysaccharide adhesive extracted from red seaweed such as *Gloiopeltis furcata*, is another consolidant traditionally employed (Yamasaki and Nishikawa 1970; Yamashita 2009c).

Mixtures of wheat flour paste (*mugi nori*) and raw lacquer (*ki urushi*) are known in Japan as *mugi urushi* and are traditionally used for the consolidation of structural damage in lacquer ware. Due to its high adhesive strength, *mugi urushi* is preferably used to consolidate structurally failed areas of the multilayered coating (Piert-Borgers 1987, p. 13) as well as for cracks and other structural damage in the wooden substrate (Kato 1988; Matsumoto and Kitamura 2008). When diluted with appropriate solvents, such as the petroleum ether ligroin or the more slowly evaporating alkyl (C<sub>5</sub>–C<sub>8</sub>) benzene HAN 8070 (Exxonmobil), *mugi urushi* can be prepared having a very low viscosity. This enables it to penetrate deeply into a damaged or porous material. As opposed to solvent diluted or non-diluted pure lacquer, *mugi urushi* has the great advantage that with the added wheat starch paste, water is introduced into the matrix. This induces the lacquer to

#### 4. Consolidation of East Asian Lacquer Objects

polymerise comparatively fast, even if it is applied in a relatively thick layer deep inside the object's coating structure (Matsumoto and Kitamura 2008). If a formulation with lesser water content is used, consolidation with lacquer is a comparatively time-consuming undertaking, as its slow polymerisation requires very long clamping times until sufficient hardening has occurred. It is known from Vietnam that lifting coating layers on lacquer paintings are often conserved by complete impregnation with raw lacquer, subsequently kept in a press for about one year to facilitate full polymerisation of the natural polymer (Herm 2009b).

According to the general approach of using similar materials for consolidation as for initial manufacture (e.g. Yamashita 2009a), it appears to be widely recommended and accepted that failing protein-based layers in lacquer coatings are consolidated with Japanese hide glue. Interestingly, however, it also seems to be common practice to use lacquer based *mugi urushi* for the consolidation of major structural damage in lacquer coatings that contain protein glue-bound foundation (*nikawa shitaji*) layers (Kato 1988; Katsumata 2003; Matsumoto and Kitamura 2008). Additionally, dilute *ki urushi* is sometimes used to 'pre-consolidate' *nikawa shitaji*, before *kokuso* (a mixture of *mugi urushi*, sawdust, finely cut hemp fibres and fine clay powder) is applied to fill in losses in the lacquer coating (Matsumoto and Kitamura 2008).

**Synthetic resins** Despite appearing not to be a popular choice in Japanese lacquer conservation, synthetic resins are known to have been used as consolidants for lifting paint layers on Japanese paintings and sculptures with lacquer grounds. Yamasaki (1957) reported that synthetic resins, such as "moderately polymerised methyl methacrylate" in diverse solvents, and aqueous solution of poly(vinyl alcohol) (PVAL) have been favoured for consolidating peeling protein-bound paint layers since the end of the 1930s. Allegedly, they replaced less satisfactorily performing rice starch paste and aqueous glue solutions. In cases of thick lifting layers, Yamasaki and Nishikawa (1970) recommended the use of 15-20 % poly(vinyl butyral) in ethyl- or butyl alcohol. For the consolidation of protein-bound grounds they suggested formulations of 5-10 % solution concentration. The effectiveness of acrylic dispersions for re-adhering warped lacquer flakes was further pointed out by Nakazato (1978). Additionally, Riederer reports on the common use of acrylic polymers and PVAL for the consolidation of lacquer coatings in Japan, whilst poly(vinyl acetates) (PVAc), epoxy resins and isocyanate were primarily chosen for "special cases" (Riederer 1979, p. 121).

#### Methods used in Western collections

The Western approach to consolidation of art and cultural heritage objects is generally driven by the aim to preserve the original material with the least possible physical and chemical interference by any added treatment agent. This includes

the feasibility of keeping the object re-treatable in the future (for a detailed discussion on reversibility, internal consolidation and re-treatability see Appelbaum 1987). East Asian lacquer is insoluble once polymerised and can only be removed by mechanical means. In cases where previous applications of lacquer on objects were deemed unsatisfactory, this cross-linked polymer has frequently caused significant problems with its removal (e.g. Chase 1988). This is why in the West lacquer is currently not widely accepted as a desirable consolidant. Furthermore, East Asian lacquer is considered too hard and strong for many coatings that contain aged and fragile components. It is held responsible for inducing further flaking of unevenly consolidated coatings, as pointed out for example by Nakajima (1988).

For lacquer ware with simplified foundation layers that contain no lacquer at all, a variety of natural and synthetic materials have been used in the past. Breidenstein (2000) reviewed a number of possible consolidants for these less prestigious types of lacquer coating. A further review will be given in the following section.

#### 4.2.2. Natural polymers

##### Protein-based glues

Animal glues have a long tradition as adhesives and consolidants for flaking East Asian lacquer coatings as much in East Asia as in the West. For multilayered coatings that contain foundation layers based on a mixture of protein binder and clay powder, protein-based consolidants are useful and have great acceptance amongst conservators.

**Cold-liquid fish glue** A common choice appears to be cold liquid fish glue for its ease of application and its reputed mechanical strength (Webb 1993, 2000; Breu and Miklin-Kniefacz 1995). However, a recent review on published data on the properties of animal glues could not ascertain this alleged strength when compared with alternative protein glues (Schellmann 2007). It rather suggested that cold-liquid fish glue had inferior strength properties than hide glues and isinglass, and that it was less stable in fluctuating environmental conditions. Uses of this type of protein glue for the consolidation of lifting decorative layers on paintings and sculptures are not reported, which suggests that cold-liquid hide glues are considered unsuitable for such layers. Also, its often unknown additives still give rise to doubts about its long-term ageing properties and whether it remains fully resoluble with time.

**Isinglass and mammalian hide glues** Sturgeon glue, or more generally isinglass (i.e. glue extracted from fish bladders), has given good results for the consolidation of Chinese screens (Piert-Borgers 1993; Breidenstein 2000). Albeit, in

#### 4. Consolidation of East Asian Lacquer Objects

some cases it has also been reported to lack sufficient adhesive strength to hold down severely lifting lacquer coatings (Miklin-Kniefacz 1995; Hatchfield et al. 2010). These contradictory results can be explained by differing layer thickness of the top lacquer layers that may have exerted different levels of stress on the bondline. With respect to the successful application of isinglass, parallels can be drawn to the consolidation of panel paintings and painted sculptures that feature similar coating structures, with brittle, protein-bound foundation layers underneath stressed top paint coats. Isinglass is a widely used consolidant for their lifting and flaking multilayered coatings because of its high mechanical strength and elasticity (e.g. Luybavskaya 1990; Sandner et al. 1990, sections 6.4.1. and 9.2.3; Habel-Schablitzky 1992; Petukhova and Bonadies 1993; Foskett 1994). Isinglass has a major advantage over mammalian hot hide glues in that it gels at a lower temperature and thus can be applied more easily, usually achieving better penetration results, too (e.g. Webb 2000, p. 165; Hagedorn 2002). This is because severely degraded lacquer coatings are generally not recommended to be heated or warmed to temperatures that would allow good penetration of hot hide glues. Aged lacquer surfaces will also be susceptible to damage by the combined exposure to water and heat (Webb 2000, p. 80), which renders hot protein glues a risky choice. On the other hand, the delayed gelation of isinglass solution may also have disadvantages: it can expose water-sensitive layers in the coating structure to unwanted swelling and leaching. This may itself cause significant additional damage to the coating and should be considered before application.

**Remarks on the stability of protein glues** A further general problem of protein glues is their affinity to shrink or swell with changing ambient humidity levels. Long term storage and display in fluctuating environmental conditions embrittle the protein glues and increase their likelihood of failure over time (Hedley 1988; Mecklenburg 1988; Mecklenburg et al. 1998; Zumbühl 2003). The degree to which a protein consolidant has the tendency to exert substantial stresses on the consolidated coating structure depends on its mechanical properties. Generally, these differ for the individual types of protein glues, and are mostly dependent on their molecular weight distribution and species of origin. A detailed review on the properties of animal glues relevant to conservation was previously published by the author of this thesis (Schellmann 2007). Considering the general sensitivity of these consolidants to changing relative humidity levels, some conservators prefer not to use protein-based consolidants under environmentally unstable conditions, but opt for synthetic polymer formulations instead (e.g. Payer et al. 1998; Schniewind 1998, p. 90).

#### Polysaccharide-based polymers

**Native starch** Starch paste with its gel-like consistency has traditionally been used for lacquer consolidation and has the advantage of introducing comparatively



little water to the coating structure. Compared with other aqueous consolidant formulations, it reduces the risk of swelling and leaching of water-sensitive layers. Its adhesion strength has been shown to be sufficient in holding previously lifting lacquer flakes in their correct position (Breidenstein 2000). However, penetration of starch into a fragile layer may be very limited due to its high viscosity and large starch molecules (Horie 1987, p. 135; Nicolaus 1998, p. 230). Pure starch films may be problematic as they form rather highly strained and brittle films, with wheat starch developing lower strains and greater adhesive strength than rice starch (van Steene and Masschelein-Kleiner 1980; Sun et al. 2010). To improve elasticity, wheat starch is therefore sometimes mixed with isinglass solutions. Starch added to isinglass solutions may also reduce the ability of the protein solution to penetrate deeply into a porous material and avoid undesired effects, such as excessive swelling, starvation of joints or formation of insufficient film thickness. In the context of paint consolidation on canvas, a detailed discussion on starch paste used as a thickening agent for isinglass is given by Springob (2001). On a Chinese lacquer screen, empirical consolidation tests with a mixture of isinglass and wheat starch have produced very satisfactory results (Breidenstein 2000).

**Starch / cellulose ethers and funori** Korn (2006) tested several polysaccharide-based consolidants on flaking Burmese lacquer coatings and found that the modified starch Kollotex 1250, a potato starch ether, resulted in successful treatment. On the other hand, cellulose ethers such as Klucel G, Tylose MH300 and methyl-cellulose provided insufficient adhesive strength (Korn 2006, pp. 132-34). This was also found for funori, despite its reported common use in Japan as an adhesive for thin lifting lacquer layers (Yamasaki and Nishikawa 1970). In the Western world, funori is widely used as a consolidant for matt paint (Winter 1984; Hansen et al. 1991; Michel et al. 2002; Swider and Smith 2005; Pataki 2007), although successful uses for the consolidation of multilayered lacquer coatings have indeed not been reported.

## Waxes and natural resins

In the past, waxes and wax-resin mixtures were regularly employed for the consolidation of damaged lacquer ware. In several instances, successful applications were reported for the stabilisation of flaking and lifting Chinese lacquer coatings (Franke 1976a,b, 1978; Chase 1988). However, wax used as a consolidant on lacquer coatings has also been held responsible for the development of further cracks on objects at the Linden Museum in Stuttgart/Germany. These cracks had appeared after the conservation work had been completed (Nakajima 1988).

As waxes alone lack sufficient strength to hold stressed lacquer flakes in place, natural resins were often added. An example of beeswax/dammar resin mixture being used for the consolidation of delaminating gilding and polychromy that

#### 4. Consolidation of East Asian Lacquer Objects

contained gesso-type foundation layers was reported by Payer et al. (1998). The effectiveness of wax-resin mixtures may however still be limited, as natural resins, such as dammar, rosin and shellac, are also only of medium strength and embrittle with age (Schniewind 1998). Hagedorn (2002) demonstrated that a solution of 20% dammar in turpentine failed to hold previously lifting lacquer flat in place.

On the whole, the use of wax-resin mixtures as a consolidant for lifting coating layers appears to be problematic. Shellac as an additive or adhesive is generally considered inappropriate by current conservation standards. This resin is known to cross-link over time, which renders it (or any consolidant that contains this resin) difficult to remove when aged (e.g. Koob 1979, 1984). Furthermore, the wax content of such consolidants has also caused problems with regards to their removability (e.g. Rivers and Umney 2003, p. 568) and may hinder future applications of East Asian lacquer. Wax reputedly does not allow lacquer to dry properly when the latter is applied over a wax coating, which is why Japanese conservators recommend not to use wax-based consolidants at all (Nakajima 1988; Matsumoto and Kitamura 2008). However, contrasting to this general and widely accepted assumption, Piert-Borgers (1993, p. 192) and Heckmann and Dei Negri (2002, p. 192) reported on their experiences that lacquer does indeed dry under these circumstances. In any case, since the mid 1990s wax-based consolidants appear to have been rarely applied and have only been used in instances where old treatments with wax required re-treatment (e.g. Breidenstein 2000).

#### 4.2.3. Synthetic polymers

Of the synthetic polymers available, a range of thermoplastic resins and their mixtures have found wide use in the consolidation of lacquer coatings and related composite materials. One of the advantages of these polymers is that they can be applied in solution with diverse organic solvents or as aqueous dispersions. The variety of options is mirrored in the types and numbers of formulations used for lacquer consolidation. Unfortunately however, the literature does not often provide detailed information on the exact type of polymer, the solvent/diluent and the actual polymer concentration of the formulations. This makes an assessment of the consolidants and application procedures rather difficult. Due to this lack of information and despite the great number of different synthetic polymers used for the consolidation of East Asian lacquer coatings, only the most common ones will be reviewed in the following paragraphs.

Special applications methods, such as that of using acrylic monomers that are polymerised in situ by electron beam, which was famously used to consolidate lacquer-based coating layers on figures of the Terracotta Army of the first Chinese emperor (Langhals and Bartelt 2003; Langhals et al. 2005) will be omitted in this survey. This method was mainly chosen to counteract the specific nature of archaeological lacquer, which developed “severe cracking and buckling of the lacquer” during drying following excavation (Thieme 2001). This example

thus did not represent the more common degradation mechanisms considered in the present work, which are caused by more normal environmental conditions encountered during display and storage in museums and collections.

## Acyclic polymers

**Acrylic solutions** Acrylics in solutions with aliphatic and aromatic hydrocarbons are desired consolidants for degraded East Asian lacquers, as their non-polarity is considered to pose the least hazard for sensitive, photodegraded surface layers of the lacquer coating (e.g. Breidenstein 2000; Webb 2000, p. 72; Schellmann 2003, pp. 18-20). The most commonly used acrylic polymers appear to be Paraloid B 72 (ethyl methacrylate/methyl acrylate copolymer), and Paraloid B 67 (isobutyl methacrylate copolymer). They are usually dissolved in hydrocarbon solvents such as toluene, xylene, acetone and ethyl acetates and have produced successful consolidation results on various lacquer objects (e.g. Yamasaki 1957; Chase 1988; Chase et al. 1988; Gillis 1998; Webb 2000; Lencz 2005; Hatchfield et al. 2010). However, high solution concentrations appear to be required for efficiently re-adhering lifting coatings. Webb (2000, p. 82) remarks that a 15% solution of Paraloid B 72 in xylene “has insufficient strength to keep distorted lacquer in place”, whilst at a 25% solution concentration this polymer will not penetrate sufficiently into the ground layer. Hagedorn 2002 reported that 10-20% solutions of these polymers in ethyl acetate or benzene may be successful after long clamping times, although in some cases she found their adhesive strength insufficient, too. Overall unsuccessful consolidation tests with Paraloid in non-polar solvents or ethyl acetate were reported by Breidenstein 2000, who suggested that too low polymer concentrations in the bondline (i.e. starved joints) may have been one of the major causes for their failure.

**Acrylic dispersions** Generally, aqueous acrylic dispersions appear to perform successfully (Miklin-Kniefacz 1995) and are recommended consolidants not only for lifting lacquer coatings but also for the paint layers of panel- and canvas paintings (Nicolaus 1998, pp. 221, 234). Nakazato (1978) reported the successful application of acrylic dispersions, particularly when applied in two stages. Often, acrylic dispersions are also chosen for applications in combination with the use of warm tacking-irons (e.g. Miklin-Kniefacz 1995; Webb 2000, pp. 83-84). Formulations based on butyl acrylate (BA) and methyl methacrylate (MMA) copolymers, such as Plextol D360 and D498, Lascaux 360 HV (MMA+BA+ acrylic acid ester) and Mowilith DM771 (acrylic acid esters) diluted with water produced good results with respect to penetration into fine cracks and small pores (Breidenstein 2000; Hagedorn 2002). For gaining sufficient adhesive strength for lifting lacquer, dispersions with a solid content of around 50% were required. Undiluted Rhoplex AC 234 with a solid content of around 46% has shown particularly good results when used for the consolidation of severely distorted pieces of lacquer coating.

#### 4. Consolidation of East Asian Lacquer Objects

Although, it has been pointed out that some damage might occur on strongly degraded lacquer surfaces due to the high pH of 9-10 of this dispersion (Webb 2000, p. 83; CAMEO 2009).

### **Poly(vinyl acetates) (PVAc)**

**Solutions and dispersions** Similarly to acrylates, PVAc polymers are also applied as solutions and dispersions, although again, often detailed information of the exact formulations is not provided. Many different PVAc formulations appear to have been used in the past for the consolidation of lifting and flaking lacquer coating structures, as well as for fragile paint layers on fine art objects (Chase 1988; Nicolaus 1998, p. 234). These polymer types have also been reported to show good stability over the period of several decades (Lencz 2005).

According to Webb (2000, p. 83), the pure PVAc homopolymer AYAF (previously Vinylite A, known in Europe as Mowilith 50) at solution concentrations of 25 % in ethanol or acetone showed good application properties and generally works well for holding down lifting coatings. However, other formulations of this polymer, such Mowilith 30/50 (containing lower molecular weight fractions of the polymer) in a 10-20 % solution in Shellsol T, have proven to produce unsatisfactory results in a study conducted by Hagedorn (2002). The main problems appeared to be long clamping times and insufficient adhesive strength, which manifested itself in the renewed lifting of the consolidated lacquer flakes some time after consolidation. These differing results may suggest that higher average molecular weight formulations, higher solution concentrations and the use of polar solvents significantly improve the performance of the PVAc (cf. Schniewind and Kronkright 1984; Schniewind 1998). Similar observations had been made for acrylic consolidants, as described in the previous paragraphs.

The PVAc dispersion CM Bond M4 is mentioned as an effective consolidant for thick, powdery ground layers of Chinese lacquer ware. However, this polymer formulation has also been found to sometimes harm sensitive, degraded lacquer surfaces, for reasons as yet unexplained (Webb 2000, p. 83). Powdery ground layers on lacquered Japanese armour have also been successfully stabilised with a two-stage application involving a 10 % Paraloid B 72 solution in xylene, followed by an unspecified 20 % PVAc solution. The latter was required to hold down the lifting urushi layers (Lencz 2005).

#### 4.2.4. Major challenges encountered during consolidation

##### **‘Memory’ of distortion**

The ‘memory’ of the lacquer layers for their distorted state is one of the most significant difficulties encountered during their consolidation (Webb 2000, pp.

62, 80). Lacquer coatings are known to have a strong tendency to revert back into their previously distorted state after flattening and reattachment. Hence, this causes many consolidants and bondlines to fail, sometimes weeks after the consolidant has been applied. In order to withstand the stresses exerted by these layers, it is therefore important that the consolidant fulfills two criteria: it is to improve the cohesive strength of a fragile layer and is also required to act as a sufficiently strong adhesive between the old, re-adhered fracture surfaces. Unsurprisingly, the best consolidation results for such cases were mostly achieved with multi-stage applications of consolidants and with those where formulations with high polymer concentrations were chosen, as mentioned earlier in this review section.

## Sensitivity to water

**Importance of pH** Water-based consolidants and adhesives generally appear to perform most successfully by increasing the elasticity of distorted lacquer coatings and enabling their flattening (Breu and Miklin-Kniefacz 1995; Miklin-Kniefacz 1995). Nevertheless, it has to be kept in mind that aged lacquer coatings may react very sensitively to these formulations, as with time their degraded surfaces become very susceptible to elevated pH. The pH of East Asian lacquer tends to range between 4.5–4.8 when new and values as low as pH 3.5 when aged (Rivers and Umney 2003, section 16.8.5.1; Schellmann 2003, pp. 23, 38). The effect of water and aqueous solutions on degraded East Asian lacquer surfaces has been discussed in detail in previous publications (e.g. Schellmann 2003; Schellmann and Rivers 2005). Hence, many synthetic polymer dispersions appear to be problematic: polymer dispersions generally contain emulsifiers that only work at specific pH values. As a consequence, acrylic dispersions are usually buffered at pH values between 7 and 9, whilst the PVAc dispersions used in conservation normally range between pH 3.5 and 7. Unless a dispersion is used that has an equally low pH as that of the degraded lacquer, it can be expected to further harm the lacquer surface during the application of the consolidant.

**Protective measures** To prevent further damage to the already photodegraded lacquer coatings, aqueous polymer formulations have to be chosen with great care. Solutions or dispersion with high pH values should generally be avoided, unless the degraded lacquer surface is temporarily coated with a protective isolation layer. This could for example be a synthetic resin dissolved in a non-polar hydrocarbon solvent, as suggested by Breidenstein (2000).

Unfortunately, temporary coatings may cause problems themselves. Coatings can infiltrate into micro-fissures on degraded lacquer surfaces (which have been observed to commonly show dimensions of up to 30  $\mu\text{m}$  in width and depth, see cross-sections in Appendix D, pp. 305, 320 and 327) and may not be fully removable at a later stage. This could impair surface appearance, mechanical properties

#### 4. Consolidation of East Asian Lacquer Objects

and possible future surface treatments with East Asian lacquer. Alternatively, traditional Japanese *urushi-gatame* or *suri-urushi* treatments may be considered, where diluted lacquer is applied to the photodegraded surface to fill the micro-cracks to different extents (Yamashita 2009b). The use of such (irreversible) treatments however requires much experience and good technical skills to be successfully applied. Current research is investigating the mechanical effects and problems associated with additional thin films on aged lacquer coatings (Elmahdy et al. 2010; Elmahdy 2010; Thei 2011; Liu (in progress)).

Generally, polymers dissolved in non-polar hydrocarbon solvents appear to be the least problematic alternative, with respect to causing further surface damage. However, as the literature review has suggested that they are less successful regarding their mechanical performance, further research is necessary to determine, why exactly they fail and in what way they might be manipulated to perform more successfully.

### 4.3. Criteria for consolidant selection

The literature review has not only demonstrated that a diverse selection of different materials are commonly used as consolidants for lifting and flaking lacquer coatings. It has also found that the same polymers and/or consolidant formulations can induce rather varying results, ranging between entirely ineffective and successful applications. Unfortunately, descriptions of why exactly some consolidants were unsuccessful in terms of their physical and mechanical behaviour are only rarely available. To clarify this issue, the following chapter sections will investigate the parameters that have the most influence on the mechanical behaviour of consolidants.

#### 4.3.1. Requirements for consolidants

**General requirements** In conservation, consolidants are required to meet a range of criteria in order to be considered an acceptable or suitable choice. Like any agents applied or added to objects during conservation, consolidants should ideally be limited to the specific purpose they are supposed to remedy, whilst otherwise having the least possible interference with the original material of the structure they are applied to. Rosenqvist (1963), Grattan (1980), Williams (1988) and others, have discussed these requirements in detail. Those that directly or indirectly have a bearing on the mechanical behaviour of the consolidants are listed below.

Consolidants are required to

- strengthen the structure uniformly, without adding new stresses to the original object due to shrinkage or swelling,

- be chemically and physically compatible with other materials involved,
- have long-term stability and not contribute to or increase degradation of the object,
- enable future re-treatment of the object and
- have good handling properties.

Assuming that a consolidant used for the stabilisation of delaminating and flaking lacquer coatings will not be visible from the object's surface, the optical properties of the consolidant are regarded of less importance in this study. The effects of colour change of various polymers and adverse visual effects of consolidants on the surface appearance of objects will thus be omitted from this discussion. Further information in this topic can be found in many publications, e.g. Horie (1987), de la Rie (1987, 1988a), Horton-James et al. (1991), Hansen et al. (1993, 1996), Down (2009) and Down (2009). Long-term chemical compatibility and stability, resolubility of the consolidant, and whether a consolidated object remains re-treatable are very important issues, but will also not be subject of this study. These aspects are further discussed in publications for example by Down and Lafontaine (1980), Howell et al. (1984), Horton-James et al. (1991), Down et al. (1996), Hansen and Bishop (1998) and Down (2009).

Indeed, it would go beyond the scope of this work to review the principles of consolidation encompassing all aspects that are relevant for conservation. As the present thesis is mainly concerned with the mechanical performance of consolidants, works by other authors should be consulted for more general or comprehensive discussions of the principles of consolidation, as provided by Ashley-Smith and Wilks (1987), Rivers and Umney (2003, Chapters 4, 12) and Schniewind (1998). Detailed aspects regarding the consolidation of paintings are further considered by Nicolaus (1998) amongst others.

**Characteristics of fractured protein-bound foundation layers** Delaminating and lifting export-type lacquer coatings have specific characteristics which influence the performance of a consolidant. Typical fracture surfaces of protein-bound foundation layers have a certain roughness which render their join with a more or less good fit. These foundation layers are also naturally characterised by significant porosity, which is a typical feature of highly filled gesso-type layers. A further essential feature to recognise – that generally applies to most aged and deteriorated coating structures – is that aged and damaged layers usually contain many additional cracks or flaws within the material structure that require stabilisation and re-adhering.

Porosity has a deleterious effect on both the elastic properties and strength of a material. Any existing pores reduce the material's cross-sectional area across which a load is applied, which reduces its strength and causes stress concentration within the material matrix. Indeed, the flexural strength of a material has been shown to decrease exponentially with volume fraction porosity (Callister, Jr. 2000,

#### 4. Consolidation of East Asian Lacquer Objects

p. 412). In order to strengthen effectively a fragile and porous structure such as aged protein-bound foundation layers, the number of pores and flaws need to be reduced, i.e. filled.

Therefore, two consolidant properties are of particular importance for the successful stabilisation of fragile foundation layers and the improvement of their mechanical performance: the consolidant has to serve as an adhesive that re-adheres the lifting coating, whilst simultaneously acting as a penetrant that internally stabilises the fragile structure or layer. How well this is achieved by a consolidant is dependent on the parameters discussed below.

##### 4.3.2. Factors influencing consolidant properties and performance

###### Adhesion

The mechanical strength of a bonded joint is dependent on the effective adhesion between the adhesive and the substrate, and on adequate cohesion within the bulk adhesive itself. Adhesion to a substrate can be achieved by mechanical interlocking through penetration of an adhesive or consolidant into a rough and porous surface, and by interfacial bonding. There are several theories that explain chemical adhesion: that of diffusion, the electronic theory and adsorption.

The **diffusion theory** assumes that mutual diffusion (inter-diffusion) occurs between polymers across their interface. This is best achieved if the constituent molecules of the polymers are relatively mobile and are characterised by similar solubility parameters. Mobility of a predominantly amorphous polymer can be promoted or improved by the addition of a solvent or the use of heat. However, diffusion is unlikely to occur if at least one of the polymers involved is or remains above its glass transition temperature ( $T_g$ ), in a crystalline or a highly cross-linked state (Kinloch 1987, pp. 66-73).

The **electronic theory** proposes that adhesion by electron transfer develops at the adhesive/adherend interface, if the two materials involved have different electronic band structures. The resulting formation of a double-layer of electrical charge will induce electrostatic forces that are thought to have a significant influence on interfacial adhesion (Deryaguin and Smilga 1969, p. 74; Kinloch 1987, p. 74). However, this theory has been extensively criticised, as these forces have been shown experimentally to be negligible when compared with secondary bonds induced by van der Waals forces (e.g. Kinloch 1987, pp. 77-78).

The **adsorption theory** is the most widely accepted theory to explain the main causes of adhesion between a substrate surface and an adhesive. It suggests that adhesion is induced by two types of interatomic and intermolecular bonds: secondary intermolecular forces and chemical adsorption that develop between the



substrate and the adhesive if they are in close molecular contact. Chemical adsorption involves primary ionic, covalent and metallic bonds. Of the secondary forces, the van der Waals interactions and hydrogen bonds play the most important role. Secondary bonds are much weaker than primary bonds, but have been shown experimentally to be sufficient to account for commonly measured joint strengths of adhesives. That is, as long as the adhesive behaves in a brittle manner and there is no great amount of plastic deformation during joint fracture. In fact, such joints usually fail at energy levels well below their theoretical strength induced by the interactions of secondary forces, due to the presence of air-filled voids, flaws and geometric features that induce stress-concentrations (Andrews and Kinloch 1973a,b, p. 79; Kinloch 1987, p. 79). Thus, in most adhesives, adhesion is only determined by these secondary forces. The development of ionic bonds may be a factor in protein adhesives (Skeist 1965, p. 8). In other polymer adhesives, primary bonds can be achieved by special methods involving chemically reactive and cross-linking adhesives and substrates.

The contribution of mechanical interlocking to adhesion generally appears to be half as important as that of the chemical interactions (Kinloch 1987, p. 60). Thus, the level of strength that can be achieved by an adhesive is predominantly governed by the bond strength that its molecules develop internally and with the substrate. The amount of energy that is required to break these forces quantifies the adhesive strength of a bond. However, in the case of very porous materials, such as gesso-type foundation layers, mechanical interlocking may be of greater importance. Their rough fracture surfaces, which need to be re-adhered, are far from ideal for achieving optimal chemical interactions, as they will neither be flat nor free from contaminants and other loose particles. The aspect of mechanical interlocking is therefore likely to have a much greater significance than under more common applications of adhesives in the field of engineering.

## Wetting

Adhesion requires intimate contact on a molecular level between the adherend (i.e. the fracture surface) and the adhesive (consolidant). If a consolidant is in the liquid phase, intimate contact is only possible provided the consolidant can displace the air and spontaneously spread (i.e. wet) the fracture surface. Wetting is also a prerequisite for penetration into pores of the substrate.

The wetting ability of a liquid consolidant applied to a solid surface is a function of the surface tensions (or surface free energy,  $\gamma_m$ ) of the substrate and the liquid, and is further controlled by the viscosity. According to the laws of thermodynamics, a liquid can spontaneously wet a surface when its surface free energy is lower than that of the solid. In other words, a wetting agent with lower surface tension has a stronger attraction to the substrate surface than to its own molecules (for detailed discussion see for example Skeist 1965, Allen 1984, Ashley-Smith and Wilks 1987, Horie 1987, pp. 18-20 or Kinloch 1987, Chapter 2).

#### 4. Consolidation of East Asian Lacquer Objects

Table 4.1.: Surface free energy (surface tension),  $\gamma_m$ , and viscosities,  $\eta$ , of some solvents commonly used for consolidants, measured at 20 °C (Masschelein-Kleiner 1981; Pietsch 2002, pp. 108-109).

SOLVENT	$\gamma_m$ [mN/m]	$\eta$ [mPa.s]
Water	72.8	0.89
Ethanol	22.9	1.07
Acetone	24.9	0.31
Ethyl acetate	24.7	0.41
Xylene	29.0	0.56
Toluene	29.1	0.54
Benzene	29.6	0.60

The fracture surfaces of foundation layers consisting of mineral filler particles and protein-based binder matrix are expected to have higher surface energy than most liquid polymer formulations that may be applied during consolidation. Organic compounds, such as polymeric adhesives, usually have relatively low surface free energies of less than 100 mN/m, as opposed to high energy surfaces, for example of metal oxides and ceramics that range at around 500 mN/m and greater (Kinloch 1987, p. 24-26). Therefore, most consolidants should be able to wet these substrates without much difficulty. Of the commonly used solvents, water has the highest surface energy and thus will be expected to show the least effective wetting of such foundation layers compared with other hydrocarbon solvents used (Table 4.1). Its wetting ability can be improved by the addition of a suitable solvent with lower surface free energy, hence the common addition of ethanol in water-based consolidants.

#### Adhesive layer thickness

A prerequisite for effective bonding between two re-adhered fracture surfaces is the formation of an adequate adhesive layer by the consolidant. In the case of rough surfaces that show limited fit – like the ones of fractured foundation layers – this bondline needs to be of sufficient thickness. Too little adhesive will fail to fill all the gaps between the two adherends and leave the joint starved. If stresses are applied to a bonded structure where even, intimate contact between the adhesive and adherend is lacking, uneven distribution of these stresses will lead to stress concentration and induce failure of the bonded structure. In practice, it is therefore generally aimed to achieve a bondline thickness of just sufficient width to fill all the gaps between the adherends and to provide intimate contact between

them (Skeist 1965).

Bondline thickness is influenced by the rheological properties of the liquid polymer, i.e. on how well the consolidant spreads between the adherends and to what degree it penetrates into the porous substrates (adherends). The spreading is dependent on the viscosity and wetting ability, and can be manipulated by the pressure per unit area that is applied to the bonded structure during clamping and subsequent drying or curing.

## Penetration ability

Porous substrates are permeable by liquid consolidants, at least to a certain degree. Provided adequate wetting of the substrate surface occurs, the transport of the consolidant into the porous substrate is governed by its permeability, i.e. its ability to let fluid flow through its interconnected network of pores. The permeability of the substrate is governed by the specific nature of the material, as well as by the viscosity of the fluid. The rate of flow is further influenced by the pressure differential across the flow path (e.g. Schniewind 1998).

As pressure impregnation or vacuum treatments are often inappropriate or difficult to realise with many art objects, most consolidation treatments take place under normal atmospheric pressure. Consequently, during simple brush-application, for example, the pressure differential is driven by gravitational forces, surface tension between the liquid consolidant and the porous substrate, and by capillary pressure (see Schniewind 1998 for a detailed discussion). Under most circumstances, the gravitational forces as well as the pore size have to be taken as a given. This means that the most influential parameters that govern penetration are the viscosity of the liquid consolidant, which principally should be as low as possible for best penetration results, and the capillary action. Respective values for some example solvents are given in Table 4.1 .

The capillary action varies for different fluids and depends on their chemical nature and interaction with the capillary walls, i.e. their surface tension. Again, the polarity of the consolidant influences its ability to penetrate into the porous substrate. Liquids of higher polarity and surface tension generally travel further in capillaries, whilst their flow rate is improved with decreasing viscosity. Also, the smaller the capillary diameter, the further a given fluid will travel (Ashley-Smith and Wilks 1987, p. 19). The strong affinity of polar fluids to polar substrates can however induce further actions that may prevent penetration: it has been shown that polar consolidants can become adsorbed by the wood substrate due to strong hydrogen bonding, which significantly reduces their mobility and penetration (Nicholas 1972, as cited by Schniewind 1998). Finally, penetration can also be hindered by an unsuitably large molecular size or spatial configuration, i.e. the extent of branching, of the dissolved polymer (e.g. Schniewind 1998, p. 563; Rivers and Umney 2003, p. 563).

#### 4. Consolidation of East Asian Lacquer Objects

(For further discussion see Masschelein-Kleiner 1981; Banik and Krist 1984, pp. 133-135; Ashley-Smith and Wilks 1987, p. 125; Schniewind 1998, p. 125).

### Viscosity ( $\eta$ )

The viscosity, being a measure of a liquid's resistance to flow, has already been mentioned as an important factor that influences wetting and penetration. Viscosity is governed by the bonding strength between the molecules of the fluid. It increases with increasing strength of the secondary forces between the molecules, which in turn rise with increasing polarity of the molecules, higher molecular weight and higher concentration in solution. Water, which forms strong hydrogen bonds between its highly polar molecules, therefore has a higher viscosity than less polar or non-polar hydrocarbon solvents, such as acetone (propan-2-one) or xylene (dimethyl benzene), as shown in Table 4.1. Fluids containing larger molecules, such as long-chain hydrocarbons, develop much higher viscosities. Hence, the viscosity of a polymer solution can be manipulated by the choice of average molecular weight of the polymer, its concentration, and the degree of bonding that develops between the molecules of the liquid and those of the polymer.

Last but not least, temperature greatly affects the viscosity of a fluid, with higher temperatures generally reducing the viscosity. Gelatin-based adhesives, such as hide glues, are a prime example for this phenomenon, as they visibly reduce their viscosity when heated and gel fast during cooling.

### Solvent action on polymers

The thermodynamic quality of a solvent determines the conformation of the dissolved polymer in solution and after drying in the solid state. Thermodynamically "good" solvents encourage polymer molecules to extend and assume greater mobility, whilst "poorer" solvents leave them in a more entangled state and packed in tighter agglomerates to avoid unfavourable contact with the solvent (Hoernschemeyer 1974; Hansen et al. 1991). Poorer solvents thus render fewer active groups within the molecules available for adsorption sites than good solvents. Attractive forces between the consolidant and the substrate are less able to develop. In polar polymers, such as poly(methyl methacrylate), the viscosity is strongly dependent on the nature of the solvent, being greater in poorer solvents (Dreval' et al. 1973).

With respect to mechanical properties, Sakuno and Schniewind (1990) demonstrated that in terms of polarity the solvent action of consolidants has a much greater effect on the adhesive strength of consolidated wood than the actual choice of polymer type. Nevertheless, Hansen et al. (1991) point out that the exact effect of the thermodynamic quality of a solvent on the mechanical properties of a

polymer is unlikely to be estimated theoretically, but requires determination by experimental means.

**Reverse migration** Reverse migration often occurs when solvent-based thermoplastic resins are applied to a porous substrate, and it manifests itself in increased polymer concentration near the outer surfaces of the consolidated structure (Payton 1984). This phenomenon is linked with the behaviour of the solvent that evaporates during drying and its interaction with the polymer. Domaslawski (1988) demonstrated that for consolidants used on stone, reverse migration could be significantly reduced by slowing down the evaporation rate of the solvent. This was also confirmed for wood substrates by Schniewind and Eastman (1994), who found evidence of increased resin concentration in wood samples consolidated with solutions of Paraloid B 72 in acetone and toluene due to high drying rates in air. In addition to the drying rate, the surface tension of the consolidant also influences polymer migration towards the evaporation surfaces. In consolidant solutions of high surface tension the constituent polymer molecules have a greater affinity for the solvent than for the substrate they are applied to. Hence, the effect of reverse migration will be more pronounced.

**Solvent retention** Solvent retention in consolidants and adhesives is an important aspect to consider when estimating or evaluating mechanical performance. Retained solvent in the polymer acts as plasticiser, it reduces the glass transition temperature,  $T_g$ , of the polymer and can induce cold flow or creep. Upon the application of stresses the polymer or bond may thus fail due to plastic deformation. In most cases, this effect appears to be most relevant for the early stages of drying, where the consolidant still contains a significant amount of solvent or diluent. Adequate clamping time is required to ensure reliable bonding of flattened, stressed layers.

The retention of solvents is governed by diffusion and hence by both the drying time and the square root of the film thickness (Newman et al. 1975, as cited by Carlson and Schniewind 1990). Clearly however, diffusion of the solvent in complex multilayered wood-polymer systems may take significantly longer than in free polymer films. Furthermore, solvents with higher boiling points are less volatile and hence generally retained for longer by resin adhesives than those with lower boiling points (e.g. Carlson and Schniewind 1990). Any solvent retained even after long drying times still has a great influence on the elasticity and strength of a bond. The degree to which these properties are affected is dependent on the chemical interaction of the solvent with the polymer. The “better” the thermodynamic quality of the solvent, the stronger appears to be its plasticising effect (Bistac and Schultz 1997). Compared with acetone and chloroform, toluene has been shown to be retained in PVAc films for much longer. This results in greater ductility and hence increased toughness of the film, i.e. the latter shows a greater strain-to-failure and lower stress to failure (Hansen et al. 1991).

#### 4. Consolidation of East Asian Lacquer Objects

(For further discussion of solvent retention in paint layers see Masschelein-Kleiner 1981; Banik and Krist 1984; Pietsch 2002.)

### Properties of the polymer molecule

**Effect of molecular weight ( $M_W$ )** The weight-average molecular weight, commonly just referred to as molecular weight,  $M_W$ , gives an indication of the average size of its constituent molecules. Many polymers are supplied stating their respective  $M_W$ , which can be used as a measure to estimate their physical and mechanical properties in solution and as dry film. In polymers, cohesion generally increases with increasing average size of the molecules. As a consequence, the viscosity of a polymer in solution is strongly influenced by the  $M_W$  (e.g. Horie 1987, pp. 15-17), and so are the mechanical strength properties of the polymer in the solid state: larger molecules increase the viscosity and render polymer films stronger than low molecular weight polymers. A good example for adhesives with significantly differing average  $M_W$  is that of mammalian bone glues and isinglass. Whilst the latter contains very large protein molecules owing to gentle extraction from sturgeon swim bladders, the bone glues are extracted by a relatively harsh treatment which breaks down the protein molecules into smaller fractions. Therefore, bone glues are more brittle and have much lower strength properties than isinglass (e.g. Schellmann 2007).

**Glass transition temperature ( $T_g$ )** The glass transition temperature,  $T_g$ , specifies the temperature region at which an amorphous material changes from the brittle, or glass-like to a more ductile (rubber-like) state. It is an important property, as it indicates the material's stiffness (reflected in the modulus of elasticity) and mechanical strength in relation to temperature. Below  $T_g$ , polymers are stiff and will break without much deformation when stressed. Above  $T_g$ , they are ductile, and will readily show deformation upon exposure to stresses. Hence,  $T_g$  is the region where the physical and mechanical properties of the polymer change drastically (e.g. Carlson and Schniewind 1990). This transition also includes large dimensional changes, as the polymer molecules take up more space in their rubbery state due to increased translational mobility and rotation about the chemical bonds of their chains. Generally,  $T_g$  rises with increasing molecular weight, increasingly bulky side groups, greater polarity and hydrogen bonding, rising number of double bonds and degree of cross-linking (e.g. Callister, Jr. 2000, p. 486). The addition of plasticisers on the other hand leads to its decrease.

The glass transition temperature is very important to consider for several reasons: Schilling (1989) points out that if an object is kept in fluctuating environmental conditions, it is generally aimed to avoid using polymers for their consolidation that have a glass transition temperature well within the same temperature range. Otherwise, the objects will be exposed to significant stresses that are caused by

the applied polymer, which experiences extreme dimensional changes under these conditions. Such additional stresses may cause damage to the object.

The glass transition temperature also has an influence on the solvent evaporation from polymer solutions and the film-forming properties of polymer particles in dispersions. In the latter, the particles can only coalesce to form a film if the drying temperature is above the polymer's  $T_g$ . In practice, this is not usually a problem, because the polymer dispersions commonly used in conservation have glass transition temperatures well below normal room temperature (e.g. Horie 1987, pp. 95, 111). Thermoplastic polymers in solution do have film-forming ability below their glass transition temperature, however they will always retain some of the solvent in the resulting film if kept under these normal conditions (i.e. if not heat-dried). This is because the restricted movement of the polymer molecules below their  $T_g$  hinders the diffusion of the remaining solvent through the film. Due to the plasticising effect of this retained solvent, the resulting solid film will consequently have a lower  $T_g$  than the initial bulk polymer. This does not apply to polymers with a  $T_g$  below room temperature: they will be in their rubbery state at normal room temperature and thus allow full solvent evaporation through the film (see Schilling 1989 for a detailed discussion).

## Application methods

There are many ways of applying consolidants to fragile and delaminating coating layers, and these have been shown to have a great influence on the overall performance of the consolidants (e.g. Schießl 1989). The most common methods appear to be the application of liquid consolidant by brush or by injection, the choice being mainly dependent on the actual shape of the damaged coating and on whether accessibility to cracks and delaminated areas is limited. Also, the physical and rheological properties of the consolidants play a role. To achieve even better penetration, exposure to a vacuum may in some cases be employed, although this type of method seems to be rarely undertaken on lacquer-coated objects.

A significant factor for the consolidation of porous materials is the possibility of applying liquid consolidants in several stages, where gradually the polymer concentration of the solution is increased. This allows the polymer to penetrate deeply into the structure whilst leaving open pores for repeated application of the polymer solution. Good results for such stabilisation treatments have been widely reported for fragile wood (e.g. Grattan 1980; Schniewind 1998, pp. 94-95). In the case of delaminating and lifting coating layers, however, multiple applications of consolidants may be more problematic due to the limited access to the fracture surfaces. It is therefore often tried to use a consolidant in a single stage application.

## 4.4. Consolidant choice for lifting lacquer coatings

The previous section clarified that many parameters influence the mechanical properties of a consolidant. Although this theoretical background helps to understand and interpret the behaviour of different consolidants applied during consolidation tests, the complexity of the influences still renders it difficult to predict the behaviour and strength properties of consolidants in situ, i.e. when applied on a fragile object. As strength improvements are relative and depend on the state of the fragile structure, suitable tests are further required that can demonstrate the possible differences in the behaviour of various consolidants.

In this research, the goal was therefore to undertake tests under comparable conditions with a broad range of polymer formulations that could be used on lacquer coating structures containing protein-bound foundation layers. A variety of different polymer formulations were chosen to be tested in the experimental part of this work (cf. Chapters 6 and 7). The range of consolidants was aimed partly to reflect previous choices reported in the literature review, and partly to select materials which were expected to display varying mechanical properties and behaviour.

Firstly, it was intended to test representative consolidants from three categories:

- water-based solutions or dispersions,
- hydrocarbon solvent-based solutions, and
- chemically reactive formulations.

Furthermore, polymers were to be chosen from five classes, again reflecting the different classes of consolidants commonly used in the conservation of flaking lacquer and paint layers:

CLASS	POLYMER
I	Protein glues based on fish and mammalian collagen
I+	Protein glue with added polysaccharide
II	<i>Urushi</i> lacquer
II+	<i>Urushi</i> lacquer with added polysaccharide
III	Acrylic resins in a) solution, and b) aqueous dispersion
IV	Poly(vinyl alcohols) in aqueous solution
V	Poly(vinyl acetates) in a) solution, and b) aqueous dispersion

Generally, one representative polymer was aimed to be tested for each of the above classes. The selection was additionally extended to include a few similar polymers with only slightly varying formulations. This was intended to provide information on whether similar polymer types would display similar mechanical



behaviour or not, and in the latter case on whether the finally selected test method would be able to measure and quantify these differences. The final selection of the consolidants will be presented in the following sections.

##### 4.4.1. Class I, Protein-based consolidants

The typical protein-based adhesives and consolidants used in conservation are derived from mammalian and fish collagen, which is transformed into gelatin by hot water extraction (e.g. Hubbard 1965; Johns and Courts 1977; von Endt 1984). Protein glues are applied as aqueous solutions which usually require heating to liquefy from their gelled state. Upon cooling, they revert back into gel-like consistency. Due to the chemical nature of their constituent amino acids, gelatin of mammalian origin generally has a higher gelation temperature than that of marine origin. The nature of the amino acids also determines the adhesive and mechanical strength properties of the individual glue types. Gelatin-based adhesives can further be manipulated by additives so that cold-liquid glue formulations are available (proprietary fish glue and some hide glues). An extensive discussion of the properties of animal glues in conservation is given by Schellmann (2007) and should be consulted for further details.

As mentioned earlier, consolidants based on mammalian or fish gelatin are often used for delaminating and flaking lacquer coatings. Of this group, three types were chosen to be tested, due to their reputedly different mechanical properties. Their differences in relevant properties are summarised as follows (see also Schellmann 2007):

- |                       |  |
|-----------------------|--|
| Cold-liquid fish glue | <ul style="list-style-type: none"><li>- medium <math>M_W</math> (Kremer Pigmente)</li><li>- achieved good consolidation results on lacquer in the past</li><li>- applied without using additional heat</li></ul>                             |
| Isinglass             | <ul style="list-style-type: none"><li>- highest <math>M_W</math> (Haupt 2004), greatest elasticity, high tensile strength</li><li>- successful consolidant in paintings conservation</li><li>- applied as moderately warm solution</li></ul> |
| Bovine hide glue      | <ul style="list-style-type: none"><li>- medium to high <math>M_W</math> (Kremer Pigmente) and tensile strength (Mecklenburg 1991), stiffer than isinglass (Simon et al. 2003)</li><li>- applied as hot solution</li></ul>                    |

#### 4. Consolidation of East Asian Lacquer Objects

##### 4.4.2. Class +, Polysaccharides (starch)

Starch is a polyglucose polymer and consists of the linear starch molecules amylose and the much larger, branched amylopectin. Their average molecular weights are around 40,000–650,000 and  $10^7$ – $10^8$  respectively, which constitute rather large molecules compared with other polymers used as consolidants (cf. Table 4.2). Whilst amylopectin is soluble in cold water, amylose merely swells to a high degree under these conditions. Starch is usually heated to its gelatinisation temperature of 55–80°C to encourage partial dissolution of the amylose and to disrupt and disperse the starch grains. Depending on the amount of stirring during heating and subsequent cooling, the average molecular mass of the polymer and the size of any agglomerates can be significantly reduced, thus influencing the viscosity and the mechanical properties of the resulting film (Horie 1987, p. 136).

##### (I+) Starch as additive for isinglass

Starch is usually applied as a gelatinised (cooked) paste dispersed in water. In this study it was added as a thickening agent to isinglass solution, as previous research by Breidenstein (2000) had shown very successful results during the conservation of Chinese lacquer screen panels. The addition of starch was considered to improve the bond strength between foundation layers and lacquer coating layers that retained a strong ‘memory’ for their previous state of distortion.

##### (II+) Starch as additive for lacquer

A further traditional starch-based material is flour paste. Wheat flour has traditionally been used as an adhesive in paper conservation, but is also commonly employed in Japan for stabilising fragile lacquer structures. Wheat flour contains gluten (protein) in addition to amylose and amylopectin, which renders it with better adhesive qualities than pure starch when applied as a paste (e.g. Horie 1987, p. 140, Matsumoto and Kitamura 2008). It also significantly improves the adhesive properties of *urushi*, which is why the Japanese use it in the form of *mugi urushi* (*urushi* mixed with wheat flour paste and diluted with hydrocarbon solvent) for the structural repair and consolidation of damaged lacquer objects. *Mugi urushi* was chosen to be included in this research in order to gain more information about its mechanical behaviour in fragile coating layers.

##### 4.4.3. Class II, *Urushi* lacquer

As introduced in Chapter section 2.1, East Asian lacquer is a natural, reactive polymer deriving from various tree species, several of which belong to the *Anacardiaceae* family. The sap from these lacquer trees is a double emulsion of water-in-oil-in-water with a slightly acidic pH of 6.4 – 6.6 at the time of collection,

#### 4.4. Consolidant choice for lifting lacquer coatings

which has the tendency to decrease further with time (Kenjo 1988; Kumanotani 1995, p. 177). The lacquer harvested in Japan and China consists of a complex mixture of various components. The base is around 55-65% of the phenolic lipid urushiol, which is a 3-substituted catechol derivative with 15 carbon atoms including up to 0-3 olefins (double bonds). This constitutes the oily phase that further contains a small percentage (2-5%) of hydrophobic (water-insoluble) glycoproteins. Around 20-30% of the sap is water in which plant gums (mono-, oligo- and polysaccharides) and enzymes (the copper glycoprotein Rhus laccase, stellacyanin and peroxidase) are dissolved (Kumanotani 1995, p. 166; Kamiya and Miyakoshi 2000). Once this sap comes into contact with oxygen and high relative humidity, the highly unstable double bonds in the urushiol in combination with the enzymes induce the lacquer sap to polymerise into a tough film (Kumanotani 1995, 1998). Lacquer is a cross-linked polymer that becomes insoluble in almost any solvent once it has hardened (Nagase 1986; Hisada et al. 2000. See also McSharry et al. 2007 for a detailed review of the chemistry of lacquer).

Even though lacquer is a cross-linking and thus irremovable consolidant, it was shown to be sometimes used to pre-consolidate fragile protein-based foundation layers, before *mugi urushi* is applied (cf. Section 4.2.1). In order to gain a better understanding of how the addition of lacquer changes the mechanical properties of the foundation, *urushi* diluted in a suitable hydrocarbon solvent was chosen to be tested as a consolidant. The type of solvent used was based on previous research by Rivers and Yamashita (Rivers 2007), who tested alternative solvents to replace the petroleum spirit ligroin, which is traditionally used in Japan for diluting lacquer, but is unavailable in Europe. They found that Exxsol DSP 80-100 or HAN 8070 (both ExxonMobil), were both suitable (see also Yamashita and Rivers 2011).

#### 4.4.4. Class III, Acrylics

Acrylic polymers typically used in conservation are based on acrylate and methacrylate, which are derived from acrylic acid and methacrylic acid respectively. Depending on their exact composition and ratio of homopolymers, the polymers can have greatly varying properties, which are extensively discussed in the literature (e.g. Horie 1987). Generally, acrylics can be applied in solution with hydrocarbon solvents or in the form of aqueous dispersions.

##### (III a) Acrylic solution

Paraloid B 72 (ethyl methacrylate and methyl acrylate copolymer, EMA/MA, at a ratio of 70:30) is one of the most popular acrylics in conservation due to its outstanding chemical stability and ageing characteristics (e.g. Down 2009). It was chosen in this study as it has been extensively used for the consolidation of fragile paint and coating layers, including those of lacquer objects. Its physical

#### 4. Consolidation of East Asian Lacquer Objects

properties are a molecular weight of around 65 000 (de la Rie 1987), a glass transition temperature of 40 °C (Lascaux 2007a) and an elastic modulus (i.e. stiffness) of 3.0 GPa (Tan et al. 2011). In many cases, Paraloid B 72 is dissolved in acetone or ethyl acetate, or in non-polar aromatic solvents such as toluene or xylene. For this study, two solvents were chosen for B 72: toluene was selected for its non-polar nature which would be the least damaging for a degraded lacquer surface. Secondly, acetone was chosen for comparison purposes, and as B 72 in acetone has recently been reported to achieve successful consolidation results on severely distorted lacquer (Hatchfield et al. 2010).

Furthermore, Paraloid B 48N was added to the list of polymers to be tested, in order to include a second acrylic resin solution and to see whether differences between various Paraloid types could be identified with a mechanical test method. Paraloid B 48 N is a methyl methacrylate/butyl acrylate (MMA/BA) copolymer of the ratio 74.5:25.5 mol % that has a molecular weight of 184 000 and a  $T_g$  of 50 °C (Lazzari and Chiantore 2000). It also contains added plasticiser (dibutyl phthalate) and an adhesion promoter (CAMEO 2009). Paraloid B 48 N tends to be slightly stiffer than Paraloid B 72, having a Young's modulus of 3.0–3.5 GPa (Tan et al. 2011). It is most commonly used on metal objects (e.g. Conservation Resources; von Looz 2001), but has been reported to be successful as an adhesive for East Asian lacquer/metal foil interfaces (Rivers and Yamashita 2006) and for marble (Tan et al. 2011). As it is more difficult to dissolve than B 72, the recommended mixture of toluene and xylene was chosen (Conservation Resources), to keep it as similar as the solvent used for the B 72.

#### (III b) Acrylic dispersion

Of the various acrylic dispersions available, it was decided to use Lascaux Medium for Consolidation (Lascaux MfC), a highly stable consolidant explicitly developed for conservation use. It consists of finely dispersed acrylate/methacrylate and styrene copolymer and includes a small amount of other minor additives required to form a stable and lasting aqueous dispersion. This formulation was specifically developed to replace the discontinued Acronal 300D, which had been a preferred consolidant for painted and water-sensitive gilt surfaces on porous, gesso-type foundation layers (Hedlund and Johansson 2005). Lascaux MfC has a relatively high molecular weight (>300 000) but nevertheless has a low viscosity and shows excellent penetration ability, according to its developers. The proprietary dispersion is supplied with 25% solid content (Hedlund and Johansson 2005; Lascaux 2007b) and was aimed to be tested at this undiluted concentration.

#### 4.4.5. Class IV, Poly(vinyl alcohols)

Poly(vinyl alcohols) are not very popular any more in conservation due to their affinity to cross-link and become insoluble with age (Horie 1987, pp. 96-99).

#### 4.4. Consolidant choice for lifting lacquer coatings

Nevertheless, this polymer type is widely used in the paint industry as it has some favourable properties. Mowiol polymers, for example, are generally known for their good cohesion and adhesion to fillers, pigments and fibres, and display notable bonding strength and pigment binding capacity. Mowiol 3-83 is a recommended base for wood primers that allegedly provides a good key for subsequent paint coats of various compositions (Clariant 1999, p. G17) and is mostly soluble in cold water. Due to its relatively average molecular weight of 14 000 and its chemical nature (containing polar –OH groups), Mowiol 3-83 has very good wettability of wood substrates and penetration ability. Its surface tension is the lowest of all Mowiol grades and lower than that of water (KSE Kuraray Specialities Europe 2002; Clariant 1999, pp. G13, G17).

Despite not being commonly used in conservation, this polymer was explicitly chosen to be included in the tests due to its alleged good mechanical properties (before aging) whilst having relatively low average molecular mass.

#### 4.4.6. Class V, Poly(vinyl acetates)

Polyvinyl acetate adhesives are frequently chosen for conservation purposes and a range of different types are available, having varying chemical, physical and mechanical properties. The molecular weights of homopolymers can differ substantially whilst their glass transition temperature usually ranges between room temperature and higher values (Horie 1987, p. 92; Kremer Pigmente 2007b). PVAc is insoluble in water, but similar to acrylates, it is available as complex copolymer formulations (with various additives) in aqueous dispersion, which have minimum film forming temperatures below 5 °C (e.g. Horie 1987, pp. 94-96).

##### (V a) PVAc solution

PVAc homopolymers are soluble in various hydrocarbon solvents, and their mechanical properties are highly dependent on the solvent used (Olayemi and Adeyeye 1982). In this study, only one PVAc solution could be tested. The choice was made for Mowilith 50 (also known as AYAF), which is a medium grade homopolymer of the Mowilith types and had been shown to be a successful consolidant for lacquer coatings. It has a molecular weight slightly below that of Paraloid B 48 N and a  $T_g$  similar to that of Paraloid B 72 (cf. Table 4.2). It is soluble in toluene, in addition to acetone and other polar solvents. For the tests, it was decided to use toluene, in order to test a further non-polar polymer formulation and to keep this solution comparable to that of the two Paraloids.

##### (V b) PVAc dispersion

From the group of PVAc-based aqueous dispersions, Mowilith DMC2 was selected, as it is one of the aqueous versions of Mowilith. The DMC2 formulation consists

#### 4. Consolidation of East Asian Lacquer Objects

of the co-polymer of vinyl acetate and di-butyl maleate (35%) dispersed in water with the addition of cellulose ether as a stabiliser (de Witte et al. 1984; Horie 1987, p. 95). It contains rather large solid particles of 0.3-2.0  $\mu\text{m}$  and is supplied at various concentrations of between 46-55 % solids content, which makes it a highly viscous formulation. It has mostly been used as a consolidant for textiles (Cocca et al. 2006) as it retains significant elasticity after drying due to its low  $T_g$  of 10 °C. In this study, it represented one of the two synthetic polymer formulations with a  $T_g$  below room temperature (together with Lascaux Medium for Consolidation). Also, this consolidant was deliberately chosen for its low pH of around 3.5, as lacquer surfaces are less sensitive to low pH than to neutral or alkaline pH. In terms of pH, this consolidant was hence the least potentially damaging of all the aqueous consolidant formulations chosen in this work.

##### 4.4.7. Summary of polymers selected for testing

Table 4.2 summarises the properties of the polymers chosen for the consolidation tests. The data in the table was drawn from various sources and studies, and this has to be kept in mind when comparing the data. It is important to note the widely varying experimental conditions under which the data was measured, as clearly can be seen for the viscosity values, which were measured under the conditions stated in the respective adjacent column. In many cases, some of the sources did not provide sufficient details on the analytical methods and conditions, so that the data may actually be difficult to compare. This problem was also pointed out by Schilling (1989), who states that  $T_g$  values published by different sources may not necessarily be comparable due to differences in measuring parameters and methods. Therefore, the listed values for the individual polymer properties should more generally serve as a rough guideline.

## 4.5. Chapter summary

The review of the materials and methods previously used to consolidate failing and delaminating East Asian lacquer coatings has shown that a great variety of stabilising agents have been employed for this purpose with varying results. The consolidants ranged from waxes to natural polymers, such as gelatin-based animal glues, starches and East Asian lacquer, to synthetic polymers based on acrylates and diverse polyvinyl derivatives. Of all these consolidants, water-based formulations generally appeared to be most successful. Examples of these were protein-based adhesives of both mammalian and marine origin, isinglass in mixtures with starch paste, as well as various polymer dispersions with relatively high solid content. Waxes and wax-based consolidants had shown to achieve some good results regarding the re-adhering of lifting lacquer. However, they had also demonstrated to potentially cause further damage and problems with future

re-treatability of the object. East Asian lacquer, applied in diluted form and with various additives by Japanese and other East Asian conservators, reportedly appeared to be a successful consolidant for flaking lacquer coatings. However, due to its cross-linking nature and its assumed high strength it still remains little accepted as a desirable consolidant in Western countries.

It was further shown that consolidants are required to serve two purposes simultaneously: that of penetrating into – and thus stabilising – a fragile, porous structure, whilst also sufficiently remaining on the fracture surfaces to re-adhere the lifting lacquer coating. In order to gain a consolidant with these properties, several parameters can be influenced: the choice of polymer with a particular molecular weight and glass transition temperature, as well as the solvent or diluent, and the solid content of the formulation, which influence the viscosity, surface tension and thus the penetration ability of the consolidant.

Based on the review of the physical and chemical factors that determine the consolidant properties, a group of polymers was chosen to be tested for their mechanical properties when used on delaminating and lifting protein-bound foundation layers of lacquer coatings. The choice comprised polymers from different classes (i.e. proteins, polysaccharides, lacquer, acrylics, PVAc and PVAI) and included both aqueous and hydrocarbon solvent-based (polar and non-polar) formulations. The exact choice of the polymers was based on successful experiences of previous research reported in the literature review and included a few additional polymers for comparison purposes. The polymers chosen for testing were cold-liquid fish glue, hide glue, isinglass (+ wheat starch paste), East Asian lacquer (+ wheat flour paste), Paraloid B 72 (in toluene and in acetone), Paraloid B 48 N (in toluene/xylene), Lascaux Medium for Consolidation (aqueous dispersion), Mowiol 3-83 (aqueous solution), Mowilith 50 (in toluene) and Mowilith DMC2 (aqueous dispersion).

#### 4. Consolidation of East Asian Lacquer Objects

Table 4.2.: Polymers selected for consolidation testing.

CLASS	POLYMER	COMPOSITION	$\bar{M}_w$	$\bar{d}$ [ $\mu\text{m}$ ]	$T_g$ °C	PH	VISCOSITY [mPa.s]	CONDITIONS % / °C	REFERENCE
I	Fish glue	cold-water fish protein	60 000	-	-3 (tuna skin gelatin)	4.0-6.0	4 000-6 000	45% solids in water	Kremer Pigmente (2007a, 2005), Johann (2006), Rahman et al. (2008)
I	Isinglass	sturgeon bladder protein	150 000 (-300 000)	-		5.5-7.5	2.5-4.3	3.5% solids aq. / 55°C	Amstel-Products, Haupt et al. (1990), Luybavskaya (1990), Roskett (1994), Haupt (2004)
I	Bovine hide glue	bovine hide protein	43 000 -73 000	-	57 (bovine gelatin)	6.5-7.4	8-24	12.5% solids aq. / 60°C	Luybavskaya (1990), Rahman et al. (2008)
+	Wheat starch paste	amylose + amylopectin	40 000 -650 000; 10 <sup>7</sup> -10 <sup>8</sup>	30-40	> room temp.	4.5	135	5% solids aq. / 25°C	van Steene and Maschelein-Kleiner (1980), Horie (1987, p.135), Zeleznak and Hoseney (1987), Nemtann and Brasoveanu (2010)
II	<i>Urushi</i> (raw)	urushiol + poly-saccharides + glycoproteins + laccase	310 (c.60%), 22 000 / 77 000 (c. 7%)		90-133	<6.4			Kenjo (1988), Obataya et al. (2001, 2002)

(Table continued on following page)



CLASS POLYMER	COMPOSITION	$\bar{M}_w$	$\bar{d}$ [ $\mu\text{m}$ ]	$T_g$ °C	PH	VISCOSITY [mPa.s]	CONDITIONS % / °C	REFERENCES
IIIa) Paraloid B72	EMA/MA (70:30)	65 000	–	40	(6.4*)	600	40 % in tol.	de la Rie (1987), Chapman and Mason (2003), Lascaux (2007a), Down et al. (1996, p.25)
IIIa) Paraloid B48N	MMA/BA + DBP + adhesion promoter	184 000	–	50	(3.8*)	200	40% in ac., 25°C	Down et al. (1996, p.25)
IIIb) Lascaux MfC	acrylic ester + MA ester + styrene	>300 000	0.03–0.3	<4 ( $M_{FFT}$ )	(6.5–) 8.5	1–5	25 % aq.disp.	Hedlund and Johansson (2005)
IV Mowiol 3-83	PVAI	14 000	–	40–80	5–5.5	3	4 % solids aq./ 20 °C	Clariant (1999)
Va) Mowilith 50	PVAc	176 000	–	35–45	(5.1*)	100–160	20 % in ethyl acetate/ 20 °C	Horie (1987, p.93), Down et al. (1996, p.24), Kremer Pigmente (2007b), Lascaux (2007c)
Vb) Mowilith DMC2	vinyl acetate + maleic acid di-n-butylester		0.3–2.0	10–15	3.5–5	5 000– 12 000	25 % aq.disp./ 20 °C	de Witte et al. (1984), Lascaux (2007c), Cocca et al. (2006)

$\bar{M}_w$ : weight-average molecular weight;  $\bar{d}$ : average particle diameter;  $T_g$ : glass transition temperature; MA: methyl methacrylate; MMA: methyl methacrylate; BA: butyl acrylate; EMA: ethyl methacrylate; DBP: dibutyl phthalate (plasticiser); PVAI: polyvinyl alcohol; PVAc: polyvinyl acetate; MFFT: minimum film-forming temperature (usually a few °C above  $T_g$ ); tol.: toluene; ac.: acetone; solids aq.: solid content in aqueous solution; aq.disp.: aqueous dispersion. Values marked with an asterisk (\*) denote pH values for unaged, dry film extracts. Values in *italics* denote those measured by the author in this study. Details provided in “Conditions” column refer to the viscosity measurements of the previous column.



# 5. Testing of Material Strength and Fracture Behaviour

## 5.1. Introduction

Having identified the materials responsible for and the loci of failure in the multilayered coating structure (Chapter 3), and the parameters that influence the properties of a consolidant (Chapter 4), the question remains how the performance of consolidants in situ can be tested most conveniently and efficiently.

It is clear that a consolidant is intended to strengthen a material or composite that has lost or is about to lose its integrity. Strength improvement, on the other hand, is a relative measure which has been shown to be directly dependent on the degree of initial degradation (Schniewind and Kronkright 1984). It is also known that when layers in composite materials are consolidated, the adhesive strength of the consolidant should not be too great, as this may induce high stresses that can cause further damage to the structure (e.g. Nicolaus 1998). To enable an informed choice of the most suitable consolidant for facilitating the desired degree of stabilisation or strengthening, it is therefore vital to understand the mechanical characteristics of the fragile structure. Furthermore, detailed knowledge is required on the way in which these characteristics change with a chosen treatment.

Unfortunately, for most object components this information is often unavailable to conservators. Materials used in the production of applied arts objects generally have a strong tendency to be inhomogeneous and technical data are rarely provided. Lacquer objects are no exception; they are based on varied natural materials assembled in complex structures, usually manufactured entirely by hand and in processes that are neither standardised, nor necessarily recorded in sufficient detail to be precisely reproducible. Furthermore, by the time such objects require conservation, these materials are mostly aged and their properties have changed in various ways and to varying degrees. Additionally to the lack of information on the aged material, the properties of the consolidants and adhesives available are – if at all – known only for the bulk material. When dispersed in a porous substrate and potentially containing numerous voids, their properties are seldom well understood.

In practical conservation it generally appears to be unfeasible to directly measure the mechanical properties of a degraded coating. Whilst it may be technically

## 5. Testing of Material Strength and Fracture Behaviour

possible to determine these properties, there are many practical limitations as such tests often require sampling of original material. Any form of destructive testing or sampling of artefacts, however, is generally to be avoided. Furthermore, tests undertaken in limited areas or on very small samples may generate data that are not necessarily representative or valid for a large area on an object that is most often unevenly degraded. Sufficient tests are usually constrained, if not by ethical considerations, then by the inaccessibility of equipment and lack of time. Comprehensive characterisation of mechanical properties is thus rarely available to conservators for most objects needing consolidation.

With these difficulties in gaining representative or widely valid data, it is not surprising that research on the mechanical properties of East Asian lacquer coating structures and related decorative coatings or composite materials has been relatively scarce. Evaluation of the suitability and success of specific consolidation treatments is still often done by personal judgement during practical handling and by visually assessing the results several weeks, months, or even years after treatment has been completed. These results are extremely valuable for conservators and should not be neglected. Nevertheless, scientific analysis can assist in ascertaining spatial distribution of consolidants and differences in their strengthening ability of a damaged structure that cannot be sufficiently determined otherwise. The following chapter therefore discusses the considerations that led to the development of a new testing methodology for failing, multilayered decorative coatings, based on the analysis of their fracture behaviour before and after consolidation.

### 5.2. Material properties definitions

For the purpose of clarity, some technical terms for mechanical properties of materials are introduced here:

**Stress** is defined as the force,  $P$ , per unit area,  $A_0$ , applied to a body. On the application of stress, a body is strained and it deforms. **Strain** is expressed as the ratio of the body's change in length ( $L-L_0$ ) to its original length ( $L_0$ ), measured in the direction of the applied stress (Fig. 5.1a). The strain can be permanent (plastic) or recoverable (elastic).

The stress/strain curves for two different materials are shown in Figure 5.1b. The slope of the curve in the linear region is defined by the ratio of stress and strain and is termed the **elastic modulus**,  $E$ . The higher the value of  $E$  the stiffer the material is. The **stiffness** (or rigidity) of a material denotes its resistance to deformation upon the application of stress. For a given applied stress a material with a low stiffness will deform more than one with a high stiffness. In Figure 5.1b material a is stiffer than material b.

All solid materials behave elastically at small strains, but there is a limit to elastic behaviour (**elastic limit**, **yield point**) beyond which the material deforms plastically. Plastic deformation, unlike elastic deformation, is not recoverable,

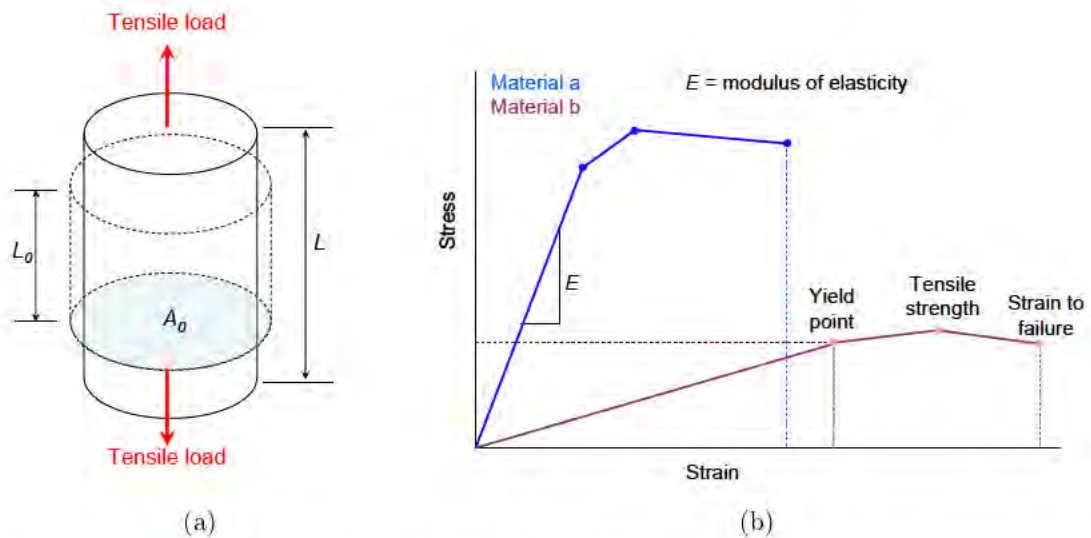


Figure 5.1.: Stress/strain behaviour of materials. (a) Schematic representation of a tensile load applied to a cylindrical body. The solid line represents the strained and elongated body. (b) Representation of stress/strain curves for two different materials, showing differences in mechanical properties.

which means that the body will remain deformed even when the applied stress is removed. The material's resistance to plastic deformation can also be defined as **hardness**. How much plastic deformation occurs before fracture is a measure of the material's **ductility**.

If an increasing load is applied, the material will reach its maximum load-bearing capacity. The stress at which this occurs is called the **(ultimate) tensile strength**. Once this load is exceeded, the material will eventually fail. Fracture does not necessarily coincide with the maximum stress due to localised deformation.

(e.g. Ashby and Jones 1996, reprinted 2001, Chapters 3, 6, 8, 13; Callister, Jr. 2000, Chapter 6 )

### 5.3. Previous research

When deciding on a suitable methodology for investigating the consolidation of lacquer coatings, previous work on the testing of coatings and their component materials needs to be considered. As lacquer is a significant component of the coatings in the present study, research on its mechanical properties is reviewed. Secondly, this chapter looks at the properties of filled polymers, as the foundations of multilayered lacquer coatings usually consist of composite material, combining clay particles with a natural polymer matrix (e.g. lacquer, starch and

protein glue). Finally, consideration is also given to previous studies in the field of conservation which involve various test methods for adhesives.

### 5.3.1. Properties of East Asian Lacquer films and coatings

Most research on lacquer coatings predominantly focuses on the analysis of the physico-chemical nature of pure lacquer films, as this type of natural polymer is of particular interest in the coating industry as a “superdurable” coating material (Kumanotani et al. 1979; see also McSharry et al. 2007). Specific physical and mechanical properties, such as glass transition temperature ( $T_g$ ) and stiffness were determined for diverse types of pure lacquer films by researchers such as Kuwata et al. (1961), Kumanotani (1995) and Obataya et al. (2002). Hisada and co-workers (2000) tested the effects of curing conditions on the tensile strength and strain at break of pure Japanese lacquer films, and found that ageing of lacquer generally renders the films stronger, stiffer and with decreased ductility.

While these results help to characterise lacquer films in isolation, very few studies appear to have been undertaken on complex lacquer coating structures. Such research of more direct practical use to conservators was undertaken by Nishiura (1984). He investigated the failure strength of traditional, high quality, multi-layered lacquer coatings with tensile tests, where the tensile load was applied in the direction perpendicular to the laminar structure of the test specimens. This study found that textile layers and the lacquer/*tonoko* mixtures in the foundation always were the least strong layers within the coating structure. Most importantly, however, Nishiura also acknowledged that the ageing properties and hence the failure strength of such coatings were largely dependent on the person who manufactured them. Great variation in the strength properties of lacquer coatings therefore have to be expected. Kenjo (1988) further demonstrated that the adhesive strength of lacquer films on wood increased significantly when they hardened more slowly at lower RH conditions, i.e. between 33 % and 55 % RH. Hence, it becomes clear that lacquer used as an artist’s material may generally vary substantially in its properties and its mechanical performance.

### 5.3.2. Properties of filled polymers and complex systems

The study by Nishiura (1984) and the survey presented in Chapter 3 has clearly shown that in lacquer coating structures the layers most in danger of failure are those consisting of mineral filler (clay powder, *tonoko*) mixed with a polymeric binder. Such foundation layers show very typical behaviour of highly filled or reinforced polymer systems. The mechanical properties of such composites are strongly dependent on the filler-to-binder ratio, usually referred to as ‘pigment volume concentration’. With increasing ratio of filler particles to binder matrix, the stiffness and toughness of the composite increase, whilst simultaneously its tensile strength decreases (Zosel 1980; Mecklenburg 1991).

Considering that foundation layers in lower-quality East Asian lacquer coatings and those applied on export ware actually contain very limited amounts of lacquer and usually surrogate binders such as protein glue, parallels can be drawn to gesso layers used on paintings and in gilding. The mechanical properties of traditional gesso formulations have been extensively investigated by Mecklenburg and coworkers (1988, 1991, 1991a, 1991b, 1998, 2007) and Michalski (1991a, 1991b). Their studies looked at complex, multilayered painting structures with all their individual components, and they analysed the mechanical behaviour of bulk material and that of the combined system. Thus, they provided a thorough understanding and model of the stress/strain behaviour of painting materials in both the glassy and the rubbery phase. Many of their findings on the effect of changing RH environments on these composite materials have already been referred to in Chapter 3 of this work.

Regarding the influence that the composition of gesso has on its mechanical properties, valuable information is also provided for example by von Endt and Baker (1991) and Mecklenburg (1991): the tensile strength of gesso layers made from chalk and rabbit skin glue was shown to be significantly lower than that of the pure glue. Additionally, a higher filler content increases the stiffness of the gesso, albeit only up to a critical filler-to-glue ratio. The latter was established to be around 13.3 (i.e. a pigment volume concentration of up to 85.5 %) for these components. With any further addition of chalk beyond this critical concentration, the stiffness of the gesso decreases. Last but not least, dimensional changes are lower in gessos with higher proportion of filler particles. Levels of total permanent shrinkage can thus vary between 2.5 and 1.0 % for gessos with chalk-to-glue ratios of around 3 and 10 respectively.

A thorough knowledge of these property relationships helps to understand the possible changes in material behaviour when an additional binder or consolidant is added to the fragile foundation layer or structure. Nevertheless, suitable mechanical strength tests are required to gain more detailed information on the actual changes induced. These are introduced in the following section.

#### **5.3.3. Methods for determining the mechanical behaviour of adhesives or consolidants**

In the field of conservation, strength properties of materials are commonly tested in bulk with conventional quasi-static tensile, compressive or flexural tests (e.g. Down and Lafontaine 1980; Schniewind and Kronkright 1984; Cuany et al. 1989; Wang and Schniewind 1985; Down et al. 1996). Moreover, adhesively bonded joints are usually evaluated using peel, tensile or shear tests (Berger 1972; Berger and Zeliger 1984; Shashoua 1993; Bradley 1984; Katz 1985; Down 1996; Schniewind 1998 amongst others). With respect to the evaluation of consolidation treatments of decorative layers, recent research investigated the mechanical properties of animal glues used as a consolidant/adhesive for the interface between

## 5. *Testing of Material Strength and Fracture Behaviour*

gesso-layers on wood substrates with shear tests (Weinbeck 2007). Peel tests were used to evaluate the performance of different adhesives on gesso-coated canvas (Sindlinger-Maushardt and Petersen 2007). Similar to the failure strength tests undertaken by Nishiura (1984) on lacquer structures reported earlier, Simon (2001) determined the failure strength of consolidated wall paintings by simple tensile tests using an end block attached to the top paint layer of the sample and a spring balance.

The results gained from these conventional test methods are very useful as they give information on the cohesive or adhesive tensile strength, elasticity and stiffness of the material. This can be used to determine or estimate differences in the material's performance during service. However, whilst these methods are simple to perform, they are not necessarily most ideal for characterising materials for conservation purposes:

Firstly, the strength values gained from conventional tests are indeed generally dependent on the specimen geometry and exact test conditions and thus do not allow for universal comparison of the measured data. Hence, these test methods are more commonly used as means for quality control. Secondly, these tests often do not satisfactorily model the failure observed on real-life objects. For example, it is easily acknowledged that an adhesive joint between two carefully prepared, flat surfaces (as required for most conventional mechanical strength test specimens) will perform significantly differently from that between two fractured, rough surfaces that needed consolidation and re-adhering. Furthermore, similar reservations apply to the direction of specimen loading, i.e. whether a tensile, compressive or sheer force is applied during testing. The loading direction strongly affects the forces leading to failure and thus significantly influences the fracture properties of the tested body. It is therefore very important to consider which loading conditions in mechanical strength tests will provide stresses that most suitably simulate those leading to failure in an object during service. Otherwise, results may not provide information that is meaningful for practical purposes.

A different approach to the mechanical failure analysis of test specimens is offered by the field of fracture mechanics. It investigates the loads under which a pre-existing flaw or crack in a material propagates and grows. Considering that Conservation deals with materials that are usually extremely flawed and damaged, this approach appeared to be a promising alternative to the conventional strength test methods commonly used.



## 5.4. Fracture mechanics approach – Choice of test method

The field of fracture mechanics – used by engineers to develop tough polymers and composites – considers the failure of materials under three loading conditions, shown in Figure 5.2 (e.g. Kinloch 1987, p. 273):

- Mode I: Cleavage or tensile-opening mode
- Mode II: In-plane (sliding) shear mode
- Mode III: Anti-plane (torsional) shear mode

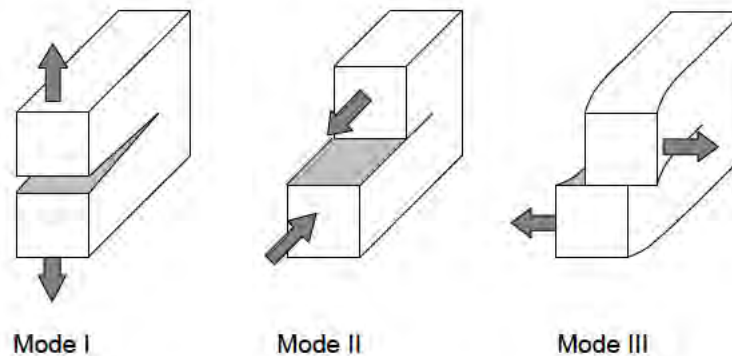


Figure 5.2.: Modes of loading of a test specimen: mode I (cleavage or tensile-opening mode), mode II (in-plane shear mode) and mode III (anti-plane/torsional shear mode).

In reality, crack development in materials occurs by a superposition of all three loading modes. This is also reflected in some conventional mechanical strength tests, such as those under shear load, where the specimens fail in mixed mode. Failure in mixed mode, however, makes the test data relatively difficult to interpret. In order to characterise the fracture behaviour of materials and the driving forces for crack propagation, the field of fracture mechanics has developed methods that investigate the loading modes individually to identify independent fracture criteria for a given joint or material. This approach assumes that crack propagation always starts from the pre-existing flaws that are present in every material. Such flaws can be voids generated during manufacture or service, or any other discontinuities in the material that originate from an abrupt change in material properties. These may be present naturally or introduced by an adhesive bond. When a force is applied to a material, stress concentration develops in the proximity of such flaws. Fracture occurs when this stress reaches a critical level, i.e. the ultimate strength of the material or the interface. Stress,  $\sigma$ , is defined as applied force,  $P$ , over area,  $A$ :

## 5. Testing of Material Strength and Fracture Behaviour

$$\sigma = \frac{P}{A} \quad (5.1)$$

The critical stress intensity factor is also known as fracture toughness,  $K_c$ , and can be defined as a function of the stress applied at fracture,  $\sigma_a$ , and the length of the flaw or crack,  $a$  (Callister, Jr. 2000, p. 199; Anderson 2005, p. 14).

$$K_c = \sigma_a \sqrt{\pi a} \quad (5.2)$$

For adhesively bonded specimens or multilayer structures the stress intensity approach is unsuitable due to the complicated interaction of dissimilar materials in this region (River 1994). However, an equivalent criterion that can be measured easily is the energy per unit area that the material can absorb before fracturing. Essentially, this is a measure of the material's resistance to stress and failure, or in other words its **toughness**. This energy is called fracture energy,  $G_c$ , and it describes the driving force needed to propagate the crack through the material.  $G_c$  varies for the different loading modes. However, it is a material property independent of the geometry of the cracked body and, ideally, even of the test conditions.

For plane strain conditions (i.e. thick layers, where the stress field is triaxial as opposed to biaxial which exists in thin layers),  $G_c$  is calculated as follows (Kinloch 1987, p. 282; Callister, Jr. 2000, pp. 116-121):

$$G_c = \frac{K_c^2}{E} (1 - \nu^2) \quad (5.3)$$

where  $E$  is the modulus of elasticity (Young's modulus),

$$E = \frac{\sigma}{\epsilon} \quad (5.4)$$

where  $\epsilon$  is the strain, which is the change of length of a stressed body,  $\Delta L$ , over its original length,  $L_o$ ,

$$\epsilon = \frac{\Delta L}{L_o} \quad (5.5)$$

and  $\nu$  is the Poisson's ratio, the ratio of the lateral strain,  $\epsilon_x$ , and the axial strain,  $\epsilon_y$ .

$$\nu = -\frac{\epsilon_x}{\epsilon_y} \quad (5.6)$$

In isotropic materials, out of all three loading conditions, mode I requires the least amount of energy to induce fracture (Kinloch 1987, p. 311). Consequently, mode I

is the most serious and potentially damaging for such materials, under which a crack always propagates perpendicular (normal) to the direction of maximum principal tensile stress.

Indeed, East Asian lacquer coatings are anisotropic composite materials. Nevertheless, considering mode I failure in such structures is a very useful approach. Mode I failure analysis has been applied extensively and successfully to similar materials such as composite laminates (e.g. Hashemi et al. 1990; Bader et al. 2000; Tzetzis and Hogg 2006; Brunner et al. 2008). Like all composite laminates, East Asian lacquer coatings most commonly fail by delamination and as shown in Chapter 3, this failure is usually a consequence of differential swelling and shrinkage of the individual layer components of the composite structure. Delamination can essentially be regarded as the propagation of a crack parallel to the laminar structure, which develops because the inter-laminar plane has the lowest resistance to failure. Mode I cleavage therefore presents the most likely failure scenario for a lacquer coating which provides sufficient energy to cause delamination.

##### 5.4.1. Testing of fracture energy under mode I – Double cantilever beam testing

The independent material property fracture energy in mode I loading,  $G_{IC}$ , can be measured with a rather simple test specimen, known as the double cantilever beam (DCB) specimen (Fig. 5.3). DCB specimens provide data for the calculation of the energy needed to initiate crack propagation and the energy still stored in the specimen, at which the crack ceases to grow (crack arrest energy). Also, information is gained on the crack growth rate stability, which is particularly interesting, because it gives an indication of whether a crack will grow catastrophically or slowly in a steady, tearing way. Provided that the DCB specimen is designed with sufficiently long beams, it gives the means to evaluate the uniformity of the material or the adhesive bond, as crack initiation and arrest can be observed repeatedly over a long distance.

In the past two decades, DCB tests in mode I loading have been widely used in the field of composites research (e.g. Hashemi et al. 1990; Blackman et al. 1995; Bader et al. 2000; Brunner et al. 2008), the testing of wood (Yoshihara and Kawamura 2006) or wood adhesive joints (e.g. River and Okkonen 1993; River 1994; Gagliano and Frazier 2001) and paint adhesion on wood (e.g. Knaebe and Williams 1993). This method has also proven to be a useful tool in the evaluation of repair treatments of fibre-reinforced composites with different adhesives (Bader et al. 2000; Tzetzis et al. 2003; Tzetzis and Hogg 2006). The great advantage of this method is that the effect of different consolidation treatments used on fractured materials can be investigated with a single type of specimen by establishing whether and to what extent a consolidant has an effect on its material properties. A specimen can first be fractured, then consolidated and finally fractured again. Not only does one thus gain directly comparable data on the fracture toughness

of the specimen before and after consolidation treatment, but also it is possible to compare the reliability of a treatment between different specimens.

## Principles of DCB analysis method

Tests to determine the mode I adhesive fracture energy,  $G_{Ic}$ , are carried out according to the standard test method ASTM D5528:94a (1994) or to the British Standard BS 7991 (2001) using DCB specimens with the geometry shown in Fig. 5.3.

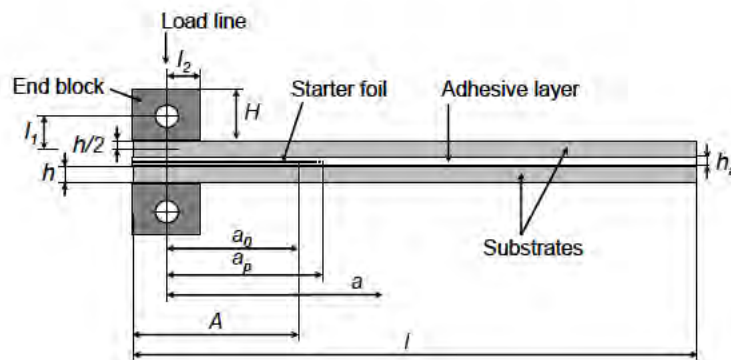


Figure 5.3.: DCB specimen with end blocks adapted from Standard BS 7991 (2001), where  $l$  is the total specimen length (150 mm),  $h$  is the thickness of the wood substrate beam (4 mm),  $h_a$  is the thickness of the adhesive (foundation) layer,  $H$  is the thickness of the end block (13 mm),  $A$  is the starter foil length from the end of the specimen (40 mm),  $a_0$  is the starter foil length from the load line (30 mm),  $a_p$  is the precrack length, measured from the load line to the tip of the mode I precrack, and  $a$  is the crack length, which is the distance between the load line and the tip of the crack on the edge of the specimen ( $> 30$  mm).

## Crack initiation

In order to analyse the fracture behaviour of a specimen, it is required that the actual onset of crack-growth is clearly defined. According to the Standard, this is done using three different criteria, which are all used for the analysis (BS 7991:2001). The values for the three crack initiation criteria NL, VIS and MAX/5% are derived from the load-displacement curve recorded during the test (Fig. 5.4). The value for each criterion encompasses the respective three values for displacement,  $\delta$ , load,  $P$ , and associated crack length,  $a$ .

NL denotes the point of deviation from linearity preceding the maximum load on the load-displacement curve, ignoring any initial deviations at the beginning of

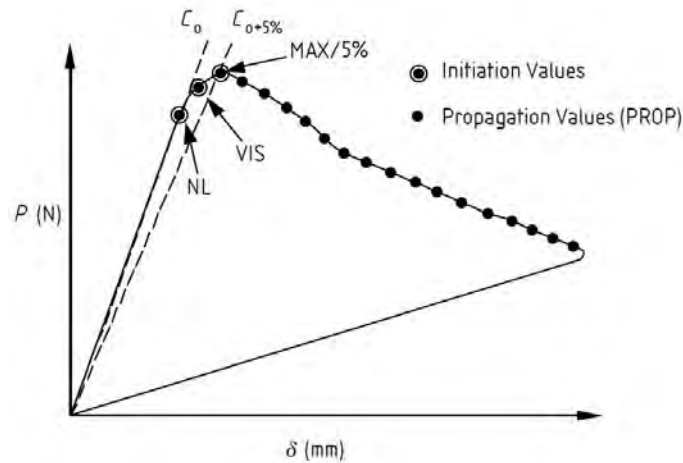


Figure 5.4.: Schematic load-displacement curve showing the initiation points NL, VIS and MAX/5% and the propagation points for mode I loading conditions (figure taken from BS 7991:2001, p.14).

the test caused by take-up of play in the loading system. A linear fit to the load-displacement curve, starting at 5% of the maximum load, determines the initial compliance of the joint,  $C_0$ . The first point of deviation from linearity is used as a consistent criterion for the determination of NL. The VIS criterion uses the first point at which the crack had been visually observed to have propagated as the onset of crack growth. The third crack initiation criterion, MAX/5%, either employs the maximum load,  $P_{\max}$ , on the load-displacement curve, or the intercept of the load-displacement curve with the linear  $C_0 + 5\%$  graph as initiation point, whichever is met first.  $C_0 + 5\%$  denotes the initial compliance increased by 5%.

The load at the intersection point of the 5% offset line with the load-displacement curve,  $P_{5\%}$ , and  $P_{\max}$  are further used to check whether linear elastic fracture mechanics (LEFM) are applicable for interpreting the test results, i.e. to determine whether the degree of nonlinear inelastic behaviour is negligible. LEFM can be employed if the ratio of  $P_{\max}/P_{5\%}$  is  $< 1.1$ . This criterion means that a non-linearity of 10% may occur before the test data are deemed too nonlinear to be interpreted by LEFM methods (Hashemi et al. 1990). If  $P_{\max}/P_{5\%}$  is  $> 1.1$  then the test is invalid.

## Mode I analysis

The fracture energy for DCB specimens, expressed as the critical energy release rate,  $G_{Ic}$ , for elastic behaviour, is calculated with three different analysis methods following BS 7991:2001. The corrected beam theory (CBT) method and the experimental compliance method (ECM) are considered to give more accurate values of  $G_{Ic}$  than the simple beam theory (SBT) approach (Hashemi et al. 1990).

## 5. Testing of Material Strength and Fracture Behaviour

The latter method is uncorrected and does not take rotational and shear deformations at the crack tip into account, rendering the values for  $G_{Ic}$  imprecise. This is particularly the case if highly anisotropic substrates are used, where corrections to the SBT are required (Blackman et al. 1991). However, the SBT method is the only method that can be used for analysing unstable crack growth behaviour, where CBT and ECM fail to give valid results, as not enough data points can be gained to construct an accurate plot of compliance versus crack length.

According to the Standard, all three analysis methods are generally to be performed for complete data analysis of the DCB tests.

### Method 1: Simple Beam Theory (SBT)

The adhesive fracture energy can be calculated using Equation 5.7.

$$G_{Ic} = \frac{P^2}{2B} \cdot \frac{dC}{da} \quad (5.7)$$

where  $P$  is the applied load measured during testing,  $B$  is the (bonded) width of the specimen,  $a$  is the crack length and  $C$  is the compliance,  $C = \delta/P$ , where  $\delta$  is the displacement.

Mostovoy et al. (1967) and Kinloch (1987, pp. 264-92) have shown according to simple beam theory that for thin adhesive layers of less than 1 mm thickness in DCB specimens with beams of rectangular cross-section the following equation applies:

$$\frac{dC}{da} = \frac{8}{E_s B} \left( \frac{3a^2}{h^3} + \frac{1}{h} \right) \quad (5.8)$$

where  $E_s$  is the independently measured flexural modulus of the substrate.

Hence,  $G_{Ic}$  can be calculated by combining Equation 5.7 and 5.8:

$$G_{Ic} = \frac{4P^2}{E_s B^2} \left( \frac{3a^2}{h^3} + \frac{1}{h} \right) \quad (5.9)$$

This method, however, underestimates the compliance and the values for  $G_{Ic}$  are not accurate. To obtain precise values for the fracture energy, correction factors need to be introduced.

### Method 2: Corrected Beam Theory (CBT)

This method uses several correction factors in the calculation of the fracture energy in order to compensate for the effects of rotation and deflection at the crack

#### 5.4. Fracture mechanics approach – Choice of test method

tip, large displacements in the test specimen and stiffening of the substrate due to the bonded end-blocks used to apply the load (Hashemi et al. 1990; Blackman et al. 1991). The adhesive fracture energy is calculated using Equation 5.10.

$$G_{Ic} = \frac{3P\delta}{2B(a + |\Delta|)} \cdot \frac{F}{N} \quad (5.10)$$

where  $\delta$  is the displacement,  $N$  is the correction factor for the end-blocks,  $F$  is the large displacement correction and  $\Delta$  is the crack-length correction.

The end-block correction factor,  $N$ , and the correction for the large displacement,  $F$ , are given by Equations 5.11 and 5.12 respectively.

$$N = 1 - \left(\frac{l_2}{a}\right)^3 - \frac{9}{8} \left[1 - \left(\frac{l_2}{a}\right)^2\right] \cdot \frac{l_1\delta}{a^2} - \frac{9}{35} \left(\frac{\delta}{a}\right)^2 \quad (5.11)$$

$$F = 1 - \frac{3}{10} \left(\frac{\delta}{a}\right)^2 - \frac{3}{2} \left(\frac{l_1\delta}{a^2}\right) \quad (5.12)$$

where  $l_1$  is the distance from the centre of the loading pin to the mid plane of the specimen beam to which the end-block is attached, and  $l_2$  is the distance between the centre of the loading pin and the edge of the end-block.

The crack length correction factor compensates for the effects of rotation and deflection at the crack tip, which make the crack length,  $a$ , effectively longer ( $a + |\Delta|$ ) than its measured value. The correction term  $|\Delta|$  is gained experimentally from the graph that plots the cube root of the normalised compliance,  $(C/N)^{1/3}$ , as a function of crack length, as shown in Fig. 5.5.

As a check on the procedure, the flexural modulus,  $E_f$ , is calculated as a function of the crack length with Equation 5.13.  $E_f$  is compared with the independently measured flexural modulus,  $E_s$ , of the substrate beams, described in Section 5.4.2.  $E_f$  can also be obtained from the gradient of the linear graph in Fig. 5.5 (Blackman et al. 1991).

$$E_f = \frac{8(a + |\Delta|)^3}{\frac{C}{N} B h^3} \quad (5.13)$$

## 5. Testing of Material Strength and Fracture Behaviour

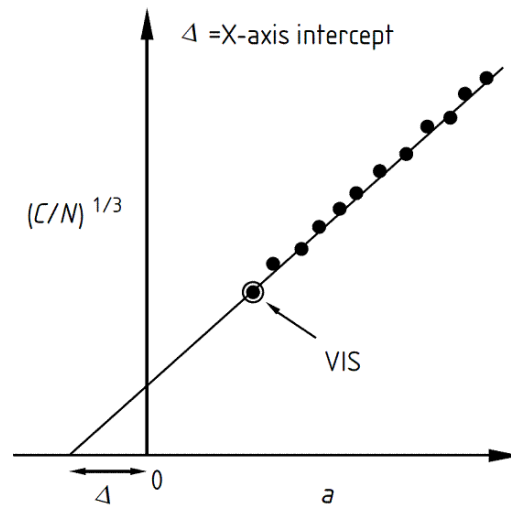


Figure 5.5.: Determination of the crack length correction factor  $\Delta$  for the corrected beam theory (CBT) method. For the linear regression analysis, the visual point (VIS) is excluded (figure taken from BS 7991:2001, p.15).

### Method 3: Experimental compliance method (ECM) or Berry's method

The compliance method calculates  $G_{Ic}$  for DCB specimens with end blocks as shown in Equation 5.14.

$$G_{Ic} = \frac{nP\Delta}{2Ba} \cdot \frac{F}{N} \quad (5.14)$$

where  $n$  is the slope of the graph plotting the logarithm of the normalised compliance,  $\log(C/N)$ , versus the logarithm of the crack length,  $\log a$  (Fig. 5.6). The correction factors  $F$  and  $N$  are the same as for the CBT method.

Generally, all three analysis methods are to be employed for a DCB test according to the standard. Depending on the substrate used and the stability of the crack growth observed during testing, the most suitable method may be chosen to be quoted after the data analysis was performed.



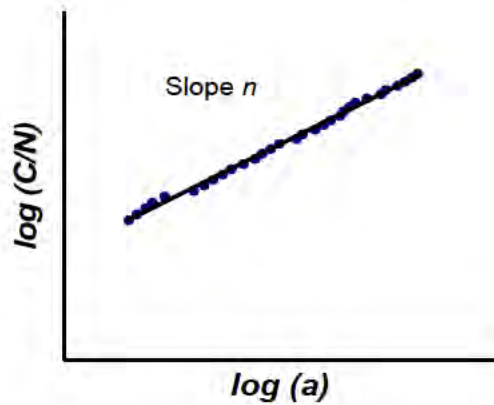


Figure 5.6.: Slope  $n$  determined for the Experimental Compliance Method (ECM) for the DCB specimen (after BS 7991:2001).

### 5.4.2. Determination of flexural modulus

The beam theory used in the calculation of the fracture energy requires the independent measurement of the flexural modulus of the DCB specimen substrate for cross check. The flexural modulus,  $E_s$ , can be determined with three-point bending tests according to ASTM D790 M (1993) and calculated using Equation 5.15.

$$E_s = \frac{L^3 m}{4Bh^3} \quad (5.15)$$

where  $L$  is the support span length,  $m$  is the slope of the linear part of the load-displacement curve,  $B$  is the beam width, and  $h$  is the beam thickness (Fig. 5.7).

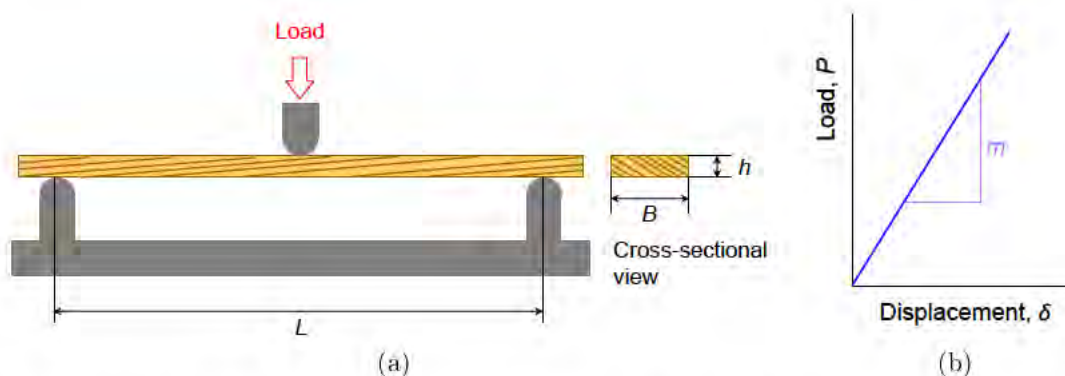


Figure 5.7.: Three-point bending test. (a) Fixture with a support span of length  $L$  and a roller applying a load on the wooden test specimen; (b) load/displacement curve with slope  $m$ .

## 5.5. Choice of materials for test specimens

In order to get a clearer understanding of the fracture behaviour of East Asian lacquer coatings, it was decided to investigate primarily foundation layers containing protein-based binder. In Chapter 3 these were shown to be a major cause for the development of flaking coatings in export ware surveyed at the V&A Museum. Even though this type of foundation layer was often only one of several types of layers prone to failure, it clearly appeared to be the most likely one to fail first. Hence it seemed a useful starting point for the development of a strategy to characterise these types of complex coatings in more detail.

To gain meaningful answers to the question of how much energy is needed to fracture a protein-bound foundation layer or its interface with the wood substrate, it was vital to simplify the tested system to the extent that any influences on the material's behaviour could be clearly ascertained and controlled. This meant that DCB specimens had to be designed which contained animal glue-bound foundation as an 'adhesive' layer between the two wooden beams. Following on from this very simplified structure, the intention was to test a second set of samples which incorporated an additional lacquer layer between the foundation and one of the wooden beams. This second set would provide information on whether the foundation failed differently if coated with lacquer, i.e. when incorporated in a multilayered composite structure.

### **Accelerated ageing versus mechanical replication of damage**

It has been acknowledged at the beginning of this chapter in Section 5.1 that the properties of aged materials in objects are difficult to characterise. To some extent, the same applies to materials that are artificially aged in a laboratory environment. Determining the 'correct' parameters for accelerated ageing experiments to give a desired result, is extremely difficult, time-consuming, and often requires sophisticated – and thus expensive – equipment. Research by Feller (1987; 1994) and others (e.g. Berger and Zeliger 1984; Thei 2010) have clearly shown that the artificial replication of specific degradation and failure patterns require extensive investigations, which in the end may still only produce specimens that have indeed the correct appearance, but not necessarily the appropriate physical and chemical properties. This is a common difficulty associated with any accelerated ageing technique, as the accelerating methodology may cause failure processes that are never seen to occur in real objects.

With new materials or newly produced objects, this is less of an issue. If sourced or manufactured in a reproducible manner, new materials can be characterised more consistently. With the knowledge of how these materials generally change during natural ageing and deterioration – information on which can at least partly be gained from respective literature – it is possible to predict a general trend of

### 5.5. *Choice of materials for test specimens*

how they are likely to behave with increasing age. ‘Baseline’ values for properties can be provided for new materials, which are assumed to characterise ‘best possible behaviour’ of the material (as it is still unaged). These present a realistic starting point from which generally known property changes will occur with time. Hence, this approach may allow conservators to attempt a more informed estimate on the altered characteristics of the aged material they are dealing with eventually.

To gain suitably damaged specimens for testing, an alternative approach can be that of directly inducing mechanical action on the specimens. In this research, it was aimed to test the scope of the proposed DCB method for replicating the damage patterns observed on real life objects to create specimens bearing great physical resemblance to these objects. The following two chapters present the manufacture of the test specimens and the results of these replication trials in more detail.



# 6. Experimental: Fracture Behaviour — Materials and Methods

## 6.1. Preparation of test specimens

Test specimens were designed and prepared in a procedure that was partly based on traditional recipes, but was adapted so as to provide the means for more controlled uniformity and reproducibility. Although it would have been possible to utilise original East Asian substrates and materials for the manufacture of test specimens, it was considered that their use would not have significantly improved the validity of this research. East Asian materials used for export-lacquer ware, such as hide glue or even some woods, are very similar to the ones supplied in central Europe, and very often, both origins do not necessarily provide much detailed technical information about their products. Hence these materials may vary substantially between suppliers or even between individual batches. For the manufacture of test specimens it was therefore decided to use Western materials as far as possible (single batches), to reduce not only costs but also to have available as much technical information on the materials as possible.

### 6.1.1. Double Cantilever Beam (DCB) specimens for initial testing

#### Wood preparation

For the substrate, a softwood was chosen with similar mechanical properties to that of Japanese cypress (*Chamaecyparis obtusa*), which is known as *hinoki* in Japanese (see Appendix B for specifications). The beams (substrates) for the DCB specimens were prepared from a thick, flat sawn, finely grained, knot-free and well seasoned log of Québec yellow pine (White pine, *Pinus strobus*) which had approximate dimensions of 650 mm (grain direction) by 300 mm (tangential face) by 78 mm (radial direction).

From this, thin boards (laminae) of 5 mm thickness were cut at an approximate 3° angle to the wood grain with a circular saw (Fig. 6.1). Grain angle was determined

## 6. Experimental: Fracture Behaviour – Materials and Methods

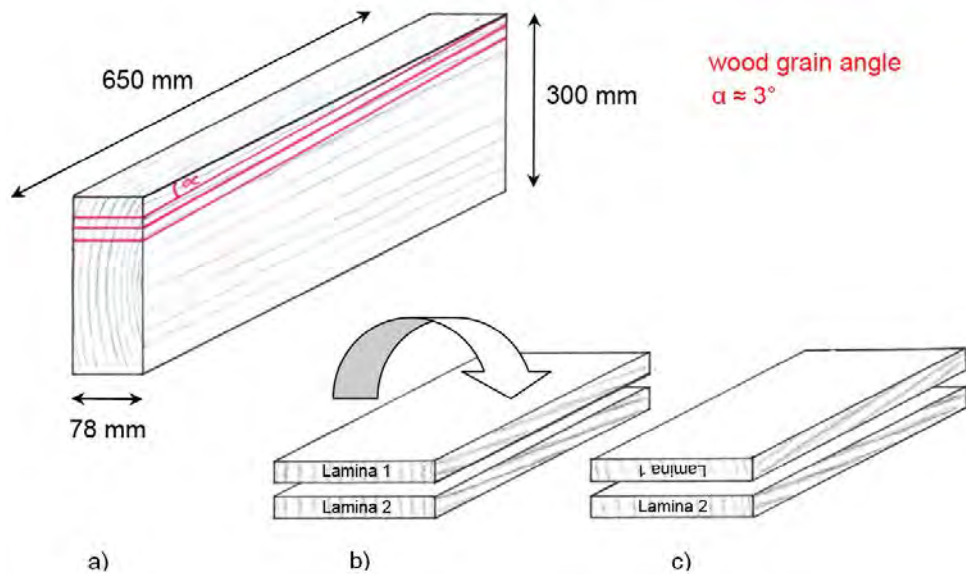


Figure 6.1.: a) Cutting of laminae from pine wood log at a  $3^\circ$  angle to the wood grain, b) pairing of consecutive lamina boards showing V-shaped alignment of wood grain on radial surface (c).

on the tangential surface and parallel lines were drawn to assist cutting. This was to ensure a consistent modulus of elasticity ( $E$ ) in each beam and helped direct the crack away from the substrates during testing. Previous research had shown that grain angles between  $3^\circ$  and  $10^\circ$  achieve this purpose successfully (Knaebe and Williams 1993).

The thin laminae were consecutively numbered, further planed to 4 mm thickness and cut each into 4 short boards of 150 mm length. Each individual small board was allocated an identification code comprising the number of the original lamina and a number indicating its position within the original board. Two boards with consecutive lamina numbers and identical position numbers were then paired together by placing them on top of each other and flipping the panel with the uneven number over its long side. This alignment ensured that the grain angle of the tangential surfaces of both plates was directed in a 'V'-shape towards their boundary (Fig. 6.1). The end of each specimen board at the open side of the 'V' was marked 40 mm from its edge for later positioning of a starter foil during bonding. The thickness of each board was measured using Vernier callipers in 3 places 30 mm from each narrow end and in two places in the centre area of the board. The thickness values were recorded to the nearest 0.01 mm and the values were averaged for 3 (or 2) data points in the length direction of the board.

## Preparation and application of foundation layer

The available literature does not provide precise details for the manufacture of animal glue/*tonoko* foundations other than simply naming the general ingredients (e.g. Quin 1882/1995, p. 21 or Stephan 1927). Therefore, experience from the preparation of gilding gesso and recommendations of two Japanese lacquer specialists, Kitagawa and Kautsch, were adopted and slightly adapted for more controlled handling of the materials. Bovine hide glue (Kremer) was chosen as a substitute for *sanzenbon nikawa* (“Three Thousand Sticks Glue”) that is typically used in Japan. Both these glues are based on bovine hide collagen. Whilst reliable technical information on *sanzenbon nikawa* is rarely obtainable, bovine hide glues can be purchased from European suppliers offering more detailed information, such as gel strength and viscosity. Choosing hide glue from European suppliers renders the manufacture of test specimens more controlled and thus reproducible.

Two different types of specimen boards were manufactured by bonding together two 78 mm wide pine boards. From these, three individual DCB specimens of 20 mm width were subsequently cut. Type A specimens were intended for testing the fracture properties of a protein-bound foundation layer that had a wood interface on both sides of the layer. Type B specimens were manufactured with a wood–foundation interface on one side and a foundation–lacquer interface on the other, which reflected more realistically the situation on real life lacquer objects.

**DCB Specimens Type A (with foundation layer only)** A 10 weight % (wt %) solution of bovine hide glue was prepared by soaking dry glue pearls in deionised water overnight and then heating the solution in a bain-marie at 60 ( $\pm 1$ ) °C water temperature for 30 minutes. The solution was strained through a clean cotton cloth to remove remaining particles and the froth that had developed upon first heating. Finely ground and sieved (through 15 den polyamide tights) Japanese *tonoko* clay powder was slowly added to the glue solution at a weight (wt) ratio of 1:1, and the mixture was carefully stirred without introducing air bubbles, whilst being kept heated in the bain-marie. It is worth mentioning at this point that previous trials for the manufacture of homogeneous test specimens had shown that *tonoko*/glue solution ratios higher than 1:1 and up to 1.15 parts of clay powder lead to problems with the even application of consecutive layers, as the paste becomes too stiff too fast upon spreading on a previously applied foundation surface. The 1:1 *tonoko*/glue mixture had a consistency similar to gesso solutions used in gilding (e.g. Michalski 1991a) and was convenient to apply in an even manner. The foundation mixture was then filtered through fine gauze (15 den polyamide tights) and swiftly applied in a layer of about 1 mm thickness to the surfaces of each pair of boards with a large, soft-haired brush. Care was taken not to introduce bubbles into the liquid foundation mixture during application. On the previously marked end of one board a 12.5  $\mu\text{m}$  thick polytetrafluoroethylene (PTFE, Teflon) starter foil was placed and two stainless

## 6. Experimental: Fracture Behaviour – Materials and Methods

steel wires with a diameter of 0.25 mm were positioned at each end of the specimen as spacers, before the two boards were carefully placed together starting from one end to prevent the entrapment of air bubbles in the joint. The bonded specimen board was then immediately placed in a steel press that had been pre-warmed to 30 °C, and it was left under a pressure of approximately 0.4 MPa at room temperature of 21.0 ( $\pm 1.5$ ) °C for 16 hours.

### **DCB Specimens Type B (with foundation layer and a lacquer coating)**

For the second type of specimens the foundation was applied with the same technique to a further eight boards, but this time only to those ones of a board pair that were marked with an odd number. The second board remained untouched. The first foundation layer was left to dry for 24 hours at 21.0 ( $\pm 1.5$ ) °C before the surface was lightly sanded with dry 150 grit (#) emery-paper to reduce unevenness. A second layer of freshly prepared foundation was then applied in the same way as described above, and the coated panels were left to dry for several days. The fully dried foundation layer was ground with #150 emery-paper until the surface was even.

After the excess dust had been wiped off the surface with a dry, clean cloth, a layer of *ki-urushi* was applied to the foundation surface with a V-shaped *urushi* brush (*kiridashi hake*), following a strict application routine based on Japanese tradition to allow even distribution of the lacquer (Fig. 6.2). Application was undertaken at room temperature of 21.0 ( $\pm 1.5$ ) °C and 37.0 ( $\pm 1.5$ ) % RH. A PTFE starter foil was placed on the fresh lacquer coat in the same position at one end of the specimen board as described for type A specimens, and the boards were placed inside a humidity box at 74.0 ( $\pm 1.5$ ) % RH at 21.0 ( $\pm 1.5$ ) °C for polymerisation of the lacquer. The boards were left in the humidity box for 1-2 days, then removed and exposed to room temperature at around 50 % RH. As the wood of the thin lacquered boards had swollen slightly in the high RH environment and thus showed a small degree of concave warping towards the lacquered surface, the coated panels were given two days to relax back into their original flat state before a second layer of *ki-urushi* was applied in the same manner as before. Polymerisation of the second layer in the high RH environment was followed by the same relaxation routine at around 50 % RH at room temperature for two days. The dried urushi lacquer surface was then polished with a #800 Japanese grindstone and a small amount of water to remove enclosed dust particles from the lacquer surface. A third, fourth and fifth layer of *ki-urushi* were consecutively applied in the same manner. The final polymerisation time after application of the fifth lacquer layer was one week in the high RH box and relaxation at room temperature around 50 % RH for a further 3 weeks. The matching untreated wood board for each coated specimen board was finally glued onto the lacquer surface with Araldite 2015 (epoxy resin) adhesive thinly spread on both joint surfaces, and the specimen was placed in a press at approximately 0.6 MPa pressure at room temperature for 24 hours.



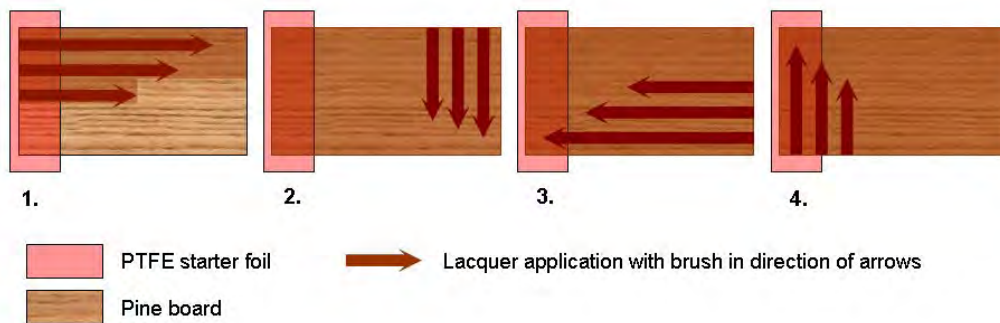


Figure 6.2.: Direction of brush strokes during application of *urushi* lacquer (1.-4.) to ensure even spreading (method based on Japanese tradition; Kurimoto 2001).

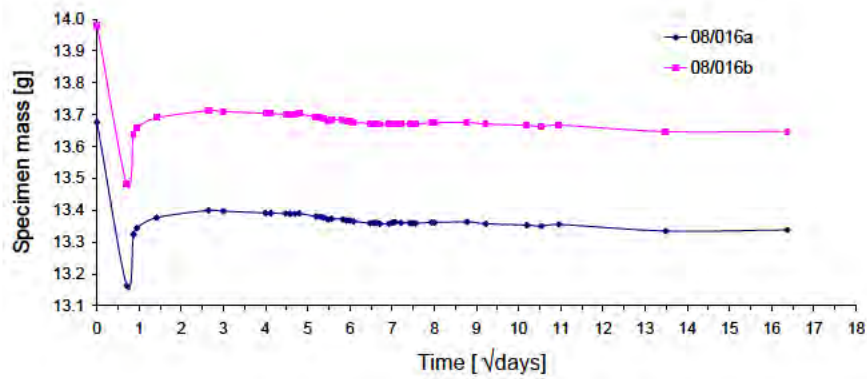
## Cutting and conditioning of DCB specimens

**DCB specimen type A** After curing the foundation for 16 hours, the bonded laminate boards were removed from the press and cut into individual specimens with a band-saw. Each board yielded 3 specimens of 21 mm width, which were then ground to a final width of 20 mm. As slight variations in the nominal dimensions could not be avoided, the actual width of each specimen was measured in 3 places, 30 mm from both ends and in the middle, with the mean value being recorded for each specimen. All specimens were individually coded with the laminate board number and their position number within each board. Altogether 60 DCB specimens were prepared (5 sets of 12 specimens each).

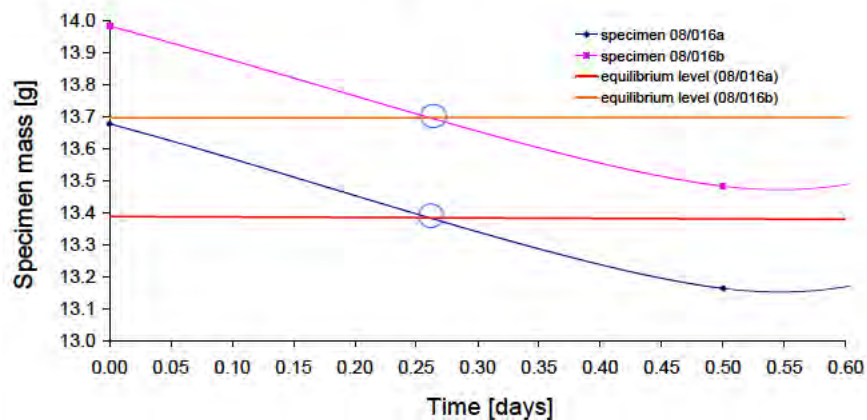
The specimens were dried and conditioned in two stages: directly after cutting they were first placed into a closed environment of near 0 % relative humidity (RH) at 21 °C temperature for 6 hours to increase the moisture gradient within the specimen. This led to accelerated initial drying. The length of time for this initial drying period was determined from preliminary drying tests, conducted to avoid “over-drying” of the test specimens. Preliminary specimens had been placed in a near 0 % RH environment for a period of twelve hours, during which time their weight was monitored at close time intervals. The drying cycle was then followed by continuous exposure to 53.0 ( $\pm 1.5$ ) % RH at 21.0 ( $\pm 1.5$ ) °C for several months during which the weight changes of the samples were recorded at increasing intervals (Graph 6.3a). In order to find a suitable time span for accelerated drying at low relative humidity, the intersection point of the desorption curve (in the area of accelerated drying) and the specimen mass at a preliminary equilibration level was determined. This preliminary equilibration level was set at 25 days, as the specimens showed only very small weight changes after this drying period. Hence, the intersection point of the graphs at 6 hours (0.25 days) was taken as a suitable time span for accelerated drying (Graph 6.3b).

After initial drying at near 0 % RH, the DCB specimens were moved into a

6. Experimental: Fracture Behaviour – Materials and Methods



(a)



(b)

Figure 6.3.: Desorption curves for two DCB specimens (150 mm x 20 mm x 8 mm) during equilibration to  $21.0 (\pm 1.5) ^\circ\text{C}$  and  $53.0 (\pm 1.5) \% \text{RH}$  over a period of 268 days, represented in (a). The initial drying phase of the specimens shows a sharp drop in specimen mass caused by the exposure to near 0 % RH for 12 hours to decrease the drying time; (b) gives a detail of the desorption curves shown in (a), showing intersections of the graphs with their respective preliminary equilibration level after approximately 6 hours.

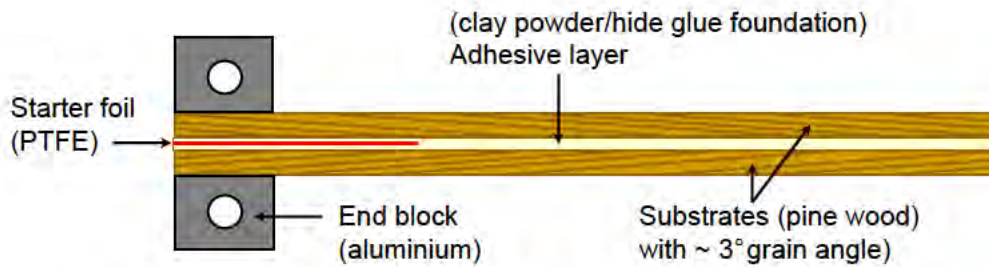


Figure 6.4.: DCB specimen (pine wood/foundation) with attached aluminium end blocks.

chamber conditioned with a saturated salt solution of magnesium nitrate to  $53.0 (\pm 1.5) \% \text{RH}$  at a temperature of  $21.0 (\pm 1.5) ^\circ\text{C}$  and then further dried for two months. Even though equilibration of the specimens with the surrounding environment was not complete after this period, weight changes of the specimens until full equilibration were only minimal, in the range of  $0.2\text{--}2 \mu\text{g}$  per 24 hours, and were thus considered negligible.

**DCB specimen type B** The lamina boards of specimen type B were cut and ground in exactly the same manner as those of specimen type A. Directly after manufacture, the individual specimens were placed in a chamber conditioned with a saturated salt solution of magnesium nitrate to  $53.0 (\pm 1.5) \% \text{RH}$  at  $21.0 (\pm 1.5) ^\circ\text{C}$ , omitting any initial accelerated drying, and equilibrated for two months. The length of equilibration time also assured that the lacquer layer was fully cured. Complete polymerisation of the *urushi* film is reported to take approximately two months (Vogl 2000).

**DCB specimen finishing before testing** Before testing, two aluminium end blocks were fixed to the wood surface on that end of the DCB specimen incorporating the starter foil. The end blocks were adhered with cyanoacrylate adhesive (Loctite SuperGlue) and a jig was used to ensure their symmetrical alignment (Fig. 6.4). On the bond line, a thin coat of proprietary solvent-based white paint (correction fluid, Tippex) was applied to create a white background, against which crack growth could be monitored more easily during testing. To enable crack length measurement, a scale with 1 mm increments was attached to one of the beams below the bond line, with its origin aligned with the loadline (i.e. the centre of the end block holes).

### 6.1.2. Consolidation of fractured DCB specimens

After initial cracking of the DCB specimens, all specimens were randomly grouped together in sets of four specimens each. Every set was allocated a consolidant. One further set of specimens was used to measure the flexural modulus of the wooden beams, which involved the additional flexing of the beams after initial cracking. This rendered these specimens incomparable with the remaining sets and hence the flexed specimens were entirely abandoned for further consolidation and testing.

#### Consolidants

Table 6.1 lists the consolidants chosen from each individual class as introduced in Section 6.1.4. The individual polymer concentrations were selected so that the formulations had roughly comparable working properties, such as sufficiently low viscosity to allow even spreadability, and were able to bond the specimens without their failing during simple handling. The working properties were determined in pre-tests. Viscosities varied between the formulations, but it was tried to keep them as similar as possible within each consolidant class.

#### Preparation of consolidants

**Set No.01 Salianski Isinglass (class I)** Raw, dried Salianski isinglass bladder (Kremer) was cut into small pieces and soaked in cold deionised water at a weight ratio of 1:9. After soaking for 16 hours the mixture was heated in a bain-marie at  $68 (\pm 1)^\circ\text{C}$  for 3 hours, then filtered through fine gauze (15 den polyamide tights) and poured thinly onto Melinex polyester film for drying (Przybylo 2006; Przybylo 2007). Fresh isinglass glue solution was prepared from the dried isinglass film with deionised water at a 10 wt % concentration and heated in a bain-marie at a water temperature of  $60 (\pm 1)^\circ\text{C}$  for a few minutes until liquid. Fast Green stain powder (Merck) was added to the glue solution at a concentration of 0.2 wt % to enable visual tracking of the consolidant distribution in cross-sections after consolidation. The solution had a pH of 5.5.

**Set No.02 Fish Glue (class I)** Cold-liquid fish glue (Lee Valley) was diluted with deionised water to a concentration of 25% solid content. The pH of the solution was determined as 4.5. Fast Green stain powder was added to the glue solution at a concentration of 0.2 wt %.

**Set No.03 Bovine Hide Glue (class I)** Bovine hide glue in cubes (Kremer) was soaked overnight in deionised water at a concentration of 10 wt % and then heated in a bain-marie at a water temperature of  $60 (\pm 1)^\circ\text{C}$  for 30 minutes. The

## 6.1. Preparation of test specimens

Table 6.1.: Selection of consolidant formulations.

CLASS	SET	CONSOLIDANT	CONCENTRATION	SOLVENT/ DILUENT	REFS. (AMONGST OTHERS)
I	01	Salianski isinglass	10 wt %	Deionised water	Miklin-Kniefacz (1995)
I	02	Lee Valley fish glue	22.5 wt %	Deionised water	Breu and Miklin-Kniefacz (1995), Webb (1998), Breidenstein (2002)
I	03	Bovine hide glue	10 wt %	Deionised water	Miklin-Kniefacz (1995), Kato (1988)
I +	04	Isinglass/wheat starch ( <i>shofu</i> )	10 wt % and 16.6 wt%, 1:1	Deionised water	Breidenstein (2000), Springob (2001)
II +	05	<i>Mugi-urushi</i>	2:1 (by wt.)	Exxsol 80-110	Matsumoto and Kitamura (2008)
II	06	<i>Ki-urushi</i>	2:1 (by wt.)	HAN 8070	Yamasaki and Nishikawa (1970), Matsumoto and Kitamura (2008)
III a)	07A	Paraloid B 72	25 wt %	Toluene	Yamasaki (1957), Chase (1988), Chase et al. (1988)
	07B	Paraloid B 72	20 wt %	Acetone	Gillis (1998)
III a)	08	Paraloid B 48 N	25 wt %	Tol./xylene 1:1 (by wt.)	
III b)	09	Medium for Consolidation	25 % solid content	–	Hedlund and Johansson (2005)
IV	10	Mowiol 3-83	25 wt %	Deionised water	Yamasaki (1957)
V a)	11	Mowilith 50	20 wt %	Toluene	Hagedorn (2002)
V b)	12	Mowilith DMC2	10 % solid content	Deionised water	

## 6. Experimental: Fracture Behaviour – Materials and Methods

solution had a pH of 6. Fast Green stain powder was added to the glue solution at a concentration of 0.2 wt %.

**Set No.04 Wheat Starch (*shofu*) and Salianski Isinglass (class I+)** Japanese precipitated – i.e. gluten free – wheat starch (Paper Nao) was prepared at a ratio of 1:5 by volume (16.6 % by weight) with deionised water and cooked based on instructions recommended by Merryl Huxtable from the V&A Museum’s Paper Conservation Department (personal communication). The mixture was gradually heated in a pan under constant and vigorous stirring, and was cooked for 15 minutes at high heat until the paste turned translucent. The paste was taken off the heat and left to stand stirring for another 10 minutes before it was transferred into a glass container and cooled down completely. Before use as a consolidant, the cool paste was pressed through fine gauze (double layer of moderately stretched 15den polyamide tights). It was further mixed at a weight ratio of 1:1 with a 10 wt % isinglass solution stained with 0.1 wt % of Fast Green, yielding a smooth thin paste with an overall solid content of 13.3 wt%.

**Set No.05 *Mugi-urushi* (class II+)** For *mugi-urushi*, Japanese medium strength wheat flour (provided by Y. Yamashita, V&A) was prepared as a paste, adding 1 part by weight of deionised water to 2 parts of Japanese medium strength wheat flour. The flour paste (66.6 % solid content) was mixed with a spatula, kneaded with the fingers until smooth and left to stand for 30 min. The paste was further mixed with filtered *ki-urushi* at a weight ratio of 1:2. The *ki-urushi* was of Chinese origin (Watanabe-Shoten) and is assumed to have a solid content (i.e. urushiol, plants gums, glycoproteins and enzymes) in water of around 70 % (Kumanotani 1995). Finally, the *urushi*/flour paste was diluted with Exxsol 80-110 (Exxon Mobil) at a weight ratio of 2:1 (rendering an approximate dispersion concentration of 46 %).

**Set No.06 *Ki-urushi* (class II)** Chinese *ki-urushi* (Watanabe Shoten) was mixed with an aromatic hydrocarbon solvent based on petroleum ether, HAN 8070, at a ratio of 2:1 by weight.

**Set No.07 Paraloid B 72 (class III a)** Paraloid B 72 (Conservation Resources) was dissolved in toluene (for type A specimens) and in acetone (for type B specimens) at a concentration of 25 wt %. Each solution was prepared by suspending in the solvent for 24 hours a cotton gauze sachet filled with the acrylate granules until the resin had dissolved completely.

**Set No.08 Paraloid B 48 N (class III a)** Paraloid B 48 N (Conservation Resources) was dissolved in a solvent mix of 50 wt % toluene (methylbenzene) to

50 wt % xylene (dimethylbenzenes) at a concentration of 25 wt % and pre-stained before application with 0.1 wt % of Solvent Blue G dye (Town End Leeds).

**Set No. 09 Lascaux Medium for Consolidation (class III b)** Lascaux Medium for Consolidation (Kremer) was used as an undiluted aqueous dispersion containing 25 % of dispersed solids, as provided by the supplier. The pH of the solution was measured as pH 7.

**Set No. 10 Mowiol 3-83 (class IV)** Mowiol 3-83 granules (Kremer) were dissolved in deionised water at a solution concentration of 20 wt %. As the solution still contained highly swollen, undissolved particles after several hours of continuous stirring at around 21 °C, the solution was briefly heated to 90 °C for 2 min, according to recommendations by Clariant (1999, p. C2.1), until full dissolution of the swollen resin particles was achieved. The poly(vinyl alcohol) (PVAL) solution was then left to cool down to room temperature before use, and a pH of 5 was measured.

**Set No. 11 Mowilith 50 (class V a)** Mowilith 50 (Kremer) was prepared in toluene at 25 wt % solution concentration by suspending a cotton gauze sachet filled with the polyvinyl acetate granules in the solvent for 48 hours until complete dissolution occurred.

**Set No. 12 Mowilith DMC2 (class V b)** The aqueous PVAC dispersion Mowilith DMC2 (Kremer), provided by the supplier at a 50 % solid content, was diluted with deionised water to a 10 wt % concentration of solids. The diluted dispersion had a pH of 3.5.

## Application of consolidants, clamping and equilibration

All solutions and dispersions were applied with a 20 mm wide bristle brush to both fracture surfaces of each DCB specimen. Application was executed with 3 brush strokes of a freshly loaded brush for each fracture surface to facilitate even consolidant distribution. The two substrates were then placed together starting from the end of the inserted starter foil to prevent enclosure of air bubbles, and the DCB specimen was placed under a weight, exerting a pressure of 23 kPa. The pressing time at room temperature depended on the type of consolidant used: solvent-based consolidants were pressed for 1 week inside a fume cupboard, whilst *urushi*-containing consolidants were pressed for 1 week in a humidity-controlled chamber at 73.0 ( $\pm 1.5$ ) % RH. All other specimens consolidated with water-based adhesives were left in the press at ambient room environment for 2 days. Only the specimens consolidated with Mowiol 3-83 were pressed for 7 days, as previous consolidation tests had shown that longer pressing time was required.

## 6. Experimental: Fracture Behaviour – Materials and Methods

After initial drying in the press, all the specimens were secured at both ends with small clamps, moved into conditioned chambers at 53.0 ( $\pm 1.5$ ) %RH and a temperature of 21.0 ( $\pm 1.5$ ) °C. Equilibration of the specimens was monitored by weighing them at regular intervals until their mass ceased to change significantly (changes  $< 0.0015$  % per 24 hours). The type A and B specimens were kept in the equilibration chamber for 2 $\frac{1}{2}$  and 3 $\frac{1}{2}$  months respectively until testing. (The varying equilibration times for the two specimen types had no particular technical reason, and were merely a consequence of testing equipment availability.)

### 6.1.3. Specimens for tensile and compression testing

#### Foundation

**Tensile specimens** The gesso-type foundation mixture, prepared to the specifications given in Section 6.1.1, was cast into silicone rubber moulds with dogbone-shaped recesses of 450  $\mu\text{m}$  depth. The surface was drawn down smooth with a razor blade. After drying for 6 hours at room temperature of around 21 °C, the specimens were carefully lifted from the mould with a thin razor blade. At this stage, the films still contained sufficient moisture to provide flexibility and to prevent damage of the specimens. Due to the shrinkage of the foundation matrix during drying, however, the dogbone-shaped specimens had developed a pronounced meniscus along the edges rendering them with irregular thickness. Therefore, the specimens were cut with a sharp blade to a smaller rectangular shape of 70 mm x 6 mm in dimensions, making use of the flat centre area of the specimen. Sample dimensions and preparation for testing followed a procedure specified by Hagan (2009). To provide a rigid gripping surface for mounting the thin films in the testing equipment, paper tabs were bonded to each narrow end of the rectangular specimen with sparingly-applied cyanoacrylate adhesive, leaving a free gauge length of 60 mm and ensuring a length to width specimen dimension of 10:1. Care was taken not to use too much adhesive to avoid contamination of the gauge length section of the specimen. The specimens were equilibrated to 53.0 ( $\pm 1.5$ ) % RH at 21.0 ( $\pm 1.5$ ) °C for several months.

Before testing, the thickness of all prepared specimens was measured with a micrometer in three positions within the gauge length. The mean thickness value for each specimen, which typically ranged between 350–380 ( $\pm 5$ )  $\mu\text{m}$ , was determined to establish the specimen's initial cross-sectional area.

**Compression specimens** Compression specimens were manufactured with the same type of foundation mixture that was used for the tensile specimens. The freshly prepared hide glue/*tonoko* mixture was cast into cylindrical silicone rubber moulds of 15 mm diameter and 3 mm depth. As problems arose with cracking caused by too rapid drying at conditions of 21 °C and approximately 50 % RH, evaporation of the water contained in the cast specimens was delayed by covering



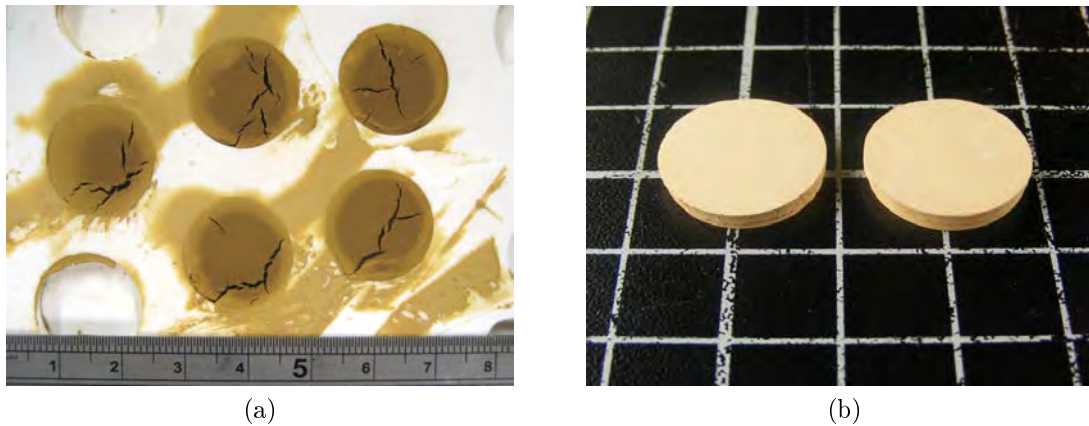


Figure 6.5.: Foundation compression specimens. (a) Unsuccessful attempt of producing specimens using foundation with a lower water content (16.5% glue solution concentration). (b) Foundation specimens made with 10% glue solution concentration after grinding of circular surfaces (grid in background equals 10 mm square)

the mould with cling film. Small holes in the film ensured adequate ventilation and effectively prevented the development of cracks within the body of the specimens. Nevertheless, the specimens shrank slightly during drying and separated from the side walls of the mould, creating slightly rough and concave surfaces on the periphery. The specimens were ground and polished with emery paper and Micro-mesh (Kremer) on their circular faces to render them absolutely parallel before being equilibrated to  $53.0 (\pm 1.5) \% \text{RH}$  at  $21.0 (\pm 1.5) ^\circ\text{C}$  for three months (Fig. 6.5a).

Trials with foundation formulations having lower water content but the same (dry) glue-protein to filler ratio were unsuccessful. Even a small reduction of water corrupted adequate dispersion of the filler particles in the glue solution, allowing only a maximum glue solution concentration of 16.5%, provided the original ratio of dry glue to filler was retained. The large surface area of the fine filler particles apparently requires a large amount of water for appropriate wetting. Specimens with reduced water content also appeared to develop more pronounced cracking during drying (Fig. 6.5a).

#### 6.1.4. Replication of lifting lacquer for empirical consolidation testing

Small pine boards of 4 mm thickness were prepared with two layers of hide glue/*tonoko* foundation and coated with 5 layers of Chinese *urushi* lacquer according to the procedure described in Section 6.1.1. After hardening of the lacquer, the boards were cut by hand with a fine hardwood backsaw into small individual

## 6. Experimental: Fracture Behaviour – Materials and Methods

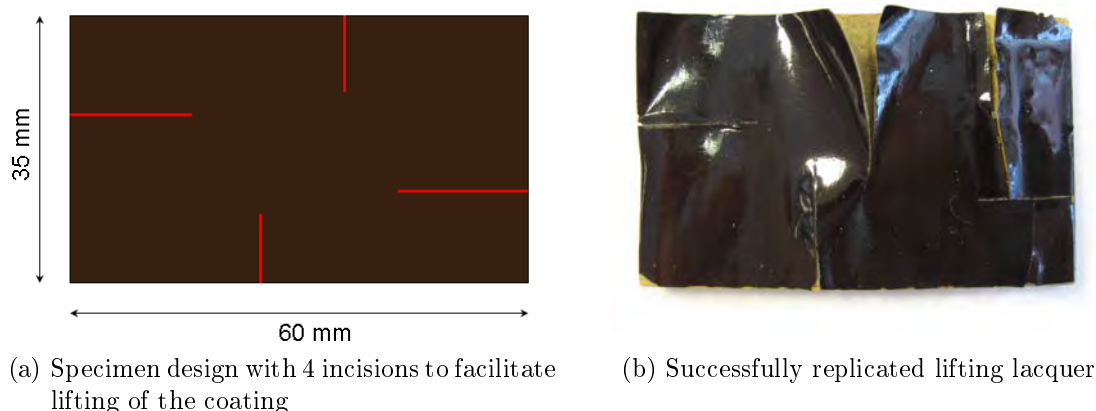


Figure 6.6.: Replication of lifting export lacquer coatings

samples of approximately 60 mm x 35 mm in size, and were conditioned under laboratory conditions at room temperature and circa 50 % RH for two months. The specimens were then placed in an RH-controlled chamber and exposed to 100 % RH for 2 days until the lacquer film and foundation layer had softened sufficiently so that 4 incisions of approximately 10-15 mm length could easily be made with a razor blade through the coating down to the wood (Fig. 6.6a). These cuts were intended to facilitate lifting of the coating during further cycling which was executed at relative humidities of near 0 % and 100 % until extensive lifting occurred. The type of cracking and lifting produced on these lacquer coatings resembled the type of damage frequently seen on lower quality Japanese lacquer ware and on Chinese lacquer objects (see Chapter 3).

### Unsuccessful approaches

During trial runs intended to establish a method and appropriate cycling conditions that would give successful results, it became clear that the replication of lifting lacquer was more difficult to achieve than originally expected. The first trial tests, where specimens were wrapped in a wet cloth for 4-5 hours before drying at room temperature in an unconditioned, dry laboratory environment at around 21 °C, initially gave very promising results, which even appeared to be reproducible. However, while at first several specimens were successfully deteriorated in this way on different occasions, reliable replication turned out to be impossible in the long run.

A second way of replicating lifting lacquer was tried, during which the samples were not directly exposed to water, but to a high humidity environment of 100 % RH in cyclic change with near 0 % RH. These conditions were achieved by placing the specimens in small chambers, in which RH was controlled by desiccated silica gel (Merck) for extremely dry conditions, and by wet towels to achieve maximum RH. Specimens were humidified for the same time period as they were

dried out, with cycles lasting between 3 and 4 days, alternating every week. The entire cycling procedure was repeated over 6 weeks, although with very limited success. Only some of the outermost edges of the specimens' four corners and the incisions in the coating had started to lift very slightly. However the lifted areas were not sufficiently large to perform useful consolidation tests.

Slightly more successful results were gained when specimens were exposed to high humidity for much longer periods than just 3-4 days. Wet cycles were extended to 2-3 weeks and dry cycles to 5 days over a period of 3 months. Unfortunately, this cycling encouraged mould growth on the specimens. With the return to an environment of 53% RH, the small wood boards also developed significant concave distortion towards their uncoated underside, despite being cut in radial direction of the growth rings. Nevertheless, these conditions finally did produce sufficiently lifting lacquer coatings, even though the lifting was less pronounced as in the initial lot produced under 'uncontrolled' conditions.

The best results were produced rather unintentionally, when specimens were kept (and accidentally forgotten) in a humid environment for two months, and mould had grown on the surfaces. When subsequently exposed to the dry RH conditions, extensive lifting of the lacquer coating developed within minutes, as shown in Figure 6.6b.

## Discussion of replication method

The types of wood boards used for the initial tests were two pieces of pine wood of unknown origin purchased at a DIY store, the first of which had fine, narrow annual growth rings, whilst the other showed much more pronounced and wider late wood grain. They further differed in the direction of cut relative to the growth rings as well as in their relative content of pine resin. These differences may well have played a vital role in their unequal behaviour, in that the samples may have experienced different degrees of dimensional changes during cycling and varying adhesion between substrate and coating.

In summary it can be stated that the artificial production of lacquer damage under controlled conditions is not a straight forward task. Even in very simple export lacquer structures that consist of a wood substrate, animal glue-bound foundation and East Asian lacquer, several factors seem to play a vital role for the overall mechanical performance of the coating structure:

- the type of pine wood used as substrate (including its state of seasoning, dimensions and direction of growth rings, and possibly the presence of natural resin)
- the total number of dry and wet cycles
- and the time length for each cycle.

In order to produce specimens with lifting lacquer for consolidation tests, more research into a suitable and reproducible method is necessary. In this work, time

constraints did not allow for a continued investigation of an improved method. Therefore, the specimens from the initial lot produced under ‘uncontrolled’ conditions and the final ‘accidental’ trial run were used for further practical testing, even though they were neither produced under identical or even comparable conditions, nor under fully controlled circumstances. This is taken into account in the interpretation of the results.

## Consolidation of lifting lacquer

Due to the limited number of samples available, only one single small board could be tested per consolidant. The choice and preparation of the consolidants followed the methods described in Section 6.1.2.

The lacquer specimens had been conditioned in a  $53.0 (\pm 0.5) \% \text{RH}$  environment at room temperature, before being exposed to  $73.0 (\pm 0.5) \% \text{RH}$  for 16 hours, allowing the lifted coating to gently soften. Application of the consolidants was undertaken with small, flat nylon hair paint brushes (Daler-Rowney) and the entire area to be consolidated was generously covered with liquid consolidant. The lifting flakes were carefully pressed down with a ‘sandwich’-structure of Melinex / 1 mm thin, clear silicone sheet / 2 mm Perspex sheet / 2 mm clear silicone sheet with the traditional Japanese *shimbari* method. The clamping method that uses thin bamboo sticks braced between an objects surface and a wooden frame surrounding the object was chosen, because the small lacquer boards had distorted in concave shape towards their back side. Hence, for such specimens conventional clamping in a flat press would not have been appropriate. The advantage of *shimbari* sticks is that they deflect elastically in the lateral direction during buckling under compression, and thus show no significant change in load which they exert on their contact area. This means that the sticks kept exerting approximately the same amount of pressure on the distorted sample boards, even whilst the latter gradually flattened under the applied load.

Ten sticks, providing a pressure of approximately 15 kPa, were braced between the silicone/Melinex sandwich block and a wooden frame surrounding the sample. Pressing times for the individual consolidants were the same as those for the DCB specimens given in Section 6.1.2. After initial drying, the specimens were placed for further drying in an environmentally controlled chamber at  $53.0 (\pm 0.5) \% \text{RH}$  and  $21.0 (\pm 1.5) ^\circ\text{C}$  for two months. This was followed by cyclic exposure to  $73.0 (\pm 0.5) \% \text{RH}$ , controlled with saturated table salt (sodium chloride + sodium ferrocyanide) solution, and  $22.5 (\pm 0.5) \% \text{RH}$ , controlled with saturated potassium acetate solution, for three and a half days each in alternating sequence. The full wet-dry cycles were repeated eight times, over eight weeks. All four surfaces on the sides of the specimen boards (i.e. where the coating could be seen in cross-section) were monitored and photographed before consolidation, after initial drying (before cycling) and after cycling: This was to monitor changes in the appearance of the adhered joints and to evaluate any possible failure of the

consolidants, which would have induced renewed delamination and lifting of the coating structure.

## 6.2. Mechanical properties testing

### 6.2.1. Mode I fracture tests

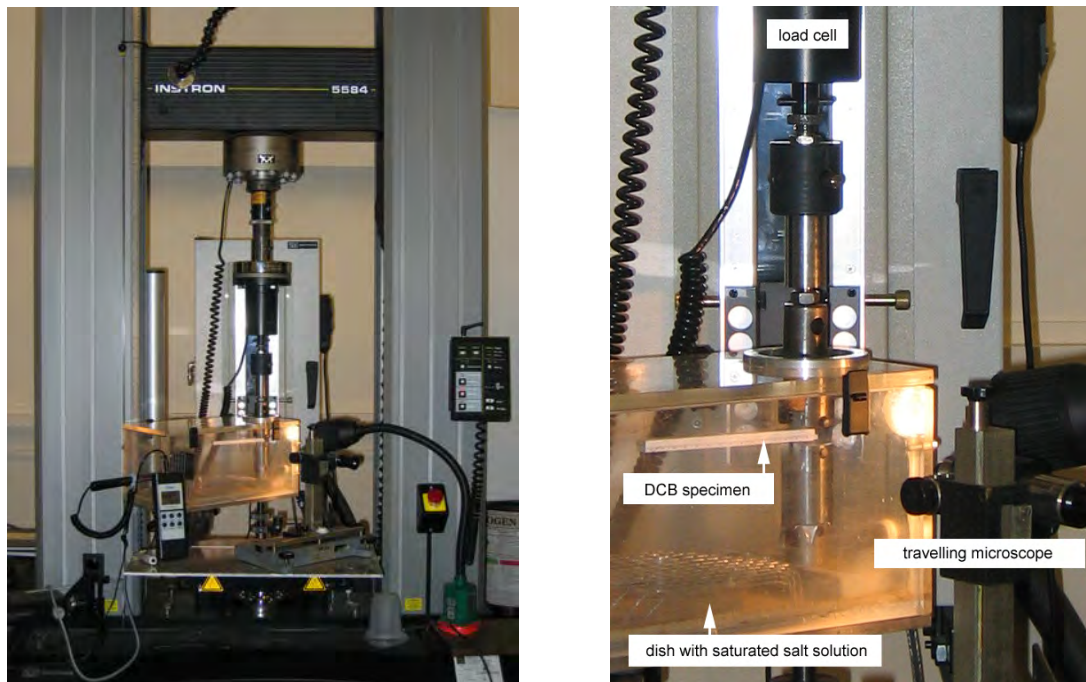
Four DCB specimens for each type of consolidation treatment were tested on an Instron 5584 universal testing machine fitted with a 5 kN loadcell. This measured the load to an uncertainty of better than 0.5%. The specimens were mounted in the testing machine fixture with 8 mm diameter pins. As the specimens were very lightweight, there was no need to support them to remain orthogonal to the loading path during testing. The tests were run at a monotonic cross-head displacement rate of 0.3 mm/min.

The load,  $P$ , crack length,  $a$ , displacement,  $\delta$ , and pip count were electronically recorded using the Bluehill software. Due to the hygroscopic nature of the test specimens, all tests were undertaken within a controlled humidity chamber at 53.0 ( $\pm 0.5$ )% RH and 21 ( $\pm 1$ ) °C. Humidity was controlled with saturated magnesium nitrate salt solution, and a small computer case fan provided adequate circulation. After mounting the DCB specimen in the testing machine fixture, the test was not started for another 30 minutes to allow the conditions within the chamber to revert back to their equilibration level of around 53% RH. The setup is shown in Fig. 6.7.

Crack propagation during testing was observed with a travelling microscope to an accuracy of  $< \pm 0.5$  mm and was manually recorded with a pip for every 1 mm increment. Crack length was monitored over a distance of at least 70 mm from the precrack.

As the fracture energy during crack initiation is significantly influenced by the radius of the crack tip (Kinloch and Williams 1980) it is necessary to ensure coherence between all the joints investigated. Therefore, all DCB specimens were initially precracked a few millimetres beyond the end of the starter foil, to create a sharp crack tip, as recommended by the British Standard (Fig. 6.8a). The test was then stopped and the specimen was completely unloaded at a rate of 5 mm/min before being reloaded for the actual test (Fig. 6.8b). At the end of the test, the specimen was unloaded again to check whether a significant offset displacement had occurred, which would indicate that plastic deformation had taken place in the specimen substrate. Due to the low loads applied during testing and the elasticity of the wood substrate it was however expected that no plastic deformation of the substrate beams would occur.

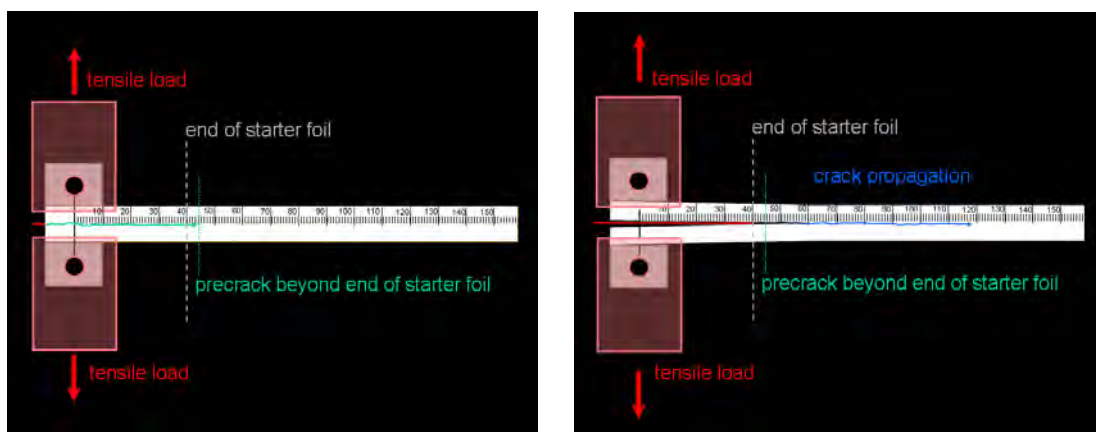
6. Experimental: Fracture Behaviour – Materials and Methods



(a) Overall view of setup with 5 kN loadcell and environmentally controlled chamber.

(b) Detail showing a DCB specimen being tested in mode I inside the RH chamber.

Figure 6.7.: Instron 5584 universal testing machine setup for DCB testing in controlled environment with humidity chamber.



(a) DCB specimen, with scale and end blocks attached, during pre-cracking.

(b) DCB specimen during testing with crack propagation in tensile loading.

Figure 6.8.: Principle of DCB testing.

## Description of failure patterns

The general failure patterns (failure loci) shown on the fracture surfaces of the DCB specimens were characterised following the definitions given by the British Standard BS EN ISO 10365 (1995). Table 6.2 summarises the possible failure patterns for the DCB specimens used in this study.

The possible failure patterns for both initial and second-phase fracture after consolidation differed for the type A and B DCB specimens.

## Data analysis

Values of  $G_{Ic}$  for crack initiation and the individual propagation points within each individual sample were calculated with a customised Excel spreadsheet according to the standard procedure of BS 7991:2001 (2001), described in Section 5.4.1. For a set of measurements the arithmetic mean,  $\bar{x}$ , of the  $G_{Ic}$  values and its standard deviation,  $s$ , were calculated (Eqns. 6.1 and 6.2 respectively).

$$\bar{x} = \sum_i \frac{x_i}{n} \quad (6.1)$$


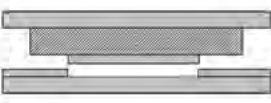

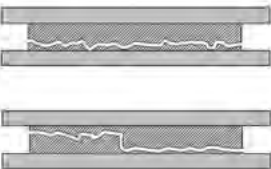
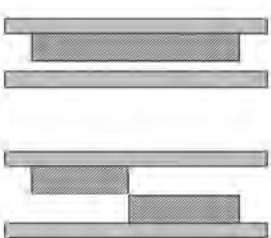

$$s = \sqrt{\sum_i \frac{(x_i - \bar{x})^2}{n - 1}} \quad (6.2)$$

where  $x_i$  is the population and  $n$  denotes the sample size (i.e. the number of calculated values). The relative standard deviation, or coefficient of variation (CoV) of the propagation values was calculated with  $100 \times s/\bar{x}$  to indicate its magnitude relative to the sample mean. Assuming that there was no systematic error present during the experiments, the arithmetic mean of the population was regarded as the true  $G_{Ic}$  value for each sample.

To compare the effect of the consolidation treatments on the fracture energy of the specimens, the difference (delta,  $\Delta$ ) between the  $G_{Ic}$  values for initial fracture and those measured after consolidation was established.  $G_{Ic}$  values were compared for individual specimens as well as for the specimen set (i.e. a set of up to four specimens). Comparing the delta mean fracture energy ( $\Delta\bar{G}_{Ic}$ ) was intended to eliminate the dependency of the means on the precise location within the specimens' fracture surfaces where the measurements were taken, which may have varied considerably within and between specimens due to their natural heterogeneity. The delta mean could be regarded as an indicator of the consolidants' ability to change the energy required for propagating a crack through the specimens, provided that the multilayered specimens were in similar condition. Therefore, both the mean fracture energy,  $\bar{G}_{Ic}$ , and the mean delta mean fracture energy,  $\Delta\bar{G}_{Ic}$ , were evaluated for each specimen set, and these results were further related to each other.

6. *Experimental: Fracture Behaviour – Materials and Methods*

Table 6.2.: Possible failure patterns on DCB specimens based on the definitions given by the Standard BS EN ISO 10365 (1995).

DESIGNATION	FAILURE PATTERN	ABBREVIATION
Cohesive substrate failure (within the wood)		CSF
Delamination failure (within substrate laminate of type B specimens only, i.e. between wood and epoxy resin layer)		DF
Cohesive failure (within foundation or lacquer)		CF
Special cohesive failure (close to interface and/or on different levels within foundation or lacquer layer)		SCF
Interfacial failure (adhesively between two adjacent layers)		AF
Adhesive-cohesive failure with peel (failure on several levels simultaneously)		ACFP



### 6.2.2. Flexural modulus of the wood substrate

The flexural modulus,  $E_s$ , of the wooden beams was determined from three-point bending tests that were performed on an Instron universal testing machine equipped with a 5 kN loadcell. The single beams of 150 mm x 20 mm x 4 mm were loaded using 10 mm diameter loading noses at a span length of 100 mm and a cross-head speed of 1 mm/min (see Fig. 5.7). The modulus was calculated using Equation 5.15.

As the flexural modulus of wood is very much dependent on the direction of the grain and the nature of the cell structure,  $E_s$  values for wood can only be precise if they are measured for each beam in its final test dimensions and prior to any application of the adhesive or consolidant. However, as the DCB specimens had to be manufactured in larger plates before being cut into individual specimens, the flexural modulus could not be measured for every specimen. Hence, the flexure test was performed on 24 specimens cut from the first 4 lamina of the original Québec yellow pine block. The mean  $E_s$  value was calculated to be 8.8 GPa ( $\pm 3\%$ ), which was in excellent agreement with the elastic modulus of 8.8 GPa reported for Japanese *hinoki* wood (Sugiyama 1983). This value was used as an approximation of the real  $E_s$  for every DCB specimen substrate in order to cross-check the  $E_s$  values calculated during DCB analysis, and to show that the test method was giving reliable results.

### 6.2.3. Tensile modulus of foundation

The Young's modulus (modulus of elasticity), elongation at break and tensile strength were determined for foundation by testing rectangular film specimens in tensile loading in general accordance with BS EN ISO 527-1 and BS EN ISO 527-3. The tests were performed on an Instron 4301 universal testing machine equipped with a 100 N loadcell inside a custom-built environmental chamber. The chamber, designed and described in detail by Hagan (2009), controlled the RH at a level of 53.0 ( $\pm 0.3$ ) % and the temperature at 21.0 ( $\pm 0.3$ ) °C during testing. The tensile specimens were mounted in the following procedure:

Firstly, the upper grip was removed from the loading rod and one paper-reinforced end of the specimen was inserted into the grip using a jig for correct perpendicular alignment. The grip was tightened and together with the specimen it was reattached to the loading rod. The partly mounted specimen was then positioned by changing the gauge length of the testing machine so that the paper-enforced end of the specimen was likewise aligned with the lower grip edge that was fixed inside the testing chamber. Before tightening the lower grip, the chamber was closed and conditioned to the set target humidity and temperature to enable the specimen to adjust to the environmental conditions. The grip was tightened from the outside of the chamber with an Allen key through a hole in the door ten

6. Experimental: Fracture Behaviour – Materials and Methods

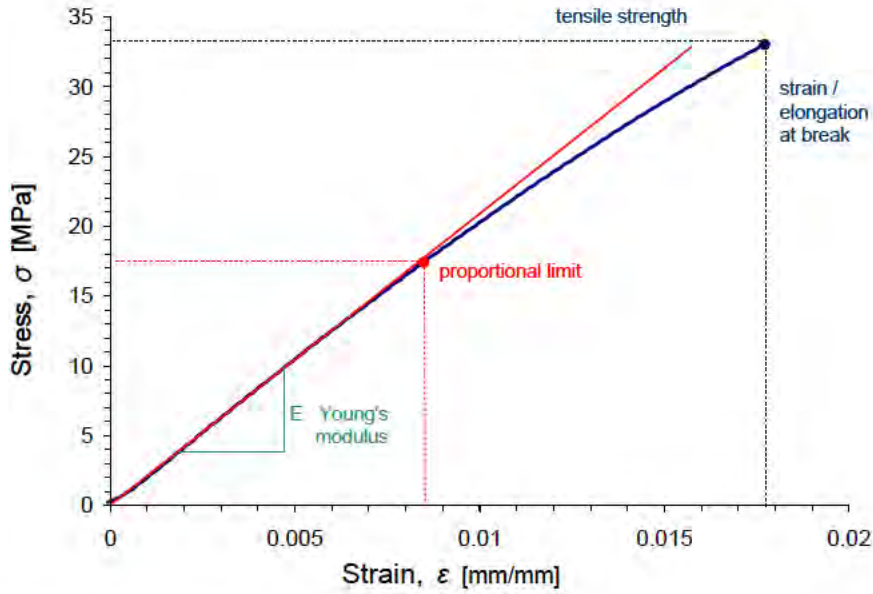


Figure 6.9.: Stress/strain curve for a foundation tensile test specimen showing the Young's modulus,  $E$ , and the tensile strength, which in this graph equals the ultimate strength of the composite.

minutes after the target conditions had been reached. This procedure facilitated testing of stress-free specimens.

The stress/strain graph was plotted (Fig. 6.9) and Young's modulus,  $E$ , was calculated using Equation 6.3 over a strain interval of  $1.5 \cdot 10^{-3}$  mm/mm.

$$E = \frac{\sigma}{\epsilon} = \frac{PL_o}{A_o\Delta L} \quad (6.3)$$

where  $\sigma$  is tensile stress,  $(P/A_o)$ ,  $\epsilon$  is tensile strain,  $(\Delta L/L_o)$ ,  $P$  is the load applied,  $L_o$  is the initial specimen length,  $\Delta L$  is the change of specimen length, and  $A_o$  is the initial cross-sectional area of the specimen.

Tensile strength (stress at failure),  $\sigma_f$ , was calculated using Equation 6.4.

$$\sigma_f = \frac{P_f}{A_o} \quad (6.4)$$

where  $P_f$  is the load applied at the point of failure.

### 6.2.4. Yield stress of foundation

The foundation specimens were brittle in tension and failed prior to obtaining maximum yield strength. The yield stress,  $\sigma_y$ , for this material was thus determined by testing cylindrical specimens in compression loading in accordance with Standard BS EN ISO 844 (2009). The tests were undertaken on an Instron 5584 universal testing machine equipped with a 100 kN loadcell at a rate of 0.5 mm/min and at environmental conditions of 21 ( $\pm 1.5$ ) °C and 53 ( $\pm 2$ ) % RH. The yield stress was defined as the first point of deviation from linearity on the stress/strain curve (Fig. 6.10).

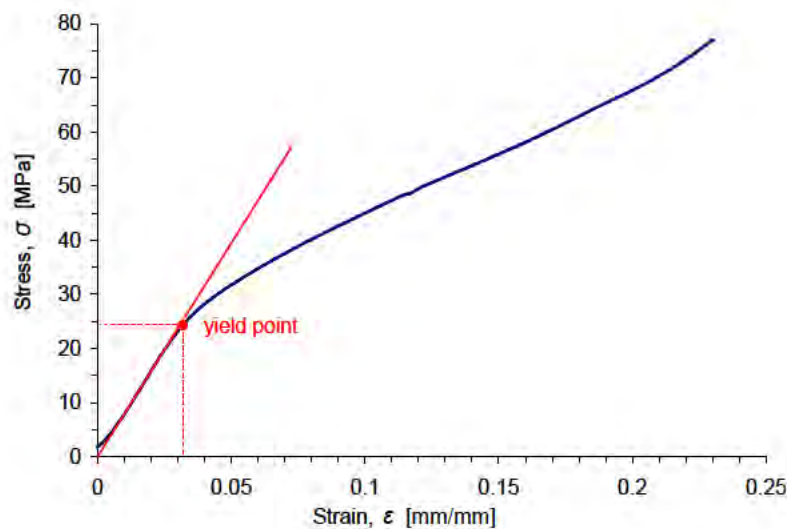


Figure 6.10.: Stress/strain curve for a cylindrical foundation specimen tested in compression at 0.5 mm/min. The yield point is defined as the first point of deviation from linearity.

## 6.3. Determination of consolidant distribution

### 6.3.1. Cross-section sampling

From each DCB specimen a cross-section sample was taken by cutting the far end of the specimen (opposite the end with the starter foil) 5 mm from the edge. The specimens were embedded into clear polyester casting resin (Tiranti), leaving the cross-section surface exposed. Prior to embedding, the specimens were sealed from five sides with a viscous dispersion of Primal B60 A (Conservation Resources, replacing Rhoplex AC 33) and colloidal silica (West System) to prevent infiltration of the casting resin into the specimen (Derrick et al. 1994). Finally, the

## 6. Experimental: Fracture Behaviour – Materials and Methods

cross-section surface was polished with #360 – #800 emery paper and polishing mesh (Micro-Mesh) up to #12000.

Embedding of the cross-section specimens was necessary due to the fragility of some of the adhesive bonds between the consolidated fracture surfaces, which easily broke open during handling. Also, the specimens consolidated with acrylic formulations required embedding as they were to be immersed in staining solution afterwards for visualising the consolidant distribution within the cross-section. Pre-tests had shown that the solvent of the staining solution quickly softened the consolidant inducing the loss of mechanical strength in the bond, and non-embedded samples would break within the consolidated layer during rinsing and drying.

### 6.3.2. Staining of consolidants

For the visualisation of binding media distribution within the consolidated DCB specimens, the consolidants were stained at two different stages of the consolidation process. The procedure was dependent on the type of polymer used: either, the consolidant itself was coloured with a stain before application on the specimen, or the cross-section was immersed into a staining bath after it had been cut from the dried, consolidated DCB specimen.

Staining before application was necessary for all protein-based consolidants (classes I and I+), as the foundation layer itself was bound with protein-based bovine hide glue. All protein glues were stained before application with Fast Green (C.I. 42053, Merck) which was added to the consolidant solution in solid powder form at a concentration of 0.1 wt%. Fast Green stains the protein matrix in a green colour which is detectable with visible light microscopy (Schramm and Hering 1988, pp. 214-216). Adhesives containing *urushi* lacquer (classes II and II+) did not require staining, as during polymerisation their colour changed to a dark brown, making them naturally detectable under a visible light microscope. Starch-based consolidants, the poly(vinyl alcohol) and the poly(vinyl acetates) (classes I+, II+, IV and V) were all stained with a 1% iodine-potassium iodide solution, known as Lugol's solution. A single drop of this solution was applied on the cross-section sample and any excess solution was wiped off after 4 seconds, before leaving the specimen to dry at room temperature. When exposed to Lugol's solution, the colour of native starches turns to a dark blue-black (e.g. Schramm and Hering 1988, p.206; Chayen and Bitensky 1991, p. 110), whereby amylose is stained dark blue and amylopectin reddish-brown to violet. Considering that precipitated (i.e. gluten-free) Japanese wheat starch consists of 25–28% amylose and 72–75% amylopectin (Van Hung et al. 2006) the colour expected after the staining is a purply brown. PVAc and partially hydrolysed PVAL, such as Mowiol 3-83, stain dark red to reddish-brown (Hayashi et al. 1982, Hirai et al. 1986, Lehmann 2004).

### 6.3. Determination of consolidant distribution

Cross-sections containing acrylates (class V) were stained with a filtered 0.2 wt % solution of Solvent Blue G (C.I. 61554, Town End Leeds) in ethanol (Lehmann 2004). The specimens were soaked in ethanol/water (2:1) for 3 minutes for initial saturation of their open pores and then immersed in the staining solution for a further 3–10 minutes. Lascaux Medium for Consolidation stained relatively fast and only required 3-5 minutes in the stain bath for effective uptake of colour. However, the Paraloid-based consolidants were less effectively stained and the respective specimens were therefore left in the staining bath for up to 10 minutes. Consolidant solution No. 07, Paraloid B 72 in acetone, was pre-stained before application with 0.1 wt % of Solvent Blue G. These specimens were not exposed to the staining bath. The specimens consolidated with Paraloid B-48 N were pre-stained and additionally stained as a cross-section to increase the staining effect. After removal from the staining bath, the specimens were thoroughly rinsed with warm water and left to dry at room temperature.

#### 6.3.3. Optical microscopy

A Zeiss AxioScope A1 optical microscope was used in reflected light geometry to examine the cross-sections taken from the consolidated DCB specimens. Examination was performed under visible light at 100 x and 200 x magnification. Images were taken using a digital camera (AxioCam ICc1) and interpreted with AxioVision Imaging (Version 4.7.2, Dec.2008) software.



# 7. Experimental: Fracture Behaviour — Results and Discussion

## 7.1. Introduction

This chapter reports the results of tests undertaken to evaluate the performance of various polymer solutions and dispersions used for consolidating fractured foundation layers, which are typical of multilayered East Asian export-type lacquer coatings. The fracture behaviour of double cantilever beam (DCB) specimens type A (foundation layer only) and type B (foundation with lacquer layer) are presented, providing data on the failure of newly prepared and equilibrated foundation layers applied to pine wood substrates. These specimens are further evaluated to determine whether the employed test method has the capability to produce fractured specimens that are suitable for subsequent consolidation testing. Leading on from the successful production of appropriate test specimens, the results of the second-phase fracture, i.e. after the application of diverse polymer formulations (consolidants), highlight the effect each consolidant has on the fracture behaviour of the foundation. To complement these findings, consideration is further given to the ability of the consolidants to penetrate into the porous structure of the specimen layers. Finally, some practical aspects are discussed regarding the application of the chosen polymer formulations during the consolidation of artificially-produced lifting coatings on sample boards.

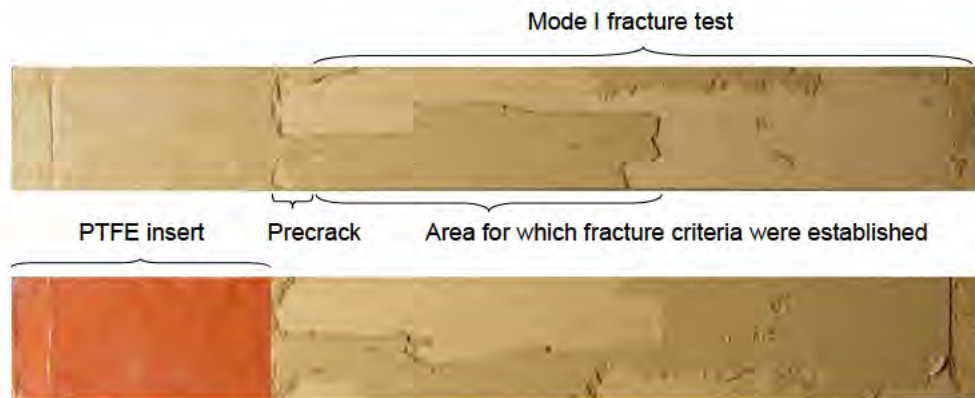
## 7.2. Initial DCB fracture tests

### 7.2.1. Fractography

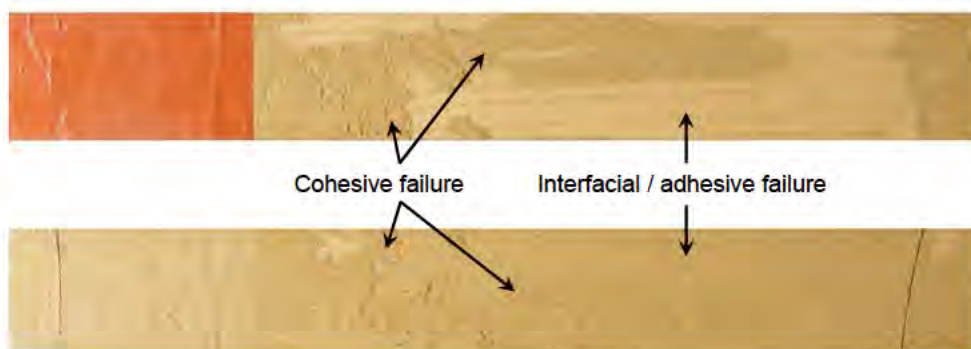
Both DCB specimen types mostly exhibited considerably stable crack propagation during testing. In a few instances, however, partly unstable fracture was observed where the crack propagated quickly over a longer distance of several millimetres before arresting. These instabilities were caused by inhomogeneities in the foundation layer and were often associated with variations in the fracture paths. The latter had either propagated interfacially (adhesively) between the

## 7. Experimental: Fracture Behaviour – Results and Discussion

foundation and the wood substrate (Fig. 7.1a), or cohesively through the foundation layer, as shown in Figure 7.1b. In the following, adhesive and cohesive failure is abbreviated as AF and CF respectively (see Section 6.2.1 for the categorisation of failure patterns). Where cohesive failure occurred, the fracture path was often observed to propagate on varying levels of the foundation. Most commonly, an individual specimen developed both AF and CF. In rare cases during testing, adhesive-cohesive failure with peel (ACFP) was observed. However, fracture loci characterised by this failure type were very small and often limited to areas along the very edges of the specimens. Typical fracture surfaces of DCB specimens types A and B are shown in Figures 7.1 and 7.2. The percentage area of the fracture surface associated with each type of fracture was measured and is summarised in Table 7.1 and Figure 7.3.



(a) Failure at the wood/foundation interface, alternating between the two wood substrate surfaces.



(b) Typical cohesive failure within the foundation in addition to interfacial failure between the wood and the foundation.

Figure 7.1.: Typical fracture surfaces of DCB specimens type A after initial testing at a rate of 0.3 mm/min. The specimen length equals 150 mm.





(a) Cohesive failure within the foundation layer and at the wood/foundation interface.



(b) Cohesive failure on varying levels of the foundation layer, but mainly close to the foundation/lacquer interface.

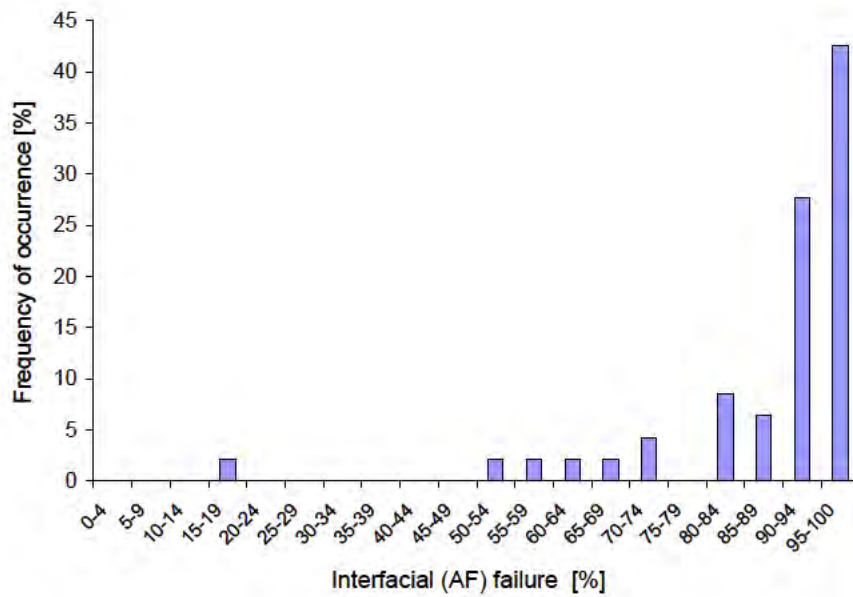


Figure 7.2.: Typical fracture surfaces of DCB specimens type B after initial testing at a rate of 0.3 mm/min. The specimen length equals 150 mm.

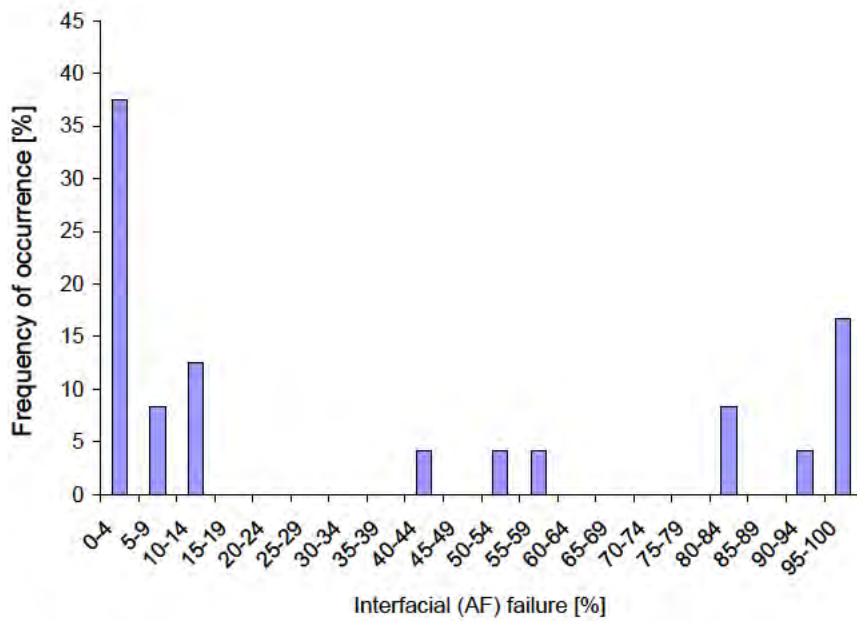
Table 7.1.: Frequency of occurrence of the degree of interfacial failure in the tested DCB specimens. The column ‘% failure of specimen’ refers to the area of fracture surface of each individual specimen, whilst the % values in the columns ‘DCB Type A’ and ‘DCB Type B’ refer to the frequency of occurrences within the entire set of specimens.

FAILURE TYPE	% FAILURE OF SPECIMEN AREA	DCB TYPE A	DCB TYPE B
Interfacial	> 50	98 %	38 %
	> 75	85 %	29 %
	> 90	70 %	21 %

7. Experimental: Fracture Behaviour – Results and Discussion



(a) DCB specimens type A.



(b) DCB specimens type B.

Figure 7.3.: Frequency of occurrence of the proportion of interfacial failure in the tested DCB specimens.

It can be seen from Table 7.1 and Figure 7.3 that the DCB specimens incorporating the foundation layer only (type A) predominantly fractured interfacially, i.e. between the foundation and the pine wood substrate. Around 70% of the type A specimens fractured with more than 90% interfacial failure, i.e. with less than 10% cohesive failure of the foundation. In contrast, the majority of the type B specimens containing the additional lacquer layer on top of the foundation showed cohesive failure within the foundation layer. More than 60% of the type B specimens failed predominantly cohesively within the foundation. Simultaneously, they displayed a comparatively larger proportion of mixed failure compared with type A.

Except for a few short wood fibres that were attached to the surface of the foundation in areas which had failed interfacially (Fig. 7.4), no significant fracture had occurred within the wood substrate. In the case of the type B specimens, failure also never developed within the lacquer layer, nor within the epoxy adhesive (with which the upper wood substrate was adhered to the lacquer surface), and neither was any interfacial failure observed between these polymer layers or the epoxy and the wood substrate. These results thus demonstrated that the method of manufacturing the type B specimens worked well and that the epoxy chosen for bonding the lacquer surface to the wood beam was suitable for this application.



Figure 7.4.: Type A DCB specimen: detail of the fracture surface of a foundation layer located between two wood interfaces before testing, showing failure on varying levels.

When cohesive failure occurred within the foundation layer of a specimen, it was observed that the fracture path had often traveled on varying levels of the layer (Fig. 7.4). This was most apparent in the type B specimens, where cohesive fracture propagated mostly along the upper part of the foundation layer very close to the lacquer interface (Fig. 7.5).

## 7. Experimental: Fracture Behaviour – Results and Discussion

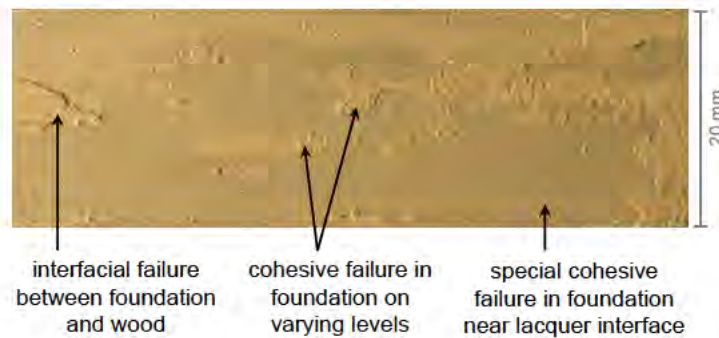


Figure 7.5.: Type B DCB fracture surface of foundation layer (detail). Failure mainly occurred near the lacquer interface. The fracture pattern resembles that shown in Figure 7.7a.

### Comparison of DCB fracture surfaces to natural damage on lacquer objects

The fracture surfaces produced by the DCB specimens tested in mode I were compared with those observed on the export-type East Asian lacquer objects within the Victoria and Albert Museum's collection, and striking similarities were revealed. Figure 7.7 presents details of typical, natural damage types observed on two nineteenth century Japanese lacquer objects. Indeed, the same failure types could be replicated with the DCB test specimens, ranging between interfacial (adhesive) and cohesive failure on different levels. Whilst sample type A produced predominantly the typical AF between the wood substrate and the foundation layer, sample type B replicated well the special cohesive failure (SCF) on varying levels, particularly in areas close to the lacquer interface. Figures 7.5 and 7.6 show examples of these. Mode I loading of DCB specimens thus appeared to be a useful method for the production of artificially damaged, multilayered lacquer coating specimens that are suitable for the application of consolidants and further testing.



Figure 7.6.: Type A DCB fracture surface (detail), resembling the naturally-induced damage on export-type lacquer coating in Figure 7.7b.

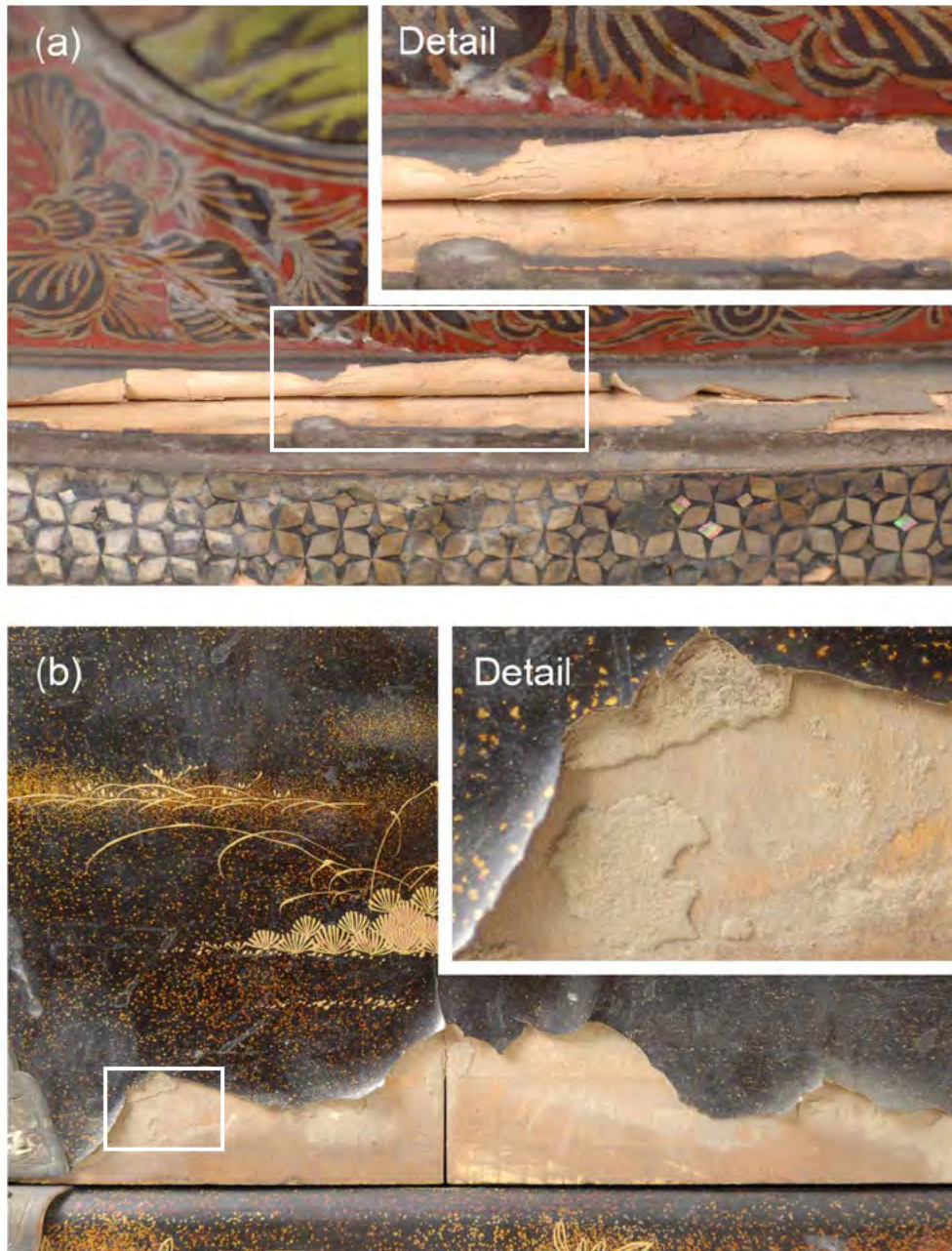
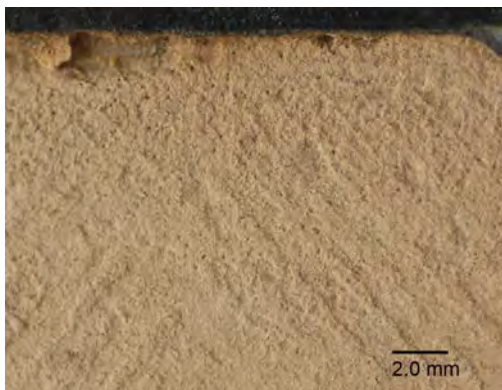


Figure 7.7.: Examples of natural coating failure observed in export-type East Asian lacquer objects: (a) Corner cabinet (V&A, 493-1872), detail of front proper left door; (b) Cabinet on stand (V&A, 303-1876), detail of cabinet back near base. (Photographs by N. Schellmann, courtesy of the V&A.)

## Morphology of fractured foundation

With respect to the surface finish of the fractured foundation layers, it was observed that many specimens contained a large number of very small air bubbles and pinhole-shaped discontinuities. These features are also typically seen in export lacquer-type objects (Fig. 7.8a), as air bubbles occur naturally during preparation and application of gesso-type foundation mixtures. They derive either from trapped air within the liquid foundation mixture that was introduced by the addition of the particulate mineral filler, and/or due to the lack of surface wetting during application with a brush. Once small pin holes are present in a foundation layer, they will become larger in diameter with every subsequent layer applied, forming funnel-shaped discontinuities in the surface. This explains why the DCB specimens type A showed on average smaller voids than those of type B. The latter were manufactured with foundation applied in two layers as opposed to the single layer in the type A specimens. Even though during manufacture care was taken to avoid the development of these discontinuities, they were present in all specimens, albeit in varying number and size (Figs. 7.8b and 7.9).



(a) Detail of Corner cabinet 493-1872 (V&A) with protein-bound foundation.



(b) Detail of typical DCB specimen type B with pinholes of varying diameter.

Figure 7.8.: Details of foundation fracture surfaces showing small air bubbles and pinhole-shaped discontinuities.

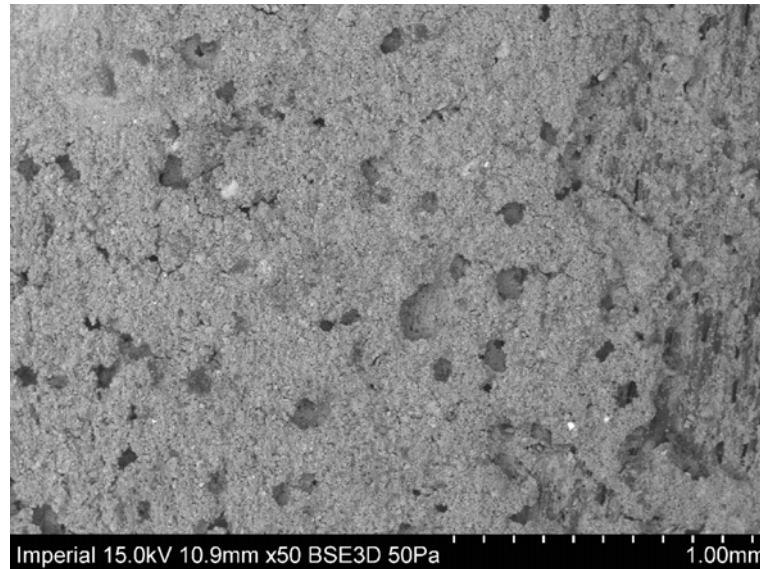


Figure 7.9.: SEM image of a DCB type B fracture surface showing irregular-shaped voids and air-bubbles in the foundation.

Analysis with a scanning electron microscope (SEM) under variable pressure revealed that on the microscopic level the fracture paths had mostly propagated along particle-matrix interfaces and through areas rich in voids. Figure 7.10 shows the morphology of a foundation fracture surface with partly exposed mineral filler particles of varying sizes. Also, areas of high polymer concentration are visible, such as the spherical-shaped agglomerate of filler particles and hide glue in the upper right quadrant of the image, or the polymer-rich area in the bottom left hand quadrant. Typically, highly filled polymers fail by debonding. Upon application of stress, voids are created around the filler particles that gradually coalesce and develop into larger holes, finally inducing fracture of the composite (Greenhalgh 2009, p. 176). However, it appeared that in the case of the foundation used here, the extensive presence of pre-existing voids also contributed significantly to the failure. Debonding could not have been solely responsible for the creation of such fracture surfaces. Typically, the voids had diameters of up to 0.2mm (Fig. 7.9), although some much larger voids of irregular size of around 0.5mm by 1mm were also observed in some specimens (Fig. 7.8b).

These findings confirmed that on both macroscopic and microscopic levels the foundation represented an extremely inhomogeneous material with many flaws.

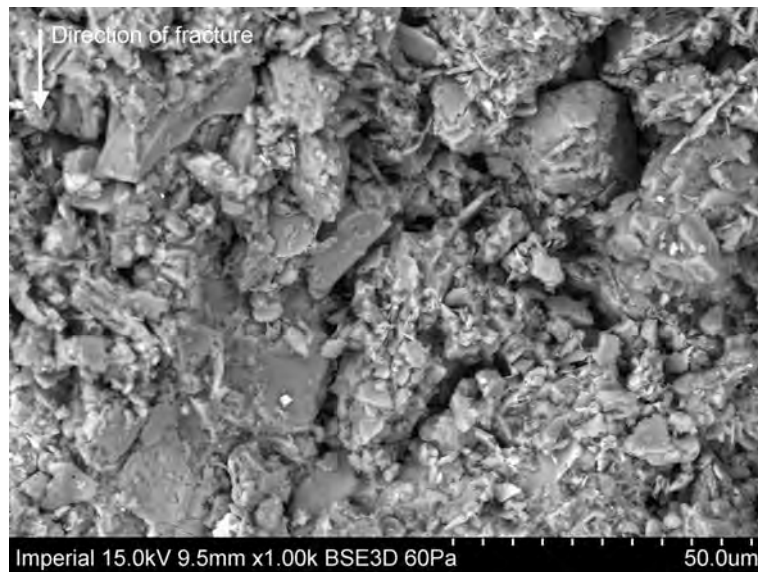


Figure 7.10.: SEM image of DCB type B foundation fracture surface at x1000 magnification.

### 7.2.2. Fracture energy $G_{Ic}$

As mentioned previously, crack growth stability in the DCB specimens was not always constant, and fracture behaviour generally ranged between stable crack propagation and propagation in an unstable manner. This was not only observed during testing, but also could be seen in the recorded data. Figure 7.11 summarises the characteristics of these two types of crack propagation, showing their main differences in terms of measured load,  $P$ , versus displacement,  $\delta$ , and crack length,  $a$ , versus displacement. For stable crack growth in DCB specimens, the  $P$  versus  $\delta$  graph is characterised by a relatively steady decrease in load during crack propagation, whilst the  $a$  versus  $\delta$  graph is nearly linear. In contrast, unstable crack growth displays clearly unsteady and non-linear graphs for load/displacement and crack length/displacement plots respectively. The graphs represented in Figure 7.11 are examples recorded during testing of types A and B DCB specimens, and they give a good indication of the data variation encountered during initial DCB testing of both specimen types.



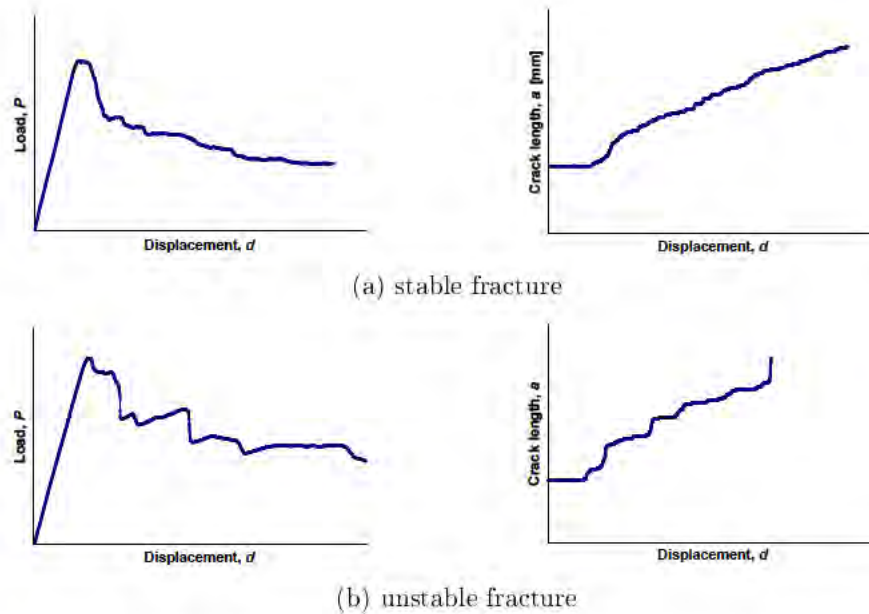


Figure 7.11.: Typical curves for (a) load,  $P$ , versus displacement,  $\delta$ , and (b) crack length,  $a$ , vs. displacement for failure types in mode I fracture testing.

Another typical example of the load versus displacement graphs recorded during testing is shown in Figure 7.12. From these data, the fracture energy,  $G_{Ic}$ , was calculated with a customised Microsoft Office Excel spreadsheet (Blackman and Kinloch 2001a, 2001b; Masania 2008) using simple beam theory (SBT), corrected beam theory (CBT) and the experimental compliance method (ECM) according to the standard procedure of BS 7991 (2001) described in Section 5.4.1. For stable crack growth, the values for  $P$  and  $a$  were extracted from the propagation points and the fracture energy was calculated with Equations 5.9, 5.10 and 5.14 for the respective methods. For unstable crack growth, known as stick-slip behaviour,  $P$  and  $a$  are normally extracted from initiation and arrest points only. However, none of the DCB specimens tested in this series showed pronounced stick-slip behaviour. Typically, this gives rise to load/displacement curves with saw-tooth shaped progression. The stick-slip behaviour observed in the tested specimens often displayed only a couple of initiation and arrest events. Therefore,  $P$  and  $a$  were extracted in the same manner as for stable crack propagation. The correction factors  $F$  and  $N$  were calculated using Equations 5.12 and 5.11 respectively, and the crack length correction,  $\Delta$ , was gained experimentally from the graph plotting the cube root of the normalised compliance versus the crack length (see Fig. 5.5). The fracture energy at crack initiation,  $G_{Ic\,init}$ , was established for the three initiation criteria, i.e. the first point of deviation from linearity (NL), the first point for which crack propagation was observed (VIS) and the point of either 5% change in compliance or the maximum load on the load-displacement

## 7. Experimental: Fracture Behaviour – Results and Discussion

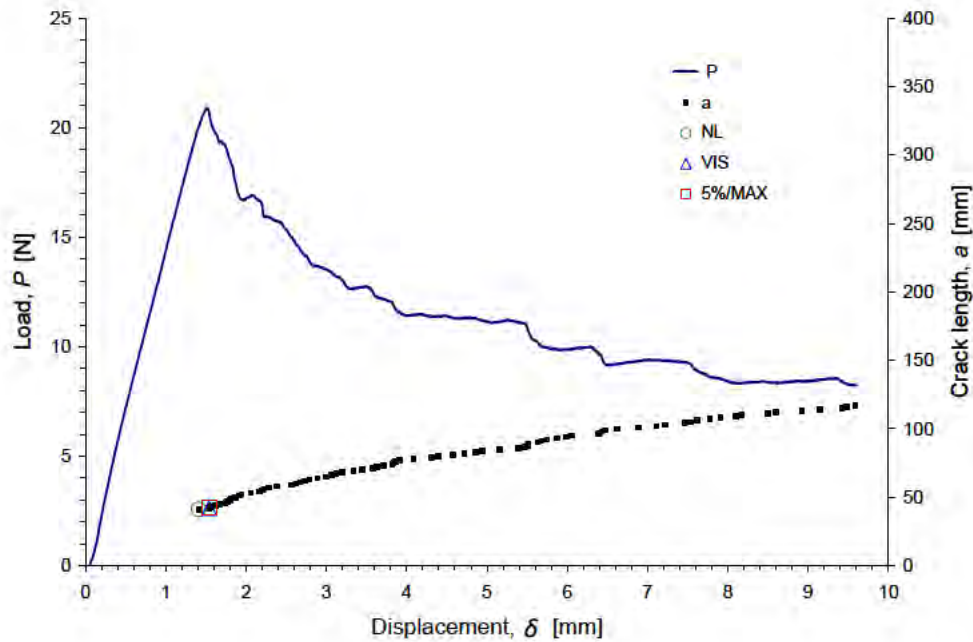


Figure 7.12.: Load,  $P$ , and crack length,  $a$ , as a function of displacement,  $\delta$ , for a DCB (type A) test.

curve (5%/MAX). The system compliance was measured for the testing setup according to the standard procedure. However, the measured load was so low that the correction factor was small, and the results were not affected by the system compliance.

A typical graph plotting fracture energy,  $G_{Ic}$ , versus crack length (in the following denoted as resistance curve or R-curve) for all three analysis methods is shown in Figure 7.13. Comparison between the  $G_{Ic}$  values established by the three different analysis methods revealed that the CBT and ECM methods gave almost identical results, whilst the values for the SBT method usually deviated slightly from the ones calculated with the two former methods. The deviation of the SBT results is consistent with the principle of the SBT method, in which the expression for the compliance of a perfectly built-in DCB specimen underestimates the true compliance of the specimen (cf. Section 5.4.1). Of course, in reality the specimen is never perfectly built-in, i.e. it is not fully restricted and so can deflect or rotate in any of the possible directions to some, albeit small degree. As no significant difference could be established between the two compliance-corrected methods, and for the purpose of clarity, only the  $G_{Ic}$  values deduced with the CBT method are referred to in the following discussion. This method is generally the one most commonly quoted (Blackman et al. 2003).

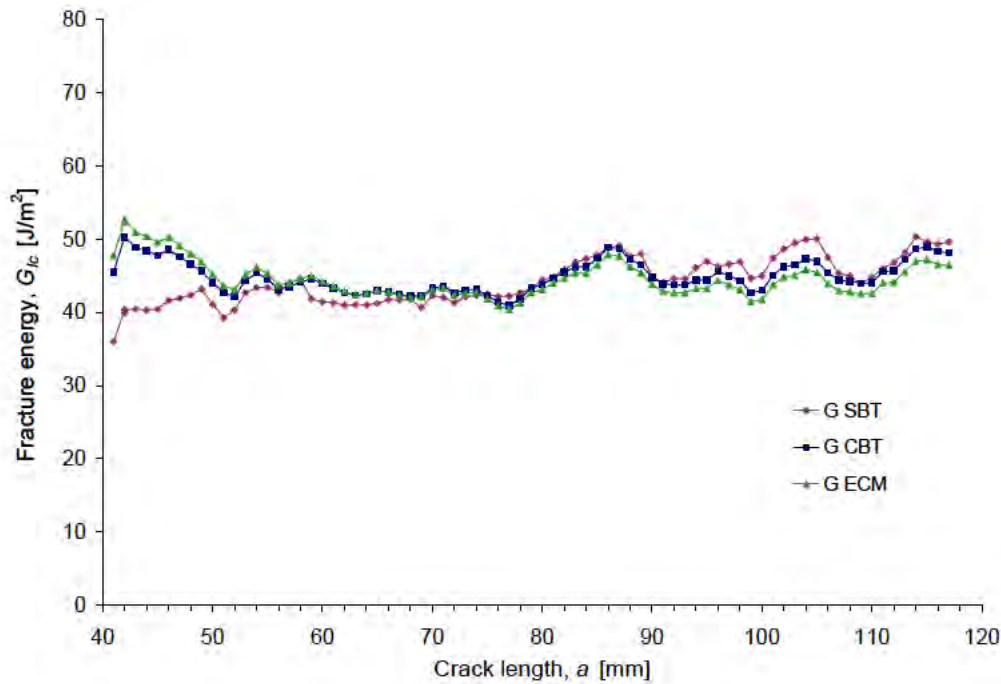


Figure 7.13.: Resistance curves for a DCB specimen during initial testing in mode I showing fracture energy,  $G_{Ic}$ , as a function of crack length,  $a$ , established by simple beam theory (SBT), corrected beam theory (CBT) and experimental compliance method (ECM).

## Crack initiation and propagation

As would be expected, the NL criterion consistently gave the lowest crack initiation values for both types A and B specimens with an average fracture energy of around  $40 \text{ J/m}^2$  ( $\pm 30\%$ ) and  $38 \text{ J/m}^2$  ( $\pm 35\%$ ) respectively. The  $G_{Ic\text{init}}$  values calculated for the VIS and 5%/MAX criteria were slightly higher and almost identical to each other at around  $45 \text{ J/m}^2$  ( $\pm 29\%$ ) and  $42 \text{ J/m}^2$  ( $\pm 37\%$ ) for types A and B respectively (Table 7.2). The average propagation values,  $G_{Ic\text{prop}}$ , for both samples reached values around  $46\text{-}47 \text{ J/m}^2$ . The good agreement between the propagation values and the same locus of failure in both types strongly implied that both specimen types were suitable for measuring the fracture energy of the materials used.

The low fracture energy values suggest that the foundation layer is a very brittle composite, requiring only little energy to be fractured in mode I. These findings agree well with general, mainly empirical observations made on the fracture behaviour of gesso-type foundation layers. Numerical values for the fracture properties of composites made from animal glue with mineral particle fillers (i.e. gesso-type materials) are not available for comparison, however, comparative data may be drawn from other highly filled polymers. Friedrich and Karsch (1981),

## 7. Experimental: Fracture Behaviour – Results and Discussion

for instance, demonstrated that above a filler volume concentration of 15% the fracture energy of silicon dioxide-filled polypropylene decreased rapidly, reaching similarly low values at high filler concentrations as the animal glue-bound foundation in the present study.

Table 7.2.: Mean fracture energy initiation values,  $G_{Ic\,init}$ , for the non-linear (NL), visual (VIS), and the 5% or maximum load (5%/MAX) criteria according to BS 7991 (2001) and the flexural modulus,  $E_f$ , of DCB specimens measured during initial fracture.

SAMPLE	$G_{Ic\,init}$ (NL) [J/m <sup>2</sup> ]		$G_{Ic\,init}$ (VIS) [J/m <sup>2</sup> ]		$G_{Ic\,init}$ (5%/MAX) [J/m <sup>2</sup> ]		$G_{Ic\,prop}$ [J/m <sup>2</sup> ]		$E_f$ [GPa]	
	$\bar{x}$	$\pm$	$\bar{x}$	$\pm$	$\bar{x}$	$\pm$	$\bar{x}$	$\pm$	$\bar{x}$	$\pm$
Type A	40	30 %	45	28 %	45	29 %	46	25 %	8.2	20 %
Type B	38	34 %	41	36 %	42	37 %	47	46 %	10.3	15 %

At first glance, the coefficients of variation (CoV, denoted by ‘ $\pm$ ’) of the measured data appear to be large. However, fracture testing of commercial materials and structural adhesives and materials has shown that mechanical property values established in this way very commonly vary by 10-20% within a set of test specimens (see for example Blackman et al. 1995, 2003). Taking into account that the average  $G_{Ic}$  values measured within each individual specimen used in this study varied by around 12% and 16% for types A and B specimens respectively (Fig. 7.14a), CoV values of up to 46% within an entire set can be considered realistic (and thus perforce acceptable) for the type of specimens used. Composite DCB specimens made from wooden substrates and highly mineral-filled adhesive based on gelatin are likely to be very inhomogeneous. Not only is there the natural variation in the wood growth, but also inhomogeneity due to manually ground clay powder, which is mixed with a protein binder and is applied by hand. This will result in considerable variation in the properties and hence in the measured data (see for instance Knaebe and Williams 1993; Reiterer and Tschegg 2002). The graphs in Figure 7.14 show the measured and calculated results for two specimens with markedly different fracture behaviour: the blue graphs are typical examples of a specimen displaying stable crack propagation, whilst the red ones are those resulting from a specimen that fractured in a very unstable manner. The variation shown between these two examples indicate the degree of scatter in the data that is to be expected from the materials employed in this study.

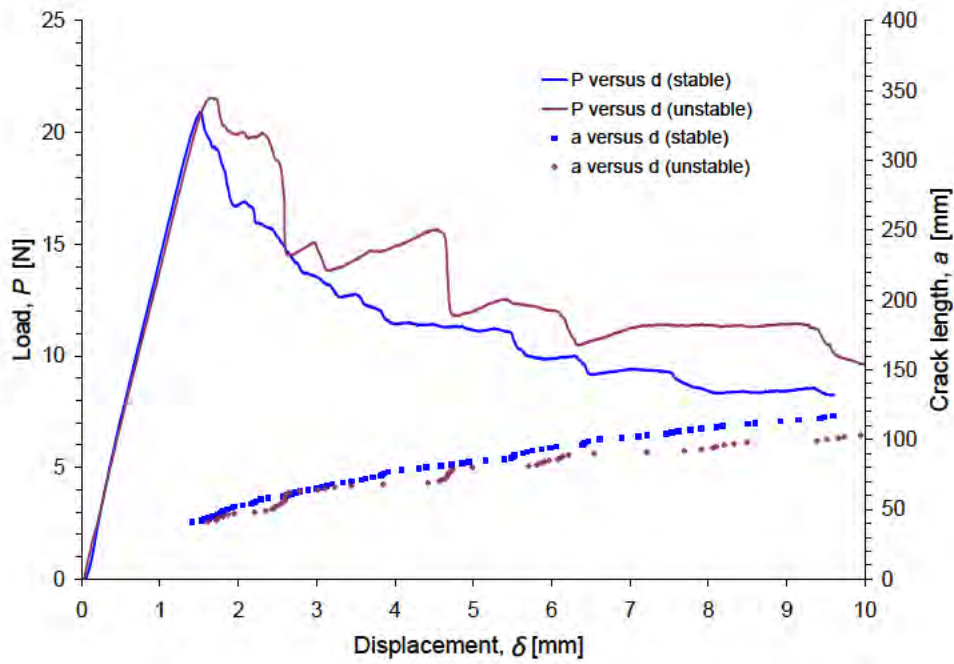
For both type A and B specimens, the R-curves showed no particular trend towards rising or falling fracture energy values with increasing crack length. This means that during fracture, no crack length dependent toughening occurred in the material. The fracture energy can therefore justifiably be quoted as a mean value in the further discussion. Furthermore, the mean  $G_{Ic}$  values for crack propagation were not significantly different from those established for initiation, and neither was a trend noticeable between initiation and propagation values. This is consistent with the absence of a rising or falling R-curve, and hence only propagation values are further referred to in this work. These results clearly showed that the DCB testing method is suitable for these kinds of materials.

### 7.2.3. Dependence of $G_{Ic}$ on layer thickness

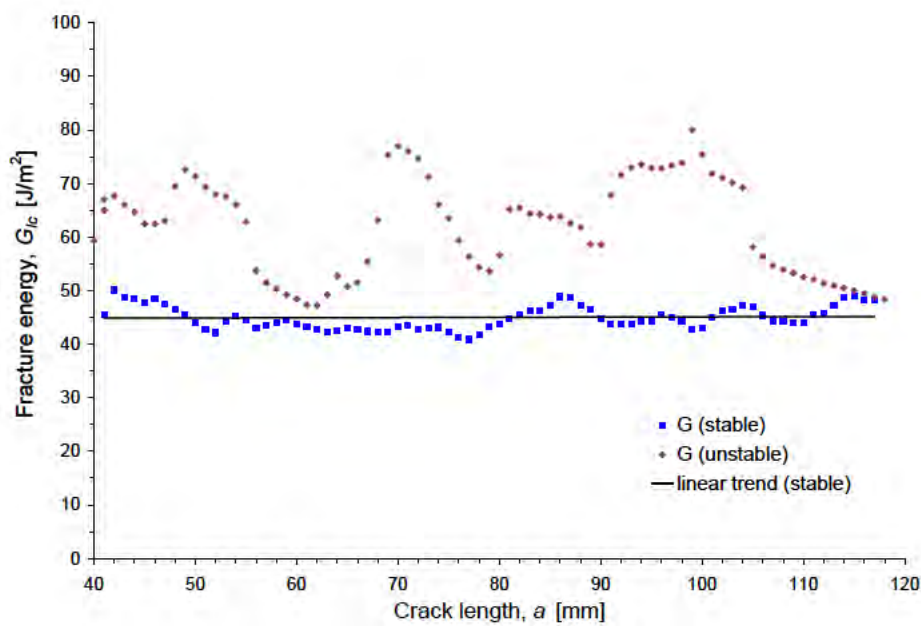
The DCB specimens used in this research were designed with foundation layers that have similar layer thicknesses to those found on real life objects. Examples of average values for foundation layers measured during the survey of the V&A lacquer objects (see Chapter 3) are shown in Table 7.3.

Figure 7.15 relates the mean  $G_{Ic}$  measured for all type A DCB specimens to their average layer thickness. The distribution of the values suggests that the fracture energy is independent of the layer thicknesses in the tested range. This is in line with the general principles of linear elastic fracture mechanics (LEFM) mode I fracture tests of relatively brittle materials. For these, the measured  $G_{Ic}$  values should be independent of the layer thickness if the latter is greater than the diameter of its plastic zone (e.g. Kinloch 1987, p. 280). The plastic zone is the area of plastic deformation that develops in the vicinity of the crack tip (Fig. 7.16). If the foundation layer thickness,  $h_a$ , were smaller than the diameter of the plastic zone, the full volume of the latter would be restricted, leading to interference with the crack tip micromechanisms and thus to a dependence of  $G_{Ic}$  on  $h_a$ .

7. Experimental: Fracture Behaviour – Results and Discussion



(a)



(b)

Figure 7.14.: Two examples of type A DCB specimens showing very stable fracture (marked in blue) and unstable failure (in red) during initial testing. The differences are clearly apparent in the graphs plotting (a) both load,  $P$ , and crack length,  $a$ , as a function of displacement,  $\delta$ , and (b) the R-curves that give fracture energy,  $G_{Ic}$ , versus  $\delta$ .

Table 7.3.: Average foundation layer thicknesses,  $h_o$ , of export-type lacquer objects from the V&A (cf. Appendix D), and of the DCB specimens.

OBJECT/SPECIMEN	FOUNDATION THICKNESS	
	$h_o$ [mm]	
Corner cabinet	0.15–0.31	
Palanquin	0.30–0.38	
Cabinet on stand	0.17–0.44	
Shrine	0.12–0.58	
DCB type A	0.32	( $\pm 18\%$ )
DCB type B	0.30	( $\pm 20\%$ )

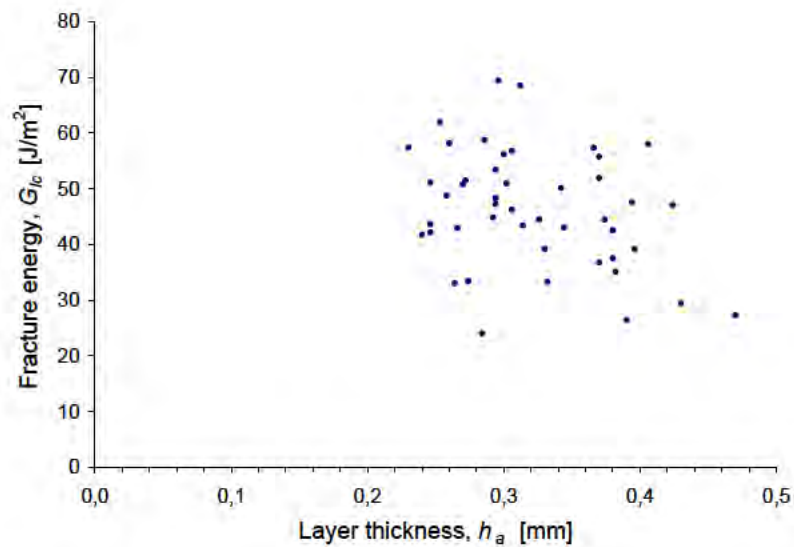


Figure 7.15.: Distribution of mean  $G_{Ic}$  (CBT) values for tested type A DCB specimens in relation to the mean thickness of the foundation layer.

## 7. Experimental: Fracture Behaviour – Results and Discussion

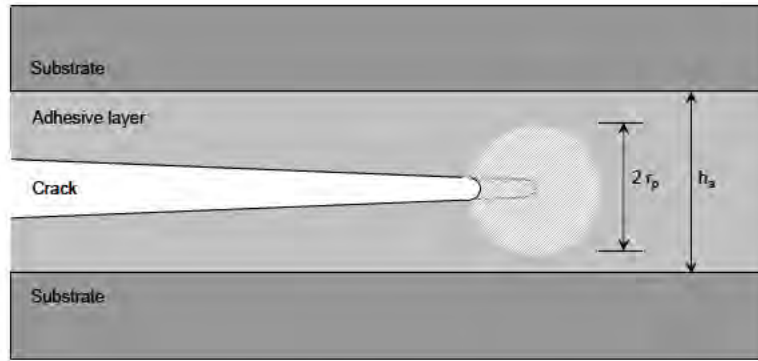


Figure 7.16.: Plastic zone ahead of crack tip (after Kinloch 1987, p.280).

To clarify the dependence of  $G_{Ic}$  on the layer thickness in the DCB specimens used in this study, the size of the plastic zone preceding the crack tip was established using Equation 7.1 (e.g. Kinloch 1987, p. 281; Anderson 2005, p. 62):

$$r_p = \frac{1}{6\pi} \left( \frac{K_{Ic}}{\sigma_y} \right)^2 \quad (7.1)$$

where  $r_p$  is the radius of the plastic zone,  $K_{Ic}$  is the mode I critical stress intensity factor (fracture toughness) and  $\sigma_y$  is the yield stress for plane strain conditions. For brittle polymers and thermosets it is assumed that  $\sigma_y \geq \sigma_f$ , where  $\sigma_f$  denotes the stress at fracture, i.e. the ultimate stress. In the worst case, a brittle material does not yield at all, and  $\sigma_y = \sigma_f$ . Using  $\sigma_f$  in Equation 7.1 thus provides the radius for the largest possible plastic zone which in reality will most likely be smaller.  $K_{Ic}$  can be calculated from Equation 7.2 (e.g. Kinloch 1987, p. 282).

$$G_{Ic} = \frac{K_{Ic}^2}{E} (1 - \nu^2) \quad (7.2)$$

where  $G_{Ic}$  is the fracture energy in mode I,  $E$  is the Young's modulus and  $\nu$  is the Poisson's ratio, i.e. the ratio of the lateral and the axial strains that result from an axial stress applied to a body during elastic deformation. For highly mineral-filled polymers,  $\nu$  was assumed to be approximately 0.4, a value used by Friedrich and Karsch (1981) for a composite not too dissimilar to the foundation material used in the present study. (Although this value was higher than the one more commonly used for industrial composite materials, which is around 0.35 (e.g. Callister, Jr. 2000, p. A11), it was shown to have no significant effect on the calculated result).

The yield stress values,  $\sigma_y$ , required for the calculation of the plastic zone size were obtained from small, cylindrical foundation specimens tested under compression



Table 7.4.: Mechanical properties of hide glue / tonoko foundation.

NAME		VALUE		UNIT	TEST TYPE / REF.
Young's modulus	$E$	2.7	( $\pm 5\%$ )	GPa	Tensile
Fracture energy	$G_{Ic}$	47	( $\pm 46\%$ )	J/m <sup>2</sup>	DCB
Yield stress	$\sigma_y$	20	( $\pm 22\%$ )	MPa	Compression / Eqn. 7.3
Stress intensity factor	$K_{Ic}$	0.39		MPa $\sqrt{m}$	Eqn. 7.2
Poissons's ratio	$\nu$	0.4			Assumed (Friedrich and Karsch 1981)

loading (see Section 6.1.3). Previously tested tensile specimens had shown brittle behaviour with failure prior to obtaining maximum yield strength, and thus had not provided the data needed. The relationship between the values of compressive yield stress,  $\sigma_{yc}$ , and tensile yield stress,  $\sigma_{yt}$ , is defined by Equation 7.3 (Huang and Kinloch 1992).

$$\sigma_{yt} = \sigma_{yc} \frac{(3^{1/2} - \mu_m)}{(3^{1/2} + \mu_m)} \quad (7.3)$$

where  $\mu_m$  is a material constant for pressure dependency, which was taken as 0.2 (Sultan and McGarry 1973, Masania 2010). The tensile yield stress,  $\sigma_{yt}$  was assumed to be identical to  $\sigma_y$ .

Table 7.4 summarises the properties established for the hide glue/tonoko foundation used in this study. From these values a plastic zone with a maximum diameter of  $d_p = 2r_p \approx 0.04$  mm was calculated. Compared with the average foundation layer thickness of the DCB specimens of  $d = 0.31$  mm ( $\pm 20\%$ ) this value is sufficiently small that  $G_{Ic}$  can be considered truly independent of the layer thickness in the DCB specimens employed in this study.

#### 7.2.4. Flexural modulus

A final confirmation for the suitability of the employed test method was given by the cross-check of the flexural modulus  $E_f$  of the DCB substrate with the independently measured flexural modulus  $E_s$ , which were established according to the procedure described in section 6.2.2 and respectively calculated using Equations 5.13 and 5.15.

## 7. Experimental: Fracture Behaviour – Results and Discussion

Within each individual specimen the variation of flexural moduli calculated was very low at an average of around 4.4% for both type A and B specimens. A typical curve plotting  $E_f$  versus  $a$  is presented in Figure 7.17. Within the specimen sets, the calculated values varied by less than 20%, which can be considered consistent results. Results for the back-calculated flexural modulus are summarised in Figure 7.18.

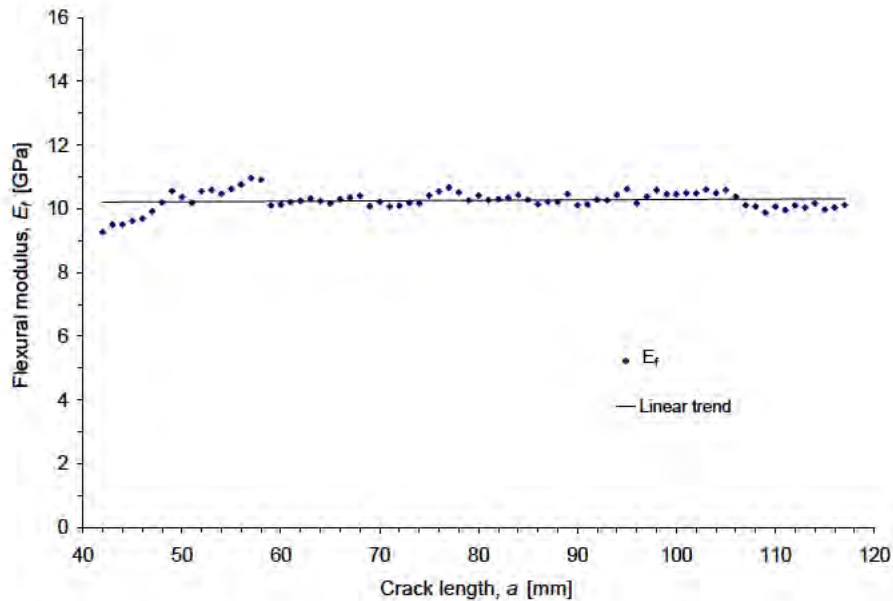


Figure 7.17.: Flexural modulus back-calculated using simple beam theory (SBT) plotted against crack length. The graph shows the typical data variation measured within single type A DCB specimens.

The specimens tested in three-point bending, which comprised 24 DCB substrates cut at a  $3^\circ$  grain angle from the first two laminae of the original pine wood block (see Section 6.1.1), had a measured flexural modulus of 8.8 GPa. Subsequent comparison with the back-calculated flexural modulus,  $E_f$ , of the type A specimens gave a very good match with values of around 8.3 GPa. However, the mean value calculated for type B specimens achieved slightly higher values of around 10.3 GPa (Table 7.2). The apparent difference between these calculated moduli was not entirely unexpected. Firstly, it was most likely to be partly due to the natural variability of the wood. Despite deriving from the same wood block, type A and B specimens contained different annual wood growth rings and therefore some variation in their mechanical properties was expected. Secondly, the more complex layer structure of the type B specimens may also have contributed to differences in  $E_f$ , as these specimens further included a lacquer and an epoxy resin layer on one side of the foundation. Any additional layer between the foundation and the wood substrate increases the thickness of the specimen and thus effectively stiffens the respective cantilever beam. Hence, slight deviation in  $E_f$

### 7.3. Second-phase DCB fracture tests (consolidated specimens)

values compared with those calculated from the more simply structured type A specimens had to be accepted. Nevertheless, any variability between the measured and the back-calculated moduli still remained well within the experimental error (Fig. 7.18), suggesting that these differences were not significant. The measured moduli for the pine wood also agreed well with the moduli reported for Japanese cypress wood, which depending on its age have been shown to range between around 8 and 10 GPa (Sugiyama 1983; Obataya 2009). This also confirmed that using the Quebec yellow pine wood in this study was a suitable replacement for the Japanese cypress wood.

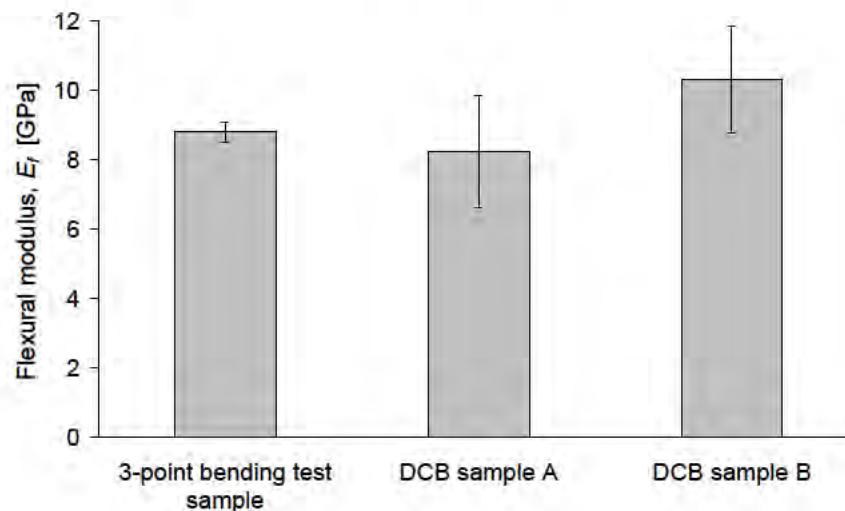


Figure 7.18.: Comparison of the flexural moduli measured by three-point bending test, and from DCB test results back-calculated with corrected beam theory (CBT). Error bars indicate, plus or minus, one standard deviation.

## 7.3. Second-phase DCB fracture tests (consolidated specimens)

To establish the effect of the consolidation treatments on the fracture behaviour of the specimens, both the fracture surfaces and the fracture energy values measured during initial and second-phase fracture were compared.

### 7.3.1. Validity of measured data

Unsurprisingly, the retesting of the previously fractured and consolidated test specimens was less straightforward than the initial testing of the newly prepared

## 7. Experimental: Fracture Behaviour – Results and Discussion

specimens. The degree of inhomogeneity within the DCB specimens had noticeably increased since initial fracture and subsequent consolidation, so that in a few specimens unstable failure was observed. In very few cases, failure and crack propagation were so inconsistent that they were difficult to monitor visually. This clearly underlines the general challenges posed by fractured and repaired test specimens, which are manufactured with rather inhomogeneous materials, as they cannot be produced truly reliably with consistent mechanical properties. Nevertheless, this study also showed that most of the DCB specimens were indeed suitable for testing and provided appropriate data from which valid trends regarding the fracture behaviour of unconsolidated and consolidated specimens could be inferred. In order to ensure the validity of the measured data, the following methodology was pursued:

The British Standard BS 7991 (2001) is applicable for test specimens that comply with linear-elastic fracture-mechanics (LEFM), i.e. for specimens that display brittle fracture without any significant plastic deformation, except that which is localised at the crack tip. Therefore, it is required to exclude any specimens from analysis that do not conform to LEFM (see Section 5.4.1 for method of determination). In this study, every specimen was checked for LEFM behaviour, but even in the event of non-conformity data analysis was still performed. For LEFM methods to apply,  $P_{\max}/P_{5\%}$  is required to be  $< 1.1$  (which effectively allows a non-linearity of 10%). However, this criterion may be difficult to meet in specimens which are as inhomogeneous as the ones used in this study. In a few instances it was observed that the failure to comply with the  $P_{\max}/P_{5\%} < 1.1$  criterion was indeed not caused by inelastic behaviour of the material, but rather by deviation from linearity during initiation due to inhomogeneities in the material. If in these cases the results for  $G_{Ic}$ ,  $E_f$ , and the overall fracture behaviour after initiation fitted the general behaviour of the specimen set, then the specimen was kept to contribute to the overall results. Obvious outliers, however, were excluded.

With respect to propagation values, a small number of specimens displayed unstable fracture. An example is the specimen for which the load-displacement curve is presented in Figure 7.19. According to BS 7991 (2001), this type of fracture behaviour cannot be considered stable. At the same time, it can neither be regarded as proper stick-slip behaviour, despite the latter being the only alternative to stable propagation given by the standard. The fracture behaviour observed in these specimens was essentially characterised by bursts of faster crack growth alongside fairly stable crack propagation. However, the standard does not provide any recommendations on how to deal with such fracture behaviour. It was therefore decided to perform all the calculations irrespective of whether the specimen had failed in a stable or unstable manner. Indeed, it was shown in this research that, in most cases, a useful value for  $G_{Ic}$  could still be calculated from the measured data. Specimens were only rejected if the back-calculated value for  $E_f$  was well outside the expected value, and in addition if the  $G_{Ic}$  value did not agree with the expected range of values within the specimen set.

### 7.3. Second-phase DCB fracture tests (consolidated specimens)

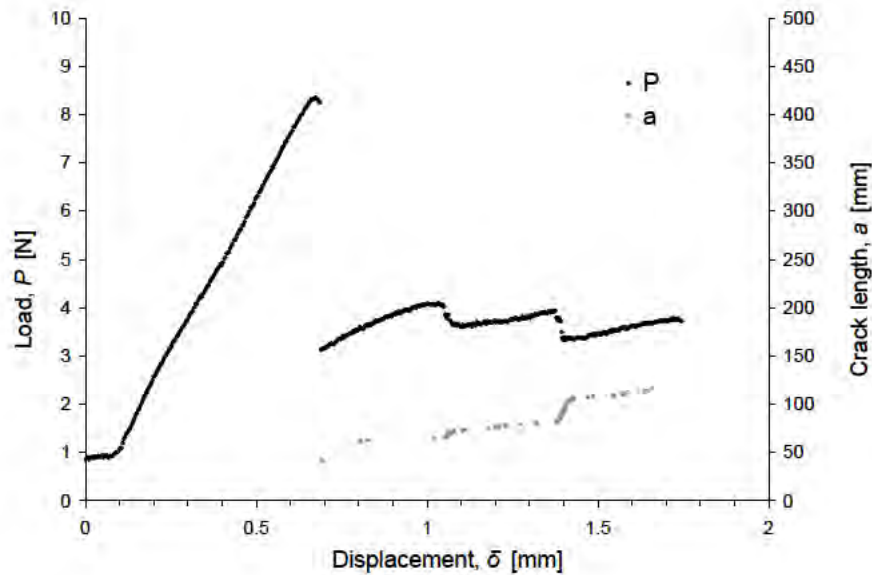


Figure 7.19.: Load versus displacement curve for a type A DCB specimen showing relatively unstable crack propagation.

Due to the natural inhomogeneity of the specimens and the variation in their fracture behaviour (regarding failure loci/fracture patterns and absolute  $G_{Ic}$  values), the test results for each individual consolidated DCB specimen were directly compared with those of the same specimen measured during initial testing. For each specimen, the relative change in fracture energy,  $\Delta G_{Ic}$ , was established by subtracting the respective  $G_{Ic}$  value measured during second-phase testing from that gained during initial fracture and expressed as a percentage. The  $\Delta G_{Ic}$  values were then averaged for every set comprising up to four DCB specimens per consolidant. This mean change,  $\overline{\Delta G_{Ic}}$ , expressed as a percentage, was regarded as a more meaningful indicator for the consolidants' ability to change the fracture energy required to propagate a crack through the specimens, as it takes into account the specific condition of each specimen. Nevertheless, for comparison purposes, absolute  $\overline{G_{Ic}}$  values for every specimen set (i.e. the average  $G_{Ic}$  value from 4 specimens) were also compared and related to the results from the  $\overline{\Delta G_{Ic}}$  values.

#### 7.3.2. Fracture results for specimen sets

In the following, the results from each set of specimens are presented. The full set of consolidations used was previously shown in Table 6.1 and described in Section 6.1.2.

## Set 01 Salianski Isinglass (Consolidant class I)

**Fractographic results** Results for specimen sets A-01 and B-01 were obtained for four specimens each. Figure 7.20 presents a typical example of fracture surfaces of a DCB specimen consolidated with 10 % Salianski isinglass solution. The colouring with Fast Green stain clearly shows where the fracture path had propagated within consolidated areas, and where it had deviated from the previous path to create entirely new surfaces (i.e. the unstained areas). In this particular example, the specimen had mostly failed within the bulk consolidant between or along its interfaces with the two fracture surfaces created during initial testing. Visually, the exact failure loci were not clearly discernible, as the bulk consolidant that had re-adhered the old fracture surfaces was not present as a pronounced layer. Any new fracture was mainly located along the interface between the wood and the foundation, whilst only very little cohesive failure had occurred within the foundation layer itself.

In general, fracture propagated in a relatively stable manner in both specimen types. Comparison of all specimens with their previous fracture surfaces (created during initial fracture) established that after consolidation failure on average occurred predominantly within the consolidant either between and/or along its interfaces with the old fracture surfaces. The area covered by this failure accounted for approximately 70 % of the type A and 80 % of the type B specimens. In set A-01, approximately 23 % of the fracture path had induced new interfacial failure between the wood and the foundation, and around 7 % of the specimen surfaces had fractured cohesively within the unconsolidated areas of the foundation layer. Specimens of set B-01 on average showed 20% special cohesive failure on different levels within consolidated and unconsolidated areas of the foundation layer.



Figure 7.20.: Fracture surfaces of DCB specimen consolidated with 10 % isinglass solution stained with Fast Green.

**Fracture energy:** The mean fracture energy measured for both specimen sets showed a rather large scatter of 43 % and 73 %, reaching  $\overline{G}_{Ic}$  values of  $47 \text{ J/m}^2$  and  $58 \text{ J/m}^2$  for specimen set A-01 and B-01 respectively. On average, isinglass solution changed the fracture energy of the foundation layer in set A-01 by a mean

### 7.3. Second-phase DCB fracture tests (consolidated specimens)

relative increase of 7%. By contrast, in set B-01 the consolidation resulted in an overall decrease in  $G_{Ic}$  values by around 9% (Table 7.5). This implied that the application of a 10% isinglass solution did not significantly change the fracture properties of the foundation layer. Considering the large amount of scatter in the samples, a similar amount of energy to that used during initial fracture had to be provided to propagate fracture during second-phase testing. Furthermore, the appearance of the new fracture surfaces suggested that the foundation layer was effectively consolidated. It showed fracture predominantly within or along the bondline between the two previously re-adhered and consolidated old fracture surfaces. This meant that the new bondline in most areas presented the locus with the lowest toughness within the DCB specimen. However, whether or not this was the case because of small-scale misalignment between the two old fracture surfaces, could not be established with certainty. Deviations of the new fracture path from the bond line into entirely new areas of the foundation layer (be it within the foundation and/or along the wood/foundation interfaces) were generally associated with irregular consolidant distribution and additional flaws in the layer. As the DCB specimens had previously been fractured, they were likely to contain many additional flaws and voids compared with their original state before initial testing. This also explains the large scatter of the measured  $G_{Ic}$  values recorded for the two specimen sets.

Table 7.5.: Mean fracture energy,  $\overline{G}_{Ic}$ , and mean relative changes in fracture energy,  $\overline{\Delta G}_{Ic}$  for specimens consolidated with 10% Salianski isinglass solution.

SET	$\overline{G}_{Ic}$ [J/m <sup>2</sup> ]	$\overline{\Delta G}_{Ic}$ [%]
A-01	47	7
B-01	58	-9

## Set 02 Fish Glue (class I)

**Fractographic results:** Four DCB specimens were tested for Set A-02. In these specimens almost 100% of the fracture path had propagated between the previously re-adhered fracture surfaces. No significant or visibly discernible failure had occurred within the consolidated foundation layer (Fig 7.21).

## 7. Experimental: Fracture Behaviour – Results and Discussion



Figure 7.21.: Example of typical fracture surface of DCB specimen type A consolidated with cold-liquid fish glue stained with Fast Green).

**Fracture energy:** All four specimens showed unstable crack growth that developed very quickly and at low loads, making crack propagation difficult to monitor visually at regular intervals. A typical load-displacement curve for specimens consolidated with fish glue is shown in Figure 7.22. As explained in the introduction to this section, this type of fracture behaviour is not truly stick-slip behaviour, which is why calculated values for  $G_{Ic}$  still gave reasonable results. Nevertheless, one of the specimens had to be excluded from the results as an outlier. The fracture energy measured for the remaining three specimens decreased on average by around 85 %, compared with the initial  $G_{Ic}$  values of the unconsolidated foundation. Absolute  $\overline{G}_{Ic}$  values for these specimens reached around  $8 \text{ J/m}^2$ .

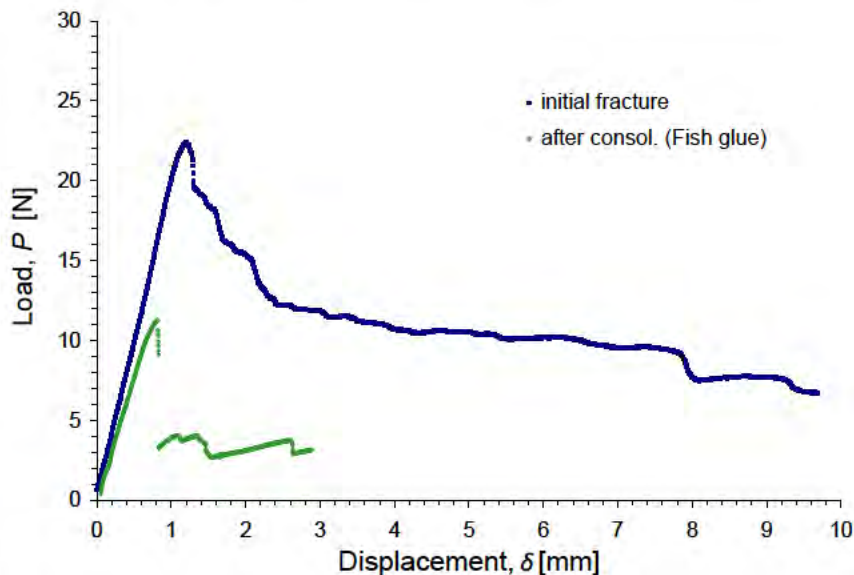


Figure 7.22.: Load as a function of displacement for a typical DCB specimen consolidated with cold-liquid fish glue tested at a rate of  $0.3 \text{ mm/min}$ .

As failure had only occurred between the previous fracture surfaces, this gen-



### 7.3. Second-phase DCB fracture tests (consolidated specimens)

erally allowed two possible conclusions. Firstly, the cold-liquid fish glue could have penetrated too well into the porous foundation leaving the joint starved of consolidant/adhesive. Alternatively, the fish glue could merely have acted as an extremely brittle adhesive between the two fracture surfaces which was insufficiently tough to sustain even small loads. An explanation can be found by considering the results gained from the specimens consolidated with isinglass and hide glue: these consolidants had been applied in the same manner as the fish glue, and the specimens showed fracture surface topographies which were similar to those of the specimens treated with fish glue. However, both isinglass and hide glue had reached much higher values for  $G_{Ic}$ , despite having been applied to the test specimens at a much lower solution concentration than the fish glue. Therefore, it was considered unlikely that starved joints were responsible for the brittle performance of specimens consolidated with fish glue. It is more probable that the weaker mechanical performance of this consolidant was due to its chemical structure. Cold-liquid fish glue, based on gelatin sourced from cold water fish skins and bones, indeed contains much shorter protein chains than isinglass extracted from fish bladders. It has also much lower network stabilisation by inter- and intramolecular bonding than mammalian collagen-based glues (Simon et al. 2003; see also Schellmann 2007).

#### Set 03 Bovine Hide Glue (class I)

**Fractographic results** All tested specimens fractured in a fairly stable manner similar to those consolidated with isinglass solution (Fig.7.23). In both sets A-03 and B-03 approximately 80 % of the fracture occurred between the consolidated/re-adhered old fracture surfaces (in both sets, two specimens each contributed to this average value with almost 100 % failure in this area). Around 15 % of the specimen area had failed with new interfacial failure between the substrate and the foundation. Around 5 % of the fracture path had propagated through entirely unconsolidated areas of the foundation layer.



Figure 7.23.: Fracture surfaces of type B DCB specimen consolidated with 10 % bovine hide glue solution stained with Fast Green.

## 7. Experimental: Fracture Behaviour – Results and Discussion

**Fracture energy** For two specimens of set A-03 that showed 100 % failure at the interface between the old fracture surfaces, consistent fracture energies of 22 and 23 J/m<sup>2</sup> respectively were measured. The other two specimens of this set, which had failed in around two thirds of their area between the consolidated/re-adhered old fracture surfaces and partly at the foundation-wood interface, reached higher fracture energy values, giving an overall mean fracture energy of 37 J/m<sup>2</sup> for the entire set. In terms of relative change between the before and after consolidation results, this meant that a mean decrease in fracture energy by 24 % was measured.

Specimen set B-03 produced slightly different results. After consolidation, a 37 % mean increase in fracture energy was established for the set, although, it should be noted that this was mainly due to the large  $\Delta G_{Ic}$  of + 158 % in one test specimen. This specimen displayed an unusually large area (> 60 %) of new interfacial failure between the wood substrate and the foundation layer. Only one other specimen also showed a relative increase in fracture energy (the one with new SCF in consolidated and unconsolidated areas of the foundation). The remaining two specimens (where failure occurred mainly between the old fracture surfaces) performed very similarly to the ones of set A-03.

Regarding the R-curves of these specimens, an attempt was made to relate changes in fracture energy to changes in the fracture path. The latter propagated either along any of the interfacial areas (either the substrate–foundation interface or the bondline area between the re-adhered old fracture surfaces) or on any level within the consolidated or unconsolidated foundation. However, whilst theoretically it is very desirable to find typical  $G_{Ic}$  values for specific failure types, in practice this approach can hardly be realised. The fractured specimens showed that wherever the fracture paths changed, different fracture types (i.e. fracture locations) occurred simultaneously over the width of the specimens. This means that the measured  $G_{Ic}$  values in these cases were the result of failure in various locations, rather than of just one type or another. Specimens that displayed greater variation in their fracture paths generally also showed greater variation in their measured R-curves. These mixed types of failure are often observed on real objects, too. Hence, this observation again supports the understanding that inhomogeneities are omnipresent in pre-fractured and consolidated material, which influence its fracture behaviour in the most varied way. From a practical point of view it therefore does not seem advisable to read too much into results that consider  $G_{Ic}$  values for very specific and detailed failure types.

## Set 04 Wheat Starch (*shofu*)/Isinglass (class I+)

**Fractographic results** All four specimens from both sets fractured in a slow and considerably stable manner.



Figure 7.24.: Type B DCB specimen consolidated with starch/isinglass showing typical fracture surfaces with a high proportion of SCF within consolidated and unconsolidated areas of the foundation, as well as some new AF and a negligible degree of failure between the old, consolidated and re-adhered fracture surfaces.

On average, specimen set A-04 showed about 60 % fracture in the bondline between the re-adhered and consolidated old fracture surfaces. Around 20 % new interfacial failure occurred between the wood substrate and the foundation layer, whilst the same amount was observed as new SCF on different levels within the consolidated foundation layer.

Set B-04 displayed a rather different behaviour: on average only 10 % of the fracture path had propagated within the bondline between the re-adhered and consolidated old fracture surfaces, whilst the remainder had created new surfaces. Of the latter, 61 % failure was SCF on different levels of the foundation layer, and 39 % failure had occurred at the interface between the wood substrate and the foundation (Fig. 7.24).

**Fracture energy** In set A-04 a relative  $\overline{\Delta G_{Ic}}$  of around 3 % was established, which denoted a change of no significance. It thus appeared that the fractured DCB specimens containing foundation only between the two wood substrates were stabilised by the starch/isinglass mixture, and that the original overall mean fracture energy was restored. However, even though the value for  $\overline{\Delta G_{Ic}}$  was very small, individual  $\Delta G_{Ic}$  values of up to  $\pm 20$  % were measured for three of the specimens. This means that the consolidant in individual cases indeed had a significant effect on the specimen's fracture energy. Nevertheless, no clear trend was apparent in whether these changes were reductions or increases.

## 7. Experimental: Fracture Behaviour – Results and Discussion

For specimen set B-04, results seemed much more obvious at first sight, as an overall increase in  $\overline{\Delta G_{Ic}}$  of around 79 % was established. However, this overall value was mainly influenced by an unusually large  $\Delta G_{Ic}$  of 330 % measured for one single specimen, whilst the other three specimens showed changes not too different from sample A-04.

All in all, the specimens consolidated with wheat starch/isinglass mixture showed on average that the original fracture energy was usually at least restored, if not increased. The mean increases tended to be larger than those reached by the specimens consolidated with hide glue and isinglass solutions. The gap-filling ability and the bonding properties of the starch/isinglass were also much more effective than those of the other protein-based consolidants. Consequently, relatively high levels of failure in previously unfractured regions of the foundation layer were observed, both in unconsolidated and consolidated areas. The levels of new failure, too, were significantly higher than those recorded for pure isinglass and hide glue.

### Set 05      *Mugi-Urushi* (class II+)

**Fractographic results** Four DCB specimens were tested of which 3 fractured in a relatively stable manner. Figure 7.25 gives an example of the typical appearance of a DCB specimen consolidated with *mugi-urushi* after testing. One specimen showed unstable fracture and slight stick-slip-like behaviour.

Overall, the fracture path had created new fracture surfaces along the interface between the wood and the unconsolidated regions of the foundation layer. On average, these covered around 65 % of the specimens' fractured area. Comparison with the initial fracture surfaces revealed that only around 20 % of the failure in the set was located in the bondline between the re-adhered and consolidated old fracture surfaces. The remaining 15 % of the failure had occurred within the unconsolidated areas of the foundation layer. It appeared that *mugi-urushi* in this set acted as an efficient adhesive between roughly structured fracture surfaces inducing predominantly new failure in unconsolidated areas of the multilayered structure. If the unstable specimen were excluded from these results, this finding would be even more obvious: in that case around 83 % of the failure would have occurred in unconsolidated areas. The failure between the old fracture surfaces appeared to have been caused by a lack of gap-filling ability of the consolidant. This was mainly due to problematic handling properties of the consolidant, which was diluted with a highly volatile solvent.)

### 7.3. Second-phase DCB fracture tests (consolidated specimens)

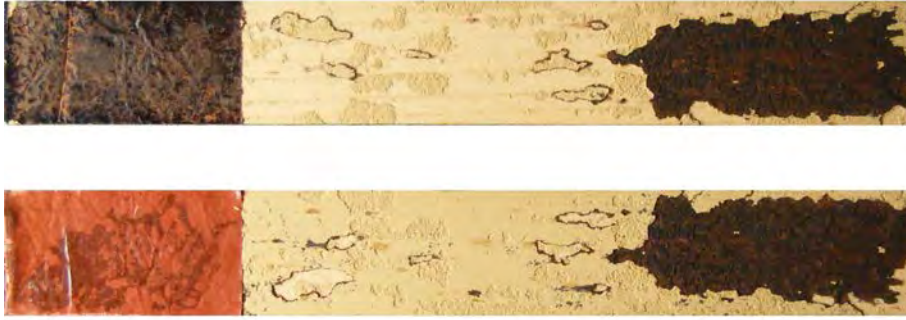


Figure 7.25.: Fracture surface of a DCB specimen consolidated with *mugi-urushi*.

**Fracture energy** Consolidation with the *mugi-urushi* nominally decreased the mean fracture energy of the sample by 5%. However, the location of the fracture path is taken into account, this result requires a rather different interpretation. The three specimens which had predominantly fractured with new AF between the wood substrate and the unconsolidated foundation layer showed an overall increase in  $\overline{\Delta G}_{Ic}$  of around 10%. Two of these specimens did not significantly change their fracture energy, but one increased by around 30% to an absolute value of 60 J/m<sup>2</sup>. This value however is not untypical for an unconsolidated foundation layer (see results of initial fracture of type A specimens in Section 7.2.2). As fracture had mainly occurred in entirely unconsolidated areas, this clearly indicated that in the majority of specimens the consolidant had successfully re-adhered the two old fracture surfaces. Furthermore, it had increased the fracture energy in the treated areas of the structure well beyond that of the foundation layer or the wood/foundation interface.

The fourth specimen was the only one that had shown a significant decrease in mean fracture energy by around 46%. This specimen had only failed by around 35% cohesively along the edges of the specimen in unconsolidated areas and otherwise fractured between the re-adhered old surfaces. It has to be pointed out that this specimen may have been slightly different than the others. During manufacture it was noticed that the solvent Exxsol DSP 80/110 evaporated rather quickly. Hence, by the time the consolidant was applied to the third specimen, a small amount of solvent had to be added to the *mugi-urushi* in order to keep its initial viscosity. However, when the fourth specimen (the one that showed unstable fracture during testing) was about to be consolidated, the necessary addition of even more solvent had most likely diluted the *mugi-urushi* too much. Eventually, the consolidant penetrated so well into the porous foundation layer that it left the interface between the two fracture surfaces starved of adhesive/bulk consolidant. Therefore, a decrease in  $\overline{G}_{Ic}$  was not surprising in this case. Clearly, such a test specimen is not ideal for testing and should be rejected. However, it was still included in this research, as it represented a typical case or problem that may be encountered in a real-life conservation scenario. As three specimens

## 7. Experimental: Fracture Behaviour – Results and Discussion

gave consistent results, the fourth was primarily used to explain the effects of the problematic application of the consolidant.

### Set 06 Raw (*Ki*) *Urushi* (class II)

**Fractographic results** Fracture of four DCB specimens consolidated with *ki-urushi* consistently produced fracture surfaces that displayed around 80 % failure in the bondline between the re-adhered and consolidated old fracture surfaces. A further 17 % of new AF occurred between the wood and the unconsolidated foundation, whilst approximately 3 % of new SCF was located on varying levels within the unconsolidated foundation layer (Fig. 7.26). Three out of the four DCB specimens tested showed considerably unstable fracture with regions of very fast crack propagation.

**Fracture energy** Figure 7.27 presents the R-curve for a DCB specimen consolidated with *ki-urushi*. The variation in the  $G_{Ic}$  values was typical for the specimens in this set. The mean fracture energies calculated for the individual specimens after consolidation had changed on average by  $\pm 15\%$  compared with their initial  $\overline{G}_{Ic}$  values measured during first fracture testing. This gave an overall  $\Delta\overline{G}_{Ic}$  of around -1 % for the sample. In other words this means that the consolidant had neither significantly strengthened nor weakened the re-adhered interface between the old fracture surfaces beyond the original strength of the foundation. However, regarding the bulk foundation into which the *ki-urushi* had penetrated, it can only be assumed that these areas were strengthened by the consolidant; no new cohesive failure had occurred in these parts of the specimens, only where it had remained unconsolidated.



Figure 7.26.: Fracture surfaces of type A DCB specimen consolidated with *ki-urushi*.

### 7.3. Second-phase DCB fracture tests (consolidated specimens)

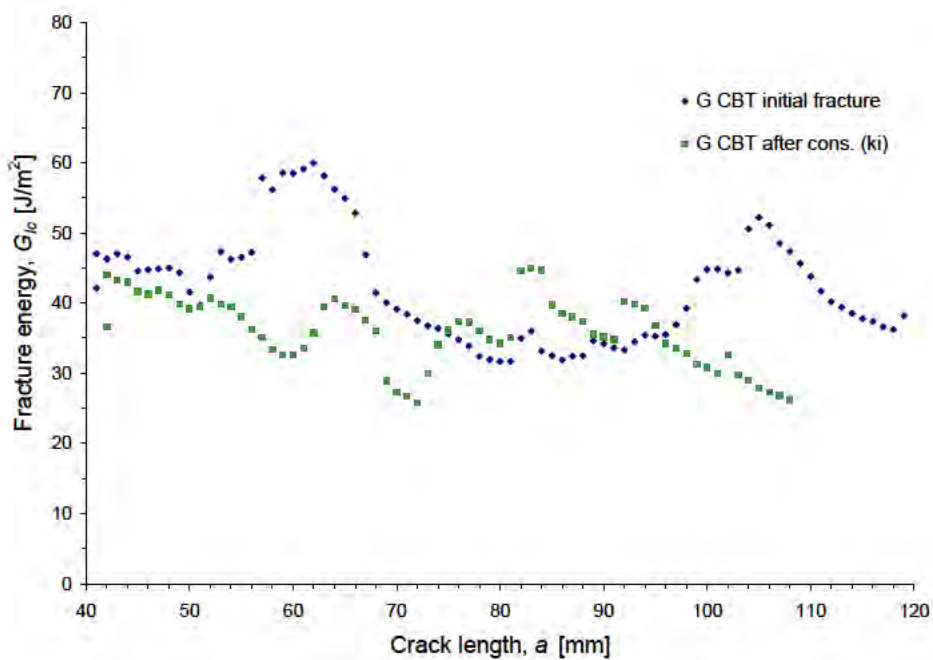


Figure 7.27.: R-curves for DCB specimen before and after consolidation with *ki-urushi*.

#### Sets 07 and 08      Paraloid B 72 and B 48 N (class III a)

Three different solutions of Paraloid resin were tested in this study. Set A-07 was consolidated with Paraloid B 72 (25%) in toluene, whilst set B-07 was treated with a 25% solution of Paraloid B 72 in acetone. For set A-08, a solution of Paraloid B 48 N was used at a concentration of 25% in toluene/xylene (1:1).

**Fractographic results** It was generally noted that the specimens in these sets were extremely sensitive to handling before and during testing. One specimen of each set A-07 and A-08 precracked during mounting in the testing machine. During DCB testing, fracture occurred very rapidly in an unstable, often stick-slip-type manner and at relatively low loads. Therefore, in most cases only a few propagation points could be recorded.

## 7. Experimental: Fracture Behaviour – Results and Discussion



Figure 7.28.: Typical fracture surfaces of a DCB specimen consolidated with Paraloid B 72 (25 %) in acetone stained with Solvent Blue G stain, showing 100 % AF between the old consolidated/re-adhered fracture surfaces.

The three specimen sets showed unanimous results with respect to their fracture surfaces in that they had failed entirely between the re-adhered and consolidated old fracture surfaces (Fig. 7.28). A distinct layer of bulk consolidant, acting as an adhesive, could not be established on any of the specimens. It appeared that they had all failed in these locations due to insufficient adhesion within a starved joint. High resin concentrations were only observed close to the specimen edges, caused most likely by resin migration towards the specimen's surface during solvent evaporation. Such behaviour is well known for polymers dissolved in fast-evaporating solvents (e.g. Payton 1984; Wang and Schniewind 1985). Figures 7.29 a–c present details of the fracture surface and show the non-uniform distribution of Paraloid B 72 resin. Similar results on the qualitative performance of Paraloid B 72 have also been reported by Horton-James et al. (1991), who investigated the consolidation of flaking paint on wood in earlier studies.

Colourless residues on the fracture surfaces of the four specimens treated with Paraloid B 48 N (set A-08) clearly suggested that these DCB specimens had failed for similar reasons. Microscopy revealed that the residues were small, colourless crystals which had formed all over the fracture surface (Fig. 7.30b). This confirmed failure due to a lack of continuous film formation and insufficient adhesion of the polymer to the foundation layer. Crystals of this type were specific to the Paraloid B 48 N and were not present on any of the specimens consolidated with Paraloid B 72. It was thus assumed that they originated from the resin formulation of the B 48 N, which apart from consisting of a methyl methacrylate copolymer and polystyrene, is also known to contain plasticiser and an adhesion promoter (CAMEO 2009). Also, the choice of solvent could have influenced the polymer's behaviour: it was observed that when dissolved in toluene, B 48 N turned milky in its appearance once xylene was added to the solution. This indicates that some coagulations may have already formed in the solution, which upon application on the fractured DCB specimen may have formed the crystals.



### 7.3. Second-phase DCB fracture tests (consolidated specimens)

It is thus questionable whether this type of resin should at all be applied in a solvent that does not fully dissolve it.

In all specimens consolidated with the Paraloid solutions, the areas of failure between the wood and the (consolidated) foundation were characterised by several phenomena:

The higher resin concentration near the specimen edges has already been described. In addition to this, irregular uptake of the consolidant was observed which was caused by the presence of natural resin inherent to the Québec yellow pine wood. This resin had partly leached from the wood into the foundation layer and thus prevented the uptake of the consolidant in the affected areas (Fig 7.31).

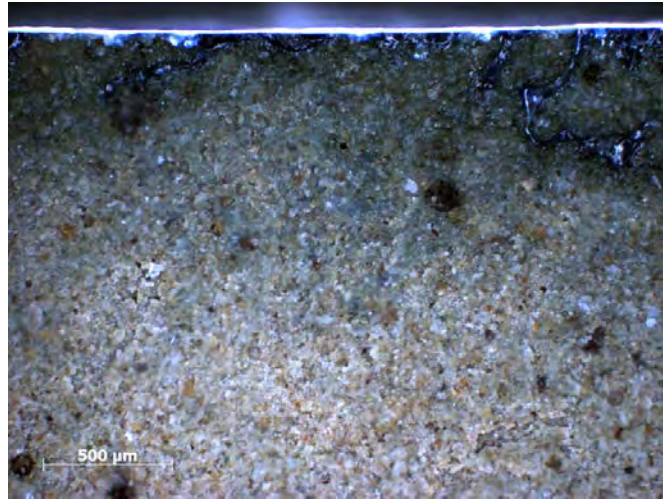
Furthermore, very fine wood fibres had remained adhered to the foundation, irrespective of the type of Paraloid used (Fig. 7.30a). However, it was noted that many wood fibres had already become loose after initial testing without fully detaching from the wood substrate. Hence, this fine wood failure was not unique to the consolidants used. Also, it was too subtle to be true substrate failure and was eventually considered negligible.

**Fracture energy** Determination of the fracture energy of these specimens was problematic, as several specimens had failed to give sufficient propagation points to calculate useful values for  $G_{Ic}$ . Entirely unusable specimens were rejected. This left three valid specimens of set A-07, two of set A-08 and another three specimens of set B-07 for calculating the fracture energy. Almost all specimens had fractured in a very unstable, stick-slip-like manner so that typical load-displacement graphs recorded gave results very similar to the one presented in Figure 7.32.

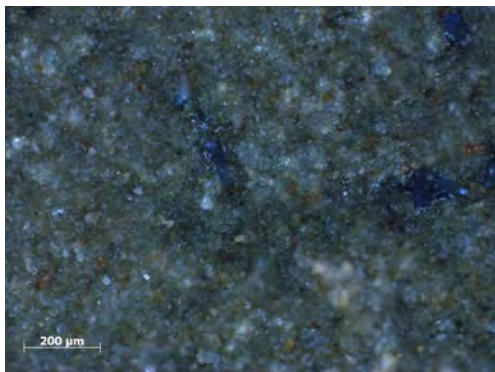
The fracture energies calculated from the second-phase test data showed a unanimous decrease in  $G_{Ic}$  values for all specimens. On average, the mean relative fracture energies of the specimens of sample A-07 (Paraloid B 72 in toluene) were reduced by around 96 % ( $\overline{G}_{Ic} \approx 2 \text{ J/m}^2$ ). Set A-08 (Paraloid B 48 N) showed relative decreases of 88 % and the specimens in sample B-07 (B 72 in acetone) had changed on average by -94 %. Both reached absolute  $\overline{G}_{Ic}$  values just slightly above  $3 \text{ J/m}^2$ .

The low fracture energy values together with the fractographic results suggested that all three Paraloid formulations neither achieved sufficient bonding between the cohesively fractured foundation interfaces, nor between the adhesively fractured foundation/wood interface. This appeared to be due to the non-uniform consolidant distribution and starved joints.

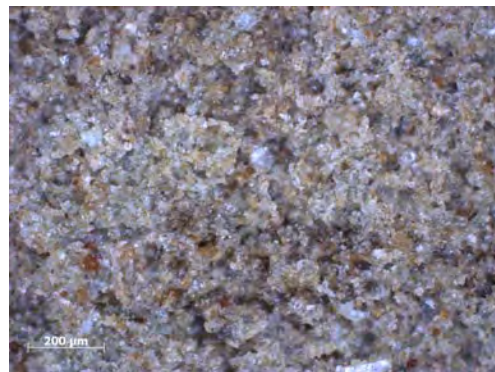
7. Experimental: Fracture Behaviour – Results and Discussion



(a) Detail showing increasing consolidant concentration towards the specimen edge.



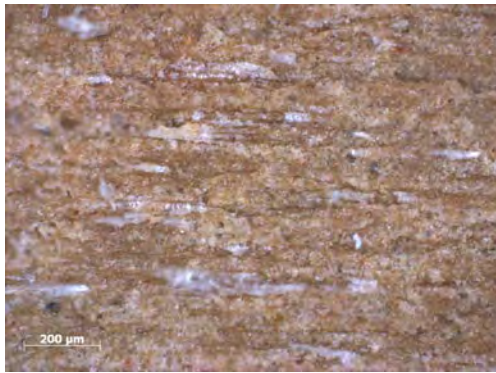
(b) Detail near the specimen edge with high resin concentration.



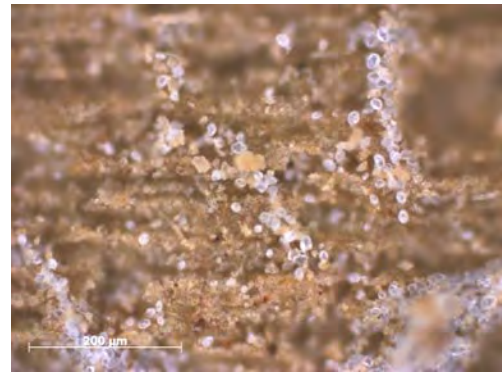
(c) Detail of the central area of the specimen with very low resin concentration.

Figure 7.29.: Fracture surface of a DCB specimen consolidated with Paraloid B 72 in acetone (stained with Solvent Blue G) showing non-uniform resin distribution in the foundation layer.

7.3. Second-phase DCB fracture tests (consolidated specimens)



(a) Fine wood fibres adhered to foundation.



(b) Detail of resin crystals on foundation.

Figure 7.30.: Fracture surfaces of DCB specimen consolidated with Paraloid B 48 N in toluene/xylene.



(a) Set A-08 specimen consolidated with Paraloid B 48 N in toluene / xylene.



(b) Set B-07 specimen consolidated with Paraloid B 72 in acetone.

Figure 7.31.: Details of fracture surfaces of DCB specimens consolidated with Paraloid solutions, stained with Solvent Blue G. Irregular uptake of the consolidant is visible in areas of leached natural pine resin (details equivalent to 60 mm x 20 mm).

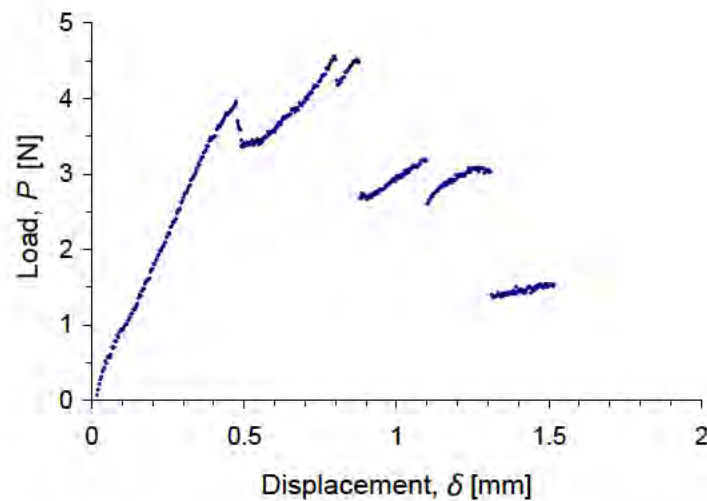


Figure 7.32.: Typical load-displacement curve for a DCB specimen consolidated with Paraloid B 72 in acetone.

### Set 09 Lascaux Medium for Consolidation (class III b)

**Fractographic results** Four specimens were tested for both sets A-09 and B-09. In the specimens of set A-09 around 73 % of the fracture path had created new interfacial failure between the wood substrate and the unconsolidated foundation layer. Approximately 26 % of the failure had occurred in the bulk consolidant/adhesive between the interfaces of the two old fracture surfaces. Areas of new cohesive failure within the foundation layer were negligible.

Figure 7.33 presents a characteristic example of the fracture surfaces from testing type B DCB specimens which were consolidated with Lascaux Medium for Consolidation. On average, half of the failure in set B-09 had occurred along the bondline of the re-adhered and consolidated old fracture surfaces, typically showing fracture within the bulk consolidant/adhesive, similar to the specimens in set A-09 (Fig. 7.34b). All remaining failure in the specimens was located within the unconsolidated foundation layer, where the fracture path had propagated as SCF on varying levels (Fig. 7.34a).

For all specimens it was noted that any areas of bulk consolidant appeared to contain a large number of small air-bubbles. These were not seen in any of the other consolidants tested (Fig. 7.34b). Furthermore, some of the voids may also have been caused and increased by partly ductile fracture processes that induced void coalescence. A white appearance of the otherwise clear consolidant indicated a change in refractive index due to an increased presence of microvoids (this phenomenon is discussed in more detail for specimen set 12 below). These findings agree with the very fine bridging of the acrylic consolidant that was observed in all specimens during some stages of the testing. The bridging contributed to

### 7.3. Second-phase DCB fracture tests (consolidated specimens)

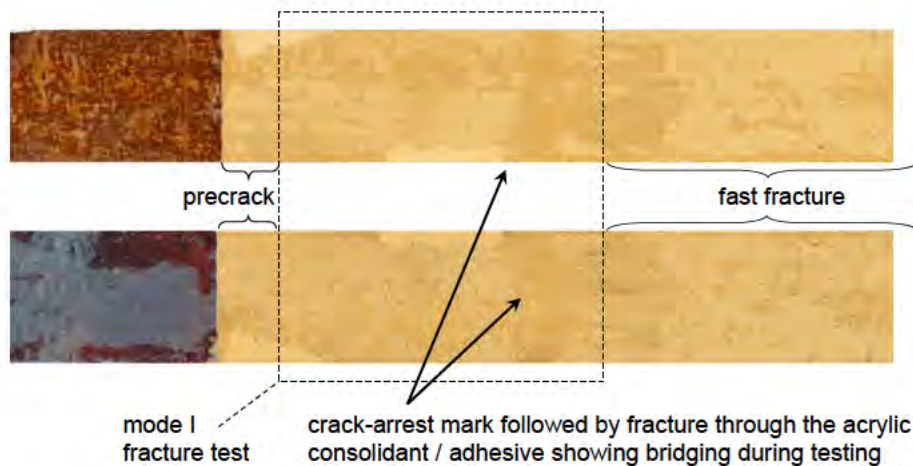
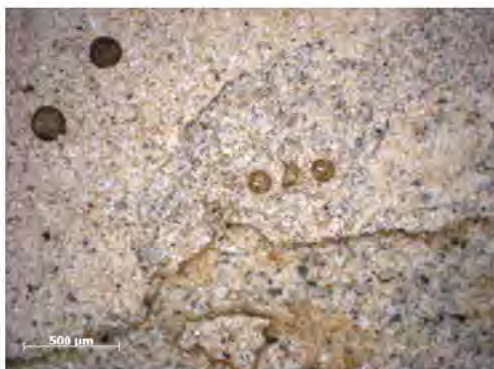
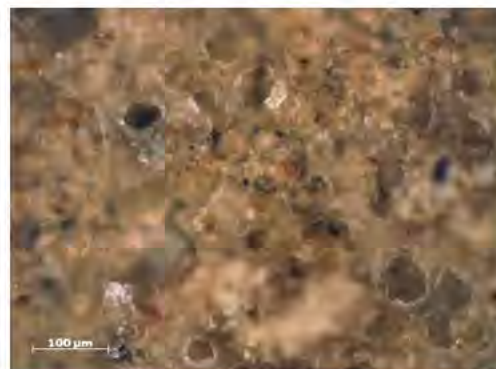


Figure 7.33.: Typical fracture surface of a type B DCB specimen consolidated with Lascaux Medium for Consolidation.

the comparatively slow fracture of the DCB specimens in a mostly stable manner. However, instabilities occurred whenever the fracture path changed its level (between interfacial fracture and failure in the consolidated or unconsolidated areas of the foundation). The specimen in Figure 7.33 clearly shows one of the causes for unstable crack propagation with subsequent fast and catastrophic failure: where the crack path changed from cohesive foundation fracture to cohesive propagation within the bulk consolidant (denoted 'crack-arrest mark ...' in the Figure), extensive bridging started to occur. At this point, the additional fracture energy required to propagate the crack through the composite and the bridges caused the crack to arrest temporarily. Once the bridges broke, the sudden excess of energy could not be dissipated in the system other than by inducing fast crack propagation (as in stick-slip failure). This resulted in catastrophic failure of the specimen.



(a) Failure on varying levels of the foundation in mainly unconsolidated areas.



(b) Fractured layer of bulk acrylic resin showing entrapped air-bubbles.

Figure 7.34.: Details of the fracture surfaces shown in Figure 7.33.

## 7. Experimental: Fracture Behaviour – Results and Discussion

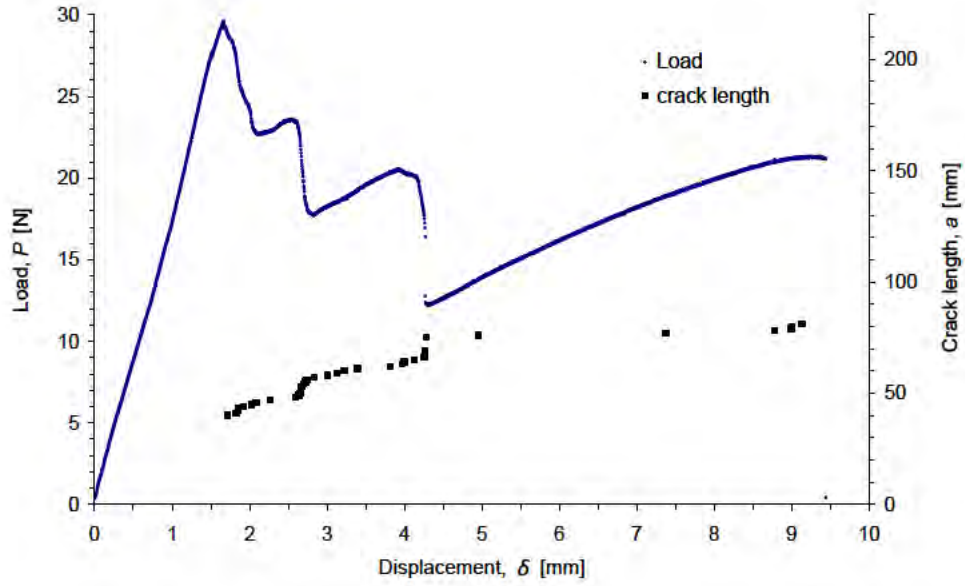
**Fracture energy** On average, absolute  $\overline{G}_{Ic}$  were measured at around  $61 \text{ J/m}^2$  in set A-09. In terms of changes in fracture energy this denoted a mean relative increase by 100 % for the specimens.

In set B-09, this behaviour was even more pronounced. Two specimens fractured within the bulk consolidant in the bondline between the re-adhered old fracture surfaces, giving  $G_{Ic}$  values of  $122 \text{ J/m}^2$  and  $173 \text{ J/m}^2$  respectively. A third specimen had shown an initial fracture energy of around  $250 \text{ J/m}^2$  at early stages of the test. However, this specimen had subsequently failed catastrophically when the fracture path changed from within the bulk consolidant in the bondline to create cohesive failure in the unconsolidated areas of the foundation. Overall, a  $\Delta\overline{G}_{Ic}$  increase of around 180 % ( $\overline{G}_{Ic} \approx 158 \text{ J/m}^2$ ) was determined for specimen set B-09. This suggested that the consolidant had penetrated well into the foundation and had reinforced the layer almost throughout its entire thickness.

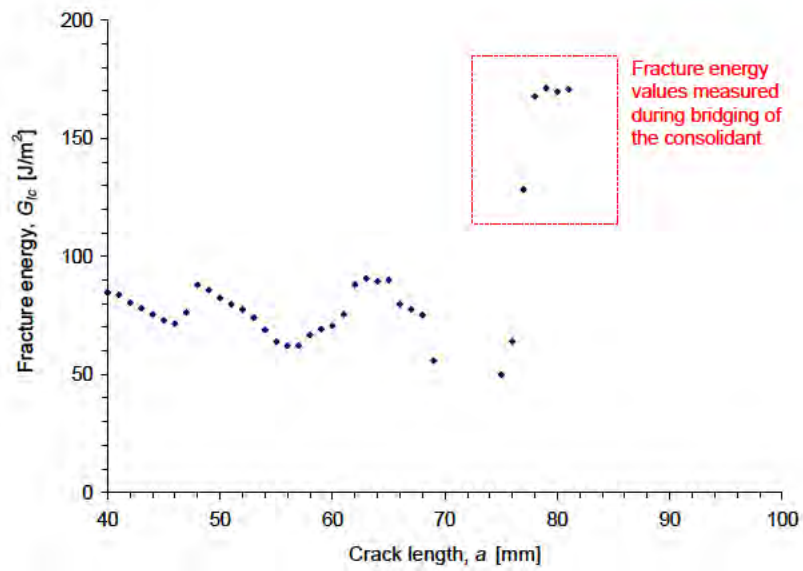
The increased fracture energy values and the reduction in bridging in set B-09 were attributed to the longer drying time of the specimens. The type B specimens had been kept in the humidity-controlled chamber for  $5\frac{1}{2}$  months after consolidation, whilst type A specimens had only cured for 3 months (cf. Section 6.1.2). During the pre-testing phase of this research it was noticed that aqueous dispersions of acrylics and polyvinyl acetate polymers changed their fracture properties rather drastically over a much longer time period during drying compared with the other consolidants used. The dispersions were very elastic to begin with and showed pronounced creep during testing, manifested in the extent of bridging. This tendency to creep decreased during the course of drying and equilibration over several weeks. Nevertheless, these specimens did not display entirely brittle fracture behaviour even after more than five months. In contrast, the aqueous and solvent-based solutions and the lacquer-based consolidants all showed brittle fracture after two months of equilibration.

The effect of bridging on can clearly be Figure 7.35 gives a typical example of the behaviour of a DCB specimen treated with Lascaux Medium for Consolidation after  $5\frac{1}{2}$  months of equilibration. These graphs were recorded for the fractured DCB specimen shown in Figure 7.33. From the load-displacement graph it can be seen that fracture was relatively stable up to a crack length of around 78 mm, despite displaying some variability in the measured data and deviation from ideal propagation in the R-curve (Fig. 7.35b). In the region between 79-82 mm crack length, the fracture surfaces of the specimen show a typical crack arrest mark. Beyond this mark, fracture had occurred within the bulk consolidant/adhesive located between the two old fracture surfaces. Related to the R-curve, it is apparent that this area corresponds with a distinct increase in fracture energy. Hence it is strongly suggested that the observed bridging of the acrylic consolidant is mainly responsible for this behaviour.

7.3. Second-phase DCB fracture tests (consolidated specimens)



(a)



(b)

Figure 7.35.: Load and crack length as a function of displacement (a) and fracture energy as a function of crack length (b) for the specimen consolidated with Lascaux Medium for Consolidation, shown in Fig.7.33.

## Set 10 Mowiol 3-83 (class IV)

**Fractographic results** Four specimens for each set A-10 and B-10 were prepared, of which one specimen broke accidentally when handling prior to testing. Judged by the appearance of its fracture surfaces, this specimen appeared to have suffered from consolidant/adhesive starvation at the interfacial joint. Failure had occurred within the bulk consolidant/adhesive between the re-adhered old fracture surfaces. After testing, the fracture surfaces of all remaining specimens also showed predominantly this type of failure (on average above 97%). Crack propagation in these specimens had developed in a considerably stable manner and no bridging of the consolidant was observed. Figure 7.36 presents typical fracture surfaces of a type B specimen, also showing small areas of new special cohesion failure in unconsolidated parts of the foundation layer.



Figure 7.36.: Fracture surfaces of DCB specimens consolidated with Mowiol 3-83 (unstained), showing failure within the bondline between the consolidated and re-adhered old fracture surfaces, and small areas of SCF within unconsolidated parts of the foundation.

Initially, the type A specimens had fractured interfacially over large areas between the wood and the foundation. During second-phase fracture, some subtle failure in the wood substrate was noticed, which was not seen on any other specimens. Where the Mowiol had re-adhered the wood substrate to the foundation layer, the fracture path had partly propagated through the uppermost layers of the wood cells during re-testing. A very thin layer of fine wood fibres thus remained adhered to the foundation. This wood failure was more pronounced than in the specimens consolidated with the Paraloid formulations. In contrast, the specimens of set B-10 did not develop this type of fracture at all. Initial testing of these specimens had mainly induced SCF within the foundation layer, and no failed interfaces between the wood and the foundation were provided.

**Fracture energy** The stability of crack propagation during testing of the DCB specimens consolidated with Mowiol 3-83 was reflected in their relatively stable R-curves (Fig. 7.37). It was established that, on average, the fracture energy values



### 7.3. Second-phase DCB fracture tests (consolidated specimens)

of the consolidated specimens had decreased by around 53 and 50 % for set A-10 and B-10 respectively. This denotes a markedly consistent result. Furthermore, the measured values can be more precisely interpreted as the actual toughness of the Mowiol 3-83 itself, as all the specimens had fractured predominantly within the bulk consolidant/adhesive.

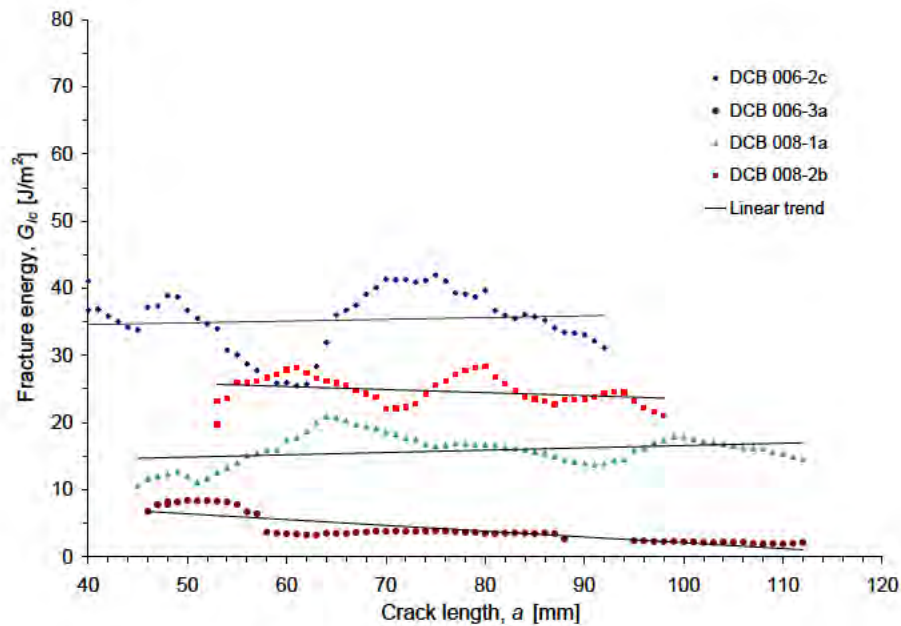


Figure 7.37.: R-curves for the four specimens of set B-10 measured during second-phase testing, after consolidation with Mowiol 3-83.

## Set 11 Mowilith 50 (class V a)

**Fractographic results** The fracture testing of the DCB specimens consolidated with Mowilith 50 produced very similar results to the specimens treated with the Paraloid solutions. One specimen fractured during handling (before testing) within the bondline between the re-adhered and consolidated old fracture surfaces. The other specimens showed partly stable and partly unstable (stick-slip-like) crack propagation during testing, and also failed within the joint between the previously re-adhered fracture surfaces (Fig. 7.38). As in the specimens consolidated with Paraloid, this fracture was mainly determined by consolidant starvation of the joints. Very fine wood fibres that remained adhered to the foundation layer (Fig. 7.39) were considered negligible. Similar fibres had already been detached during initial fracture and hence did not indicate any noteworthy change in fracture behaviour.

## 7. Experimental: Fracture Behaviour – Results and Discussion



Figure 7.38.: Fracture surface of DCB specimen consolidated with Mowilith 50 (20%) in toluene, stained with Lugol's solution.

Staining of the fracture surfaces with Lugol's solution revealed irregular consolidant uptake in those areas where natural wood resin had leached into the structure. Again, a very similar appearance of the staining pattern was reported for the Paraloid solutions (see Fig. 7.31). In all other areas of the specimens the Mowilith 50 solution appeared to have penetrated well into the previous fracture surfaces. Increased concentrations of the PVAc resin (i.e. bulk resin) were neither visible on the wood surface nor on the foundation. Figure 7.39 shows a detail of the typical appearance of a refractured foundation layer previously consolidated with Mowilith 50. (Note that the darker appearance of some areas does not indicate higher concentrations of stained resin. It merely arose from areas of shadow in fine surface recesses parallel to the direction of crack propagation).

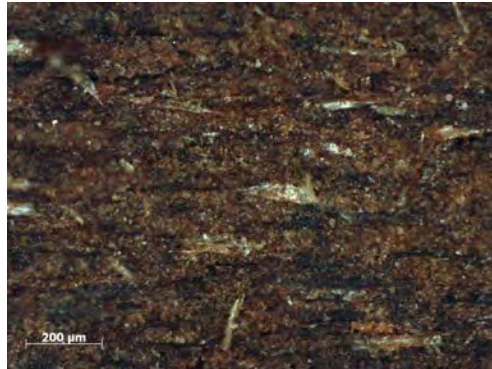


Figure 7.39.: Detail of fracture surface of DCB specimen consolidated with Mowilith 50 (20 %) in toluene after staining with Lugol's solution.

**Fracture energy** For specimen set A-11, overall mean fracture energy values were measured at around  $2 \text{ J/m}^2$ . Thus, all specimens had shown a consistent decrease in fracture energy by between 93 to 95 % of their original value measured during initial fracture testing. These results, too, were similar to the values measured for the Paraloid-treated specimens.

## Set 12 Mowilith DMC2 (class V b)

**Fractographic results** Fracture results were gained from three specimens. On average, around two thirds of their fracture area (68 %) showed failure in the bondline between the re-adhered and consolidated old fracture surfaces. Approximately 27 % of the crack path propagated interfacially between the wood substrate and the unconsolidated foundation layer, whilst 5 % had created new cohesive failure within the foundation. In all fractured areas where the wood substrate had previously been re-adhered to the foundation layer, many fine wood fibres remained adhered to the foundation layer after second-phase testing. The same behaviour had previously been observed in the specimens consolidated with Mowiol 3-83 (Fig. 7.41a). Despite the low solid content of the Mowilith DMC2 dispersion (10 % by weight), the consolidant appeared to have formed a film on the previous fracture surfaces. This is illustrated in Figure 7.41a, which also suggests that the consolidant has penetrated very little into the foundation, as the foundation has not taken up much of the stain.

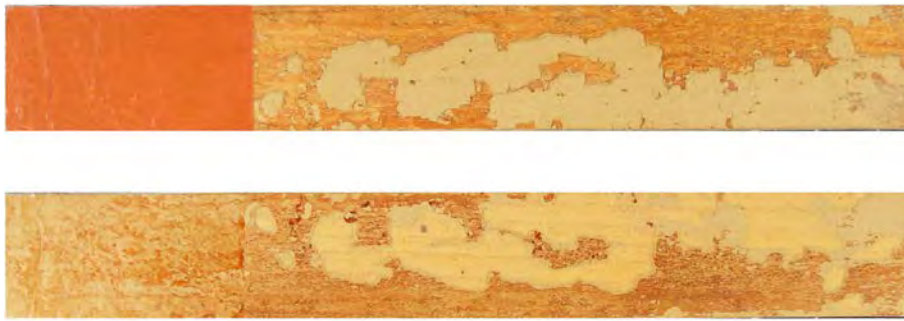
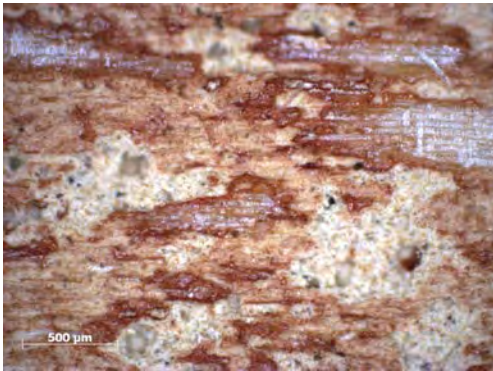


Figure 7.40.: Fracture surfaces of specimen consolidated with Mowilith DMC2 dispersion (10 % solid content), stained with Lugol's solution.

Another notable feature of these specimens was that, during testing, fine bridging of the PVAc polymer was observed where the crack path propagated cohesively within the bulk polymer. This phenomenon revealed that the consolidant did not fracture in a brittle manner, but with considerable deformation. This also explains the variation between partly stable and partly unstable crack propagation, which was observed in the specimens whenever the path changed between the different levels of the layered structure. Similar behaviour was previously reported for the specimens consolidated with Lascaux Medium for Consolidation. Figure 7.41b shows a detail of the typical appearance of a cohesively failed polymer that had retained a notable degree of plasticity. In such materials, microvoids grow and coalesce with increasing plastic strain into larger voids that finally result in total failure of the specimen (e.g. Anderson 2005, pp. 219-23). The characteristic dimples seen in the polymer layer in Figure 7.41b were a clear sign of such ductile fracture. The fine bridging that occurred during testing of the specimens is evident in Figure 7.42.

## 7. Experimental: Fracture Behaviour – Results and Discussion



(a) Detail showing fracture on varying levels of the partly consolidated foundation layer with some wood fibres adhered to the consolidant.



(b) Cohesively failed Mowilith DMC2 layer showing significant plastic deformation (ductile drawing and void coalescence) which caused the bridging observed.

Figure 7.41.: Details of fracture surfaces of DCB specimen consolidated with Mowilith DMC2, stained with Lugol's solution.

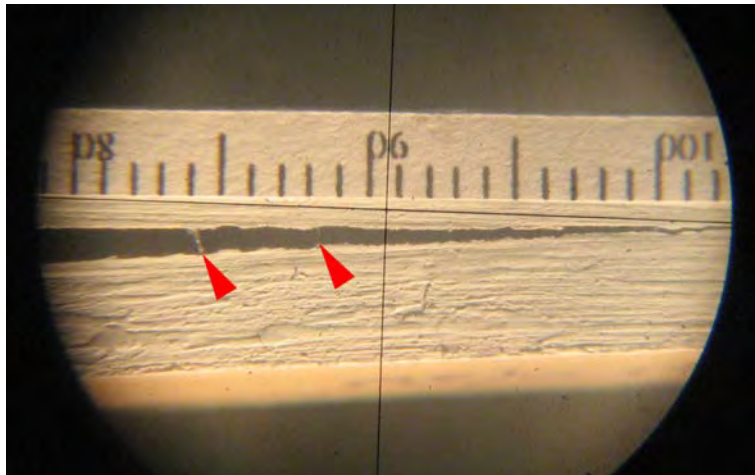


Figure 7.42.: Detail of DCB specimen consolidated with Mowilith DMC2 during testing, viewed through travelling microscope. Very fine bridging of the consolidant can be observed between the two fracture surfaces at 84 mm and 88 mm (marked with red arrows).

**Fracture energy** Fracture energy values measured for these specimens were variable, which conformed with the observation of the partly unstable fracture behaviour on varying levels and the bridging of the consolidant. To fracture (or rupture) the polymer bridges whilst propagating the crack at the crack-tip, additional energy was required, which led to the relatively high fracture energy values. Also, true brittle fracture could not be investigated in isolation in these areas, which is reflected in the variability of the measured data. For the specimen

### 7.3. Second-phase DCB fracture tests (consolidated specimens)

set, a  $\overline{G}_{Ic}$  value of  $130 \text{ J/m}^2$  ( $\pm 34 \%$ ) was measured, which denoted an increase in  $\overline{\Delta G}_{Ic}$  by  $72 \text{ J/m}^2$  ( $\pm 35 \%$ ). This meant that average increases in fracture energy of around  $126 \%$  were reached when specimens were consolidated with a  $10 \%$  solid content aqueous dispersion of Mowilith DMC2. These were by far the highest increases recorded for any of the consolidants tested in this series.

#### 7.3.3. Summary of DCB fracture tests

##### Results for type A and B specimens

The  $\overline{G}_{Ic}$  values measured for each specimen set of type A and B before and after consolidation respectively are summarised in Figures 7.43 and 7.44. The first light-grey bar in every chart represents the overall mean fracture energy of all DCB specimens of the respective type during initial fracture, whilst the darker grey bars next to each coloured one refer to the four selected specimens used in the respective set. The overall values (coloured bars) indicate the general performance of the consolidants, i.e. the average fracture energy for the set, assuming that all test specimens were more or less equal in their properties before consolidation treatment.

To eliminate the lack of randomness in these samples and to reduce the systematic error contained in the absolute mean  $G_{Ic}$  values, the relative changes in fracture energy,  $\overline{\Delta G}_{Ic}$ , were also compared. An overview of the  $\overline{\Delta G}_{Ic}$  values for all specimen sets are given in Figure 7.45.

In addition to the fracture energy results, the percentage of new failure created after second-phase fracture (Fig. 7.46) gave complementary information on whether the fracture occurred within the bondline between the old fracture surfaces or in entirely new areas of the foundation. These results helped to evaluate whether the consolidants were efficient bonding agents within the joints, and whether they were likely to facilitate new failure in previously unfractured areas of the material.

From the bar graphs in Figures 7.43 and 7.45a, which show  $\overline{G}_{Ic}$  and  $\overline{\Delta G}_{Ic}$  values, it can be seen that the **cold-liquid fish glue**, the three **Paraloid solutions** and the **Mowilith 50** all failed to strengthen the test specimens. Fracture unambiguously occurred only in the bondline, as these consolidants penetrated too well into the fracture surfaces and lacked sufficient gap-filling ability. In the specimens consolidated with fish glue, hardly any failure occurred in previously unfractured areas of the specimens, and in those treated with Paraloid, virtually no failure in new loci was observed (Fig. 7.46). The Paraloid B 72 dissolved in acetone – which was the only Paraloid solution tested on the type B specimens – showed almost identical results to those of the Paraloid formulations dissolved in the benzenes. From these limited tests, the choice of solvent (whether polar or non-polar) did not appear to have much influence on the mechanical performance of the consolidants at the given solution concentration of  $25 \%$  resin content (and provided the consolidant was applied in a single brush application).

7. Experimental: Fracture Behaviour – Results and Discussion

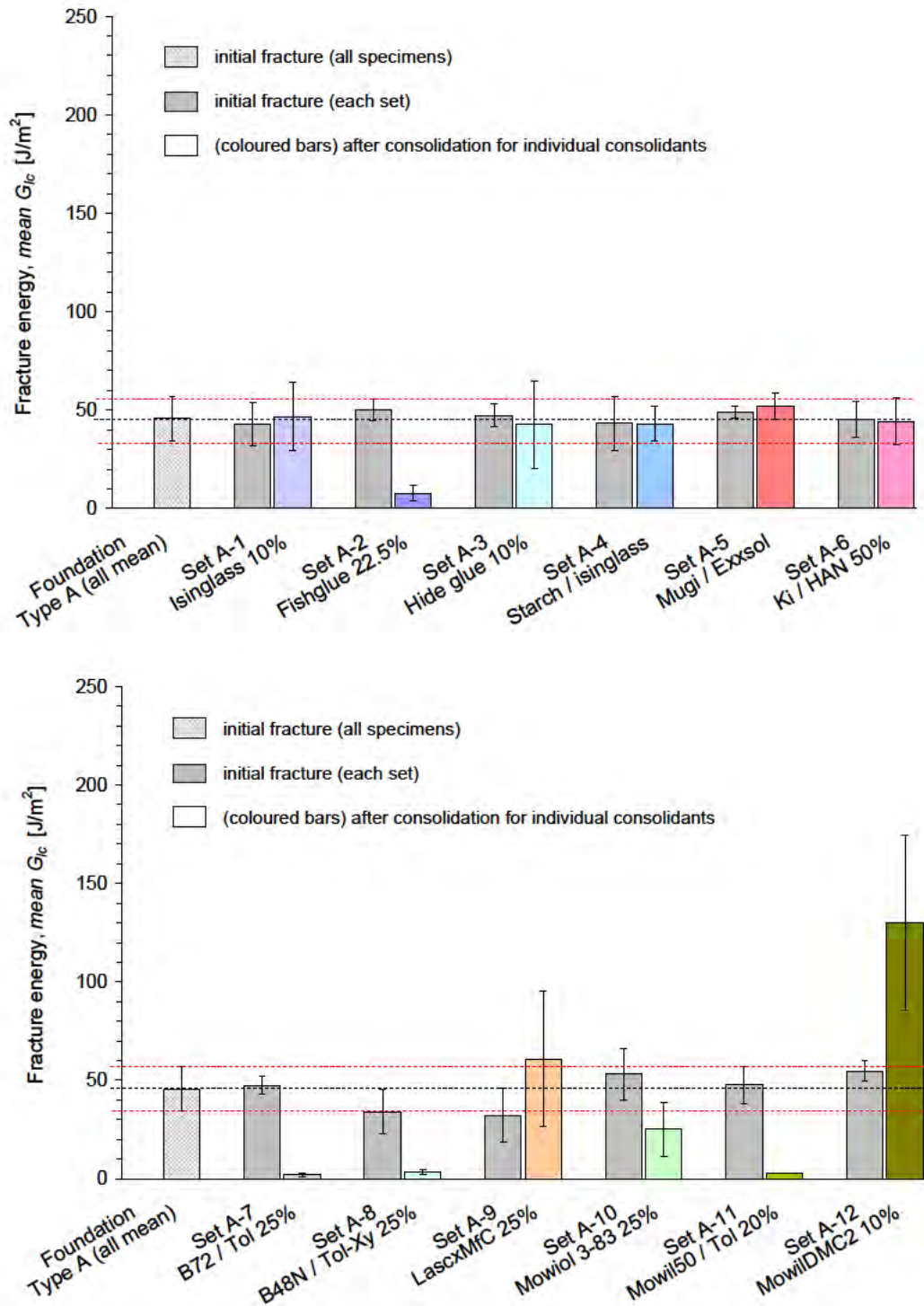


Figure 7.43.: Mean fracture energy,  $\overline{G}_{Ic}$ , values for each DCB specimen set of type A before and after consolidation. Error bars indicate, plus or minus, one standard deviation.

### 7.3. Second-phase DCB fracture tests (consolidated specimens)

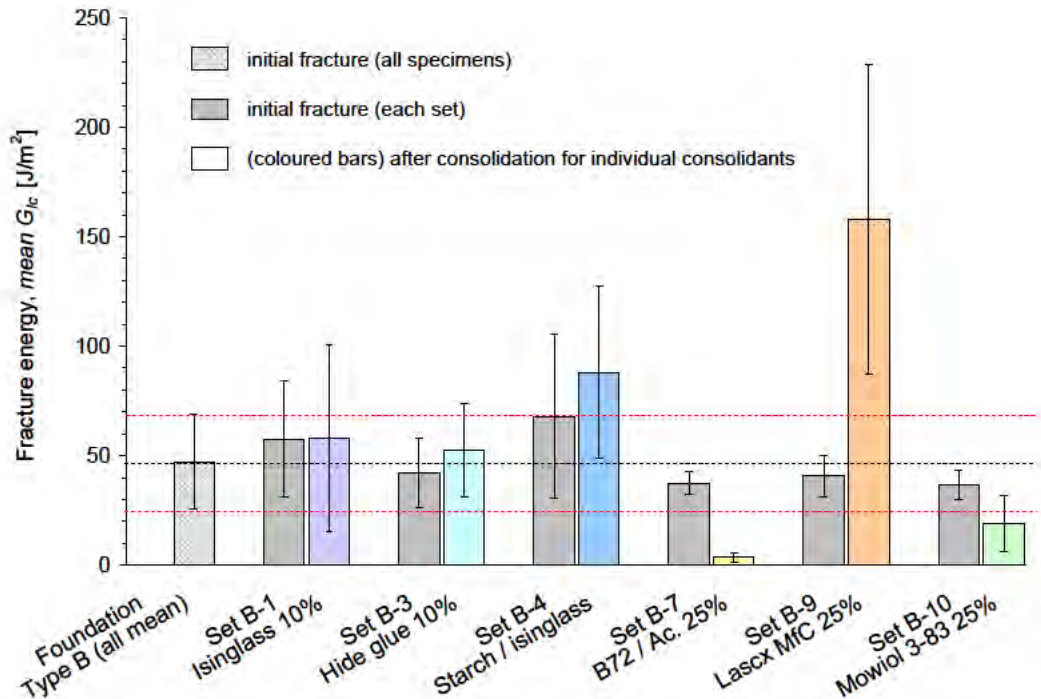


Figure 7.44.: Mean fracture energy,  $\overline{G}_{Ic}$ , values for each DCB specimen set of type B before and after consolidation. Error bars indicate, plus or minus, one standard deviation.

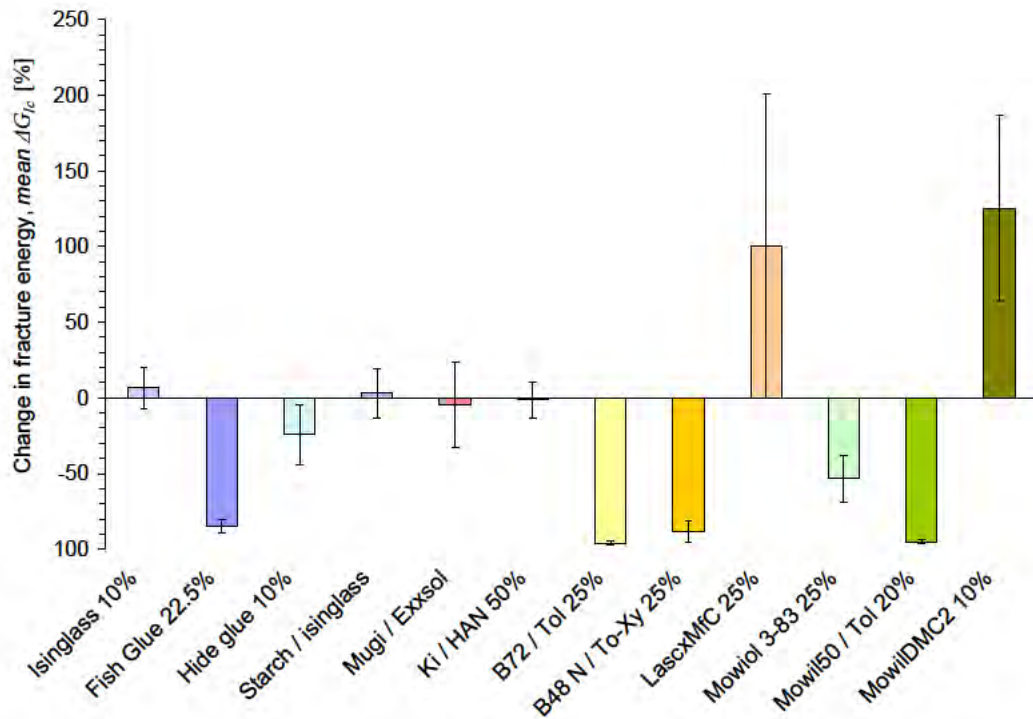
The **Mowiol 3-83** had induced some degree of strengthening, despite not being able to restore the fracture energy of the specimens to their original level measured during initial fracture. Results for types A and B specimens were practically the same, and both showed failure almost entirely within the bondline and at fracture energy levels of around half their original value.

The other **protein-based consolidants** (i.e. all but the cold-liquid fish glue) and the **lacquer-based formulations** formed a group of consolidants that showed some similarities, but also differences in their performance:

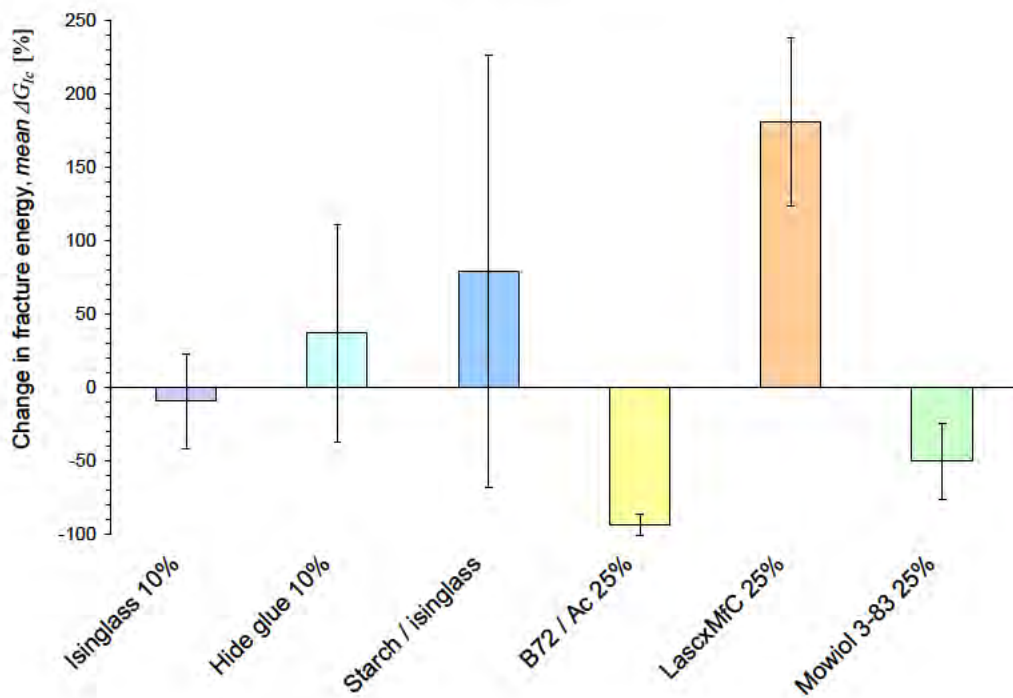
For type A specimens, all these consolidants displayed overall fracture energy values more or less within the range measured during initial fracture. As would be expected, only the scatter of the data was larger after consolidation. The  $\overline{\Delta G}_{Ic}$  values for these consolidants were generally minimal in the type A specimens.

For type B specimens, only three of the **protein glues** were tested (and none of the lacquer-based consolidants) and the results for these consolidants were different to the ones recorded for type A. Isinglass and hide glue appeared to show inverse results for relative changes in  $G_{Ic}$  (Figs. 7.45 a–b), although the respective positive and negative changes cancelled each other out when the average for both type A and B values was considered. Both consolidants also showed a similar extent of fracture in new areas of the specimens (Fig. 7.46). However in the spec-

7. Experimental: Fracture Behaviour – Results and Discussion



(a) Type A specimen sets.

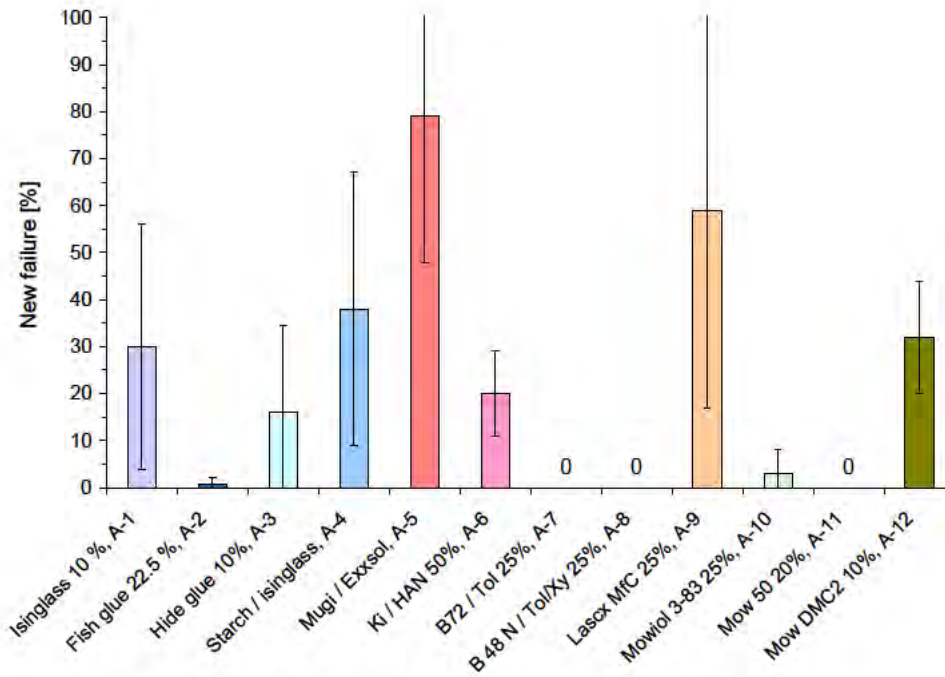


(b) Type B specimen sets.

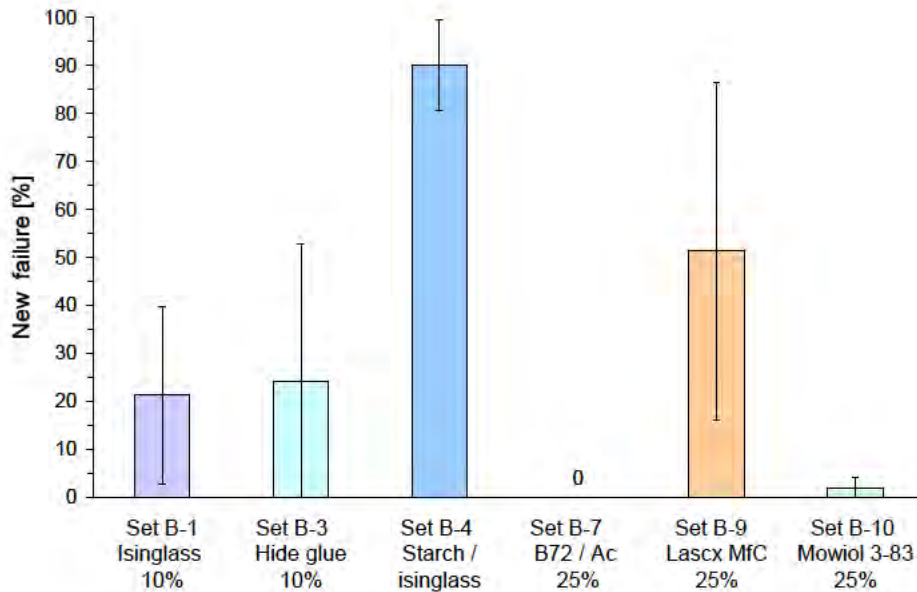
Figure 7.45.: Effect of consolidation expressed as mean relative changes in fracture energy,  $\overline{\Delta G}_{Ic}$ , measured for types A and B samples during second-phase DCB testing. Error bars indicate, plus or minus, one standard deviation.



### 7.3. Second-phase DCB fracture tests (consolidated specimens)



(a) Type A specimen sets.



(b) Type B specimen sets.

Figure 7.46.: Comparison of the percentage of failure in new areas of the DCB specimens determined after second-phase fracture. The remaining failure had developed within the bondline, following the fracture path from initial testing either within the bulk consolidant or within the joint that was starved of consolidant/adhesive. Error bars indicate, plus or minus, one standard deviation.

## 7. Experimental: Fracture Behaviour – Results and Discussion

imens consolidated with the starch/isinglass formulation exceptionally high levels of new failure occurred in the type B specimens. This behaviour was reflected in the significantly higher fracture energy values for the type B specimens compared with the type A results for the same consolidant. Considering that the fracture energies were on average higher for type B specimens than for type A, the question arose whether the longer equilibration times for these specimens played a significant role in achieving higher values during fracture testing. Unfortunately, however, a comprehensive analysis of the influence of equilibration times could not be pursued in this study, due to the limited number of tests undertaken.

The **lacquer-based consolidants**, which were only tested on type A specimens and which showed similar  $\overline{G}_{Ic}$  and  $\overline{\Delta G}_{Ic}$  values, differed greatly with respect to their failure paths. The specimens consolidated with *mugi-urushi* had failed by nearly 80 % failure in previously unfractured areas and thus performed similarly to those treated with the starch/isinglass mixture with around 90 % new failure. These two consolidants achieved the highest percentage of new failure for all consolidants tested, which suggested that the starch content acted as a very efficient adhesive and gap-filler. In contrast, the *ki-urushi* failed predominantly along the old fracture path. However, despite seemingly lacking gap-filling ability, fracture energy values similar to those measured during initial testing were achieved.

By far the highest average increases in fracture energy were measured for the two synthetic polymer dispersions: the **Lascaux Medium for Consolidation** (acrylic) and the **Mowilith DMC2** (PVAc). Levels well above 100 % of their original fracture energy value were reached by both consolidants in the type A specimens. In the type B specimens, the Lascaux MfC even showed mean increases as high as 180 %. The large increases in fracture energy in the type B specimens were mainly explained by the much longer equilibration time of these specimens. Tests had shown that within the first few months after application of acrylic or PVAc-based aqueous dispersions, their mechanical properties changed significantly. Extended drying increased the measured fracture energy for at least a period of up to 3<sup>1</sup>/<sub>2</sub> months after consolidant application. Comparison between the Mowilith DMC2 and the Lascaux MfC also revealed that the specimens consolidated with the acrylic dispersion displayed, overall, a greater percentage of fracture in new areas of the foundation. Hence it was concluded that the Lascaux MfC had not only well re-adhered the fracture surfaces, but also most effectively consolidated the bulk foundation layer well beyond its original strength, compared with all other consolidants tested.

### Overall mean results for DCB tests

The overall mean results of the DCB fracture tests for both specimen types A and B are summarised in Table 7.6. The results in the table suppose that the given consolidant is applied to the fragile material in a single application only, and in the specific formulation stated in Section 6.1.2 and Table 6.1. Such a table

### 7.3. Second-phase DCB fracture tests (consolidated specimens)

provides good support for choosing a useful consolidant for foundation material, as fracture energy values and their changes, and the distribution of fracture loci can be directly compared:

If a consolidant is required that re-establishes the previous fracture behaviour of the fragile material, a polymer formulation that can induce similar fracture energy levels during testing after application has to be chosen. This criterion is fulfilled by the isinglass, hide glue, *mugi-urushi* and *ki-urushi*. However, differences in their behaviour lie in the location of the fracture paths. From this point of view the *mugi-urushi* performed worst, as the respective specimens showed by far the highest degree of new fracture in previously undamaged areas. Furthermore, this failure only occurred in entirely unconsolidated areas, suggesting that relatively greater levels of strength (or toughness) were reached in those parts of the layer into which the consolidant had successfully penetrated. *Ki-urushi* performed better with its specimens fracturing less in previously unfractured areas. However, the fact that none of the new failure occurred in consolidated areas also indicated that similar strength increases to those with the *mugi-urushi* were reached. The hide glue and isinglass on the other hand merely showed 25 % of new failure or less, and the respective failure paths were shown to propagate partly through consolidated areas of the specimens. This fracture behaviour suggested relatively uniform fracture properties between unconsolidated and consolidated areas. Hence, such consolidants would be desirable in cases where a fragile material were to be stabilised with lower risk of future damage incurring in new areas.

Consolidants applied to those specimen sets which failed at the lowest  $G_{Ic}$  values (marked in bold red in Table 7.6, e.g. Paraloid or Mowilith 50) may not be useful in practice in most cases, as re-fracture will occur when a low amount of energy, i.e. a small force, is applied to the system. Such energy levels are easily reached (and exceeded) during ordinary handling of an object. Despite achieving only relatively low  $G_{Ic}$  values in the specimens consolidated with the Mowiol 3-83 (marked in blue italics in the Table), this PVAI consolidant may however still have useful properties. This formulation has the advantage of failing reliably and almost entirely within the bondline between the re-adhered old fracture surfaces. Nevertheless, at the same time it provides some, albeit relatively small degree of stabilisation. Thus, if reliable fracture within areas of previous damage is categorically desired, a consolidant like Mowiol 3-83 may be an appropriate choice.

Similar considerations apply to the consolidants that greatly increase the fracture energy of the stabilised foundation, i.e. the Lascaux MfC, the Mowilith DMC2, and to a certain degree the starch/isinglass (respective values marked in blue italics). Strength improvements of this magnitude may be desirable in specific cases, for example where layers are particularly load-bearing. However if these consolidants fail to disperse uniformly within the structure, they pose the risk of creating areas within the specimen with very different mechanical properties, which might be cause for further damage in the future. Therefore, the data in

## 7. Experimental: Fracture Behaviour – Results and Discussion

Table 7.6 give a somewhat incomplete picture unless the penetration ability of the consolidants is added. This aspect is looked at in the following section.

Table 7.6.: Summary of fracture testing results for all DCB specimens (type A and B), giving average values. (Note that the results in the table suppose that the given consolidant is applied to the fragile material in a single application only, and in the specific formulation stated in Section 6.1.2 and Table 6.1.)

MATERIAL / CONSOLIDANT	$\overline{G}_{Ic}$	$\overline{\Delta G}_{Ic}$	BL FAILURE [%]	NEW CF		NEW AF	
	[J/m <sup>2</sup> ]	[%]		[%]	CONS. AREAS	[%]	CONS. AREAS
Foundation (uncons.)	46	/	/	39	/	61	/
Isinglass	53	– 1	75	14	half	11	none
Fish glue	<b>8</b>	– <b>85</b>	99	1	none	0	none
Hide glue	48	7	80	5	half	15	none
Shofu / isinglass	<i>66</i>	41	36	37	half	27	little
Mugi-urushi	46	– 5	21	15	none	64	none
Ki-urushi	44	– 1	80	3	none	17	none
Paraloid B 72 (tol)	<b>2</b>	– <b>96</b>	100	0	/	0	/
Paraloid B 72 (ac)	<b>4</b>	– <b>94</b>	100	0	/	0	/
Paraloid B48 N	<b>3</b>	– <b>88</b>	100	0	/	0	/
Lascaux MFC	<i>109</i>	<i>140</i>	45	25	half	30	none
Mowiol 3-83	<i>22</i>	– 52	97	2	little	1	none
Mowilith 50	<b>2</b>	– <b>95</b>	100	0	/	0	/
Mowilith DMC2	<i>129</i>	<i>126</i>	68	5	none	27	none

‘BL’ failure denotes the extent of failure within the bondline, i.e. between the re-adhered old fracture surfaces, ‘CF’ stands for cohesive failure within the foundation and ‘AF’ refers to new adhesive failure observed at the interface between the foundation and the wood surface. The column denoted ‘cons. areas’ describes whether some of the new failure occurred in loci that had been penetrated by consolidant. Values in bold red mark fracture energy values that were too low for effective stabilisation of the layer, values in *blue italics* mark greatly increased fracture energy values after consolidation.

## 7.4. Examination of DCB cross-sections

### 7.4.1. Bondline thickness and penetration behaviour

The bondline thickness and penetration behaviour of the consolidants were assessed by examining cross-sections, which were cut from the ends of the DCB specimens before second-phase fracture. Optical microscopy under reflected, visible light was used, following the procedure described in Section 6.3. On the micrographs, penetration depth was ascertained by evaluating the spatial distribution of the individual stains used. Dark-coloured areas were interpreted as containing a high consolidant concentration, and areas appearing lighter-coloured as containing lower polymer concentrations. Examples of unstained cross-section micrographs are presented in Fig. 7.47. Specimen type A (Fig. 7.47a) contains only the foundation layer sandwiched between the two wood substrates. Specimen type B (Fig. 7.47b) shows a layer of lacquer (black colour) on top of the foundation and a layer of epoxy resin (dark-greyish appearance) between the lacquer and the top wood substrate. Average foundation layer thickness was 0.32 mm and 0.30 mm (excluding lacquer and epoxy resin layers) before consolidation for types A and B respectively (cf. Table 7.3).

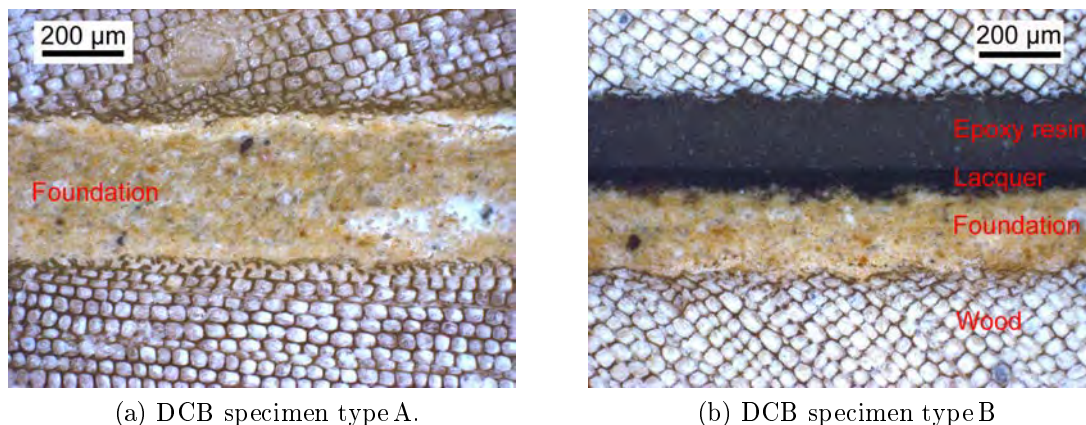


Figure 7.47.: Examples of DCB cross-section micrographs with unstained foundation layers: (a) type A contains foundation only sandwiched between the two wood substrates, (b) type B shows a lacquer layer (black colour) on top of the foundation and a layer of epoxy resin (dark-greyish appearance) between the lacquer and the top wood substrate. (As the foundation layer of the specimens is so brittle, the variation in layer thickness between some of the specimens did not have any effect on their fracture behaviour, and can hence be ignored.)

Considering that the ‘sandwich’ structure of the specimens represented a considerably inhomogeneous, pre-fractured and consolidated composite material, sub-

stantial variability in the appearance of the bondline and consolidant penetration into the structure was expected. Hence, broad trends were established to give a qualitative indication of the consolidants' performances, rather than statistically analysing the exact bondline thicknesses and penetration depths. A table summarising the reported results is given at the end of this section (cf. Table 7.7 on page 220).

### **Protein based consolidants (class I)**

Viewed in cross-section, the DCB specimens treated with the protein-based consolidants displayed overall similar results:

Fish glue, isinglass and hide glue all showed good potential to penetrate well into the porous foundation layer and to a certain degree also into the adjacent wood substrate. Examples of cross-section micrographs for these consolidants are presented in Figs. 7.48 and 7.49. In the Figures, the previous fracture surfaces, to which the consolidants were applied, are marked with red arrows.

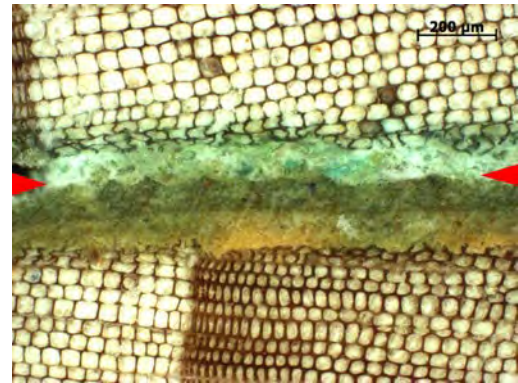
The micrographs show that consolidant penetration varied. In many areas, the proteins had fully dispersed throughout the entire layer thickness (Figs. 7.48 a, c and e). These alternated with areas of more restricted penetration, where up to one half of the layer thickness were sometimes left unconsolidated (Figs. 7.48 b, d and f). Both full and partial penetration were about equally observed in all these specimens. Even though visual examination of the cross-sections did not reveal any clear explanations for this phenomenon, it was assumed that the acknowledged inhomogeneity of the foundation layer was the predominant cause for the non-uniform consolidant penetration. On average, the protein-based consolidants penetrated up to approximately 200  $\mu\text{m}$  from the fracture surfaces into the foundation layer. Isinglass and hide glue often showed deeper penetration, with a penetration depth,  $d_{pf}$ , of up to 250 and 270  $\mu\text{m}$  respectively. Where the consolidant reached the wood/foundation interface (or was directly applied to it), an average penetration depth,  $d_{pw}$ , of up to 50  $\mu\text{m}$  into the wood substrate was noted (cf. Table 7.7 on page 220).

Another striking feature of these protein-based consolidants was their general ability to disperse through the foundation layer thickness without creating pronounced or abrupt new interfaces in areas where penetration was incomplete. Figures 7.48 a, d and f show typical examples of this behaviour: the green-stained consolidant clearly appeared lighter in colour (i.e. less saturated, indicating a lower concentration of the consolidant) with increasing distance from the surface it was applied to. This suggested a more gradual transition in properties between the consolidated and unconsolidated areas of the layer. The only exceptions in this regard were the specimens consolidated with the cold-liquid fish glue. Despite similar appearance of the consolidant, a further region displaying a colour gradient could be identified in these specimens in the middle of their foundation layer in many areas (Fig. 7.48b). The cause for this lighter colour

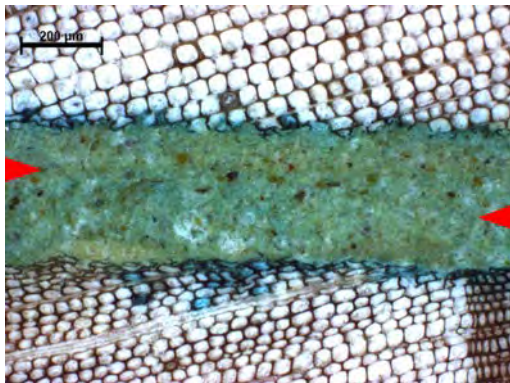
#### 7.4. Examination of DCB cross-sections



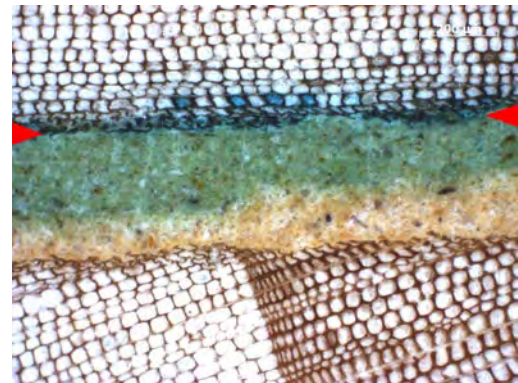
(a) Cold-liquid fish glue (type A); showing good penetration, but leaving voids in the bond along the old fracture surfaces.



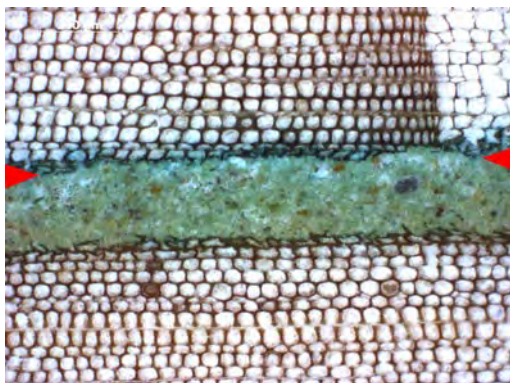
(b) Cold-liquid fish glue; revealing a strong tide-line near centre of layer and voids in bondline (filled with polishing dust).



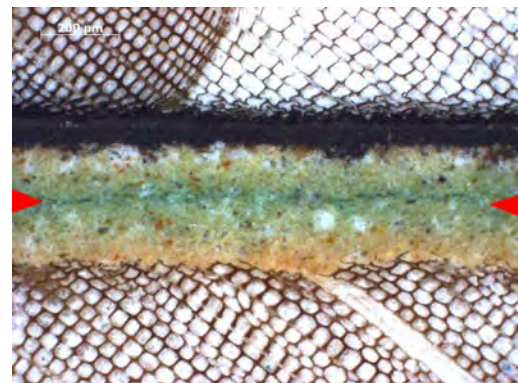
(c) Salianski isinglass (type A); displaying no visible bondline and penetration through entire foundation layer.



(d) Salianski isinglass applied to wood/ foundation interface (type A specimen); showing partial penetration.



(e) Bovine hide glue (type A specimen); uniform consolidant distribution through entire foundation layer.



(f) Bovine hide glue (type B specimen); showing faint bondline with higher consolidant concentration.

Figure 7.48.: Cross-sections of DCB specimens consolidated with protein-based polymer formulations, stained with Fast Green. Red arrows mark previous fracture surfaces to which the consolidant was applied.

## 7. Experimental: Fracture Behaviour – Results and Discussion

appearance is unclear, although, it may be explained as a tide line caused by some of the additives contained in cold-liquid fish glue. Such additives include preservatives/bactericides (phenols), colour brighteners (titanium dioxide) and deodorising agents (Lee Valley Tools Ltd. 2007; Kremer Pigmente 2007a).

With respect to the discernibility of the bondline between the old fracture surfaces, the protein-based consolidants differed significantly. In the specimens consolidated with isinglass and hide glue the old fracture surfaces showed a near-perfect fit with no visible bondline. There was also hardly any indication of higher consolidant concentration at the interface of the old fracture surfaces (i.e. no visible bulk polymer) in the specimens consolidated with fish-glue and isinglass. However, faster gelation of the hide glue at room temperature may explain why this consolidant remained at slightly higher concentrations in the bondline than the isinglass (indicated by darker green appearance). The specimens consolidated with the cold-liquid fish glue showed old fracture paths that had either almost entirely re-opened and/or still contained many large, unfilled voids (Fig. 7.48a). In Figure 7.48b the typical voids and open fracture path are obscured by polishing dust, which appears whitish on the micrograph. Voids of this kind were not found to be present in the specimens consolidated with isinglass and hide glue.

These results support the previously reported data on the fracture behaviour of the DCB specimens. Clearly, the fish glue showed unsatisfactory  $G_{IC}$  results and almost 100 % failure between the re-adhered old fracture surfaces due to starvation of the bondline and/or the lack of bonding strength of the protein matrix. Consolidation with isinglass and hide glue approximately re-established the initial fracture properties of the specimens, because these polymers were not only similar to the original binder of the foundation, but they also penetrated relatively deeply and uniformly through the entire layer. The almost invisible bondline and the perfect fit of the fracture surfaces also suggested that no new interfaces were created by these consolidants. Hence, no signs were found to assume that abrupt changes in mechanical properties within the consolidated structure were to be expected.

**Starch- and protein-based consolidant (class I+)** The specimens consolidated with the starch/isinglass mixture showed a very uniform bondline between the old fracture surfaces, with  $d_{bl} = 10$  to  $20 \mu\text{m}$ . The bondline appeared to contain a relatively high concentration of isinglass, indicated by the dark green staining in Fig. 7.49b. Staining with iodine-potassium iodide ( $\text{I}_2\text{KI}$ , Lugol's solution) revealed that the starch fraction in the consolidant had entirely remained in the bondline between the old fracture surfaces, acting as an excellent gap-filler. Simultaneously, the starch served as a thickening agent for some of the isinglass (Fig. 7.49 a), which thus remained at higher concentrations in the bondline. These results confirmed previous research by Breidenstein (2000), who suggested that starch/isinglass-based consolidants formed a relatively thick adhesive layer underneath re-adhered lacquer flakes. Her findings were based on X-ray analysis

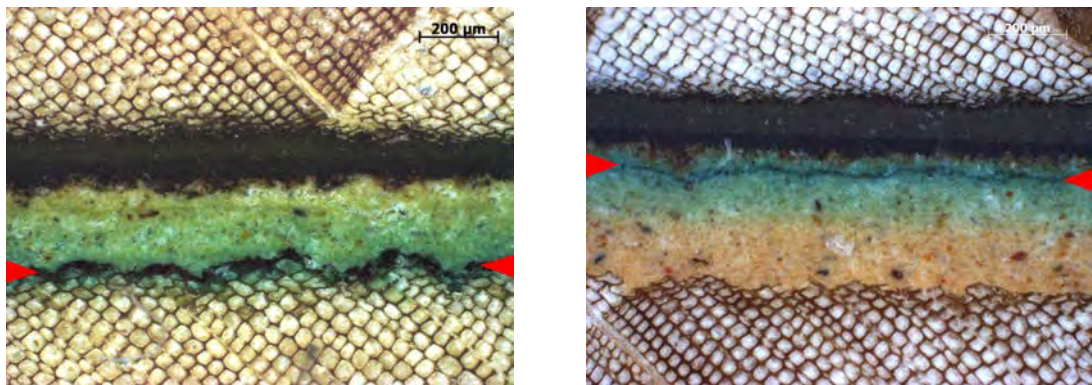


#### 7.4. Examination of DCB cross-sections

undertaken after the consolidant had been marked with iodine-containing contrast solution. In hindsight, however, this method was slightly limited in that it was not able to show the rather different penetration behaviour of the isinglass and starch fractions contained in the consolidant. The comparatively simple method of cross-section analysis and staining, which was used in the present study, clearly revealed that the isinglass had penetrated deeply into the foundation layer, achieving a similar distribution throughout the layer thickness as observed for the pure isinglass or bovine hide glue solutions. The starch on the other hand showed no penetration and remained consistently visible in the bondline.

These results clearly revealed the reason for the relatively higher fracture energy of the DCB specimens consolidated with starch/isinglass: whilst the isinglass penetrated and stabilised the foundation layer uniformly and almost through its entire thickness, the starch effectively bonded the two previous fracture surfaces. This efficient bonding was manifested in the lowest percentage of bondline failure (cf. Table 7.6). Lower levels were reached by the specimens consolidated with the *mugi-urushi* (which alongside *urushi* also contained wheat flour paste).

It can thus be concluded that the addition of starch to a protein-based glue increases the bonding ability between foundation fracture surfaces, the bondline thickness and the fracture energy in relation to the pure protein glue. At the same time, the starch does not significantly change or limit the penetration behaviour of the protein fraction. This is a useful finding, which may help to improve the performance of consolidants that so far display unsatisfactory properties. The cold liquid fish glue may be an example, as its specimens suffered from unacceptably low  $G_{Ic}$  and bondlines with poorly filled gaps which were starved of consolidant, when used at the concentration tested in this research.



(a) Bondline at wood/foundation interface, stained with Fast Green and  $I_2KI$  solution.

(b) Distribution of isinglass fraction stained with Fast Green (starch unstained).

Figure 7.49.: Cross-sections of type B DCB specimens consolidated with starch/isinglass. Red arrows mark previous fracture surfaces to which the consolidant was applied.

## Lacquer-based consolidants (class II and II+)

The cross-sectional examination of the specimens treated with the two lacquer-based consolidants confirmed the general knowledge about these consolidant formulations (Matsumoto and Kitamura 2008). Both the pure *ki-urushi* and the *mugi-urushi* diluted in hydrocarbon solvent penetrated to some extent into the porous foundation layer. In the foundation, penetration depths of between approximately 50  $\mu\text{m}$  and 170  $\mu\text{m}$  were recorded. They also appeared to vary depending on the amount and type of solvent used in the formulations. Penetration into the wood was limited to a maximum of 40  $\mu\text{m}$ . Typical examples for *ki-urushi* diluted with HAN 8070 are shown in Figures 7.50a–b. In this micrograph the solvent can be seen to have carried different fractions of the lacquer to varying extent into the foundation layer, indicating chromatographic effects. This appeared to be less the case with the *mugi-urushi* (Fig. 7.50c–d), which may have been due to the much faster evaporating solvent (Exxsol DSP 80-110) used in this instance. The two lacquer-based consolidants showed rather sharp tide-lines, suggesting the creation of new interfaces with significantly different mechanical properties. This was noted in almost all specimens.

Unsurprisingly, the gap-filling capacity of the diluted *ki-urushi* was rather poor. Also, all the specimens suffered from an unsatisfactory fit between the re-adhered old fracture surfaces. The specimens were hence left with many voids along the bondline, which can be seen in Figures 7.50a–b despite being slightly obscured by white polishing dust. If these findings are related to the fracture energy of 44  $\text{J}/\text{m}^2$ , which was only slightly below the value measured for unconsolidated foundation, it may be concluded that effective bonding only took place where the fracture surfaces were in close contact. Judged by the cross-sections, the level of contact appeared to be rather limited.

The *mugi-urushi* seemed to have variable gap-filling ability. In any areas where consolidant penetration was relatively deep (Fig. 7.50d), any voids between the old fracture surfaces were not effectively filled. In those areas with little penetration, fewer or no voids remained. The variable performance appeared to be primarily a result of the very fast evaporating solvent used (Exxsol DSP 80-100). Initially, dilution of the *mugi-urushi* was high (providing good penetration), whilst moments later the solvent had significantly evaporated, so that the consolidant was much more viscous upon application (hence working well as a gap-filler, but unsatisfactorily as a penetrant). A slower evaporating solvent, such as the HAN 8070 used for the *ki-urushi*, would have been a better choice in this instance.

Despite containing a wheat flour paste (starch) that efficiently bonded the fracture surfaces, the *mugi-urushi* did not increase the overall fracture energy of the consolidated specimens as much as the starch/isinglass mixture. This was mainly because second-phase fracture occurred in entirely unconsolidated areas of the foundation. The relatively high bonding strength achieved between the fracture surfaces after consolidation was attributed to the wheat starch paste.

#### 7.4. Examination of DCB cross-sections

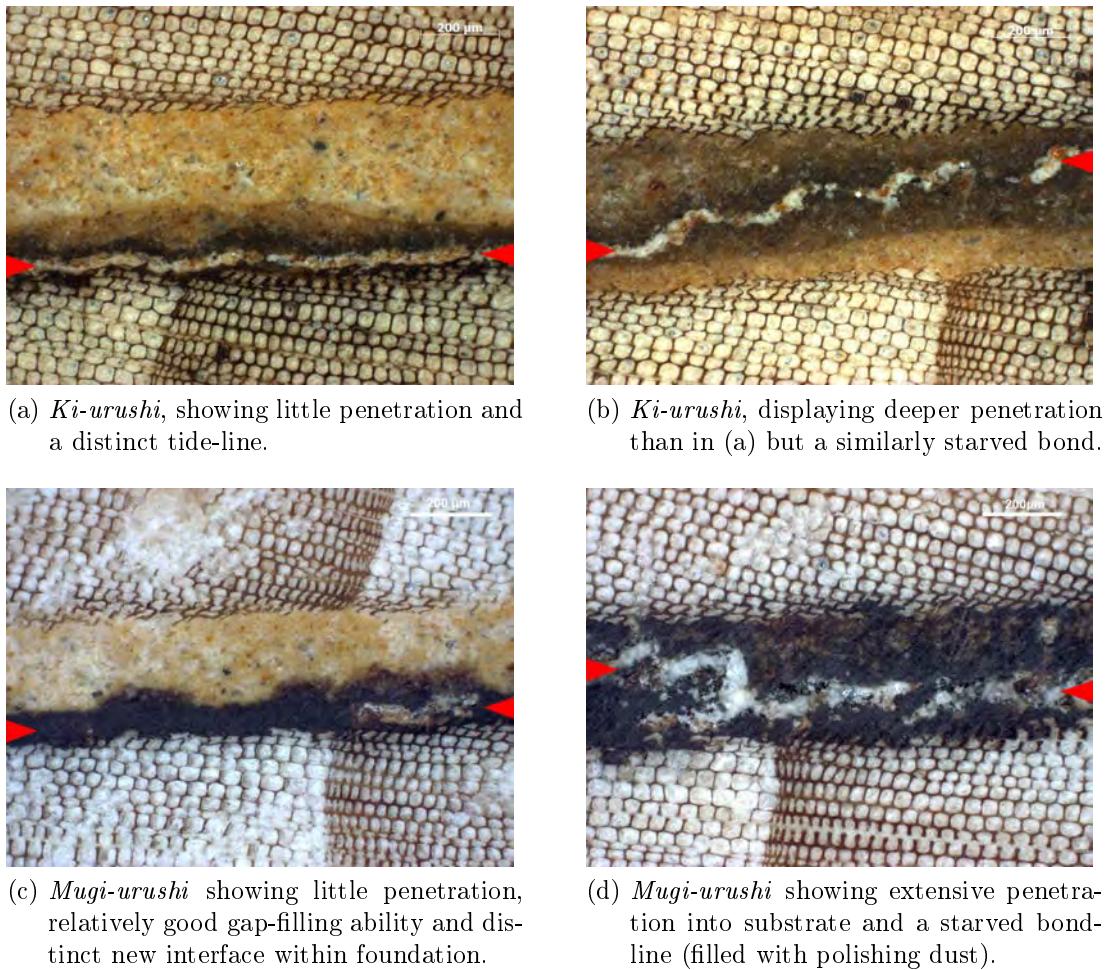


Figure 7.50.: Cross-sections of type A DCB specimens consolidated with traditional formulations based on East Asian lacquer.

Although the starch fraction could not be stained with Lugol's solution due to the very dark colour of the *mugi-urushi*, it was assumed that it had remained primarily within the bondline, as for the starch/isinglass mixture. However, unlike the isinglass, the *urushi* fraction had not penetrated as efficiently through the foundation layer, leaving significant parts of the foundation unconsolidated. Therefore, consolidation with the *mugi-urushi* had rendered specimen areas with very different mechanical properties, causing the specimens to fail largely in new and unconsolidated parts of the layer structure.

Overall, the two lacquer-based consolidants performed unsatisfactorily at the given formulations and concentrations. The HAN 8070 used for the *ki-urushi* was shown to be a more appropriate solvent to achieve slightly better consistency in penetration behaviour. The maximum penetration depths were however very similar for both formulations. The addition of wheat flour paste significantly improved the bonding ability between the fracture surfaces. It is thus conceivable

that alternative lacquer-based consolidant formulations may achieve a better balance between their penetration and the strengthening behaviour. However, these results also show that efficient bonding of fracture surfaces in conjunction with good consolidant penetration will most likely strengthen the consolidated material to a level well beyond its original strength. This might well induce other mechanical damage in its own right in the future.

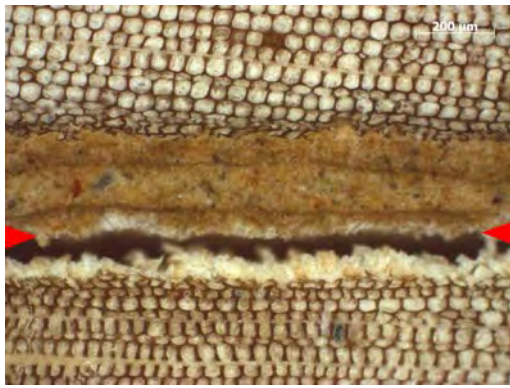
### Acrylate-based consolidants (class III)

**Acrylic solutions (class III a)** The acrylate-based consolidants dissolved in toluene (tol.), toluene/xylene (tol./xyl.) and acetone (ac.) showed very similar results in cross-section. These polymer solutions appeared to have penetrated very well into the foundation layer, extending over approximately between 50% (B 72 in acetone) and up to 100% (B 72 in toluene and B 48 N in tol./xyl.) of the entire layer thickness. In all specimens, the old fracture paths were clearly visible, as the polymer solutions had left large voids between the old fracture surfaces (Fig. 7.51). The pre-stained solution of Paraloid B 72 in acetone clearly suggested starvation of the joint: it had penetrated in such a way that the resin concentration was visibly lower along the old fracture path than further away from it (Fig. 7.51c). Despite these higher polymer concentrations in some areas, no abrupt and sharp new interfaces were identified. More distinct tide-lines produced by the consolidant and irregular polymer distribution were typically visible in all the specimens consolidated with Paraloid B 72 in toluene or B 48 N in tol./xyl. (Fig. 7.51a–b). Bulk consolidant located in the bondline was generally only noted in very few and restricted areas, such as the one shown in Figure 7.51b. The bridging of the resin seen in the image was caused by the staining process during cross-section examination. Exposure to the ethanol-containing dye induced the specimen to first swell and subsequently dry. This caused the bondline to open up, which consequently strained the softened consolidant. Polymer transport into the wood substrate could not be established for the non-polar solutions, because the staining method used was not ideal. It rendered the wood cells with remnants of stain and thus disguised any possible polymer deposition within the cells. The pre-stained Paraloid B 72 in acetone showed resin penetration into the wood by up to 40  $\mu\text{m}$  (cf. Table 7.7 on page 220).

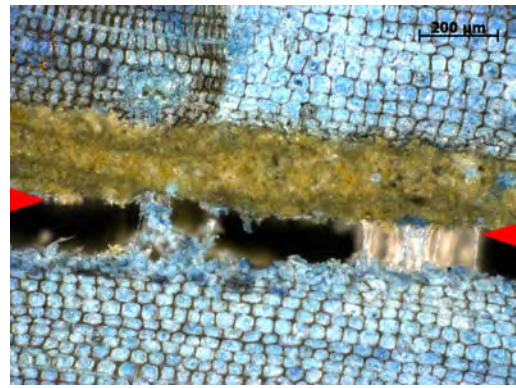
In the DCB specimens consolidated with the three acrylic solutions, the starved bondline was thus confirmed to have caused the low fracture energy values of less than 5  $\text{J}/\text{m}^2$ . This result was similar to that of the specimens treated with *ki-urushi*. It suggested that polymer solutions in hydrocarbon solvents at concentrations of up to 25% resin content generally penetrated so well into the porous foundation that insufficient consolidant remained between the fracture surfaces to provide effective bonding. Penetration of acrylates applied in solutions of aromatic hydrocarbons was almost complete, whilst acetone-based solutions penetrated only partially into the foundation layer. This difference was understood to be caused

#### 7.4. Examination of DCB cross-sections

by several factors: partly, the faster evaporation of the acetone which restricted polymer movement due to a faster increase in viscosity. Additionally, the polar acetone causes greater swelling of polar substrates, such as the protein-bound foundation layer and the wood (cf. Schniewind 1998). Therefore, it would be expected that this solvent reduced the polymer penetration in comparison with a non-polar solutions of the same polymer.



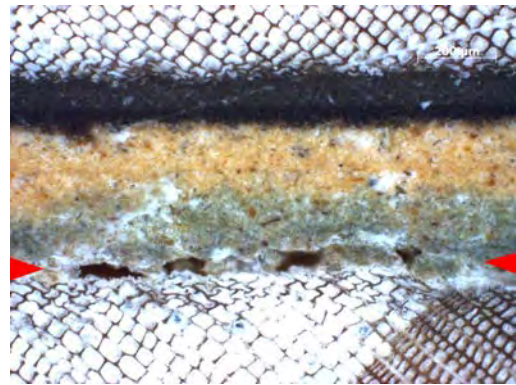
(a) Paraloid B 72 in toluene (type A); with characteristic tide-lines and irregular resin concentration in the centre of the layer and close to the wood interfaces.



(b) B 48 N in toluene/xylene (type A); after staining, showing similar non-uniform consolidant distribution as (a) and some consolidant bridging in the bondline.



(c) Paraloid B 72 in acetone (type B); showing visible old fracture path and a typical starved bondline, with higher concentration of consolidant away from the bond.



(d) Paraloid B 72 in acetone (type B); large voids are visible along the old fracture path and the consolidant has penetrated without creating sharp new interfaces.

Figure 7.51.: Cross-sections of specimens consolidated with acrylate-based consolidant solutions, partly stained with Solvent Blue G.

**Acrylic dispersion (class III b)** The results for the specimens consolidated with the acrylic dispersion Lascaux Medium for Consolidation (MfC) contrasted with those noted for the acrylic solutions. Lascaux MfC was very effective in filling voids within the joints, despite in some parts containing many small air-bubbles. Bondlines were generally relatively uniform at around 20-40  $\mu\text{m}$  and

## 7. Experimental: Fracture Behaviour – Results and Discussion

distinguishable from the surrounding foundation without staining (Fig. 7.52a). Staining with Solvent Blue G clearly increased the discernibility of the penetration depth of the polymer. It revealed that in some areas the consolidant had dispersed through the entire thickness of the layer, whilst in others it had penetrated less far. Typical penetration depths were measured to extend over around half the foundation layer thickness, i.e. up to approximately 160  $\mu\text{m}$  (Fig. 7.52b). Penetration into the wood substrate was minimal at below 20  $\mu\text{m}$ . In the foundation, the interfaces between the consolidated and unconsolidated areas appeared relatively pronounced in some parts of the specimens, whilst in others they showed a more gradual drift. It is therefore possible that zones with abrupt mechanical property changes were introduced into the specimens by the consolidant.

These results demonstrated similarities to those gained from the specimens consolidated with the starch/isinglass: both polymer formulations displayed excellent void-filling properties and  $\overline{G}_{Ic}$  values which were significantly higher than those of the specimens during initial fracture (cf. Table 7.7 on page 220). In the specimens treated with Lascaux MfC, almost half of the fracture paths had propagated through the bondline, and approximately a further 15% through new but consolidated parts of the foundation. Overall failure in consolidated areas was hence very similar to that recorded for the starch/isinglass, although a higher percentage of the Lascaux MfC specimens had failed within the bondline. This is an interesting finding as it demonstrates that acrylic copolymer dispersions, such as the Lascaux MfC, can achieve similar penetration, void-filling and fracture results to those of traditional two-phase consolidants like the starch/isinglass. The overall results for the Lascaux MfC also suggested that the properties of this acrylic dispersion may be optimised by a reduction of the polymer concentration through dilution with water. The penetration ability of the dispersion could thus be improved whilst the relatively high fracture energy values and the bondline thickness would be expected to be reduced.

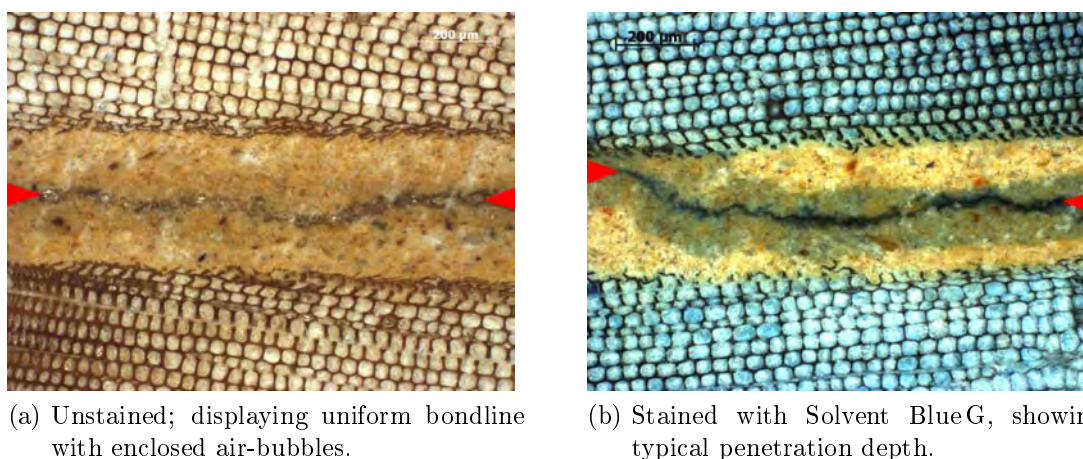


Figure 7.52.: Cross-sections of type A DCB specimens consolidated with the acrylate-based dispersion Lascaux Medium for Consolidation.

### Poly(vinyl alcohol) (class IV)

In the cross-section specimens consolidated with the Mowiol 3-83 the distribution of the consolidant was clearly visualised using Lugol's solution. This showed that the resin had penetrated typically between 20-250  $\mu\text{m}$  into the foundation. In terms of uniformity, it appeared not very different from the Lascaux MfC (cf. Table 7.7). However, in some locations the cross-sections displayed more pronounced interfaces between consolidated and unconsolidated areas. An example of this phenomenon before and after staining is presented in Figure 7.53. Staining also revealed that in most cases the consolidant had effectively filled the voids in the bondline between the old fracture surfaces (Fig. 7.53b), reaching typical bondline thicknesses of up to 20  $\mu\text{m}$ . Interestingly, the Mowiol 3-83 was the only consolidant tested that had fractured almost entirely within the consolidant in the bondline, despite having displayed effective bonding between the fracture surfaces and good gap-filling properties. This meant that the  $\overline{G}_{IC}$  values measured for the DCB specimens represented the best results that could possibly be achieved with this consolidant formulation.

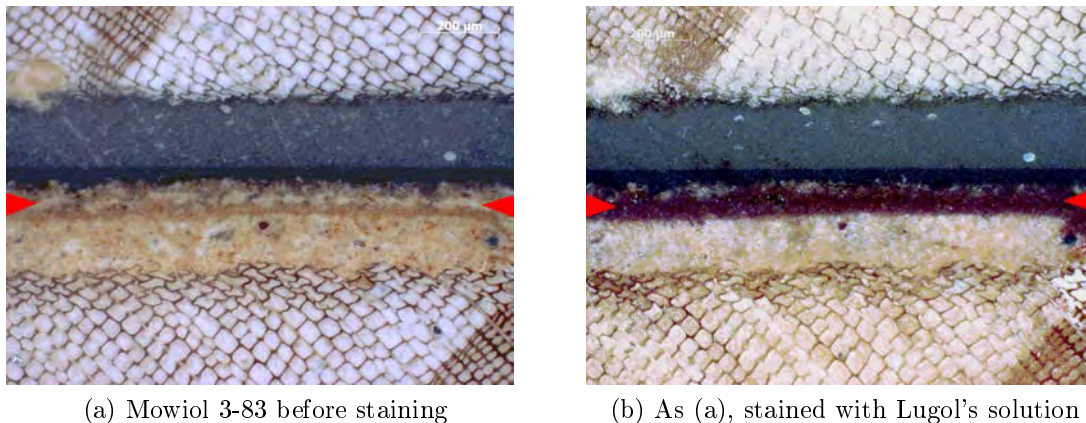


Figure 7.53.: Type B DCB cross-section specimen consolidated with the poly(vinyl alcohol) Mowiol 3-83.

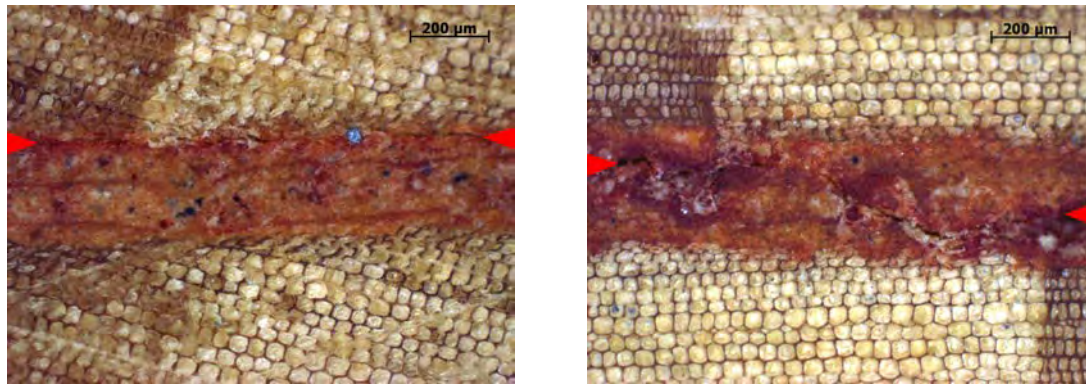
### Poly(vinyl acetate)-based consolidants (class V a and b)

The penetration performances of the poly(vinyl acetate) formulations showed differences between each other, which were similar to the ones noted between the acrylate-based solutions and dispersions described earlier. The Mowilith 50 dissolved in toluene penetrated similarly to the Paraloid-based solutions in aromatic hydrocarbons. It mostly dispersed very well through the entire layer thickness in a rather irregular manner, and created irregular tide-lines (Fig. 7.54a) and resin concentrations in areas where many cracks had interrupted the foundation layer (Fig. 7.54b). The joint between the old fracture surfaces was generally starved of

## 7. Experimental: Fracture Behaviour – Results and Discussion

consolidant, thus providing no effective bondline. Penetration into the wood was limited to below 50  $\mu\text{m}$ .

In contrast, the aqueous PVAc dispersion MowilithDMC2 proved to be a very efficient gap-filler despite its low solid content of 10 %. It filled even large irregular voids of up to 180  $\mu\text{m}$  width very effectively. However, penetration into the foundation layer was limited to about 30-50  $\mu\text{m}$  (Figs. 7.55), which were the lowest values measured for any of the tested consolidants. This meant that this polymer formulation served more as an adhesive at the bondline than as a consolidant for the porous foundation layer, even when highly diluted. The lack of penetration at this low solid content suggests that the polymer molecules in the dispersion were generally too large for the pore sizes of the foundation layer. Unfortunately, information on the molecular weight of the MowilithDMC2 was not available to confirm this. It was concluded that Mowilith DMC2 should be considered unsuitable as a penetrant for such layers.

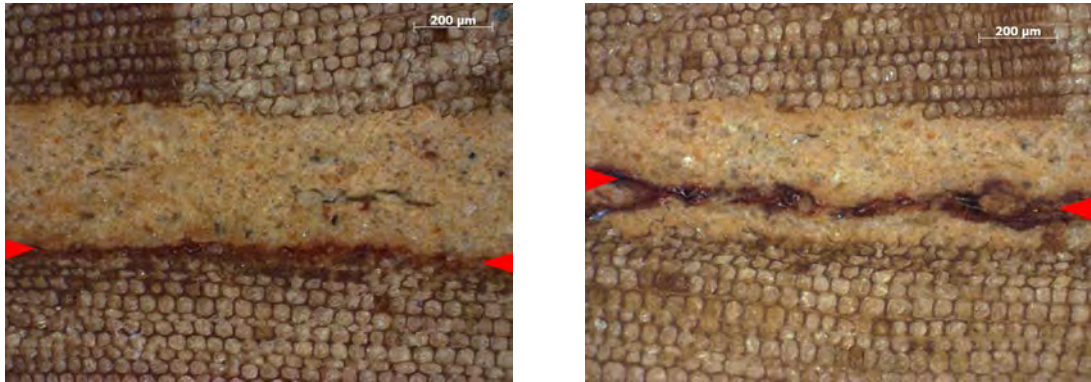


(a) Full penetration throughout the foundation layer and distinct tide-lines.

(b) Areas of higher consolidant concentration and voids along the old fracture surfaces.

Figure 7.54.: Type A DCB cross-sections consolidated with the poly(vinyl acetate) solution Mowilith 50 and stained with Lugol's solution.





(a) Thin and uniform bondline with very restricted penetration of the consolidant.

(b) Good gap-filling ability, a thick bondline and very little consolidant penetration.

Figure 7.55.: Cross-sections of type A specimens consolidated with the poly(vinyl acetate) dispersion Mowilith DMC2, stained with Lugol's solution.

## Summary of penetration behaviour

Table 7.7 summarises the results of the penetration behaviour of the consolidants, which were discussed in the previous section.

This Table clearly shows that the non-aqueous consolidants mostly displayed insufficient adhesive bonding between the fracture surfaces and thus failed as effective consolidants for fractured foundation layers. The protein-based consolidants that were applied as warm solutions, i.e. hide glue and isinglass, showed ideal properties in that they rendered the fracture surfaces of the foundation layer with perfect fit. This was achieved by the softening of the layer. Also, these consolidants did not develop visible bondlines consisting of bulk polymer that could adversely influence the uniform distribution of mechanical properties in the consolidated layer. The starch/isinglass mixture showed both deep penetration and a significant bondline due to its two-phase composition of dissolved protein and dispersed starch. The most efficient gap-fillers were the Mowilith DMC2 and the Lascaux MfC, which also achieved the highest fracture energy values. However, despite this similarity and the much greater dilution of the PVAc dispersion, the two dispersions showed disparate penetration behaviour.

## 7. Experimental: Fracture Behaviour – Results and Discussion

Table 7.7.: Summary of the penetration- and fracture behaviour of the consolidants. (Note that the results in the table suppose that the given consolidant is applied to the fragile foundation in a single application only.)

CLASS	CONSOL.	Solvent	CONC.	PENETRATION DEPTH			NEW	GAP-	$\overline{G}_{Ic}$	BLF
			$\phi$ [wt %]	$d_{bl}$ [ $\mu\text{m}$ ]	$d_{pf}$ [ $\mu\text{m}$ ]	$d_{pw}$ [ $\mu\text{m}$ ]	INTER- FACES	FILLING ABILITY		
I	Isinglass	water	10	n.a.	130–270	$\leq 50$	0	n.a.	53	75
I	Fish glue	water	22.5*	<i>starved</i>	100–200	$\leq 50$	+(TL)	<i>poor</i>	<i>8</i>	99
	Hide									
I	glue	water	10	n.a.	100–250	$\leq 50$	0	n.a.	48	80
I +	Starch/is.	water	13.3	10-20	130–270	$\leq 50$	0 / +	excellent	66	36
	Mugi-	Exxsol								
II +	urushi	80-100	(2:1)	?	50–170	$\leq 30$	++	variable	46	<i>21</i>
	Ki-	HAN								
II	urushi	8070	(2:1)	<i>starved</i>	50–170	$\leq 40$	+	<i>poor</i>	44	80
III a)	Par.B 72	tol.	25	<i>starved</i>	200–320	?	+(TL)	<i>poor</i>	<i>2</i>	100
III a)	Par.B 72	acet.	25	<i>starved</i>	100–200	$\leq 40$	0	<i>poor</i>	<i>4</i>	100
III a)	Par.B48N	tol/xy1	25	<i>starved</i>	200–320	?	+(TL)	<i>poor</i>	<i>3</i>	100
III b)	Lasc.MfC	water	25	20–40	100–160	$\leq 20$	0 / +	excellent	109	45
IV	Mow 383	water	25	10–20	60–250	?	0 / +	good	22	97
V a)	Mow. 50	tol.	20	<i>starved</i>	200–320	$< 50$	+(TL)	<i>poor</i>	<i>2</i>	100
V b)	M. DMC2	water	10	30–180	30 – 50	–	++	excellent	129	68

' $\phi$ ' gives the polymer concentration, where values marked with an asterisk (\*) refer to the solid content of the formulation given by the manufacturer.  $d_{bl}$  is the typical bondline thickness,  $d_{pf}$  the typical penetration depth in the foundation layer, and  $d_{pw}$  that in the wood substrate. Any '?' identifies results that remained unclear due to a lack in optical discernibility between the consolidant and its adjacent material. The column 'Interfaces' refers to whether new abrupt interfaces were introduced by the consolidant, ranging from no or minimally visible interfaces (0) to very pronounced ones (++). '(TL)' indicates that such interfaces were present as tide-lines. The columns denoted ' $\overline{G}_{Ic}$ ' and 'BLF' give the mean fracture energy and the extent of bondline failure. Results in *red italics* mark those properties that are the most undesirable for a consolidant used for foundation applied on wood.

### 7.4.2. Notes on the efficiency of the stains used

Generally, the visualisation of the consolidant distribution was most successful with the stains that were added to the liquid consolidant before their application to the DCB test specimens. Both the Fast Green and the Solvent Blue G used for the proteins and the Paraloid B 72 in acetone respectively provided visibly clear results. It was assumed that the stains had fully chemically bonded to the polymer without leaving excess stain molecules in the aqueous or solvent solutions that could have adulterated the true polymer distribution due to chromatographic effects within the specimens. Areas of high consolidant concentration appeared in more intense colour, whilst lighter colour shades of the stain indicated gradually lower concentrations (see Figs 7.48a,f; 7.49a-b and 7.51d).

Staining after consolidation, which had to be performed on the starch, some of the acrylates, the PVAL and PVAc formulations, proved to be more problematic. Firstly, embedding of the specimens into clear casting resin was absolutely vital, as all specimens swelled during stain application. Upon subsequent drying they were hence prone to breakage within the foundation layer or at its interface with the wood substrate. This effect was reduced by the embedding, even though fracture within the foundation layers occurred on several occasions nevertheless.

The Lascaux MfC was successfully stained with Solvent Blue G when present in bulk and when more finely dispersed in the foundation layer (Fig. 7.52b). However, the acrylate-based solutions of Paraloid B 72 and B 48 N stained less effectively and had to be kept in the staining bath for twice as long as the Lascaux MfC (cf. Section 6.3.2). Even after increased staining time, the dispersed consolidant was only faintly visible as darker shaded areas within the foundation layer (Fig. 7.51b). All the specimens that were stained after consolidation had to be lightly polished prior to visual examination, as in some areas bulk acrylic consolidant had leaked out of the cross-section plane. This excess polymer partly disguised the foundation layer and the stained, dispersed consolidant and therefore had to be removed.

The starch was stained quickly, easily and very clearly with Lugol's solution, which provided a blue-black appearance of the polysaccharide along the bondline (Fig. 7.49a). In the specimens consolidated with starch/isinglass, the two-stage staining routine worked well. Pre-staining of the isinglass showed the distribution of the protein, whilst complementary staining for starch clearly revealed the different distribution of the polysaccharide fractions of the consolidant.

The staining results for the PVAL and the PVAc, which were also undertaken with Lugol's solution, were more challenging to interpret. In general, Lugol's solution stained the PVAL in a very dark brownish-red and the PVAc in a lighter red to reddish-brown colour. However after drying, the Mowiol 3-83 and to a certain extent also the Mowilith DMC2 only clearly retained this colouration in the bulk polymer in the bondline. The stained polymer fraction that was dispersed in the foundation became almost invisible again, as its coloured appearance faded away

during drying (Figs 7.54c–d). Repeated application of Lugol’s solution increased the colouration of the polymer, but also caused the cross-section to swell increasingly and to fracture further upon drying. In the case of Mowiol 3-83, which remains water-soluble after drying, the PVAI leached out of the bondline once the cross-section was repeatedly exposed to the staining solution. Examination of these specimens under the optical microscope was therefore undertaken directly upon the application of Lugol’s solution before drying. The appearance of freshly stained Mowiol 3-83 is presented in Figure 7.53b.

### 7.5. Empirical evaluation of consolidants

Before drawing the final conclusions regarding the performance of the tested consolidants, the following section of this chapter briefly considers their handling properties. These were noted during the consolidation of DCB specimens and empirical tests involving the artificially-produced lifting lacquer sample boards. Empirical evaluation of the polymer formulations was desirable in order to gain a more complete picture of their differences and similarities encountered during practical conservation. The better conservators are able to understand whether and to what degree the handling properties translate into overall consolidant performance, the easier it will be in the future to choose an optimal consolidant for a specific purpose.

#### 7.5.1. Wetting and handling properties deduced from DCB specimens

Generally, all consolidants showed suitable wetting of the fracture surfaces upon application. Subtle differences were however observed for some formulations:

**Paraloid, Mowilith 50, *mugi-* and *ki-urushi*** The consolidants containing hydrocarbon solvents (i.e. Paraloid, Mowilith 50, *mugi-* and *ki-urushi*) showed instantaneous wetting of the wood and foundation surfaces and were mostly spread uniformly by a single brush stroke. Slight difficulties in the uniform spreading of the acetone and Exxsol-based formulations arose as these solvents evaporated very fast upon consolidant application. This increased their viscosity to such an extent that consolidant spreading and re-adhering of the fracture surfaces had to be executed very quickly.

**Lascaux Medium for Consolidation and Mowiol 3-83** Similarly efficient wetting was achieved by the Lascaux MfC and the Mowiol 3-83, although spreading of these formulation was much easier. The very good wetting properties were somewhat surprising as the other water-based formulations had displayed less

ideal performance. The good wettability of the foundation and wood surfaces by the Lascaux MfC was attributed to a small amount of non-ionic surfactants and solvent contained in the aqueous acrylic dispersion. These are specifically added by the manufacturer to promote wetting and uniform film formation (Hedlund and Johansson 2005). The aqueous solution of the pure PVAI resin owes its good performance to its chemical nature: Mowiol 3-83 has a relatively low molar mass of 14 000 (for comparison, pig gelatin has a molecular weight of  $\approx 110\,000$ ) and its molecules contain many polar hydroxyl ( $-\text{OH}$ ) groups. Both these properties promote good wetting and penetration ability of polar materials, such as wood or foundation (KSE Kuraray Specialities Europe 2002, Clariant 1999, p.G17).

**Isinglass, hide and fish glue, starch/isinglass** The protein-based formulations showed relatively good wetting, although the action of several brush strokes was required to spread the consolidants uniformly. This was necessary as otherwise some little air-bubbles remained entrapped between the foundation surface and the liquid consolidant film (particularly where the consolidant covered small voids that were contained in the fracture surfaces, such as the ones shown in Fig. 7.8 on page 160). In this group, the starch/isinglass mixture showed slightly better wetting than the isinglass and hide glue, whilst fish glue was marginally less easy to apply uniformly. The better performance of the polysaccharide/protein formulation could be explained by its higher solid content which resulted in a greater abundance of hydroxyl groups that have an affinity to polar surfaces. However, the verification of the exact reason for the slightly varying behaviour of the pure protein glues was beyond the scope of this research. Possible explanations include the varying chemical nature of the proteins and additives in the fish glue or variations in pH. It is known that pH has an effect on the surface tension of proteinaceous solutions, although its effect is somewhat inconsistent (Sauer and Aldinger 1939, Pitzen 1991).

**Mowilith DMC2** The wettability of the Mowilith DMC2 was adequate, but uniform spreading of the diluted aqueous dispersion required slightly more action of brush strokes to remove tiny bubbles trapped on the fracture surfaces. Technical data on Mowilith DMC2 is scarce, and again reasons for this less optimal wetting performance could not be established. Nevertheless, it can be safely stated that strong dilution of the Mowilith DMC2 from originally 50 % down to 10 % solid content does not render a dispersion with wetting properties as good as those of the Lascaux MfC. It may be presumed that this is partly caused by the relative reduction of surface active agents that are contained in the original, undiluted dispersion.

## Summary

Failing foundation layers are best wetted with consolidants that contain hydrocarbon solvents. These are closely followed by aqueous consolidants that contain small polymer molecules with polar side groups or additives such as surfactants. Pure protein-glues also work well, but may leave small areas unwetted unless spreading is aided with mechanical action, i.e. brushing motion. Strong aqueous dilution of polymer dispersions may be disadvantageous for achieving optimum wetting results. Furthermore, solvent evaporation from the consolidants containing Exxsol DSP 80-100 and acetone was found to be very fast and disadvantageous, as it increased the viscosity at inconvenient rate. Fast solvent evaporation rendered the consolidants difficult to spread uniformly on the fracture surfaces, unless they were applied in generous amounts.

### 7.5.2. Consolidation of lifting lacquer specimens

The consolidation and flattening of the artificially-produced lifting lacquer specimens under comparable conditions proved to be more difficult than anticipated. Due to the extremely limited number of test specimens available, which left only a single specimen for each consolidant, the most appropriate application method for each consolidant could not be established individually. This, however, would have been necessary to compensate for the diverse handling properties of the polymer formulations. Application was mostly influenced by the different evaporation rates of their solvents, but also by the very variable states of lifting of the coating reproduced on the sample boards. Some of the lifting areas would have required softening of the lacquer before they could be flattened. Others were sufficiently flexible and did not call for special treatment. Nevertheless, all consolidants were applied in a similar manner and at generous amounts. This aimed to facilitate softening of the lacquer and to prevent consolidant starvation within the bond. The consolidated layers on the specimen boards were left to dry in a shimbari frame pressed down with bamboo sticks according to the procedure described in Section 6.1.4 on page 142.

### Surface appearance

The use of one and the same application method for all test specimens is generally a necessary prerequisite for the comparability of test results. However, the method chosen in this study – unsurprisingly – rendered consolidated test specimens with very unsatisfactory appearance. In a real conservation application this appearance would have been unacceptable:

Generally, too much consolidant was applied on the specimens, causing the lacquer coating to soften excessively and to develop irregular and dimpled surfaces.

### 7.5. Empirical evaluation of consolidants

Two typical examples of the consolidated test specimens are presented in Figures 7.56a–b which clearly show this problematic appearance. To a certain extent, both the water- and solvent-based polymer formulations had induced this unwanted effect. However, no general trends could be established as to whether these effects were typical for a particular solvent, diluent or consolidant type. It was therefore concluded that the uniform application method used for flattening and consolidating the rather varied lifting lacquer layers on the test specimens was after all inappropriate. Neither did this preparation and treatment method produce very useful nor truly comparable test specimens. The attempt of further evaluating the consolidant performance by surface appearance was therefore abandoned.

However, despite the problems regarding the surface appearance, the specimens were nevertheless investigated in more detail to deduce some useful observations with respect to specimen shrinkage and consolidant failure.



(a) Specimen consolidated with Mowiol 3-83 in the areas towards the rear and the front end of the board.



(b) Test specimen consolidated with hide glue in the area of the upper half of the board.

Figure 7.56.: Lifting lacquer test boards after consolidation showing uneven appearance of the lacquer surface. (Board size 35 x 60 mm)

## Dimensional changes of coating and substrate

On all specimens it was noticed that after consolidation the coating was protruding by up to 1 mm over the edges of the wood substrate. This was only the case on those sides of the specimens that were cut parallel to the wood grain, and it was more predominant the larger the consolidated area of the previously lifting lacquer coating (Fig. 7.57a). The end-grain sides did not show any such protrusions (Fig. 7.57b). This suggested that the dimensional changes in the specimens were not caused by swelling and expansion of the coating induced by the introduction of water or solvent during consolidation. It was induced by shrinkage of the wood substrate during the production process of the lifting lacquer, i.e. during initial RH-cycling of the specimens. Indeed, it had been shown by Miura (2000) that urushi coatings show less dimensional change than Japanese cypress (*hinoki*) wood when exposed to RH changes. In the case of the lifting lacquer sample boards, the shrinkage of the wood substrate relative to its coating was increased, as the coating had lifted from the substrate during RH-cycling and thus did no longer pose any restraint for the wood. Subsequent wood shrinkage further increased the delamination of the coating. The example presented in Figure 7.58 clearly shows this phenomenon. The specimen with the coating protrusion of almost 1 mm (Fig. 7.57a) had substantially lifted before consolidation in exactly the respective coating location (seen in the right half of the image). At the same time, the wood did not show any shrinkage in the areas where the coating was still attached to the substrate. This was explained by the fact that the intact and well attached coating posed a restraint to the wood, which prevented the latter from excessive dimensional changes during cycling RH conditions and thus from developing large-scale permanent shrinkage.



Figure 7.57.: Back side of lifting lacquer specimen board consolidated with Lee Valley fish glue. The formerly lifting coating is protruding over the edge of the substrate (a), whilst the specimen sides along the end-grain show no such coating protrusion (b).



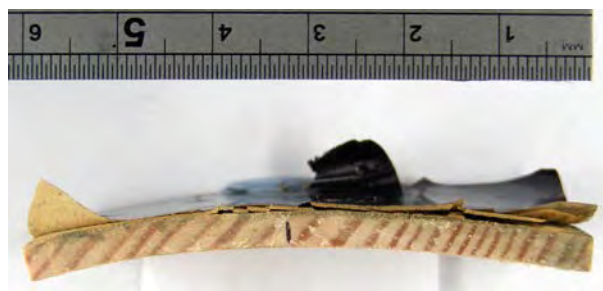


Figure 7.58.: Side view of lifting lacquer specimen shown in Fig. 7.57a before consolidation. A large area of the coating is lifting.

### Failure of consolidants during drying and RH-cycling

The main reason for cycling the lacquer boards after consolidation was to assess the polymers' ability to firmly secure the flattened flakes in their position. In other words it was tried to find whether the consolidants had a tendency to develop brittle failure or creep in changing environmental conditions. However, this assessment was difficult, due to the limited number of specimens available, the rather incomparable extent of lifting of the lacquer coatings, and the uneven surface appearance of the consolidated specimens. Therefore, only a few results could be deduced:

**Observation on firmly re-attached coatings** The specimens consolidated with isinglass, hide glue, fish glue, *ki-urushi*, Lascaux MfC, Mowiol 3-83, Mowilith 50 and Mowilith DMC2 all successfully flattened the lifting lacquer (*mugi-urushi* and the Paraloid solutions in toluene and tol./xyl. were not tested). The tested consolidants also stabilised the previously lifting areas well in their fixed position even after RH-cycling (including eight wet-dry cycles over a period of two months). No changes were recorded after the cycling. If present, any irregularities along the bondlines appeared to have been solely induced by the application method and by uneven pressing during drying. Problems with uneven pressing had occurred as some specimen boards were distorted in shape. The distortions had developed during initial cycling. It was clear that the pronounced curvature of some of the boards had prevented uniform pressure in some areas close to the edges of the panel ends, which resulted in some small gaps along the re-adhered fracture surfaces. Hence, the irregularities along the edges were clearly found not to be caused by later creep or failure of the consolidant.

**Observations on failed coatings** Only two specimens suffered failure of the adhesive bond between the re-adhered old fracture surfaces: firstly the one consolidated with Paraloid B 72 in acetone (other Paraloid-based formulations were not tested due to their poor performance in the DCB tests), and secondly, albeit to

## 7. Experimental: Fracture Behaviour – Results and Discussion

a much lesser extent, the specimen consolidated with Mowiol 3-83. Even though these specimens had been kept in the press for 7 days after consolidant application, re-lifting of the lacquer coating occurred shortly after removal from the press and during further drying at 53 % RH and room temperature (Fig. 7.59b). This failure however only affected selected areas of the previously lifting coating. In the Paraloid sample, the failed areas were the ones which had previously lifted the furthest away from the wood substrate. This can be seen in Figure 7.59a, which shows the specimen's state of lifting before consolidation. No additional or increased failure was observed during or after the RH-cycling.

**Failure of Paraloid B 72** Examination of the re-lifted coating using the optical microscope showed that consolidant distribution was similarly irregular as observed in the respective DCB specimens (Fig. 7.59c, and see Figs 7.29). Figure 7.59d further revealed that the consolidant had failed whilst developing very fine polymer bridges, which still remained visible on the rough fracture surfaces. This confirmed that the Paraloid had retained sufficient acetone solvent to display significant creep even after one week of clamping, and to cause failure of the bond. (Solvent retention in acrylic polymers has previously been discussed by Carlson and Schniewind (1990) and Hansen et al. (1991) amongst others.) Nevertheless, the remaining and successfully flattened areas of the coating suggested that it was still possible to apply the polymer solution in a manner that rendered the consolidation treatment effective. Thus, this example demonstrated again that application techniques during consolidation are as vital as the choice of polymer formulation in the first place. Some consolidants – even if they have the tendency to fail during drying – may actually be applied in a way that avoids their immediate failure.

Last but not least these observations also confirmed that the effect of consolidant migration towards the outer edges of the specimen was not only specific to the DCB specimens used in this study, but appeared to be the general behaviour of the Paraloid B 72 in acetone even under mimicked conservation applications.

**Stability of Mowiol 3-83** The Mowiol 3-83 sample had only shown some slight detachment of the re-adhered coating in the centre part of the specimen (cf. 7.56a). This failure, however, was not as significant as the one reported for Paraloid B 72. The slight detachment had solely occurred in areas of the specimen which had previously been difficult to consolidate, due to restricted accessibility with a brush. During consolidant application it was noted that consolidant uptake in these areas was very limited. Hence it was not surprising that further lifting occurred after specimen removal from the press. All other fracture surfaces that had been well accessed by the consolidant had remained stable even during RH cycling.

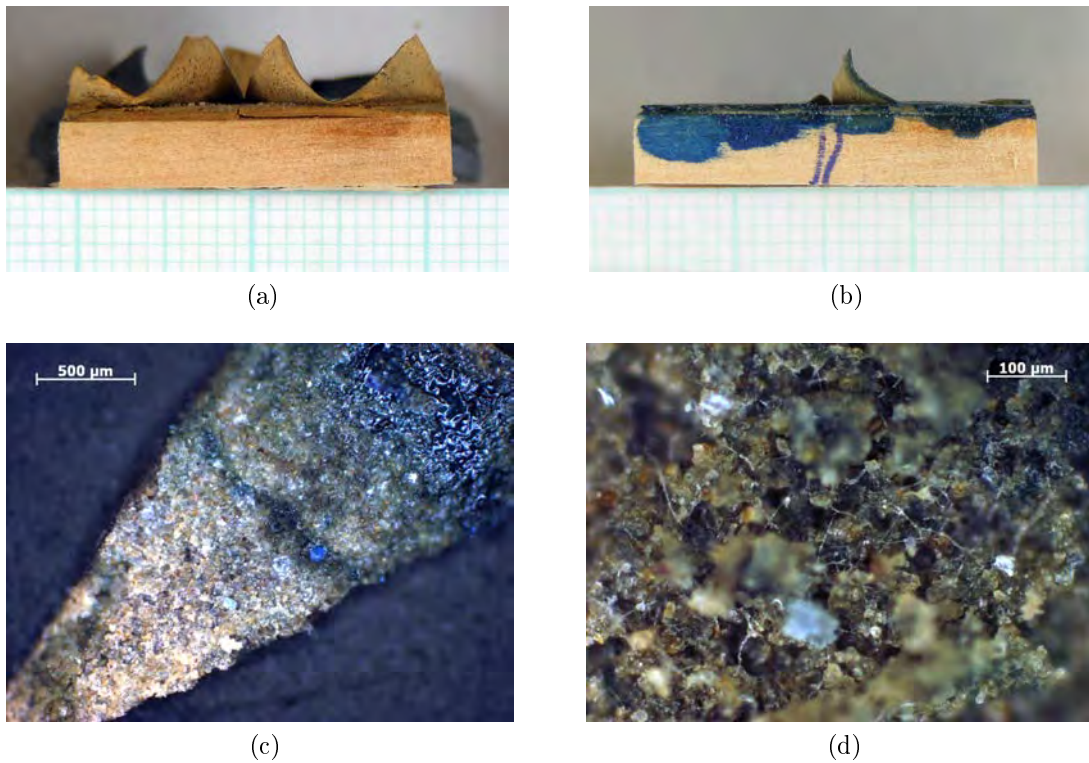


Figure 7.59.: Lifting lacquer specimen board (23 mm x 30 mm) consolidated with Paraloid B 72 in acetone (stained with Solvent Blue G). (a) Specimen before consolidation, and (b) after consolidation and 1 month drying (before RH-cycling). (c) Detail of the previously re-adhered flake (reverse side) that is shown to be lifting in (b). It reveals irregular consolidant distribution with higher resin concentration towards the outside edge of flake. (d) Detail from the lighter-coloured foundation area of the same flake with remnants of fine resin bridges that had developed during failure of the re-adhered/consolidated fracture surfaces.

## Summary

The empirical consolidation tests showed that all tested polymer formulations had sufficiently good wetting and handling properties to be used as possible consolidants. The solutions based on the solvents Exxsol 80-100 and acetone were less easy to apply due to very fast evaporation rates that rapidly increased the viscosity of the consolidants. For practical purposes, these solvents are therefore not ideal, unless used at lower resin concentrations. Principally, all tested consolidants were capable of stabilising previously lifting and re-adhered areas of the coatings flat in place. Only the specimen consolidated with Paraloid B 72 in acetone showed inconsistent bonding ability. Despite providing some effective bonding that remained intact even after the RH cycling, this consolidant displayed

## 7. *Experimental: Fracture Behaviour – Results and Discussion*

significant bond failure by fine bridging, i.e. cohesive failure of the consolidant induced by creep. Paraloid in other solvents was not tested on lifting lacquer sample boards and was thus not available for comparison. The two synthetic polymer dispersions Lascaux MfC and Mowilith DMC2, had rendered test specimens with stable bonds, despite having shown significant creep and consolidant bridging during the DCB fracture tests. It is assumed that failure was prevented mainly due to the well-filled bondlines and the high fracture energies which had been previously established.

Whilst this empirical test method generally showed that some useful information on consolidant behaviour could be gained, adjustments to this approach would be required if similar tests were to be undertaken again in the future. More meaningful and representative results on consolidant performance could be achieved if more specimens with simulated damage were available. In this way specimens could be chosen that show very similar areas of lifting, and generally more areas could be consolidated. This would enable a better understanding of whether a consolidant generally performs acceptably or not. As pointed out in Section 6.1.4 this would however require further research into the reliable manufacture of boards with lifting lacquer coatings. In this study, this manufacture had caused significant problems, and it was beyond the scope of the project to address this issue in more detail.

### **7.6. Discussion of experimental results and conclusions**

The observations made during and after the consolidation of the lifting lacquer samples confirmed again that the strengthening of such damaged multilayered coatings is a complex undertaking that involves the simultaneous control of many parameters. Choice of adhesive, solvent/diluent and concentration of the consolidant formulation are one set of factors that influence the success of the stabilisation treatment. The degree of lifting, the size of the area and the thickness of the delaminating layer are further parameters, and they matter greatly. Flakes that are hard and brittle and curl away from foundation layers or the substrate, must be softened and rendered compressible to facilitate flattening. To successfully achieve this, the direct softening action of a consolidant can be employed if carefully controlled. However, the tests on the lifting lacquer boards have shown that excess consolidant can easily cause extensive harm to the surface appearance. In such cases, multi-stage methods involving pre-softening – for example by raised RH or exposure to solvents and/or heat – would be a more appropriate choice. Suitable methods of coating softening and alternative ways of consolidant application are clearly a topic that would merit further research and practical experiments. Here, it would have gone beyond the scope of this work to address these issues in more detail.

Disregarding the problem of reversing the spatial distortion of the lifting coating, the main aim of this chapter was to investigate the behaviour of consolidants that may be used to stabilise fragile coating layers that are assumed to have relatively undistorted fracture surfaces. The consolidants have to serve two functions simultaneously: to re-adhere the flakes in the desired position and to strengthen the surrounding material structure. Effective stabilisation of a coating structure thus stands and falls with the ability to form a stable and sufficiently strong bond in the joint, and to restore or improve the cohesive strength of the weakened material. The experiments reported in this study have revealed the extent to which the tested consolidants were capable of achieving these requirements.

### 7.6.1. State of bondline and accuracy of joint fit

The DCB fracture tests and the cross-section analysis showed that the foremost problem with effective consolidation of delaminating coating layers is the lack of suitable fit between the two surfaces resulting from fracture. Several polymer formulations tested displayed undesirable fracture properties mainly because the joint between the re-adhered fracture surfaces was starved of consolidant (i.e. adhesive) and contained many unfilled voids. It is therefore essential that the consolidants used have either sufficient gap-filling ability or provide other means of improving the fit of the joint.

Two factors significantly improved the effectiveness of a bond and the accuracy of joint fit: firstly, the use of water-based polymer formulations and/or secondly, the presence of a sufficiently large consolidant fraction that remained on the fracture surfaces to fill any voids.

Except for the cold-liquid fish glue, which already failed under very small tensile loads most likely due to the chemical nature of its gelatin molecules, all the water-based consolidants showed overall effective consolidation results. This was not very surprising, as the presence of water caused the protein-bound foundation layers to swell and soften. Even though swelling is often not desirable during consolidation, as it induces additional stresses to the material and may lead to unevenness of the surface, this action does have great benefits: it generally enables better accuracy of fit between the fracture surfaces of protein-bound foundation. A near-perfect fit in the joints was thus noted for all water-based consolidants that were applied warm (isinglass and hide glue). In the cross-sections of these specimens, the original fracture surfaces could hardly be identified visually. Good fit was also achieved with the fish glue and the Mowiol 3-83.

In contrast, the non-aqueous polymer formulations (acrylics, PVAc and lacquer in ketone or hydrocarbon solvents) contained many voids between the old fracture surfaces. Whilst displaying hardly any efficient gap-filling and bonding ability due to starved joints, these polymer formulations only achieved unsatisfactory results.

## 7. Experimental: Fracture Behaviour – Results and Discussion

Significant accumulations of bulk consolidant (serving as an adhesive layer) were observed in several specimens. In these cases, irregularities in the joint were filled with polymer, which provided very effective bonds. During second-phase fracture, these specimens either showed relatively little failure within the bondline, or displayed higher fracture energies than during initial fracture. This behaviour applied to the specimens consolidated with the starch/isinglass mixture, *mugi-urushi*, Lascaux MfC, or Mowilith DMC2. The PVAc dispersion Mowilith DMC2 was most effective in filling any voids, as the polymer almost entirely remained in the joint. It thus served primarily as an adhesive between the fracture surfaces. Its penetration ability very limited. The Lascaux MfC, on the other hand showed much more effective penetration despite also forming an effective adhesive layer in the joint. It clearly showed that the acrylic dispersion contained polymer fractions that were able to penetrate deeply into the porous foundation layer, whilst some other fractions remained on the surface. From the point of view of fulfilling both effective adhesive action and good penetration ability, the Lascaux MfC showed almost ideal properties, albeit with too little failure within the bondline.

Consolidant formulations that contained more than one polymer phase clearly displayed outstanding properties. Examples for these were the starch/isinglass and the *mugi-urushi*. Both contained a starchy phase in addition to a protein solution or a lacquer emulsion, respectively. In both cases, the dissolved polymer penetrated deeply into the foundation, whilst the dispersed starch remained in the joint and contributed significantly to improved adhesion between the re-adhered surfaces. Of all consolidants tested, these two formulations showed the lowest extent of bondline failure. This was partly attributed to more efficient gap-filling properties of the starch and partly to improved adhesion due to a greater abundance of polar hydroxyl groups provided by the starch molecules. In contrast, both the diluted *ki-urushi* and the pure isinglass solution had not shown visible accumulation of bulk polymer between the re-adhered fracture surfaces. They had also failed to a much higher extent within the bondline. Therefore, if more reliable failure within the bondline were required for a specific task, the addition of starch-containing pastes to consolidants should be avoided.

### 7.6.2. Implications of Penetration Depth

Whilst the formation of an effective bond between the fracture surfaces is one prerequisite for effective consolidation, uniform consolidant application and penetration into the composite laminate are another. Any non-uniform distribution leaves the risk of creating new interfaces between consolidated and unconsolidated material with markedly different mechanical properties. In the tests reported in this work, the consolidants had shown rather varied penetration ability, not only amongst the different formulations, but more importantly also within single test specimens, i.e. for individual consolidants. This may have been partly due to the application technique of using a brush. Despite having applied generous amounts

of consolidant, non-uniform application can never be ruled out entirely. Special application techniques, such as vacuum infusion, might reduce this problem and could in some cases facilitate or at least encourage more efficient consolidant distribution. Nevertheless, brush application is one of the most common methods and hence it provided a realistic testing scenario. Even if the most suitable application techniques were employed, aged and damaged composite material may by itself still prevent ideal consolidant distribution. The fracture testing of the DCB specimens clearly showed that failure in the composite sometimes developed on several levels simultaneously. Despite the fracture path propagating in two locations parallel to each other, only one of these paths represented the principle failure locus. Any secondary path often merely remained as flaws and voids enclosed by material matrix. During consolidation, such flaws can remain inaccessible to a consolidant unless further damage occurs. The high likelihood of irregular consolidant penetration is therefore a problem inherent to the nature of deteriorated composite materials. In practice, ideal consolidation of these structures – be it on test specimens or on real objects – is unlikely. In this respect, the pre-fractured and consolidated DCB specimens constituted a very suitable representation of the situation encountered by conservators on real objects.

### 7.6.3. Level of strengthening and significance of $G_{Ic}$

The aim of stabilising a damaged coating layer beyond its original mechanical strength properties is generally to be approached with careful and critical consideration. This is particularly the case given the difficulties with achieving uniform consolidant penetration. In conservation, therefore, tough adhesives and consolidants are not necessarily desirable for many applications. If it is expected that new interfaces are introduced to a material inbetween unconsolidated and consolidated areas, then consolidants should be avoided which give rise to significantly higher fracture energies than that of the original material. They can induce new stresses in the composite, and potentially cause even further damage with time. Consolidants to which these characteristics may apply were the Mowilith DMC2, or the Lascaux Medium for Consolidation at the concentration tested in this study. Certainly the *mugi-urushi* is a problematic consolidant in this respect, which showed only negligible failure in consolidated areas of the specimen.

In many conservation-related cases, low toughness adhesives are deliberately chosen in view of this possible future damage to the object. This may somewhat be counter-intuitive to the more common expectations of engineers and material scientists, who usually try to improve the strength properties of materials by using stronger adhesives and more efficient bonding techniques. In conservation applications, failure is mostly preferred to occur in the same locations as before, i.e. within the bondline between the consolidated and re-adhered old fracture surfaces, rather than in previously undamaged areas of the original material. Such failure is best achieved with consolidants that allow fracture to occur at relatively low  $G_{Ic}$  values in the material they are applied to.

## 7. *Experimental: Fracture Behaviour – Results and Discussion*

From this point of view, a low fracture energy consolidant, such as the Mowiol 3-83, may indeed have desired properties for certain applications, where reliable bond-failure is required. The fracture tests showed that this PVAI's inability to restore the original fracture resistance of the test specimen ensured exclusive fracture in the bondline. Furthermore, the low fracture energy of the Mowiol3-83 bonds (which was lower than that of the unconsolidated foundation) implies that abrupt, great changes in mechanical properties are less likely expected at newly created interfaces between unconsolidated and consolidated foundation. The relatively limited penetration depth observed for this consolidant in some areas can therefore be considered unproblematic. Overall, Mowiol3-83 gave the most uniform results of all consolidants during fracture testing and showed very good wetting and handling properties. It thus appeared to be a very consistent stabilising agent, albeit one with only moderate strengthening ability. The empirical consolidation test on the lifting lacquer boards certainly showed that this polymer solution, if uniformly applied, was capable of successfully consolidating and re-adhering lifting lacquer coating and foundation of approximately 0.22 mm thickness. It even sustained exposure to RH cycling over two months.

Knowing the level of fracture energy at which a consolidated material fails does greatly help in choosing a suitable consolidant, although clearly, it cannot be the only criterion upon which a consolidant is chosen. It is rather required to make choices on the basis of the most appropriate balance of properties.<sup>1</sup> When tables are consulted that list consolidant properties (e.g. Tables 7.6, 7.7 and 7.8), other relevant aspects have to be kept in mind: for example whether an undesired property can be compensated for by other means and whether multiple treatments are possible. Sticking with the example of the Mowiol3-83, its rather low fracture energy could be altered by adding some Mowiol of higher polymerisation grade. Of all available Mowiol grades Mowiol3-83 has the lowest molecular weight at 14 000 (for comparison, pig gelatin  $\approx$  110 000) (Clariant 1999; Simon et al. 2003). It can thus be assumed that grades with a higher degree of polymerisation, i.e. higher average molecular weight, would improve the bond strength between the re-adhered fracture surfaces. Assuming that different fractions of Mowiol grades would penetrate to varying extent into the porous foundation layer (similar to the starch/isinglass), higher bonding strength could be achieved whilst retaining some degree of consolidant penetration. Considering the aspect of re-treatability and multiple applications, polymers with properties such as those of the Mowiol also have a further advantage. Mowiol3-83 is a recommended base for wood primers that provides a good key for subsequent paint coats of various compositions (Clariant 1999, p. G17). Polymers with such properties have the additional benefit of allowing future application of further consolidants, should they be required.

---

<sup>1</sup>Note that, as discussed earlier in this work, important properties such as the consolidants' chemical stability, aging properties and appearance were deliberately omitted from the present research in order to focus on the determination of mechanical properties and fracture behaviour.



### 7.6.4. Suitability of consolidants for protein-based foundations in lacquer coatings

The performance of the consolidants as adhesives between the fracture surfaces, penetrants and overall toughening agents is summarised in Table 7.8.

Table 7.8.: Summary of the consolidant performance for protein-bound foundations of East Asian lacquer coatings. (Note that the results in the table suppose that the given consolidant is applied to the fragile foundation in a single application only. The toughening effect refers to the performance of the entire specimen, rather than to an individual layer)

CLASS	CONSOLIDANT	SOLVENT	CONCENTR. [WT %]	EFFECTIVE ADHESIVE	EFFECTIVE PENETRANT	TOUGHENING EFFECT
I	Isinglass	water	10	✓	✓	0
I	Fish glue	water	22.5	x	✓	-
I	Hide glue	water	10	✓	✓	0
I +	Starch/isingl.	water	13.3	✓✓	✓	+
II +	Mugi-urushi	Exxsol 80-100	~ 46	✓	✓	0 (+)
II	Ki-urushi	HAN 8070	~ 46	✓	✓	0
III a)	Paraloid B 72	toluene	25	x	✓✓	--
III a)	Paraloid B 72	acetone	25	x	✓	--
III a)	Paraloid B 48N	toluene / xylene	25	x	✓✓	--
III b)	Lascaux MfC	water	25	✓✓	✓	++
IV	Mowiol 3-83	water	25	✓	✓	-
V a)	Mowilith 50	toluene	20	x	✓✓	--
V b)	Mow. DMC2	water	10	✓✓	x	++

Fields marked with '✓' and '✓✓' specify whether adhesive properties and penetration ability are good or very good, respectively. In the same columns, 'x' indicates the lack of effective adhesion or penetration. The toughening effect is distinguished by '0' (more or less unchanged), '+' (increased), '++' (much increased), '-' (reduced), and '--' are for starved joints which gave low  $G_{Ic}$  values under these conditions.

### Protein-based consolidants

Apart from the cold-liquid fish glue, the protein-based consolidants were shown to be very effective stabilising agents for the type of fragile foundation layer and lifting multilayered lacquer coating tested. Both isinglass and hide glue more or less restored the previous fracture properties of the foundation, whilst also penetrating relatively well and uniformly. Consolidation with the starch paste/isinglass mixture tended to result in slight increases in the fracture energy of

## 7. Experimental: Fracture Behaviour – Results and Discussion

foundation layers, but predominantly differed from the other two protein solutions in that it induced more failure in previously unfractured areas of the consolidated specimen. From the point of view of restoring the original fracture properties of protein-bound foundation layers, the common use of protein-based consolidants at a concentration of 10 % solid content generally appears to be an appropriate choice. Cold-liquid fish glue that is also commonly used for re-adhering lifting lacquer clearly displayed insufficient adhesive properties when diluted to half of its original solid content (22.5 %). It was found that the fish glue solution at this level of dilution does not sufficiently strengthen a delaminating export-type lacquer coating, despite having successfully re-adhered the coating of the replicated lifting lacquer boards and having sustained some RH cycling without bond failure.

### Lacquer-based consolidants

*Ki-urushi* diluted with a non-polar hydrocarbon solvent did not appear to have any mechanical advantage over a consolidation treatment with isinglass and hide glue solutions, both of which produced similar fracture surfaces and negligible changes in the fracture energy of the foundation. As opposed to the protein-based consolidants, *ki-urushi* displayed inefficient gap-filling ability, which explained the consistent failure in the bondline between the old fracture surfaces. The *mugi-urushi*, on the other hand, clearly acted as an effective gap-filler and adhesive, and thus solely induced fracture in unconsolidated areas of the foundation. As a consequence, no data could be gained on the increase in fracture energy within the consolidated areas. This implied that the areas of the specimen into which the consolidant had penetrated were significantly strengthened.

The use of lacquer-based consolidants has been a controversial choice for many conservators in the Western hemisphere. They may be a very good choice for lacquer-based foundations and layer structures that have an overall high lacquer content. However, for protein-based foundations this study showed that these consolidants had no mechanical advantage over other polymer formulations tested. Indeed, uniform consolidation with lacquer-based consolidants was shown to be difficult to achieve and they tended to create new, pronounced interfaces in the foundation. These can induce detrimental stresses to the structure in the future. In the case of *mugi-urushi* such stresses are likely to be higher than those induced by raw *ki-urushi*, as shown by Thieme (2001). Taking into account the insolubility of lacquer matrix after polymerisation, re-treatment will hardly be possible, in case it should be required in the future. The use of these consolidants for typical export-type lacquer coatings may after all not be the most appropriate choice.

## Acrylic and PVAc solutions

The Paraloid solutions and the Mowilith 50 in hydrocarbon solvents and ketone all fractured in the joint between the re-adhered fracture surfaces. As the joints appeared to have failed entirely due to consolidant starvation and lack of adhesive, no effective bonding was achieved. Subsequently, the fracture energy values measured were only those of the weak bond. Polymer penetration into the foundation layer was very successful for all these consolidants, although, no fracture data could be obtained for the consolidated areas. Hence, no true toughening effect could be established for these polymer solutions. The results strongly suggested that both the Paraloids and the Mowilith 50 solutions at the given concentrations are a problematic choice, when a lifting coating with protein-bound foundation is to be consolidated in a single application. Options for multi-stage applications might however be worth considering for further testing in the future, considering the excellent and good polymer penetration achieved with the non-polar and polar solutions respectively. In any case, solvent-containing polymer formulations show significant propensity for creep due to prolonged solvent retention. Consequently, they have to be clamped or pressed for much longer times than the water-based consolidants used in this study. Despite long clamping, bond failure between the re-adhered fracture surfaces remains a realistic problem, as was shown for the Paraloid B 72 in acetone. In wood consolidation, multi-stage applications with acrylic solutions have proven to be useful (e.g. Lencz 2005). However, it remains to be investigated in more detail whether successful application techniques can be found for these consolidants that render them useful for delaminating export-type lacquer coatings.

## Acrylic and PVAc dispersions

Both polymer dispersions tested showed large increases in fracture energy and significantly ductile behaviour of the bulk consolidant during crack propagation. Ductility was shown to decrease with drying time over several months, whilst the fracture energy increased significantly. Large  $G_{Ic}$  increases were shown for the Lascaux MfC and similar increases can be assumed for the Mowilith DMC2, too (the latter was tested after shorter drying time). Mowilith DMC2 had given the highest  $G_{Ic}$  values for all the type A specimens. Considering that the Mowilith dispersion hardly penetrated into the foundation layer, it cannot be regarded as a suitable consolidant for such material. However, the Lascaux MfC showed very good penetration, and film-forming ability in the bondline, making it a very efficient consolidant. The high fracture energy level that results from consolidation with this acrylic co-polymer may be disadvantageous in some cases, as it can strengthen parts of the material far beyond their original state, i.e. when it was new. On the other hand, this may be a desired property. Nevertheless, the performance of this dispersion might be improved if it were used at a lower solution concentration. Accumulation of bulk polymer in the bondline between

the fracture surfaces would most likely be reduced this way, whilst polymer distribution within the foundation layer could possibly be improved. Considering that it is recommended by the developer and manufacturer to dilute the Lascaux MfC (Hedlund and Johansson 2005; Lascaux 2007b), this consolidant promises to have very good properties at a lower solution concentration. Further testing of its fracture energy and overall fracture behaviour at diluted concentrations is therefore endorsed.

### 7.6.5. Remarks on the DCB test method

Overall, the test results have shown that the fracture mechanics approach is useful for analysing the mechanical performance of various consolidants for delaminating multilayered coating layers. The DCB method was suitable for replicating specimens that showed similar damage to that observed on real objects. At the same time, it provided baseline values of their fracture properties and overall fracture behaviour during initial testing.

Unsurprisingly, the retesting of the consolidated specimens gave more variable data than the initial testing. These resulted from more unstable crack growth caused by increased specimen inhomogeneity. This is the natural behaviour expected of a damaged, porous material that was stabilised with a consolidant by brush-application. For mechanical properties testing, the presence of such irregularities in both aged objects and test specimens usually implies that any data measured or collected will always show great scatter. This is why for most mechanical test methods large numbers of samples are required in order to render the measured data statistically valid. The great advantage of using a fracture mechanics approach and the DCB method for testing is that specimens can be tested twice; once to create the initial fracture damage, and a second time after the specimens were consolidated. The direct comparison between the same test specimens enables the direct evaluation of every single consolidant application. This simulates well the situation encountered when consolidating a fractured area on a real object. The results supply information of whether a specific consolidant application has worked or not, and why. Uniformity of the consolidation can be evaluated with the same specimens, because fracture is repeatedly observed over a long distance in a single specimen. A further advantage is that only very few test specimens are required by the standard test method, as a large number of data are gained from each specimen. In contrast, this is not the case for many conventional mechanical strength test methods, which usually only generate one value per test specimen. In the DCB tests, validity of the data is ensured by testing a set of minimum 4 specimens. Comparison between these specimens enables the evaluation of whether a consolidant acts consistently.

Instead of trying to perform elaborate statistical analyses on the measured data, it appeared much more useful and meaningful to establish whether a few trials were sufficient to achieve consistent results with regards to overall specimen behaviour

after consolidation. After all, this is one of the essential challenges of practical consolidation on real objects. A treatment is required to work, ideally with simple application and usually on limited and inhomogeneous areas. It was shown in this chapter that this aim was achieved by combining the DCB test method with the cross-section analysis and by adding some practical trials on replicated damaged coating structures. The tests undertaken revealed clear trends in the effects of polymer formulations on the fracture properties of the degraded and flawed composite specimens. Despite the scatter of the data, the information gained on well defined criteria – such as the independent material property fracture energy, the locus of failure and the penetration behaviour of the consolidant in the flawed structure – gives a greatly improved understanding of the consolidant performance in situ. This information can provide the means to choose and/or modify a suitable consolidant for a specific material.

### **Applicability of methodology for practical conservation**

Even though in this study most of the analysis was undertaken with sophisticated laboratory equipment, the presented test methodology has a wide scope for use even in more modestly equipped work environments.

DCB test specimens are relatively easy to manufacture and the fracture tests can be performed even without access to highly technical equipment: instead of employing a universal testing machine, DCB specimens can be fractured either by hand or using a simple construction that involves for example a bench vice, which is commonly available in many conservation studios. Fig. 7.60 shows a simplified model for a possible setup. The vice grips are equipped with holders for steel bolts (e.g. made from  $\geq 1$  mm thick sheet metal), which are used to mount the end blocks of the DCB specimen. Once mounted, the vice grips are gradually opened by turning the vice handle. Crack propagation on the specimen is observed using a loupe, whilst the displacement of the wood substrates can be measured with Vernier callipers. Even though fracture energy values cannot be precisely established in this way, the measured values for displacement to failure can be compiled. Larger displacement upon fracture implies a greater fracture energy of the failing specimen. From these data, relative differences in fracture energies can be estimated for different specimens. Furthermore, the overall fracture behaviour of the specimen may be observed. This reveals whether a crack develops rapidly, or in a steady and slow manner. Conservators can thus develop a comparative idea of the differences between the mechanical behaviour of the tested specimens. Whether or not crack length and displacement are recorded, the fracture surfaces in any case provide qualitative information about the exact location of the fracture paths. Also, information can be gained on whether the consolidants achieve a desired stabilising effect or not in the areas required.

Cross-section specimens cut from the ends of the DCB specimens prior to second phase fracture serve as a useful means for establishing the consolidant distribu-

## 7. Experimental: Fracture Behaviour – Results and Discussion

tion. To clearly reveal the presence of consolidant within the layer, the polymer formulations can be stained before application on the specimens. Alternatively, the entire cross-section specimen can be exposed to a stain bath. Either way, a simple light microscope with minimum  $\times 30$  (or better  $\times 50$ ) magnification will suffice in most cases to reveal helpful information on the consolidant distribution and the state of the bondline area between the re-adhered fracture surfaces. The Fast Green, Lugol's solution and the Solvent Blue G stains used for marking the consolidants were all shown to be sufficiently visible under the light microscope. Hence, this method of examination could dispense with the need for fluorescent microscopy.

Overall, the DCB method appears to be a very versatile and widely applicable test method that can be adapted without great effort and high expense for work bench application in conservation studios.

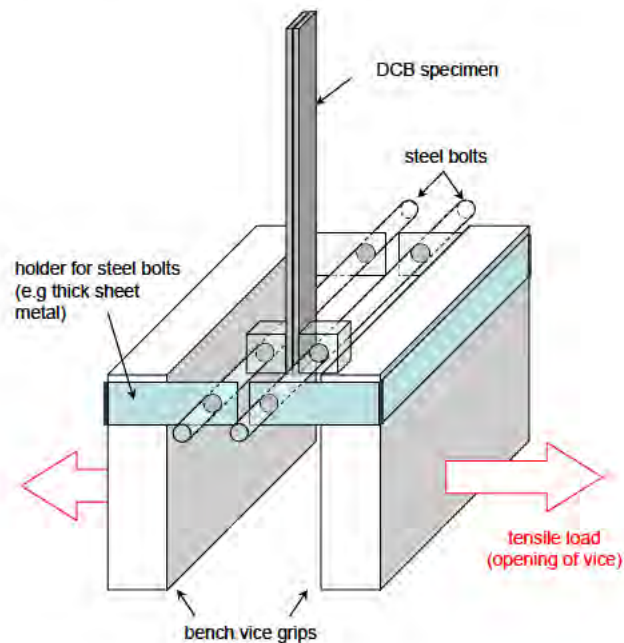


Figure 7.60.: Adapted DCB method using a simple bench vice.

### 7.7. Chapter summary

This chapter reported the results gained from both the fracture tests and the cross-section analysis of the DCB specimens, as well as from the empirical consolidation trials of the replicated lifting lacquer sample boards. Initial fracture of DCB specimens provided data on the independent material property fracture energy in mode I,  $G_{Ic}$ , of protein-bound foundation layers, and it was shown to

produce suitable test specimens for further consolidation tests. Typical  $G_{Ic}$  values for the foundation were measured at around  $47 \text{ J/m}^2$  and were established to be independent of the foundation layer thickness in the specimens. The test method was further demonstrated to be suitable for characterising and analysing the mechanical performance of consolidants that were used to stabilise the pre-fractured specimens. Changes in  $G_{Ic}$  were successfully measured for different specimens consolidated with polymer formulations based on proteins, lacquer, acrylics, poly(vinyl alcohols) or poly(vinyl acetates). Additional information on the mechanical properties of the material and the uniformity of the consolidation treatment were provided by a comparison between failure loci on the fracture surfaces, and the stability and rate of crack growth. The tests revealed measurable differences in the fracture behaviour of specimens treated with the consolidants, despite increased inhomogeneity in the consolidated specimens.

With respect to restoring the mechanical fracture properties of protein-bound foundation layers of export-type lacquer coatings, the most promising results were achieved by the isinglass and hide glue solutions. Addition of starch to isinglass strengthened the foundations as it provided very effective bonding in the joints. Mowiol 3-83 showed some degree of strengthening, but provided only half of the original fracture energy of the foundation in the bondline between the old fracture surfaces, thus inducing failure entirely in the bondline. All consolidants based on polymers dissolved in hydrocarbon solvents failed at very low loads in the bondline between the re-adhered old fracture surfaces due to consolidant starvation. They thus proved to be unsuitable for consolidating fractured foundation layers, when used in a single application at the given solution concentration. The lacquer-based consolidants restored the original toughness of the foundation in the bonded joint, however showed no mechanical advantage over the protein-based consolidants tested. Mowilith DMC2 and Lascaux MfC demonstrated very effective bonding between the re-adhered fracture surfaces. Furthermore they induced large increases in resistance to fracture in the foundation and at its interface with the wood. Mowilith DMC2 however is unsuitable for consolidation of the foundation layer due to the lack of penetration ability. Lascaux MfC showed very promising strengthening potential, but requires further investigation into its mechanical performance at lower solution concentrations.

The tests also showed that when dealing with inhomogeneous materials, such as lacquer coatings with protein-bound foundation layers on wood, it is of great advantage to use the same specimens for pre- and post-consolidation fracture tests. This facilitates direct comparison between individual specimens and significantly reduces the scatter of values measured for a complete specimen set. It also more realistically simulates the material behaviour on real-life objects. Suggestions of how the presented methodology can be adapted for use without access to sophisticated analytical equipment demonstrated the great potential of the fracture mechanics approach for the field of conservation.





## 8. Conclusions

The primary aim of this work was to investigate the mechanical performance of consolidants used for the stabilisation of delaminating and flaking multilayered decorative coatings on wooden substrates. A new systematic approach to consolidant testing was presented by considering the fracture properties of the least tough layer in this structure and the changes induced by selected consolidants. Using the example of East Asian lacquer coatings with gesso-type foundation layers, a comprehensive research methodology was developed. This started with the identification of the main fracture loci and failure causes for a group of badly damaged lacquer objects, and was followed by a discussion of the aspects that enable and influence their consolidation. Once the materials were selected for testing, suitable test methods were chosen for investigating the fracture properties of test specimens and the penetration ability of the consolidant. Dummy specimens with delaminated coating layers were produced to gain additional information on the handling properties of the consolidants, and to assess their performance in situ when applied to a structure that resembled a real object.

### 8.1. Failure causes in export-type lacquer coatings

To clarify which layers are most prone to failure, a small survey was undertaken, which examined East Asian lacquer objects that showed severe delamination and flaking coating layers. The layered structure of these coatings was revealed by cross-sectional analysis under the optical microscope. The binding media in the foundation layers were identified with the aid of chemical stains and optical microscopy under incident visible and blue light. A cross-check of the analysis results was performed using Fourier-transform infrared spectroscopy (Herm, 2009a) and pyrolysis-gas chromatography/mass spectrometry (Schilling, 2010a). The cross-check confirmed that analysis by optical microscopy in combination with chemical staining is a useful method for the identification of component binding media in export-type East Asian lacquer coatings. The results gave clear indications of typical failure types that occur in such coating structures, and helped to explain the probable causes of the deterioration mechanisms involved in the development of severe and progressive flaking. The group of objects most affected by this type of damage was shown to be export-type lacquer ware and more common-quality Japanese and Chinese lacquer objects. It was found that cohesive and some adhesive failure were the most prevalent failure types. Failure occurred predominantly at or near the interface of lower foundation layers which were bound

## 8. Conclusions

with a low lacquer concentration or cheaper surrogates. Most commonly, the binding medium of the failing layer was based on protein or starch. Changes in humidity clearly appeared to be the driving force for inducing fracture of these foundation layers, which hence resulted in the delamination of the multilayered coating structures.

## 8.2. Fracture behaviour of foundation layers

### 8.2.1. Initial fracture behaviour

The survey had specified East Asian export-type lacquer coatings with protein-bound foundation layers as the most susceptible to delamination failure. Based on the results, the fracture properties of unconsolidated and consolidated foundation layers were investigated. The standardised double cantilever beam (DCB) test method, used in fracture mechanics, was adapted and newly applied to determine the independent material property fracture energy,  $G_{Ic}$ , and the fracture behaviour of brittle, protein-bound (gesso-type) foundation layers on wooden substrates. Initial fracture of DCB specimens, which contained foundation and lacquer layers between wood substrates, successfully replicated fracture damage that had been observed on the objects of the survey. The initial testing provided base-line values for the fracture energy and the fracture behaviour of the test specimens. Furthermore, the fracture energy was shown to be independent of the foundation layer thickness used between the DCB substrates.

Once fractured, the specimens were consolidated with different polymer formulations. Twelve consolidants were selected from different polymer classes, including protein-based glues, East Asian lacquer, poly(vinyl alcohol), poly(vinyl acetates), and acrylates. Both solutions and dispersions of the polymers were included in the tests. The choice of the polymer, the solution/dispersion concentration and the solvent or diluent was based on common practice in the conservation of decorative coatings, as well as on their handling properties. The principal aim was to cover a wide range of consolidants which were thought to induce varying levels of strengthening on the test specimens. A few formulations were also included that were expected to perform not too dissimilarly to others of the same class. This was intended to test the scope of the DCB method, and whether this method was capable of distinguishing between the mechanical performance of test specimens consolidated with the various polymer formulations.

### 8.2.2. Fracture behaviour after consolidation

The re-fracture of the DCB specimens after consolidation provided data for direct comparison with those measured during initial testing. Measurable differences

induced by the consolidants could be established, despite an increased inhomogeneity within the consolidated layer. The latter was noted during second-phase fracture. Additional details on both the mechanical properties of the material and the uniformity of the consolidation treatment were gained by comparing the failure loci on the fracture surfaces and the stability and rate of crack growth produced during both test phases. Complementary information regarding the consolidant distribution and penetration ability was provided by cross-section microscopy of specimens cut from the DCB specimens. To visualise consolidant distribution, the polymers contained in the cross-section specimens were coloured with various stains (Fast Green, Lugol's solution and Solvent Blue G) and examined under visible light. The results on the consolidant distribution agreed well with the determined fracture properties of the DCB specimens.

With respect to restoring the mechanical fracture properties of protein-bound foundation layers of export-type lacquer coatings, the most promising results were achieved using the isinglass and hide glue solutions. Consolidant distribution within the foundation layers was uniform throughout the specimen. The addition of starch paste to isinglass solution increased the toughness of foundations that were consolidated with this mixture, as it provided improved adhesion in the joints. Mowiol 3-83 showed some level of strengthening, but provided only half of the original fracture energy of the foundation within the bondline between the old fracture surfaces. Hence, failure in these specimens occurred entirely in the bondline, despite the fact that the PVAI had only shown partial penetration into the foundation layer. All the consolidants based on polymers dissolved in hydrocarbon solvents (Paraloid and Mowilith 50) failed at very low loads within the bondline between the re-adhered old fracture surfaces. Penetration of these consolidants was ideal, but adhesive starvation occurred within the bondline, leading to exclusive failure in this location. These polymer formulations thus proved to be unsuitable for consolidating fractured foundation layers when used in a single application and at the given solution concentration. The lacquer-based consolidants restored the toughness of the bond in the joint, but showed no mechanical advantage over the protein-based consolidants that were tested. Uniform penetration was difficult to achieve, and the tested formulations tended to introduce areas with markedly different mechanical properties within the layer. Mowilith DMC2 and Lascaux MfC demonstrated effective bonding between the re-adhered fracture surfaces and induced large increases in resistance to fracture, both within the foundation and at its interface with the wood. Nevertheless, Mowilith DMC2 is considered unsuitable for the consolidation of the protein-bound foundation layer due to its lack in penetration ability. Lascaux Medium for Consolidation, on the other hand, showed very promising strengthening potential and polymer distribution within the specimens.

## 8. Conclusions

### 8.2.3. Advantages of test methodology

The DCB tests reported in this work further demonstrated that lacquer coatings with protein-bound foundation layers on wood are relatively inhomogeneous composites. When dealing with such materials, it was shown to be advantageous if the same specimens were used for pre- and post-consolidation fracture tests. This facilitates direct comparison between individual specimens and significantly reduces the scatter of values measured for complete specimen sets. Furthermore, the process of consolidation on real-life objects and subsequent material behaviour are more realistically modeled than in previous methods. To date, details of the mechanical behaviour of unconsolidated and consolidated coatings could not be easily and reliably obtained by conservators. The proposed application of the fracture mechanics approach offers a mechanical test method that can provide these data. In addition, the method can be adapted for use without access to sophisticated analytical equipment, and hence has great potential and wide scope for use in the field of conservation. The presented test methodology promises to be a significant step towards a better understanding of the fracture behaviour of fragile coatings and the strengthening potential of consolidant formulations.

### 8.3. Future Work

The investigations into the mechanical properties of consolidants reported in this work have demonstrated that the methodology used can give vital and new information on the fracture behaviour of consolidated coating layers. Furthermore, they are a valuable starting point for further research in a field that still poses many unanswered questions.

#### Choice of consolidants

It was beyond the scope of this work to test more than twelve different polymer formulations at more than one specific concentration. However, the test results suggested that alterations to the formulations of some consolidants might improve their physical and mechanical performance when acting as stabilising agents for fractured foundation layers. Modifications to some of the tested consolidants would hence be useful to investigate. Additionally, other polymers that have been employed successfully for the consolidation of flaking lacquer coatings or similar materials in the past should be considered. These include for example other poly(vinyl acetates), poly(vinyl butyrals) or cellulose ethers. Particular attention should be paid to the performance of consolidant formulations at different polymer concentrations and viscosities. These parameters are known to have significant effects on the penetration behaviour of some polymers, and thus also significant repercussions for the fracture properties of the stabilised material or structure.

## Fracture energy of consolidated layers

The fracture energy values reported in the graphs and tables of the results section were based on overall results for an entire specimen. No distinction was made whether or not the specimen had fractured in consolidated or unconsolidated regions of the layer structure. Hence, true fracture energy results had to be put into perspective by considering the loci of the fracture paths. In addition, several specimens failed entirely within bonds that were starved of consolidant/adhesive, where the measured fracture energy was only that of the insufficiently bonded joint. Consequently, no information was gained on the toughness of those areas which were actually well penetrated by the consolidants (and thus assumed to be stabilised). Further DCB tests are required to understand the level to which consolidants such as the Paraloid solutions change the fracture energy of a stabilised layer, and how they could perform in a multi-stage application. The latter would involve firstly stabilisation of the porous layer through effective penetration, and secondly re-adhering of the fracture surfaces. Following this approach, modified test specimens and test series could be developed that would ensure fracture in either purely consolidated areas or within bulk consolidant in the bondline between fracture surfaces. In this way, the ability of the consolidants to strengthen a porous material and to bond two fractured surfaces could be investigated separately. The fracture energy of standard materials commonly used in conservation could thus be compiled in a database, which in the future could help conservators choose consolidants by their fracture properties.

## Improvements for adapted DCB method for bench applications

The simplified DCB test set-up proposed in Section 7.6.5 for bench application in conservation studios could also be further improved. To render the test setup most useful for consolidant evaluation, it would be helpful if this method were combined with independently established data that relate the measured displacement and crack length with the resulting fracture energy. Using standardised materials and substrates, a look-up table could be compiled that would allow a rough estimate of the fracture energy to be read off for any known displacement and crack length.

## Replication of lifting lacquer

The replication of dummy-specimens with lifting lacquer coatings in a reproducible manner was shown to be difficult to achieve. The exact failure mechanisms that were experienced by the coating of the sample boards are still not fully understood, and hence reliable manufacture of useful specimens was unsuccessful in this work. However, the testing of potentially suitable consolidants on dummy-specimens with lifting lacquer coatings was shown to contribute valuable

## 8. *Conclusions*

information on their handling properties and fracture behaviour. Therefore, more research is encouraged in this field, to find a more reliable reproduction method for lifting coating layers on sample boards. Moreover, the controlled application of consolidants on such dummy specimens merits further investigation, in order to find ways to alleviate problematic side-effects encountered during the consolidation process, such as the over-softening of coating layers.

### **Interlaminar failure**

This work concentrated on determining the fracture energy values that can be achieved by individual consolidants, once they are applied to a fragile material. However, it was beyond the scope of this study to investigate the magnitude and nature of the forces that the coating on a real object is exposed to, which can lead to its failure. To relate these forces to the fracture energy values achieved by the consolidants, the forces exerted on each individual layer need to be understood. A parametric study can be conducted to investigate the various environmental factors responsible for failure, and the corresponding effects on the stress/strain behaviour of the materials. Therefore, if one quantifies the forces that the fragile layer has to sustain, then truly informed choices can be made on an ideal consolidant that will effectively strengthen the fragile composite to a level that is required for the prevention of further damage.

# References

- K.W. Allen. Adhesion and adhesives - some fundamentals. In N. Brommelle, E.M. Pye, P. Smith, and G. Thompson, editors, *Adhesives and Consolidants. Preprints of the contributions to the Paris Congress, 2-8 September 1984*, pages 5–12, International Institute for Conservation, London, 1984.
- Amstel-Products. Product information for technical gelatin / hide glue. url <http://www.amstelproducts.nl/technicalgelatin.html>. Last accessed Feb. 2007.
- T.L. Anderson. *Fracture Mechanics – Fundamentals and Applications*. Taylor and Francis, Boca Raton/London/New York, 3rd edition, 2005.
- E.H. Andrews and A.J. Kinloch. Mechanics of adhesive failure I. *Proceedings of the Royal Society of London. Series A, Mathematical and Physical Sciences*, 332(1590):385–399, 1973a.
- E.H. Andrews and A.J. Kinloch. Mechanics of adhesive failure II. *Proceedings of the Royal Society of London. Series A, Mathematical and Physical Sciences*, 332(1590):401–414, 1973b.
- B. Appelbaum. Criteria for treatment: Reversibility. *Journal of the American Institute for Conservation*, 26(2):65–74, 1987.
- M.F. Ashby and D.R.H. Jones. *Engineering Materials 1. An Introduction to their Properties and Applications*. Butterworth-Heinemann, Oxford/Auckland/Boston..., 2nd edition, 1996, reprinted 2001.
- J. Ashley-Smith and H. Wilks, editors. *Science for Conservators 3: Adhesives and Coatings*. Conservation Unit of the Museums & Galleries Commission/Routledge, London/New York, 1987.
- ASTM D5528:94a. Standard test method for mode I interlaminar toughness of unidirectional fibre-reinforced polymer matrix composites. ASTM International, West Conshohoken, 1994.
- ASTM D790 M. Standard test method for flexural properties of unreinforced and reinforced plastics and electrical insulating materials [metric]. ASTM International, West Conshohoken, 1993.
- M.G. Bader, I. Hamerton, J.N. Hay, M. Kemp, and S. Winchester. Double cantilever beam testing of repaired carbon fibre composites. *Composites Part A: Applied Science and Manufacturing*, 31:603–608, 2000.
- G. Banik and G. Krist, editors. *Lösungsmittel in der Restaurierung*. Verlag Der Apfel, Wien, 1984.

## References

- G.A. Berger. Testing adhesives for the consolidation of paintings. *Studies in Conservation*, 17:173–194, 1972.
- G.A. Berger and W.H. Russell. Investigations into the reactions of plastic materials to environmental changes. Part 1. The mechanics of the decay of paint films. *Studies in Conservation*, 31(2):49–64, 1986.
- G.A. Berger and W.H. Russell. An evaluation of the preparations of canvas paintings using stress measurements. *Studies in Conservation*, 33:187–204, 1988.
- G.A. Berger and W.H. Russell. Interaction between canvas and paint film in response to environmental changes. *Studies in Conservation*, 39:73–86, 1994.
- G.A. Berger and H.I. Zeliger. The procedure of developing an adhesive for paintings: the importance of valid tests. In Norman Brommelle, Elizabeth M. Pye, Perry Smith, and Garry Thompson, editors, *Adhesives and Consolidants. Preprints of the contributions to the Paris Congress, 2-8 September 1984*, pages 13–17, International Institute for Conservation, London, 1984.
- S. Bistac and J. Schultz. Study of solution-cast films of PMMA by dielectric spectroscopy: influence of the nature of the solvent on  $\alpha$  and  $\beta$  relaxations. *International Journal of Adhesion and Adhesives*, 17(3):197–201, 1997.
- B.R.K. Blackman and A.J. Kinloch. Fracture tests for structural adhesive joints. In D.R. Moore A. Pavan and J.G. Williams, editors, *Fracture Mechanics Testing Methods for Polymers, Adhesives and Composites*. Elsevier Science, Amsterdam, 2001a.
- B.R.K. Blackman and A.J. Kinloch. Linear-elastic fracture-mechanics (LEFM) test protocols download: DCB (LB) Spreadsheet (Excel). URL <http://www3.imperial.ac.uk/meadhesion/testprotocols/lefm>, 2001b. Last accessed 15 Nov. 2008.
- B.R.K. Blackman, J.P. Dear, A.J. Kinloch, and S. Osiyemi. The calculation of adhesive fracture energies from double-cantilever beam test specimens. *Journal of Materials Science Letters*, 10:253–256, 1991.
- B.R.K. Blackman, J.P. Dear, A.J. Kinloch, H. MacGillivray, Y. Wang, J.G. Williams, and P. Yayla. The failure of fibre composites and adhesively bonded fibre composites under high rates of test. Part I: Mode I loading - experimental studies. *Journal of Materials Science*, 30:5885–5900, 1995.
- B.R.K. Blackman, A.J. Kinloch, M. Paraschi, and W.S. Teo. Measuring the mode I adhesive fracture energy,  $G_{Ic}$ , of structural adhesive joints: the results of an international round robin. *International Journal of Adhesion and Adhesives*, 23:293–305, 2003.
- F. Bonanni. *Techniques of Chinese Lacquer - The classic eighteenth-century treatise on Asian varnish*. F. Perugini, translator/editor. The J. Paul Getty Museum, Los Angeles, 1720/2009.



- S. Bradley. Strength testing of adhesives and consolidants for conservation purposes. In Norman Brommelle, Elizabeth M. Pye, Perry Smith, and Garry Thompson, editors, *Adhesives and Consolidants. Preprints of the contributions to the Paris Congress, 2-8 September 1984*, pages 22–25, International Institute for Conservation, London, 1984.
- L. Bratasz, R. Kozlowski, A. Kozłowska, and S. Rivers. Conservation of the Mazarin Chest: Structural response of Japanese lacquer to variations in relative humidity. In J. Bridgland, editor, *Preprints of the ICOM-CC 15th Triennial Meeting, New Delhi, 22-26 September 2008*, volume 2, pages 1086–1093, Allied Publishers, New Delhi, India, 2008.
- I. Breidenstein. Konzeptionelle Überlegungen zur Restaurierung eines Chinesischen Lackparavents. In M. Kühenthal, editor, *Japanische und Europäische Lackarbeiten/Japanese and European Lacquerware*, pages 561–585. Arbeitshefte des Bayerischen Landesamtes für Denkmalpflege 96. Lipp, München, 2000.
- I. Breidenstein. ‘Sawed, divided, cut, cleft and split asunder’: Eighteenth-century Chinese export lacquer screens in Europe - two restoration cases. In P. van Duin and H. Piena, editors, *The Meeting of the East and West in the Furniture Trade, Proceedings of the 6th International Symposium on Wood and Furniture Conservation*, pages 59–64, Stichting Ebenist, Amsterdam, 2002.
- Z. Breu and S. Miklin-Kniefacz. Bericht zur Restaurierung des Lackparavents aus dem Napoleonzimmer Schloss Schönbrunn, Wien. In S. Miklin-Kniefacz, editor, *Zur Restaurierung der Vieux-lacque-Tafeln in Schönbrunn: Grundlagen und Vorarbeiten*, Wissenschaftliche Reihe Schönbrunn, pages 7–13. Schloss Schönbrunn, Wien, 1995.
- A.J. Brunner, B.R.K. Blackman, and P. Davies. A status report on delamination resistance testing of polymer-matrix composites. *Engineering Fracture Mechanics*, 75(9):2779 – 2794, 2008.
- BS 7991. Determination of the mode I adhesive fracture energy  $G_{Ic}$  of structural adhesives using the double cantilever beam (DCB) and tapered double cantilever beam (TDCB) specimens. BSI, Teddington, 2001.
- BS EN ISO 10365. Adhesives – designation of main failure patterns. BSI, Teddington, 1995.
- BS EN ISO 527-1. Plastics - determination of tensile properties - Part 1. General principles. BSI, Teddington, 1996.
- BS EN ISO 527-3. Plastics - determination of tensile properties - Part 3. Test conditions for films and sheets. BSI, Teddington, 1996.
- BS EN ISO 844. Rigid cellular plastics - determination of compression properties. BSI, Teddington, 2009.
- V. Bucur. *The Acoustics of Wood*. Springer Verlag, Berlin/Heidelberg, 2006.

## References

- A. Buder and S. Wülfert. Herstellung und Auswertung von Dünnschliffen im Rahmen kunsttechnologischer Untersuchungen. *Zeitschrift für Kunsttechnologie und Konservierung*, 11(1):83–96, 1997.
- W.D. Callister, Jr. *Material Science and Engineering - An Introduction*. John Wiley & Sons, New York/Chichester/Weinheim, 5th edition, 2000.
- CAMEO. Conservation and Art Material Encyclopedia Online, 2009. Database entry for Paraloid B48N. URL <http://cameo.mfa.org/index.asp>. Last accessed 11 Aug. 2010.
- S.M. Carlson and A.P. Schniewind. Residual solvents in wood-consolidant composites. *Studies in Conservation*, 35:26–32, 1990.
- Center for Wood Anatomy Research. Technology Transfer Fact Sheet: Pinus strobus. Online database. URL <http://www.fpl.fs.fed.us/documnts/TechSheets/SoftwoodNA/htmlDocs/pinusstrobusmet.html>. Last accessed 14 April 2011.
- S. Chapman and D. Mason. Literature review: The use of Paraloid B72 as a surface consolidant for stained glass. *Journal of the American Institute for Conservation*, 42(2):381–392, 2003.
- W.T. Chase. Lacquer examination and the treatment at the Freer Gallery of Art: Some case histories. In N.S. Brommelle and P. Smith, editors, *Urushi - Proceedings of the Urushi Study Group, 10-27 June 1985, Tokyo, Japan*, pages 95–111, The Getty Conservation Institute, Marina del Rey, California, 1988.
- W.T. Chase, P.R. Jett, S.P. Koob, and J. Norman. The treatment of a Chinese red lacquer stationary box. In J.S. Mills, P. Smith, and K. Yamasaki, editors, *The Conservation of Far Eastern Art. Preprints of the Contributions to the Kyoto Congress, 19-23 September 1988*, pages 142–145, International Institute for Conservation, London, 1988.
- J. Chayen and L. Bitensky. *Practical Histochemistry*. John Wiley & Sons, Chichester/New York/Brisbane, 2nd edition, 1991.
- G. Chiavari and R. Mazzeo. Characterisation of paint layers in Chinese archaeological relics by pyrolysis-GC-MS. *Chromatographia*, 49(5/6):268–272, 1999.
- Clariant. Mowiol Poly(vinyl alcohol) product information booklet, 1999. URL <http://www2.cbm.uam.es/confocal/Manuales/mowiol.pdf>.
- M. Cocca, L. D'Arienzo, L. D'Orazio, G. Gentile, C. Mancarella, E. Martuscelli, and C. Polcaro. Water dispersed polymers for textile conservation: a molecular, thermal, structural, mechanical and optical characterisation. *Journal of Cultural Heritage*, 7(4):236 – 243, 2006.
- Conservation Resources. Technical information on Paraloid B48N. Online product catalogue. URL [www.conservationresources.com/Main/section\\_40/section40\\_02.htm](http://www.conservationresources.com/Main/section_40/section40_02.htm). Last accessed 01 Mar. 2011.

- F. Cuany, V. Schaible, and U. Schießl. Studien zur Festigung biologisch geschwächten Nadelholzes: Eindringvermögen, Stabilitätserhöhung und feuchtephysikalisches Verhalten. *Zeitschrift für Kunsttechnologie und Konservierung*, 3(2):249–292, 1989.
- W. de Kesel and G. Dhont. *Coromandel Lacquer Screens*. Art Media Resources, Chicago, 2002.
- R. de la Rie. The influence of varnishes on the appearance of paintings. *Studies in Conservation*, 32(1):1–13, 1987.
- R. de la Rie. Photochemical and thermal degradation of films of dammar resin. *Studies in Conservation*, 33:53–70, 1988a.
- R. de la Rie. *Stable Varnishes for Old Master Paintings*. PhD thesis, University of Amsterdam, 1988b.
- R. de la Rie, S.Q. Lomax, M. Palmer, and C.A. Maines. An investigation of the photochemical stability of films of the urea-aldehyde resins Laropal A 81 and Laropal A 101. In *Preprints of the ICOM-CC 13th Triennial Meeting Preprints, Rio de Janeiro, 22-27 September 2002*, volume 2, pages 881–887, James & James (Science Publishers) Ltd./ICOM Committee for Conservation, London, 2002.
- E. de Witte, S. Florquin, and M. Goessens-Landrie. Influence of the modification of dispersions on film properties. In N. Brommelle, E.M. Pye, P. Smith, and G. Thompson, editors, *Adhesives and Consolidants. Preprints of the contributions to the Paris Congress, 2-8 September 1984*, pages 32–35, International Institute for Conservation, London, 1984.
- M. Derrick, L. Souza, T. Kieslich, H. Florsheim, and D. Stulik. Embedding paint cross-section samples in polyester resin: problems and solutions. *Journal of the American Institute for Conservation*, 33(3):227–245, 1994.
- M.R. Derrick, C. Druzik, and F. Preusser. FTIR analysis of authentic and simulated black lacquer finishes on eighteenth century furniture. In N.S. Brommelle and P. Smith, editors, *Urushi - Proceedings of the Urushi Study Group, 10-27 June 1985, Tokyo, Japan*, pages 227–234, The Getty Conservation Institute, Marina del Rey, California, 1988.
- M.R. Derrick, D. Stulik, and J.M. Landry. *Infrared Spectroscopy in Conservation Science*. The Getty Conservation Institute, Los Angeles, 1999.
- B.V. Deryaguin and V.P. Smilga. *Electronic Theory of Adhesion: Fundamentals and Practice*. McLaren & Son, London, 1969.
- W. Domaslowski. The mechanism of polymer migration in porous stone. In A. Vendl, B. Pichler, J. Weber, and G. Banik, editors, *Wiener Berichte über Naturwissenschaft in der Kunst*, volume 4/5, pages 402–425. Orac, Wien, 1988.
- J. Down and R. Lafontaine. A preliminary report on the properties and stability of wood adhesives. In *CCI Furniture and Wooden Objects Symposium, Ottawa*,

## References

- 2-3 July 1980, pages 55–64, Canadian Conservation Institute, Ottawa, Ontario, 1980.
- J.L. Down. Adhesive testing at the Canadian Conservation Institute, past and future. In N. Brommelle, E.M. Pye, P. Smith, and G. Thompson, editors, *Adhesives and Consolidants. Preprints of the contributions to the Paris Congress, 2-8 September 1984*, pages 18–21, The International Institute for Conservation, London, 1984.
- J.L. Down. Epoxy resin adhesives: report on shear strength retention on glass substrates. *Journal of the International Institute for Conservation - Canadian Group*, 21:28–35, 1996.
- J.L. Down. Poly(vinyl acetate) and acrylic adhesives: a research update. In J. Ambers, C. Higgitt, L. Harrison, and D. Saunders, editors,  *Holding It All Together. Ancient and Modern Approaches to Joining, Repair and Consolidation*, pages 91–98. Archetype Publications/The British Museum, London, 2009.
- J.L. Down, M.A. MacDonald, J. Tétreault, and R.S. Williams. Adhesive testing at the Canadian Conservation Institute: An evaluation of selected poly(vinyl acetate) and acrylic adhesives. *Studies in Conservation*, 41(1):19–44, 1996.
- V.E. Dreval', A.Y. Malkin, A.A. Tager, and G.V. Vinogradov. Viscosity, rubber elasticity, and viscoelasticity of concentrated polymer solutions. *Mechanics of Composite Materials*, 9(4):639–645, 1973.
- A.E. Elmahdy. *Understanding the Behaviour of Urushi Lacquers using Optical and Numerical Techniques*. PhD thesis, Wolfson School of Mechanical Engineering, Loughborough University, UK, 2010.
- A.E. Elmahdy, P.D. Ruiz, R.D. Wildman, J.M. Huntley, and S. Rivers. Stress measurement in East Asian lacquer thin films owing to changes in relative humidity using phase-shifting interferometry. *Proceedings of the Royal Society A: Mathematical, Physical and Engineering Science*, published online. URL <http://rspa.royalsocietypublishing.org/content/early/2010/11/22/rspa.2010.0414.abstract>, 2010.
- European Confederation of Conservator-Restorers' Organisations. E.C.C.O. Professional Guidelines. URL <http://www.ecco-eu.org/about-e.c.c.o./professional-guidelines.html>, 2001.
- R.L. Feller. Cross-linking of methacrylate polymers by ultraviolet radiation. Papers presented at the New York Meeting, Division of Paint, Plastics and Printing Ink Chemistry. *American Chemical Society*, 17(2):465–470, 1957.
- R.L. Feller. Dammar and mastic varnishes: Hardness, brittleness and change in weight upon drying. *Studies in Conservation*, 3(4):162–174, 1958.
- R.L. Feller. Thermoplastic polymers currently in use as protective coatings and potential directions for further research. *Institute for the Conservation of Cultural Material Bulletin*, 10(2):5–18, 1984.

- R.L. Feller. Some factors to be considered in accelerated-ageing tests. In *AIC Preprints of Papers Presented at the 15th Annual Meeting in Vancouver, Canada, 20-24 May 1987*, pages 57–67, American Institute for Conservation, Washington, D.C., 1987.
- R.L. Feller. *Accelerated Aging: Photochemical and Thermal Aspects*. The Getty Conservation Institute, Los Angeles, 1994.
- R.L. Feller and M. Curran. Solubility and crosslinking characteristics of ethylene/vinyl acetate copolymers. *Bulletin of the IIC-American Group*, 11(1): 42–45, 1970.
- R.L. Feller and M. Curran. Changes in solubility and removability of varnishes with age. *Bulletin of the IIC-American Group*, 15(2):17–26, 1975.
- S. Foskett. An investigation into the properties of isinglass. *Scottish Society for Conservation and Restoration Journal*, 5(4):11–14, 1994.
- J.C. Frade, M.I. Ribeiro, J. Graca, and J. Rodrigues. Applying pyrolysis-gas chromatography/mass spectrometry to the identification of oriental lacquers: study of two lacquer shields. *Analytical and Bioanalytical Chemistry*, 395(7): 2167–2174, 2009.
- A. Franke. Ostasiatische Lackarbeiten und das Problem ihrer Konservierung. *Arbeitsblätter für Restauratoren*, 1:1–10, 1976a.
- A. Franke. Restaurierung eines kaiserlich-chinesischen Thronsessels mit zugehörigem Paravent. In *Jahrbuch Preussischer Kulturbesitz*, pages 97–99. Stiftung Preußischer Kulturbesitz, Berlin, 1976b.
- A. Franke. The use of beeswax and resin in the restoration of East Asian lacquer work. In N.S. Brommelle, A. Moncrieff, and P. Smith, editors, *Conservation of Wood in Painting and the Decorative Arts. Preprints of the Contributions to the Oxford Congress, 17-23 September 1978*, pages 45–47, International Institute for Conservation, London, 1978.
- K. Friedrich and U.A. Karsch. Failure processes in particulate filled polypropylene. *Journal of Materials Science*, 16(8):2167–2175, 1981.
- J.M. Gagliano and C.E. Frazier. Improvements in the fracture cleavage testing of adhesively-bonded wood. *Wood and Fiber Science*, 33(3):377–385, 2001.
- H. Garner. Technical studies of oriental lacquer. *Studies in Conservation*, 8(3): 84–97, 1963.
- K.Z. Gillis. After the deluge: The conservation of two Chinese chests. In *WAG Postprints - Alexandria, Virginia*, URL [http://cool.conservation-us.org/coolaic/sg/wag/1998/WAG\\_98\\_gillis.pdf](http://cool.conservation-us.org/coolaic/sg/wag/1998/WAG_98_gillis.pdf). American Institute for Conservation Wooden Artifacts Group, Washington, D.C., 1998.
- A. Golloch and M.M. Sein. Vom Baumsaft zum Kunsthandwerk - Lackarbeiten aus Myanmar. *Chemie unserer Zeit*, 38(3):190–200, 2004.

## References

- D.W. Grattan. Consolidants for degraded and damaged wood. In *Proceedings of the Furniture and Wooden Objects Symposium*, pages 27–42, Canadian Conservation Institute, Ottawa, 1980.
- E.S. Greenhalgh. *Failure Analysis and Fractography of Polymer Composites*. Woodhead Publishing Ltd., Oxford/Cambridge/New Delhi, 2009.
- A. Habel-Schablitzky. Fischblasenleim - Geschichte und Eigenschaften sowie Anwendung in der Holzrestaurierung. Diploma thesis, Fachhochschule Köln, Germany, 1992.
- E. Hagan. *The Viscoelastic Properties of Latex Artist Paints*. PhD thesis, Imperial College London, UK, 2009.
- B. Hagedorn. Zur Restaurierung eines französischen Lackmöbels aus Schloss Wilhelmsthal/Restoring a French lacquered bureau from Wilhelmsthal Palace. In M. Kühenthal, editor, *Japanische und Europäische Lackarbeiten/Japanese and European Lacquerware*, Arbeitshefte des Bayerischen Landesamtes für Denkmalpflege 96, pages 517–536. Lipp, München, 2002.
- E.F. Hansen and M.H. Bishop. Factors affecting the re-treatment of previously consolidated matte painted wooden objects. In V. Dorge and F.C. Howlett, editors, *Painted Wood - History and Conservation. Proceedings of the AIC-WAG Symposium in Williamsburg, Virginia, 11–14 November 1994*, pages 484–497, The Getty Conservation Institute, Los Angeles, 1998.
- E.F. Hansen, M.R. Derrick, M.R. Schilling, and R. Garcia. The effects of solution application on some mechanical and physical properties of thermoplastic amorphous polymers used in conservation: Poly(vinyl acetate)s. *Journal of the American Institute for Conservation*, 30(2):203–213, 1991.
- E.F. Hansen, R. Lowinger, and E. Sadoff. Consolidation of porous paint in a vapour-atmosphere. *Journal of the American Institute for Conservation*, 32(1):1–14, 1993.
- E.F. Hansen, S. Walston, and M.H. Bishop. Matte paint - its history and technology, analysis, properties, and conservation treatment, with special emphasis on ethnographic objects. *WAAC Newsletter*, 18(2):15–24, 1996.
- S. Hashemi, A.J. Kinloch, and J.G. Williams. Mechanics and mechanisms of delamination in a poly(ether sulphone)-fibre composite. *Composites Science and Technology*, 37:429–462, 1990.
- P. Hatchfield, D. Johnson, J. Pace, and A. Tijong. Pride and place: the conservation and display of a seventeenth century Coromandel lacquer panel within the context of Acton Collection at Villa La Pietra in Florence. In *Multidisciplinary Conservation: a Holistic View for Historic Interiors. Proceedings of the Joint Interim-Meeting of five ICOM-CC Working Groups, Rome 23-26 March 2010*, ICOM Committee for Conservation, Rome, 2010.
- M. Haupt, D. Dyer, and J. Hanlan. An investigation into three animal glues. *The Conservator*, 14:10–16, 1990.

- T. Haupt. Zubereitung von Störleim - Auswirkungen der Zubereitungstemperatur und -zeit auf Viskosität, Gelierverhalten und Molekulargewicht. *Zeitschrift für Kunsttechnologie und Konservierung*, 18(2):318–328, 2004.
- S. Hayashi, T. Hirai, N. Hojo, H. Sugeta, and Y. Kyogoku. Blue complex formation of poly(vinyl acetate) with iodine-iodide. *Journal of Polymer Science, Part B: Polymer Letters Edition*, 20(1):69–73, 1982.
- L. He, M. Nie, G. Chiavari, and R. Mazzeo. Analytical characterization of binding medium used in ancient Chinese artworks by pyrolysis-gas chromatography/mass spectrometry. *Microchemical Journal*, 85(2):347 – 353, 2007.
- G. Heckmann. Bericht zur Begutachtung des Vieux-lacque-Zimmers, Schloss Schönbrunn, Wien. In S. Miklin-Kniefacz, editor, *Zur Restaurierung der Vieux-lacque-Tafeln in Schönbrunn: Grundlage und Vorarbeiten*, volume 1. Wissenschaftliche Reihe Schönbrunn, Wien, 1995.
- G. Heckmann and J. Dei Negri. *Japanlack Technik - Urushi No Waza*. Nihon Art Publishers, Ellwangen, 2002.
- G. Hedley. Relative humidity and the stress/strain response of canvas paintings: uniaxial measurements of naturally aged samples. *Studies in Conservation*, 33: 133–148, 1988.
- H.P. Hedlund and M. Johansson. Prototypes of Lascaux's Medium for Consolidation. Development of a new custom-made polymer dispersion for use in conservation. *Restauro*, 111(6):432–439, 2005.
- A. Heginbotham. On the procedure of separating multilayered coating samples for PyGC/MS analysis. J. Paul Getty Museum, Los Angeles, California. Personal communication, 2010.
- A. Heginbotham and M. Schilling. New evidence for the use of South Asian raw materials in seventeenth century Japanese export lacquer. In S. Rivers, R. Faulkner, and B. Pretzel, editors, *East Asian Lacquer: Material Culture, Science and Conservation*, page forthcoming, Archetype, London, 2011.
- A. Heginbotham, H. Khanjian, R. Rivenc, and M. Schilling. A procedure for the efficient and simultaneous analysis of Asian and European lacquers in furniture of mixed origin. In J. Bridgland, editor, *Diversity in Heritage Conservation - Tradition, Innovation and Participation. Preprints of ICOM-CC 15th Triennial Conference New Delhi, 22-26 September 2008*, volume 2, pages 1100–1108, Allied Publishers, New Delhi, 2008.
- C. Herm. Pigment- und Bindemittel-Analysen der Farbfassung der Terrakotta-Armee. In *Zweite Konferenz zur Chinesisch-Deutschen Zusammenarbeit in der Denkmalpflege, Forschungsbericht 8*, Bayerisches Landeamt für Denkmalpflege - Zentrallabor, München, 1993.
- C. Herm. Laboratory report no. 09/Schellmann, Dissertation Project Nanke Schellmann: several lacquer objects. Unpublished, Hochschule für Bildende Künste Dresden, 2009a.

## References

- C. Herm. Conversation on the uses of diluted raw lacquer for conservation in Vietnam. Hochschule für Bildende Künste Dresden. Personal communication at a meeting on 1 Feb. 2009, 2009b.
- C. Herm. Hochschule für Bildende Künste Dresden. Personal communication, e-mail from 03 July 2011, 2011.
- Kaoru Hidaka. The history and the characteristics of exported urushiware. In *Textbook - Japanese Lacquer - Intermediate*, pages 13–19. National Research Institute for Cultural Properties Tokyo, 2009.
- T. Hirai, A. Okazaki, and S. Hayashi. Effect of sequence distribution of poly(vinyl alcohol-vinyl acetate) on the coloring reaction with iodine. *Journal of Applied Polymer Science*, 32(3):3919–3928, 1986.
- M. Hisada, Y. Ohno, E. Obataya, B. Tomita, and M. Norimoto. Effects of curing on the material properties of Japanese lacquer film. *Wood Research*, 87:30–31, 2000.
- D. Hoernschemeyer. The influence of solvent type on the viscosity of concentrated polymer solutions. *Journal of Applied Polymer Science*, 18:61–75, 1974.
- T. Honda, R. Lu, R. Sakai, T. Ishimura, and T. Miyakoshi. Characterization and comparison of Asian lacquer saps. *Progress in Organic Coatings*, 61:68–75, 2008.
- T. Honda, R. Lu, N. Kitano, Y. Kamiya, and T. Miyakoshi. Applied analysis and identification of ancient lacquer based on pyrolysis-gas chromatography/mass spectrometry. *Journal of Applied Polymer Science*, 118(2):897–901, 2010.
- C.V. Horie. *Materials for Conservation - Organic consolidants, adhesives and coatings*. Conservation and Museology Series. Butterworth-Heinemann, Oxford, 1987.
- D. Horton-James, S. Walston, and S. Zounis. Evaluation of the stability, appearance and performance of resins for the adhesion of flaking paint on ethnographic objects. *Studies in Conservation*, 36:203–221, 1991.
- R. Howell, A. Burnstock, G. Hedley, and S. Hackney. Polymer dispersions artificially aged. In N.S. Brommelle, E. Pye, P. Smith, and G. Thompson, editors, *Adhesives and Consolidants. Preprints of the contributions to the Paris Congress, 2-8 September 1984*, pages 36–43, International Institute for Conservation, London, 1984.
- Y. Huang and A. J. Kinloch. Modelling of the toughening mechanisms in rubber-modified epoxy resin. Part II: A quantitative description of the microstructure-fracture property relationship. *Journal of Materials Science*, 27(10):2763–2769, 1992.
- J.R. Hubbard. Animal glues. In I. Skeist, editor, *Handbook of Adhesives*, pages 114–125. Reinhold Publishing Corp., New York, 4th edition, 1965.



- D.O. Hummel and F. Scholl. *Atlas of Polymer and Plastics Analysis*, volume 1. Spectra nos. 2584 and 2585. Hanser, München/Wien/Weinheim/New York, 2nd edition, 1978.
- J. Hutt. A Japanese lacquer chest in the V&A: A seventeenth-century wedding casket for the Dutch market. *Apollo*, CXLVII(433):3–9, 1998.
- J. Hutt. A Japanese export lacquer chest in the Victoria and Albert Museum: Some further observations. *Apollo*, CXLIX(445):22–24, 1999.
- J. Hutt. East and West in Japanese export lacquerware: Some problem pieces in the Victoria and Albert Museum. In *Ostasiatische und Europäische Lacktechniken/East Asian and European Lacquer Techniques*, pages 19–26, München, 2000. ICOMOS Hefte des Deutschen Nationalkomitees XXXV, Lipp.
- ICCROM/Tobunken. Urushi 2009 – International Course on the Conservation of Japanese Lacquer, 1-16 September 2009, Tokyo/Japan, 2009. Visit to urushi-coating workshop owned by O. Moriei in Ninohe, Joboji machi, Iwate Prefecture on 08. Sept. 2009.
- ICOM. *ICOM Code of Ethics for Museums*. International Council of Museums, Paris, 2006.
- O. Impey. Japanese export lacquer of the 17th century in lacquerwork in Asia and beyond. In W. Watson, editor, *Lacquerwork in Asia and Beyond, Colloquies on Art and Archaeology in Asia No.11*, number 11, pages 124–158. University of London, Percival David Foundation of Chinese Art, London, 1982.
- O. Impey. Japanese export lacquer. In J. Bourne, editor, *Lacquer: An International History and Collector's Guide*, pages 123–135. Crowood Press, Marlborough, 1984.
- O. Impey. Japanese export lacquer: the fine period. In M. Kühnenthal, editor, *Ostasiatische und Europäische Lacktechniken/East Asian and European Lacquer Techniques*, pages 11–18. ICOMOS Hefte des Deutschen Nationalkomitees XXXV, München, 2000a.
- O. Impey. A brief account of Japanese export lacquer of the seventeenth century and its use in Europe. In M. Kühnenthal, editor, *Japanische und Europäische Lackarbeiten/Japanese and European Lacquerware*, Arbeitshefte des Bayerischen Landesamtes für Denkmalpflege 96, pages 14–30. Lipp, München, 2000b.
- O. Impey and C. Jorg. *Japanese Export Lacquer 1580 –1850*. Hotei Publishing, Leiden, 2005.
- A. Jefferson and S. Wangchareontrakul. Long-chain phenols: Urushiol, laccol, thitsiol and phenylalkyl catechol compounds in Burmese lac from *Melanorrhoea usitata*. *Journal of Chromatography A*, 367:145 – 154, 1986.
- C. Jin, C. Sano, and J. Kumanotani. A study on the deterioration of urushi (oriental lacquer) by micro FT-IR ATR spectroscopy: Strategies for the judge-

## References

- ment of urushi in ancient cultural properties. In M. Kühnenthal, editor, *Japanische und Europäische Lackarbeiten/Japanese and European Lacquerware*, Arbeitshefte des Bayerischen Landesamtes für Denkmalpflege 96, pages 149–160. Lipp, München, 2000.
- Deffner & Johann. Leime. In *Gesamtkatalog 2007/2008*, pages 186–188. Deffner & Johann GmbH, Schweinfurt, 2006.
- P. Johns and A. Courts. The relationship between collagen and gelatin. In A.G. Ward and A. Courts, editors, *Food Science and Technology of Gelatin*, pages 137–177. Academic Press, London, 1977.
- M. Johnson and E. Packard. Methods used for the identification of binding media in Italian paintings of the fifteenth and sixteenth centuries. *Studies in Conservation*, 16:145–164, 1971.
- Christiaan Jorg. Japanese export lacquer for the dutch market. In *Ostasiatische und Europäische Lacktechniken/East Asian and European Lacquer Techniques*, pages 43–46. ICOMOS Hefte des Deutschen Nationalkomitees XXXV, Lipp, München, 2000.
- M. Jorjani, G. Wheeler, C. Riccardelli, W. Soboyejo, and N. Rahbar. An evaluation of potential marble repair. In J. Ambers, C. Higgitt, L. Harrison, and D. Saunders, editors, *Holding It All Together. Ancient and Modern Approaches to Joining, Repair and Consolidation*, pages 143–149. Archetype Publications/The British Museum, 2009.
- Y. Kamiya and T. Miyakoshi. The analysis of urushi by pyrolysis-gas chromatography and mass spectrometry. In M. Kühnenthal, editor, *Ostasiatische und Europäische Lacktechniken/East Asian and European Lacquer Techniques*, pages 107–120. ICOMOS Hefte des Deutschen Nationalkomitees XXXV, München, 2000.
- Y. Kamiya, R. Lu, T. Kumamoto, T. Honda, and T. Miyakoshi. Deterioration of surface structure of lacquer films due to ultraviolet irradiation. *Surface and Interface Analysis*, 38:1311–1315, 2006.
- H. Kato. The restoration of urushiware for export with animal glue and urushi. In N.S. Brommelle and P. Smith, editors, *Urushi - Proceedings of the Urushi Study Group, 10-27 June 1985, Tokyo, Japan*, pages 81–84, The Getty Conservation Institute, Marina del Rey, California, 1988.
- H. Kato. Historical study on the restoration of urushiware. In M. Kühnenthal, editor, *Japanische und Europäische Lackarbeiten/Japanese and European Lacquerware*, Arbeitshefte des Bayerischen Landesamtes für Denkmalpflege 96, pages 49–60. Lipp, München, 2000.
- S. Katsumata. Restoration of "Fupei makie knife-urn". In *Urushi 2005, International Course on Conservation of Japanese Lacquer*, pages 74–77. National Research Institute for Cultural Properties, Tokyo, 2003.

- K.B. Katz. The quantitative testing and comparisons of peel and lap/sheer for Lascaux 360 H.V. and Beva 371. *Journal of the American Institute for Conservation*, 24(2):60–68, 1985.
- V. Kautsch. Foundations for Japanese export lacquer. Lacquer specialist, Tokyo, Japan. Personal communication, email from 15 Feb. 2008.
- S. Keck. Mechanical alteration of the paint film. *Studies in Conservation*, 14: 9–30, 1969.
- T. Kenjo. Studies on the analysis of lacquer, II. Infrared spectrometry of lacquer films. *Scientific Papers on Japanese Antiques and Art Crafts*, 23:32–39, 1978. (As referenced by Derrik et al. 1988).
- T. Kenjo. Scientific approach to traditional lacquer art. In N.S. Brommelle and P. Smith, editors, *Urushi - Proceedings of the Urushi Study Group, 10-27 June 1985, Tokyo, Japan*, pages 155–162, The Getty Conservation Institute, Marina del Rey, California, 1988.
- N. Khandekar. Preparation of cross-sections from easel paintings. *Reviews in Conservation*, 4:1–13, 2003.
- A.J. Kinloch. *Adhesion and Adhesives: Science and Technology*. Chapman and Hall, London, 1987.
- A.J. Kinloch and J.G. Williams. Crack blunting mechanisms in polymers. *Journal of Materials Science*, (15):987–996, 1980.
- T. Kishima, S. Okamoto, and S. Hayashi. *Genshoku Mokuzai Daizukan (Atlas of Wood in Colour)*. Hoikusha, 3rd edition, 1983. (In Japanese).
- M. Kitagawa. Production of export lacquer (nikawa/tonoko) foundation. Japanese lacquer specialist. Personal communication, email from 25 Jan. 2008.
- M. Kitagawa. Japanese lacquer specialist. Personal communication to A. Heginbotham, as cited by A. Heginbotham and M. Schilling (2010), 2010.
- K. Kitamura. Some thoughts about conserving urushi art objects in Japan, and an example of conservation work. In N.S. Brommelle and P. Smith, editors, *Urushi - Proceedings of the Urushi Study Group, 10-27 June 1985, Tokyo, Japan*, pages 113–119, The Getty Conservation Institute, Marina del Rey, California, 1988.
- S. Kitamura. The restoration of Japanese urushi objects. In *Conservation of Urushi Objects - International Symposium on the Conservation of Cultural Property - 1993*, pages 75–89, National Research Institute for Cultural Properties, Tokyo, 1995.
- S. Kitamura. Die Restaurierung alter japanischer Lackarbeiten/Restoration of ancient Japanese urushi art objects. In M. Kühnlenthal, editor, *Japanische und Europäische Lackarbeiten/Japanese and European Lacquerware*, Arbeitshefte des Bayerischen Landesamtes für Denkmalpflege 96, pages 61–72. Lipp, München, 2000.

## References

- S. Kitamura. Conversation on practical aspects of East Asian lacquer manufacture and conservation by Japanese lacquer masters during a visit to Nara/Japan. Private Lacquer Conservation Studio. Personal communication, 28 Aug. 2009.
- M. Knaebe and R.S. Williams. Determining paint adhesion to wood using a uniform double-cantilever beam technique. *Journal of Testing and Evaluation (JTEVA)*, 21(4):272–279, 1993.
- S.P. Koob. The removal of aged shellac adhesive from ceramics. *Studies in Conservation*, 24:134–135, 1979.
- S.P. Koob. The continued use of shellac as an adhesive – why? In N. Brommelle, E.M. Pye, P. Smith, and G. Thompson, editors, *Adhesives and Consolidants. Preprints of the contributions to the Paris Congress, 2-8 September 1984*, page 103. International Institute for Conservation, London, 1984.
- M. Korn. Birmanische Lackarbeiten des Ethnologischen Museums Berlin - Herstellungstechnik, Untersuchung, Konservierung am Beispiel der Kosmetikdose IC 180 a-c. Diploma thesis, Fachhochschule für Technik und Wirtschaft, Potsdam, Germany, 2006.
- Kremer Pigmente. Online product details for bone glue (63000), hide glue (63010-63020), rabbit skin glue (63025, 63028, 23052), gelatin (63040), isinglass (63100), Salianski-isinglass 63110, fish glue (63550), Franklin Hide Glue (63500 - 63512). URL <http://www.kremer-pigmente.de/shopint/>. Last accessed 12 Jan. 2007.
- Kremer Pigmente. Natürliche Leime und Aquarellbinder. In *Kremer Pigmente Preisliste 2005/2006*, pages 58–61. Kremer Pigmente GmbH & Co. KG, Aichstetten, Germany, 2005.
- Kremer Pigmente. Fish glue, product data sheet. URL <http://kremer-pigmente.de/shopint/publishedfiles/63550e.pdf>. Kremer Pigmente GmbH & Co. KG, Aichstetten, Germany, 2007a. Last accessed 23 Jan. 2007.
- Kremer Pigmente. Technical data sheet for Mowilith (67000-67040) vinyl acetate. URL <http://kremer-pigmente.de/shopint/publishedfiles/67000-67040e.pdf>, 2007b.
- KSE Kuraray Specialities Europe. Mowiol - Technical data sheet, October 2002.
- J. Kumanotani. The chemistry of Japanese lacquer: an ideal model of coatings in future. In *New Results in the Field of Paints, Inks and Pigments. Proceedings of the 13th FATIPEC Congress in Cannes/Antibes/Juan-les-Pins, France, 2 - 7 May 1976*, pages 360–369. Fédération d'Associations de Techniciens des Industries des Peintures, Vernis, Emaux et Encre d'Imprimerie de l'Europe Continentale, 1976.
- J. Kumanotani. Urushi (oriental lacquer) – a natural aesthetic durable and future-promising coating. *Progress in Organic Coatings*, 26(2-4):163–195, 1995.

- J. Kumanotani. Enzyme catalyzed durable and authentic oriental lacquer: a natural microgel-printable coating by polysaccharide-glycoprotein-phenolic lipid complexes. *Progress in Organic Coatings*, 34(1-4):135–146, 1998.
- J. Kumanotani, M. Achiwa, R. Oshima, and K. Adachi. Attempts to understand Japanese lacquer as a superdurable material. In *International Symposium on the Conservation and Restoration of Cultural Property - Cultural Property and Analytical Chemistry*, pages 51–62, National Research Institute of Cultural Properties, Tokyo and Tsukuba, Japan, 1979.
- M. Kurimoto. Workshop on Japanese lacquer techniques (personal communication). Victoria and Albert Museum, London, Apr. - Jun. 2001.
- T. Kuwata, J. Kumanotani, and S. Kazama. Studies on phenolic resins. IV. Physical and chemical properties of coating films of Japanese lac (urushi) (Rigidity modulus-temperature relations measured by torsional pendulum method). *Bulletin of the Chemical Society of Japan*, 34(11):1678–1685, 1961.
- R.H. Lafontaine and P.A. Wood. The stabilization of ivory against relative humidity fluctuations. *Studies in Conservation*, 27:109–117, 1982.
- J.B. Lambert, J.S. Frye, and G.W. Cariveau. The structure of oriental lacquer by solid state nuclear magnetic resonance spectroscopy. *Archaeometry*, 33(1): 87–93, 1991.
- H. Langhals and D. Bartelt. Die Restaurierung des größten archäologischen Fundes - ein chemisches Problem: die Erhaltung der Farbfassungen der chinesischen Terrakotta-Armee in Lintong. *Angewandte Chemie*, 115:5854–5859, 2003.
- Heinz Langhals, Daniela Bartelt, and Sandra Bucher. Das Grabmal des ersten chinesischen Kaisers: Eine konservatorische Herausforderung. *Chemie unserer Zeit*, 39:196–211, 2005.
- Lascaux. Acrylic resin Paraloid B72, online product information. Online catalogue. URL [www.lascaux.ch/pdf/en/produkte/restauro](http://www.lascaux.ch/pdf/en/produkte/restauro), 2007a. Last accessed 15 Mar. 2007.
- Lascaux. Lascaux polyvinyl acetate and acrylic dispersions. Mowilith DMC2, Medium for Consolidation. Online product information. URL [www.lascaux.ch/pdf/en/produkte/restauro](http://www.lascaux.ch/pdf/en/produkte/restauro), 2007b. Last accessed 01 Feb. 2007.
- Lascaux. Mowilith 30, 50, 60, DMC2. Online product information. URL [www.lascaux.ch/pdf/en/produkte/restauro](http://www.lascaux.ch/pdf/en/produkte/restauro), 2007c. Last accessed 15 Mar. 2007.
- M. Lazzari and O. Chiantore. Thermal-ageing of Paraloid acrylic protective polymers. *Polymer*, 41(17):6447 – 6455, 2000.
- Lee Valley Tools Ltd. High Tack Fish Glue (56k6001), material safety data sheet. Received from [customerservice@leevalley.com](mailto:customerservice@leevalley.com), Ottawa, 2007.
- M. Lehmann. Langfristige Schädigung von Wandmalerei durch die Wirkung eingebrachter Kunststoffe am Beispiel der Gewölbmalereien in der Krypta

## References

- der Quedlinburger Stiftskirche St. Servatius. *Zeitschrift für Kunsttechnologie und Konservierung*, 18(1):71–92, 2004.
- B. Lencz. The development of conservation of Japanese armors and lacquerware in Hungarian public collections. In *The Role of Urushi in International Exchange. Proceedings of the 27th International Symposium on the Conservation and Restoration of Cultural Property, 3-5 December 2003*, pages 191–200. National Research Institute for Cultural Properties/Tokyo National Museum, Tokyo, 2005.
- X. Liu. *Modelling Environmental Ageing Behaviours of East Asian Lacquer (Urushi)*. PhD thesis, Wolfson School of Mechanical and Manufacturing Engineering, Loughborough University, England, (in progress).
- R. Lu, Y. Kamiya, and T. Miyakoshi. Applied analysis of lacquer films based on pyrolysis-gas chromatography/mass spectrometry. *Talanta*, 70:370–376, 2006.
- E.A. Luybavskaya. Investigation of properties of protein glues. In K. Grimstad, editor, *Preprints of the ICOM-CC 9th Triennial Meeting, Dresden, German Democratic Republic, 26-31 August 1990*, volume 1, pages 47–50, ICOM Committee for Conservation, Los Angeles, 1990.
- E. Martin. Some improvements in techniques of analysis of paint media. *Studies in Conservation*, 22:63–67, 1977.
- K. Masania. Excel Spreadsheet for LEFM DCB analysis, (customised version). Imperial College London, Department of Mechanical Engineering. Personal communication, 2008.
- K. Masania. *Toughening Mechanisms of Silica Nanoparticle-Modified Epoxy Polymers*. PhD thesis, Imperial College London, Department of Mechanical Engineering, 2010.
- L. Masschelein-Kleiner. *Les Solvants*. Institut Royal du Patrimoine Artistique, 1981.
- R. Mateo-Castro, J.V. Gimeno-Adelantado, F. Bosch-Reig, A. Doménech-Carbó, M.J. Casas-Catalán, L. Osete-Cortina, J. De la Cruz-Cañizares, and M.T. Doménech-Carbó. Identification by GC-FID and GC-MS of amino acids, fatty and bile acids in binding media used in works of art. *Fresenius' Journal of Analytical Chemistry*, 369:642–646, 2001.
- T. Matsumoto and S. Kitamura. European Project. Restoration of old Japanese lacquer ware from European museums, and Workshop, 11-14 Nov. 2008. Museum for East Asian Art, Cologne. Personal communication, 2008.
- M. Matteini and A. Moles. *Naturwissenschaftliche Untersuchungsmethoden in der Restaurierung*. Callwey Verlag, München, 1990.
- C. McSharry, R. Faulkner, S. Rivers, M.S.P. Shaffer, and T. Welton. The chemistry of East Asian lacquer: A review of the scientific literature. *IIC Reviews in Conservation*, 8:29–40, 2007.

- M.F. Mecklenburg. The effects of atmospheric moisture on the mechanical properties of collagen under equilibrium conditions. In *16th AIC Annual Meeting, New Orleans*, pages 231–244, American Institute for Conservation, Washington D.C., 1988.
- M.F. Mecklenburg. Some mechanical and physical properties of gilding gesso. In D. Bigelow, editor, *Gilded Wood Conservation and History*, pages 163–170. Sound View Press, Madison, Connecticut, 1991.
- M.F. Mecklenburg. Determining the acceptable ranges of relative humidity and temperature in museums and galleries. Part 1, Structural response to relative humidity. Technical report, Smithsonian Museum Conservation Institute, 2007.
- M.F. Mecklenburg and C.S. Tumosa. An introduction into the mechanical behavior of paintings under rapid loading conditions. In M.F. Mecklenburg, editor, *Art in Transit - Studies in the Transport of Paintings. International Conference on the Packing and Transportation of Paintings*, pages 137–171, National Gallery of Art, Washington/London, 1991a.
- M.F. Mecklenburg and C.S. Tumosa. Mechanical behaviour of paintings subjected to changes in temperature and changes in relative humidity. In M.F. Mecklenburg, editor, *Art in Transit - Studies in the Transport of Paintings. International Conference on the Packing and Transportation of Paintings*, pages 173–216. National Gallery of Art, Washington, 1991b.
- M.F. Mecklenburg, C.S. Tumosa, and D. Erhardt. Structural response of painted wood surfaces to changes in ambient relative humidity. In *Painted Wood - History and Conservation. Proceedings of the AIC-WAG Symposium in Williamsburg, Virginia, 11–14 November 1994*, pages 464–483. Getty Conservation Institute, Los Angeles, 1998.
- R.J. Meilunas, J.G. Bentsen, and A. Steinberg. Analysis of aged binders by FTIR spectroscopy'. *Studies in Conservation*, 35:33–51, 1990.
- S. Michalski. Crack mechanisms in gilding. In D. Bigelow, editor, *Gilded Wood Conservation and History*, pages 171–181. Sound View Press, Madison, Connecticut, 1991a.
- S. Michalski. Paintings - their response to temperature, relative humidity, shock and vibration. In M.F. Mecklenburg, editor, *Art in Transit - Studies in the Transport of Paintings. International Conference on the Packing and Transportation of Paintings*, pages 223–248, National Gallery of Art, Washington/London, 1991b.
- F. Michel, T. Geiger, A. Reichlin, and G. Teoh-Sapkota. Funori, ein japanisches Festigungsmittel für matte Malerei. *Zeitschrift für Kunsttechnologie und Konservierung*, 16(2):257–275, 2002.
- S. Miklin-Kniefacz. Untersuchungsbericht über geeignete Klebemedien zur Scholleniederlegung an ostasiatischen Lacktafeln. In S. Miklin-Kniefacz, editor, *Zur*

## References

- Restaurierung der Vieux-lacque-Tafeln in Schönbrunn: Grundlagen und Vorarbeiten*, Wissenschaftliche Reihe Schönbrunn, pages 16–21. Schloss Schönbrunn, Wien, 1995.
- S. Miklin-Kniefacz. The conservation and restoration treatment of the Chinese lacquered panels of the "Japanese Room" of the Palais Esterhazy. In *Preprints of the ICOM-CC 12th Triennial Meeting, Lyon, 29 Aug. - 3 Sept. 1999*, volume 2, pages 847–851. James & James (Science Publishers) Ltd./ICOM Committee for Conservation, 1999.
- John S. Mills and R. White. *The Organic Chemistry of Museum Objects*. Butterworth-Heinemann, Oxford/Auckland/Boston, second edition, 1999.
- S. Miura. The conservation of the Golden Hall (Konjikido) of Chusonji Temple at Hiraizumi. In M. Kühnenthal, editor, *Ostasiatische und Europäische Lacktechniken/East Asian and European Lacquer Techniques*, pages 144–148. ICOMOS Hefte des Deutschen Nationalkomitees XXXV, Lipp, München, 2000.
- S. Miura and T. Ogawa. Study on the relation between the occurrence of cracks on urushi coating and climate change after the intervention of the shelter for the Golden Hall of Chusonji. *Science for Conservation (Hozon Kagaku)*, 38: 31–38, 1999.
- Moss & Co. Timber Merchants. Online product catalogue. url <http://www.mosstimber.co.uk/wp-content/themes/moss/assets/brochure.pdf>. Last accessed 10 Mar. 2011.
- S. Mostovoy, P.B. Crosley, and E.J. Rippling. Use of crack-line-loaded specimens for measuring plane-strain fracture toughness. *Journal of Materials*, 2(3):661–681, 1967.
- R. Murakami, F. Tanaka, and M. Norimoto. Relationship between bending quality and wood species. *Wood Research*, 89:21–22, 2002.
- K. Murose. The restoration of cultural properties in Japan. In *International Course on Conservation of Urushi*, pages 23–30, Department of Restoration Techniques, Tokyo National Research Institute for Cultural Properties, Tokyo, 2001.
- Y. Nagase. *Urushi-no-hon (The Book of Urushi)*. Kensei-sha, 1986. (In Japanese).
- T. Nakajima. Conservation of Chinese urushi: methods and difficulties. In N.S. Brommelle and P. Smith, editors, *Urushi - Proceedings of the Urushi Study Group, 10-27 June 1985, Tokyo, Japan*, pages 87–89, The Getty Conservation Institute, Marina del Rey, California, 1988.
- T. Nakazato. Techniques for and restoration of urushi art (Japanese lacquer art). In *International Symposium on the Conservation of Cultural Property - Conservation of Wood - 1977*, Proceedings, pages 175–183, Tokyo National Research Institute of Cultural Properties, Tokyo, 1978.



- M. Nemtanu and M. Brasoveanu. Aspects regarding the rheological behaviour of the wheat starch treated with accelerated electron beam. *Romanian Journal of Physics*, 55(1–2):111–117, 2010.
- D.J. Newman, C.J. Nunn, and J.K. Oliver. Release of individual solvents and binary solvent blends from thermoplastic coatings. *Journal of Paint Technology*, (47):70–78, 1975.
- D.D. Nicholas. Characteristics of preservative solutions which influence penetration into wood. *Forest Products Journal*, 22(5):31–36, 1972.
- K. Nicolaus. *Handbuch der Gemälderestaurierung*. Könemann Verlagsgesellschaft, Köln, 1998.
- N. Niimura. Determination of the type of lacquer on East Asian lacquer ware. *International Journal of Mass Spectrometry*, 284:93–97, 2009.
- N. Niimura and T. Miyakoshi. Characterization of natural resin films and identification of ancient coating. *Journal of the Mass Spectrometry Society of Japan*, 51(4):439–457, 2003.
- N. Niimura and T. Miyakoshi. Structural study of oriental lacquer films during the hardening process. *Talanta*, 70(1):146 – 152, 2006.
- N. Niimura, T. Miyakoshi, J. Onodera, and T. Higuchi. Characterization of *Rhus vernificera* and *Rhus succedanea* lacquer films and their pyrolysis mechanisms studied using two-stage pyrolysis-gas chromatography/mass spectrometry. *Journal of Analytical and Applied Pyrolysis*, 37(2):199 – 209, 1996.
- K. Nishikawa. Conservation of urushi and urushi objects in Japan. In *Conservation of Urushi Objects. Proceedings of the International Symposium on the Conservation and Restoration of Cultural Property, 10-12 November 1993, Tokyo*, pages 17–24, Tokyo National Research Institute for Cultural Properties, Tokyo, 1993.
- T. Nishiura. Experimental study on the adhesion strength of lacquer coating. In *Preprints of the ICOM-CC 7th Triennial Meeting, Copenhagen, 10-14 September 1984*, pages 84.16.1 – 84.16.7, ICOM Committee for Conservation, Los Angeles, 1984.
- NRICPT. *Urushi 2005, International Course on Conservation of Japanese Lacquer*. National Research Institute for Cultural Properties, Tokyo, 2005.
- NRICPT. *Textbook - Japanese Lacquer - Basics*. National Research Institute for Cultural Properties, Tokyo, 2008.
- NRICPT. *Textbook - Japanese Lacquer - Intermediate*. National Research Institute for Cultural Properties, Tokyo, 2009.
- S. Nöth. Untersuchung zum Eindringverhalten von Klebmitteln bei der Festigung: Die Markierung von festigungsrelevanten Klebmitteln mit dem Fluorochrom Fluorescein-Isothiocyanat. Diploma thesis, Staatliche Akademie der Bildenden Künste Stuttgart, Germany, 2005.

## References

- E. Obataya. Effects of ageing and heating on the mechanical properties of wood. In Luca Uzielli, editor, *Wood Science for Conservation of Cultural Heritage - Florence 2007. Proceedings of the International Conference held by COST ACTION IE0601 in Florence, Italy, 8-10 November 2007*, pages 16–23, Firenze University Press, Florence, 2009.
- E. Obataya, Y. Ohno, M. Norimoto, and B. Tomita. Effects of oriental lacquer (urushi) coating on the vibrational properties of wood used for soundboards of musical instruments. *Acoustical Science and Technology*, 22(1):27–34, 2001.
- E. Obataya, Y. Furuta, Y. Ohno, M. Norimoto, and B. Tomita. Effects of aging and moisture on the dynamic viscoelastic properties of oriental lacquer (urushi) film. *Journal of Applied Polymer Science*, 83(11):2288–2294, 2002.
- T. Ogawa and T. Kamei. The fracture of lacquer films on oriental lacquerware resulting from absorption and desorption of water. In M. Kühnenthal, editor, *Japanische und Europäische Lackarbeiten/Japanese and European Lacquerware*, Arbeitshefte des Bayerischen Landesamtes für Denkmalpflege 96, pages 161–170. Lipp, München, 2000.
- J.Y. Olayemi and A.A. Adeyeye. Some properties of polyvinyl acetate films cast from methanol, acetone and chloroform as solvent. *Polymer Testing*, 3(1): 25–35, 1982.
- T.M. Olstad and I. Kucerova. COST Action IE0601 Wood Science for Conservation of Cultural Heritage (WoodCultHer) Focused Meeting: Consolidation, reinforcement & stabilisation of decorated wooden artefacts. Report, 30-31 Mar. 2009. 2009. URL <http://www.docstoc.com/docs/21015974/COST-Action-IE0601>. Last accessed 02. Feb 2011.
- W. Ostwald. Iconoscopic studies I. Microscopic identification of homogenous binding mediums. *Technical Studies in the Field of the Fine Arts*, 4(3):135–144, 1936.
- A.J. Panshin and C. de Zeeuw. *Textbook of Wood Technology*. McGraw-Hill, New York, 4 edition, 1980.
- A. Pataki. Konsolidierung von pudernden Malschichten mit Aerosolen. *Restauro*, 2:110–117, 2007.
- C. Payer, M.C. Corbeil, C. Harvey, and E. Moffatt. The interior decor of the Ursuline Chapel in Quebec City. Research and conservation. In V. Dorge and F.C. Howlett, editors, *Painted Wood - History and Conservation. Proceedings of the AIC-WAG symposium in Williamsburg, Virginia, 11–14 November 1994*, pages 301–317, The Getty Conservation Institute, Los Angeles, 1998.
- R. Payton. The conservation of an eighth century B.C. table from Gordion. In N.S. Brommelle, E.M. Pye, P. Smith, and G. Thomson, editors, *Adhesives and Consolidants. Preprints of the Contributions to the Paris Congress, 2-8 September 1984*, pages 133–137. International Institute for Conservation, London, 1984.

- T. Petukhova and S.D. Bonadies. Sturgeon glue for painting consolidation in Russia. *Journal of the American Institute for Conservation*, 32(1):23–31, 1993.
- B. Piert-Borgers. *Restaurieren mit Urushi - Japanischer Lack als Restaurierungsmittel*. Kleine Monographien. Museum für Ostasiatische Kunst, Köln, 1987.
- B. Piert-Borgers. Aspects and problems of the application of urushi in the restoration of objects from European collections. In *Conservation of Urushi Objects. International Symposium on the Conservation of Cultural Property, 10-12 November 1993*, pages 147–165, Tokyo National Research Institute for Cultural Properties, Tokyo, 1993.
- Barbara Piert-Borgers. Untersuchungen zum Fassungs Aufbau von Koromandel-lacken - Vorüberlegungen zu einem Projekt. In M. Kühenthal, editor, *Ostasiatische und Europäische Lacktechniken/East Asian and European Lacquer Techniques*, pages 92–106. ICOMOS Hefte des Deutschen Nationalkomitees XXXV, Lipp, München, 2000.
- A. Pietsch. *Lösemittel – Ein Leitfaden für die restauratorische Praxis*, volume 7 of *VDR Schriftenreihe zur Restaurierung*. Verband der Restauratoren (VDR), Bonn, 2002.
- V. Pitthard, S. Wei, S. Miklin-Kniefacz, S. Stanek, M. Griesser, and M. Schreiner. Scientific investigations of antique lacquers from a 17th-century Japanese ornamental cabinet. *Archaeometry*, 52(6):1044–1056, 2010.
- C. Pitzen. Die Modifizierung von Glutinleimen - Möglichkeiten der Anpassung an objektspezifische und verarbeitungstechnische Bedingungen nach Literaturangaben des 18. bis 19. Jahrhunderts. Diploma thesis, Fachhochschule Köln, Germany, 1991.
- J. Plesters. Cross-sections and chemical analysis of paint samples. *Studies in Conservation*, 2:110–157, 1956.
- M. Przybylo. Langzeit-Löslichkeit von Störleim - Tatsache oder Märchen? *VDR Beiträge zur Erhaltung von Kunst- und Kulturgut*, 1:117–123, 2006.
- M. Przybylo. Anleitung zur Leimherstellung aus getrockneten Zuchtstör-Schwimmbblasen, 2007. URL <http://www.stoerleim.de/Unterordner/Leim.Herstellung.pdf>. Last accessed 22 Aug. 2008.
- M. Qin, J.D. Mitchell, and O. Vogl. Oriental lacquer. 10. The South East Asian lacquer. *Journal of Macromolecular Science - Pure and Applied Chemistry, Part A*, 33(12):1791–1803, 1996.
- Quebec Wood Export Bureau. White pine, pinus strobus. Online wood database. Softwood and value added softwood lumber. URL <http://www.quebecwoodexport.com/eng/softwood/whitepine.htm>. Last accessed 14 Apr. 2011.

## References

- J.J. Quin. *Urushi - The Technology of Japanese Lacquer*. The Caber Press, Portland, Oregon, 1882/1995. (Originally published as: Report by Her Majesty's Acting Consul at Hakodate on the Lacquer Industry of Japan, London: Harrison and Sons, 1882).
- M.S. Rahman, G. Said Al-Saidi, and N. Guizani. Thermal characterisation of gelatin extracted from yellowfin tuna skin and commercial mammalian gelatin. *Food Chemistry*, 108(2):472 – 481, 2008.
- A. Reiterer and S. Tschegg. The influence of moisture content on the mode I fracture behaviour of sprucewood. *Journal of Materials Science*, 37:4487–4491, 2002.
- J. Riederer. Restaurierung mit Kunstharzen in Japan. *Restauro*, 2:118–126, 1979.
- U. Ring. Chemical analysis of East Asian lacquer (Qi-lacquer). In C. Blänsdorf, E. Emmerling, and M. Petzet, editors, *Die Terrakottaarmee des Ersten Chinesischen Kaisers Qin Shihuang/The Terracotta Army of the First Chinese Emperor Qin Shihuang*, pages 463–494. Arbeitshefte des Bayerischen Landesamtes für Denkmalpflege 83, Lipp, München, 2001.
- B.H. River. Fracture of adhesive-bonded wood joints. In A. Pizzi and K. L. Mittal, editors, *Handbook of Adhesive Technology*, chapter 9, pages 151–177. Marcel Dekker, Inc., New York, 1994.
- B.H. River and E.A. Okkonen. Contoured wood double cantilever beam specimen for adhesive joint fracture tests. *Journal of Testing and Evaluation (JTEVA)*, 21(1):21–28, 1993.
- S. Rivers. On the conservation of the Mazarin Chest. In *The Role of Urushi in International Exchange: Proceedings of the 27th International Symposium on the Conservation and Restoration of Cultural Property, 3-5 December 2003*, pages 150–158, Tokyo National Research Institute for Cultural Properties/Tokyo National Museum, Tokyo, 2005.
- S. Rivers. Conversation on suitable solvents used for diluting urushi lacquer. Victoria and Albert Museum, London. Personal communication, 2007.
- S. Rivers and N. Umney. *Conservation of Furniture*. Butterworth-Heinemann, Oxford/Auckland, 2003.
- S. Rivers and Y. Yamashita. A cross-cultural approach to lacquer conservation: consolidation of metal foil (hymon, kanagai and kirikane) decoration on the Mazarin Chest. In D. Saunders, J.H. Townsend, and S. Woodcock, editors, *The Object in Context - Crossing Conservation Boundaries. Contributions to the Munich Congress, 28 Aug. - 1 Sept. 2006*, pages 286–292, International Institute for Conservation, London, 2006.
- S. Rivers, R. Faulkner, and B. Pretzel, editors. *East Asian Lacquer: Material Culture, Science and Conservation*, Archetype, London, 2011.

- A.M. Rosenqvist. New methods for the consolidation of fragile objects. In Garry Thomson, editor, *Recent Advances in Conservation. Contributions to the IIC Rome Conference, 1961*, pages 140–144, Butterworths, London, 1963.
- T. Sakuno and A.P. Schniewind. Adhesive qualities for consolidants for deteriorated wood. *Journal of the American Institute for Conservation*, 29(1):33–44, 1990.
- I. Sandner, B. Bünsche, G. Meier, H. P. Schramm, and J. Voss. *Konservierung von Gemälden und Holzskulpturen*. Deutscher Verlag der Wissenschaften, Berlin, 1990.
- E. Sauer and W. Aldinger. Oberflächenspannung und Schaumbildung bei Glutininlösungen. *Kolloid-Zeitschrift*, 88(3):329–340, 1939.
- S. Schaefer. Fluorescent staining techniques for the characterisation of binding media within paint cross-section and digital image processing for the quantification of staining results. In T. Bakkenist, R. Hoppenbrouwers, and H. Dubois, editors, *Early Italian Paintings – Techniques and Analysis*. Limburg Conservation Institute, 1997.
- V. Schaible. Überlegung zum Phänomen der Schüsselbildung an Leinwandgemälden. *Zeitschrift für Kunsttechnologie und Konservierung*, 4(2):235–250, 1990.
- N. Schellmann. Aqueous cleaning of East Asian lacquer: A preliminary investigation of the effect of pH and ionic concentration on gloss and colour. Master of Arts thesis, Royal College of Art, London, UK, 2003.
- N. Schellmann. Delamination and flaking of East Asian export lacquer coatings on wood substrates. In S. Rivers, R. Faulkner, and B. Pretzel, editors, *East Asian Lacquer: Material Culture, Science and Conservation*, pages 107–120, Archetype, London, 2011.
- N. Schellmann and S. Rivers. Aqueous cleaning of photodegraded East Asian lacquer: a preliminary investigation of the effect of pH and ionic concentration on gloss and colour. *Zeitschrift für Kunsttechnologie und Konservierung*, 19(2):369–376, 2005.
- N.C. Schellmann. Animal glues: a review of their key properties relevant for conservation. *Reviews in Conservation*, 8:55–66, 2007.
- U. Schießl. Konservierungstechnische Beobachtungen zur Festigung wässrig gebundener Malschichten auf Holz. *Zeitschrift für Kunsttechnik und Konservierung*, 3(2):293–320, 1989.
- M.R. Schilling. The glass transition of materials used in conservation. *Studies in Conservation*, 34:110–116, 1989.
- M.R. Schilling. Report of analysis results for East Asian export-type lacquer samples. Getty Conservation Institute, Los Angeles, California. Personal communication, Dec. 2010 – Jan. 2011, 2010a.

## References

- M.R. Schilling. Email regarding the analysis of East Asian export-type lacquer samples / Anacard marker compounds. Getty Conservation Institute, Los Angeles, California. Personal communication, 10 Dec. 2010, 2010b.
- M.R. Schilling. Emails regarding the analysis of East Asian export-type lacquer samples / fatty acids. Getty Conservation Institute, Los Angeles, California. Personal communication, 31 Jan. 2011, 1/2 Feb. 2011, 2011.
- A.P. Schniewind. Consolidation of wooden panels. In K. Dardes and A. Rothe, editors, *The Structural Conservation of Panel Paintings. Conference proceedings, J. Paul Getty Museum, April 1995*, pages 87–107, The Getty Conservation Institute, Los Angeles, 1998.
- A.P. Schniewind and P.Y. Eastman. Consolidant distribution in deteriorated wood treated with soluble resins. *Journal of the American Institute for Conservation*, 33(3):237–255, 1994.
- A.P. Schniewind and D.P. Kronkright. Strength evaluation of deteriorated wood treated with consolidants. In N. Brommelle, E.M. Pye, P. Smith, and G. Thompson, editors, *Adhesives and Consolidants. Preprints of the contributions to the Paris Congress, 2-8 September 1984*, pages 146–150. International Institute for Conservation, London, 1984.
- H.P. Schramm and B. Hering. *Historische Malmaterialien und ihre Identifizierung*. Akademische Druck- und Verlagsanstalt, Graz, 1988.
- Y.R. Shashoua. Mechanical testing of resins for use in conservation. In *Preprints of the ICOM-CC 10th Triennial Meeting, Washington, D.C., 22-27 August 1993*, volume 2, pages 580–585. ICOM Committee for Conservation, 1993.
- A. Simon, Y. Grohens, L. Vandanjon, P. Bourseau, E. Balnois, and G. Levesque. A comparative study of the rheological and structural properties of gelatin gels of mammalian and fish origin. *Macromolecular Symposia*, 203(1):331–338, 2003.
- S. Simon. Die Evaluierung von Produkten und Verfahren zur Wandmalereikon-servierung als Konservierungswissenschaftliche Fragestellung. In J. Pursche, editor, *Konservierung von Wandmalerei - Reaktive Behandlungsmethoden zur Bestandserhaltung*, pages 48–60. Arbeitshefte des Bayerischen Landesamtes für Denkmalpflege 104, Lipp, München, 2001.
- S. Simon, Z. Zhang, T. Zhou, and C. Herm. Scientific investigations of the ground layer of the terracotta figures. In C. Blänsdorf, E. Emmerling, and M. Petzet, editors, *Die Terrakottaarmee des Ersten Chinesischen Kaisers Qin Shihuang/The Terracotta Army of the First Chinese Emperor Qin Shihuang*, pages 495–522. Arbeitshefte des Bayerischen Landesamtes für Denkmalpflege 83, Lipp, 2001.
- K. Sindlinger-Maushardt and K. Petersen. Methylcellulose als Klebemittel für die Malschichtfestigung auf Leinwandbildern - Untersuchungen zur Klebkraft und

- zur mikrobiellen Resistenz. *Zeitschrift für Kunsttechnologie und Konservierung*, (2):371–382, 2007.
- I. Skeist. Introduction to adhesives. In *Handbook of Adhesives*, pages 3–13. Reinhold Publishing Corp., New York, 4 edition, 1965.
- C. Springob. Stärkekleister als Verdickungsmittel von Störleim zur Malschichtfestigung. *Zeitschrift für Kunsttechnologie und Konservierung*, 15(1):111–132, 2001.
- K. Stephan. *Die Lackierkunst der Völker in der Vergangenheit und Gegenwart - Technische Erläuterungen für Maler und Lackierer*, volume 1. Süddeutsche Malerzeitung, München, 1927.
- H. Sugiyama. Japanese representative woods - hinoki and sugi. In *International Symposium on the Conservation and Restoration of Cultural Property. The Conservation of Wooden Cultural Property*, pages 83–91, Tokyo National Research Institute of Cultural Properties, Tokyo, 1983.
- J.N. Sultan and F.J. McGarry. Effect of rubber particle size on deformation mechanisms in glassy epoxy. *Polymer Engineering and Science*, 13(1):29–34, 1973.
- S. Sun, J.R. Mitchell, W. MacNaughtan, T.J. Foster, V. Harabagiu, Y. Song, and Q. Zheng. Comparison of the mechanical properties of cellulose and starch films. *Biomacromolecules*, 11(1):126–132, 2010.
- N. Suzuki. On the concept of the restoration and reproduction of cultural properties in Japan. In *The Role of Urushi in International Exchange. Proceedings of the 27th International Symposium on the Conservation and Restoration of Cultural Property, Tokyo, 3-5 December 2003*, pages 96–103, National Research Institute for Cultural Properties/Tokyo National Museum, Tokyo, 2005.
- J.R. Swider and M. Smith. Funori: Overview of a 300-year-old consolidant. *Journal of the American Institute for Conservation*, 44(2):117–126, 2005.
- Y. Taguchi, H. Kato, and C. Takahashi. Technical studies by reproducing urushiware made for export. *Science for Conservation (Hozon Kagaku)*, 40:84–92, 2001. (In Japanese, abstract in English).
- T. Tan, N. Rahbar, A. Buono, G. Wheeler, and W. Soboyejo. Sub-critical crack growth in adhesive/marble interfaces. *Materials Science and Engineering: A*, 528(10-11):3697–3704, 2011.
- J. Thei. Difficulties and challenges regarding the artificial ageing of Japanese lacquer samples. Imperial College London, Department of Mechanical Engineering. Personal communication, 2010.
- J. Thei. *Artificial Ageing of Japanese Lacquerware and Comparison of Conservation Treatments for Photodegraded Japanese Lacquer Surfaces*. PhD thesis, Imperial College London, 2011.

## References

- C. Thieme. East Asian Lacquer - the ground layer for the polychromy on the Terracotta Army. In C. Blänsdorf, E. Emmerling, and M. Petzet, editors, *Die Terrakottaarmee des Ersten Chinesischen Kaisers Qin Shihuang/The Terracotta Army of the First Chinese Emperor*, pages 425–462. Arbeitshefte des Bayerischen Landesamtes für Denkmalpflege 83, Lipp, München, 2001.
- G. Thomson. New picture varnishes. In G. Thomson, editor, *Recent Advances in Conservation. Contributions to the IIC Rome Conference, 1961*, pages 176–184, Butterworths, London, 1963.
- K. Toishi and H. Washizuka. *Characteristics of Japanese Art that Condition its Care*. Japanese Association of Museums, Tokyo, 1987.
- J.S. Tsang and R.H. Cunningham. Some improvements in the study of cross sections. *Journal of the American Institute for Conservation*, 30(2):163–177, 1991.
- D. Tzetzis and P.J. Hogg. Bondline toughening of vacuum infused composite repairs. *Composites Part A: Applied Science and Manufacturing*, 37(9):1239–1251, 2006.
- D. Tzetzis, P.J. Hogg, and M. Jogia. Double cantilever beam mode I testing for vacuum infused repairs of GFRP. *Journal of Adhesion Science and Technology*, 17(3):309–328, 2003.
- P. Van Hung, T. Maedac, and N. Morita. Waxy and high-amylose wheat starches and flours: characteristics, functionality and application. *Trends in Food Science and Technology*, 17:448–456, 2006.
- G. van Steene and L. Masschelein-Kleiner. Modified starch for conservation purposes. *Studies in Conservation*, 25:64–70, 1980.
- O. Vogl. Oriental lacquer, poison ivy, and drying oils. *Journal of Polymer Science: Part A: Polymer Chemistry*, 38:4327–4335, 2000.
- D.W. von Endt. Technological modifications of protein materials and the effect on stability. Protein adhesives. In C. L. Rose and David W. von Endt, editors, *Protein Chemistry for Conservators*, pages 39–46. American Institute for Conservation, Washington D.C., 1984.
- D.W. von Endt and M.T. Baker. The chemistry of filled animal glue systems. In Deborah Bigelow, editor, *Gilded Wood Conservation and History*, pages 155–162. Sound View Press, Madison, Connecticut, 1991.
- G. von Looz. Restaurierung und Technologie dreier Bronzegefäße: Römischer Luxus nördlich der Alpen. *Restauro*, 107(6):464–468, 2001.
- S. Wang. *Xiushilu jieshuo*. Cultural Relics Press (wenwu chubanshe), Beijing, 1983. (As referenced by W. de Kesel and G. Dhont (2002), p. 101).
- Y. Wang and A.P. Schniewind. Consolidation of deteriorated wood with soluble resins. *Journal of the American Institute for Conservation*, 24(2):77–91, 1985.



- M. Webb. Conservation treatment of lacquer in the Royal Ontario Museum. In *Conservation of Urushi Objects: International Symposium on the Conservation and Restoration of Cultural Property*, pages 1–16, Tokyo National Research Institute for Cultural Properties, Tokyo, Japan, 1993.
- M. Webb. Methods and materials for filling losses on lacquer objects. *Journal of the American Institute for Conservation*, 37(1):117–133, 1998.
- M. Webb. *Lacquer - Technology and Conservation*. Butterworth-Heinemann, Oxford, 2000.
- M. Webb. The autofluorescence of Asian lacquer. In S. Rivers, R. Faulkner, and B. Pretzel, editors, *East Asian Lacquer: Material Culture, Science and Conservation*, Archetype, London, 2011.
- H. Weinbeck. Materialeigenschaften von tierischen Leimen als Festigungs- und Klebemittel im Verbund Malschicht - Holzbildträger. Seminararbeit, Hochschule für Bildende Künste Dresden, Germany, 2007.
- S. Weintraub, K. Tsujimoto, and S.Y. Walters. Urushi and conservation: The use of Japanese lacquer in the restoration of Japanese art. *Ars Orientalis (Freer Gallery of Art, Smithsonian Institution, University of Michigan)*, 11: 39–62, 1979.
- M. A. Williams. An assessment for wooden objects consolidation: Notes on the 1984 WAG/AIC Thinktank. In *Wooden Artifacts Group Preprints, New Orleans Meeting*, American Institute for Conservation, Washington D.C., 1988.
- John Winter. Natural adhesives in East Asian paintings. In N. Brommelle, E.M. Pye, P. Smith, and G. Thompson, editors, *Adhesives and Consolidants. Preprints of the contributions to the Paris Congress, 2-8 September 1984*, pages 117–120. International Institute for Conservation, London, 1984.
- R. Wolbers and G. Landrey. The use of direct reactive fluorescent dyes for the characterization of binding media in cross sectional examinations. In *Preprints of the 15th AIC Annual Meeting, Vancouver*, pages 168–202, American Institute for Conservation, Washington D.C., 1987.
- X. Wu and G. Wu. Studienbericht der chinesischen Lackarbeiten-Gruppe über die altertümlichen Lacktafeln in Schönbrunn. In S. Miklin-Kniefacz, editor, *Zur Restaurierung der Vieux-lacque-Tafeln in Schönbrunn: Grundlage und Vorarbeiten*. Wissenschaftliche Reihe Schönbrunn, Wien, 1995.
- K. Yamasaki. Review of conservation of old art objects in Japan. *Studies in Conservation*, 3:83–88, 1957.
- K. Yamasaki and K. Nishikawa. Polychromed sculptures in Japan. *Studies in Conservation*, 15:278–293, 1970.
- Y. Yamashita. *Concept concerning the conservation and restoration of urushi-ware and preliminary investigation*, chapter 6.1, pages 87–88. Tokyo National Research Institute for Cultural Properties, 2009a.

## References

- Y. Yamashita. *Techniques*, chapter 6.2, pages 89–94. Tokyo National Research Institute for Cultural Properties, Tokyo, 2009b.
- Y. Yamashita. *Conservation of exported urushiware and its problems*, chapter 6.3, pages 95–107. Tokyo National Research Institute for Cultural Properties, Tokyo, 2009c.
- Y. Yamashita and S. Rivers. Conservation of the photodegraded surface of the Mazarin Chest. In Shayne Rivers, Rupert Faulkner, and Boris Pretzel, editors, *East Asian Lacquer: Material Culture, Science and Conservation*, Archetype, London, 2011.
- H. Yoshihara and T. Kawamura. Mode I fracture toughness estimation of wood by DCB test. *Composites Part A: Applied Science and Manufacturing*, 37(11): 2105 – 2113, 2006.
- K.J. Zeleznak and R.C. Hosney. The glass transition in starch. *Cereal Chemistry*, 64:121–124, 1987.
- A. Zosel. Mechanical behaviour of coating films. *Progress in Organic Coatings*, 8:47–79, 1980.
- S. Zumbühl. Proteinische Leime - ein vertrauter Werkstoff? Aspekte zum feuchtphysikalischen Verhalten von Gelatine. *Zeitschrift für Kunsttechnologie und Konservierung*, 17(1):95–103, 2003.

## A. Staining Assays

### **Ponceau S (for proteins)**

(Schramm and Hering 1988, p. 216)

Concentrated Ponceau S (Acid Red 112, C.I. 27195, sodium salt of a diazo compound) in 1% aqueous acetic acid solution.

1. Soak sample in 1% aqueous acetic acid solution for 1-5 minutes (depending on how much the sample soaks up the liquid).
2. Stain sample in Ponceau S solution for 5 minutes.
3. Rinse with a few drops of deionised water.

### **Amido Black AB2 (for proteins)**

(Martin 1977)

1g Amido Black 10B (Naphthol blue black,  $C_{22}H_{14}N_6O_9S_2Na_2$ , C.I. 20470)

450 ml 1N acetic acid ( $CH_3COOH$ )

450 ml 0.1 M aqueous sodium acetate ( $Na(CH_3COO) + 3H_2O$ ) solution

100 ml glycerine

1. Soak sample in 1% aqueous acetic acid solution for 5 minutes.
2. Stain sample in Amido black solution for 15 minutes.
3. Rinse with 1% aqueous acetic acid solution.

### **Sudan Black B (for oils)**

(after Schramm and Hering 1988, p. 216)

Concentrated solution of Sudan Black B (C.I. 26150) in isopropanol. The solution should be filtered before staining.

1. Soak sample in deionised water/ethanol (1:1) for 5 minutes.
2. Stain sample in Sudan Black B solution for 5-15 minutes.
3. Rinse with deionised water/ethanol (1:1) solution.

## A. Staining Assays

### **Nile Blue sulphate (for oils)**

(after Schramm and Hering 1988, p. 216)

5 ml of 0.5% sulphuric acid ( $\text{H}_2\text{SO}_4$ )

50 ml of concentrated Nile Blue A (C.I. 51180) solution in water  
(boiled and filtered)

1. Soak sample in deionised water/ethanol (1:1) for 5 minutes.
2. Stain sample in bath of Nile Blue sulphate for 15-30 minutes.
3. Rinse thoroughly with hot water for 1-2 minutes.

### **Lugol's / $\text{I}_2\text{KI}$ solution (for starch, PVAc and PVAI)**

(e.g. Lehmann 2004)

Lugol's solution, i.e. aqueous solution of  $0.01\text{mol/l}$  iodine-potassium iodide,  $\text{I}_2\text{KI}$ .

1. Apply one drop on the cross-section and leave to soak for 30 seconds.
2. Remove (soak up) excess stain with soft tissue.

### **Solvent Blue G (for acrylics)**

(after Lehmann 2004)

0.2 wt % solution of Solvent Blue G (C.I. 61554) in ethanol.

1. Soak sample in ethanol/water (2:1) for 3 minutes.
2. Immerse sample in staining bath for 3-5 minutes for Lascaux MfC, and up to 10 minutes for Paraloid types.
3. Rinse thoroughly under running warm water.

## B. Wood Specifications

	JAPANESE CYPRESS (HINOKI)	REFERENCE	QUEBEC YELLOW PINE	REFERENCE
ELASTIC MODULUS	8–10 GPa	Sugiyama 1983; Obataya 2009	8–10 GPa	Center for Wood Anatomy Research; Chapter section 7.2.4
MODULUS OF RUPTURE	75 MPa	Kishima et al. (1983)	65	Quebec Wood Export Bureau
DENSITY	410 / 480 kg/m <sup>3</sup>	Bucur (2006, p.167) Murakami et al. 2002	420kg/m <sup>3</sup>	Moss & Co. Timber Merchants



## C. List of Materials and Suppliers

CATEGORY	PRODUCT NAME	PRODUCT No.	SUPPLIER
<i>Polymers</i>			
Acrylics	Lascaux Medium for Consolidation	81012	Kremer Pigmente GmbH Co. KG 88317 Aichstetten, GERMANY <a href="http://www.kremer-pigments.com">www.kremer-pigments.com</a>
	Paraloid B 48 N	SY48N	Conservation Resources UK Ltd., Oxford, UK <a href="http://www.conservation-resources.co.uk">www.conservation-resources.co.uk</a>
	Paraloid B 72	SY7	
	Primal B60A (Rhoplex B60A)	SY29C	
Cyanoacrylate adhesive	Loctite SuperGlue gel		Henkel Loctite Ltd., IRELAND <a href="http://www.loctiteproducts.com">www.loctiteproducts.com</a>
Epoxy resin	Araldite 2015		Huntsman Advanced Materials Americas LLC, USA <a href="http://www.huntsman.com">www.huntsman.com</a>
Lacquer	<i>Ki-urushi</i> (Standard raw lacquer of Chinese origin, processed in Japan)	A01	Watanabe-Shoten, Ueno, Tokyo, JAPAN <a href="http://www1.odn.ne.jp/j-lacquer/home_eng.html">http://www1.odn.ne.jp/j-lacquer/home_eng.html</a> <a href="mailto:j-lac@par.odn.ne.jp">j-lac@par.odn.ne.jp</a>
Poly(vinyl acetates)	Mowilith 50	67040	Kremer Pigmente, GERMANY
	Mowilith DMC2	76582	
Poly(vinyl alcohol)	Mowiol 3-83	2517100	Deffner & Johann Roethlein-Schweinfurt, GERMANY <a href="http://www.deffner-johann.de">www.deffner-johann.de</a>
Protein glues	Hide glue in cubes (from bovine hides, 230 - 270 Bloom)	63020	Kremer Pigmente, GERMANY
	High tack fish glue	56K60.01	Lee Valley Tools Ltd. Ottawa, CANADA <a href="http://www.leevalley.com">www.leevalley.com</a>

## C. List of Materials and Suppliers

CATEGORY	PRODUCT NAME	PRODUCT No.	SUPPLIER
	Salianski isinglass (from sturgeon bladder)	63110	Kremer Pigmente, GERMANY
Wheat starch	Shofu for Restoration		Paper Nao 4-37-28 Hakusan Bunkyo-ku Tokyo 112-0001, JAPAN
<b><i>Cross-section specimens</i></b>			
Casting resin	Clear casting resin AM	405-210	Tiranti, London, UK
	Liquid hardener	405-810	www.tiranti.co.uk
Stains	Amido Black 10B (C.I. 20470)	101167 104022	Merck, Darmstadt, GERMANY www.merck-chemicals.de
	Fast Green (C.I. 42053)		
	Nile Blue A (C.I. 51180)	N5632	Sigma-Aldrich Co. Ltd., Gillingham, Dorset, UK www.sigmaaldrich.com
	Lugol's solution	109261	Merck, Darmstadt, GERMANY
	Ponceau S (C.I. 27195)	115927	
	Solvent Blue G (C.I. 61554)		Town End (Leeds) Plc. Leeds, UK www.dyes.co.uk
	Sudan Black B (C.I. 26150)	199664	Sigma-Aldrich Co. Ltd., UK
Thickening agent	Colloidal silica/ Silicon dioxide (amorphous)	406	West System Inc., Bay City, MI, USA. www.westsystem.com
Polishing	Micro Mesh (grit # 240 - # 1200)		DICTUM GmbH, Metten, GERMANY www.more-than-tools.de
<b><i>DCB specimens</i></b>			
Brushes	ProArte Series 28 Wash (soft)	50608607	CASS Art, London, UK www.cassart.co.uk
	Skyists Japan Series 632 1" (bristle)		
	Tanaka bake (flat urushi brush)		Watanabe-shoten 6-5-8 Ueno, Taito-ku, Tokyo 110-0005, JAPAN, j-lac@par.odn.ne.jp



CATEGORY	PRODUCT NAME	PRODUCT No.	SUPPLIER
Clay powder	<i>Tonoko</i>	716362	DICTION GmbH, Metten, GERMANY
Gauze filter	15 den - 17dtx ladies' rayon tights (colourless)	715949	NUR DIE GmbH, Rheine, GERMANY, www.nurdie.de
Grindstone	King, 800 grit (Japanese water stone)	711001	DICTION GmbH, Metten, GERMANY
White paint	Snopake Hi-Tech correction fluid	13139	Snopake, London, UK
Wood	Québec Yellow Pine		Moss & Co (Hammersmith) Ltd., London, UK www.mosstimber.co.uk
<b><i>Solvents</i></b>			
	Acetic acid (glacial)		DBH Laboratory Supplies, Poole, UK
	Ethanol		Tel: +44 202 669700
	Glycerine		
	Toluene (methylbenzene)		
	Xylene (dimethylbenzene)		
	Exxsol DSP 80-100		ExxonMobil Chemical Belgium
	HAN 8070		c/o ExxonMobil Chemical Ltd, Mailpoint 77 Cadland Road, Hardley, Southampton SO45 3NP Hampshire, UK
	Hydrochloric acid		DBH Laboratory Supplies, Poole, UK
	Isopropanol		
	Sulphuric acid		
<b><i>RH control</i></b>			
Humidity chambers	Lock and Lock boxes	812.00122	John Lewis, London, UK
		812.00123	Tel: +44 20 7629 7711
	Computer case fans, DC plugs and sockets, Hexagonal tap spacers	ZT88V, L49AY, JK10, QT90	Maplin Electronics Rotherham, UK www.maplin.co.uk
Salts	Magnesium nitrate	291064Y	DBH Laboratory Supplies, Poole, UK
	Potassium acetate	295814P	
	Silica gel (self-indicating)	30062	

### *C. List of Materials and Suppliers*

CATEGORY	PRODUCT NAME	PRODUCT No.	SUPPLIER
	Sodium acetate	27653.235	VWR International, 3001 Leuven, BELGIUM <a href="https://uk.vwr.com/app/Home">https://uk.vwr.com/app/Home</a> <a href="mailto:uksales@uk.vwr.com">uksales@uk.vwr.com</a>
	Sodium chloride (table salt with anti-caking agent sodium ferrocyanide)		Tesco, London, UK